THE EFFECTS OF TYPICAL CONSTRUCTION DETAILS ON THE STRENGTH OF COMPOSITE SLABS

by

Angela Sellars Terry

Thesis submitted to the faculty of the
Virginia Polytechnic Institute and State University
in partial fulfillment of the requirements for the degree of

MASTER OF SCIENCE

in

Civil Engineering

APPROVED:

W. Samuel Easterling, Chairman

Thomas M. Murray

Richard M. Barker

June 1994
Blacksburg, Virginia 24061

THE EFFECTS OF TYPICAL CONSTRUCTION DETAILS ON THE STRENGTH OF COMPOSITE SLABS

by

Angela Sellars Terry

Committee Chairman: W. Samuel Easterling
Civil Engineering

ABSTRACT

This study investigates the effects of typical construction details on the strength of steel deck reinforced concrete composite slabs. Past research on composite slabs has been centered primarily around single span, single panel width slabs with unrestrained ends. The test specimens in this study are more representative of actual slab construction. The effects of multiple spans, multiple panels, end restraint from pour stops, and deck anchorage from shear studs and welds are investigated. The results of this experimental study are analyzed using methods given in the Steel Deck Institute *Composite Deck Design Handbook*. The models were found to conservatively predict the strength of the composite slabs. Recommended modifications to the calculation methods are given.

ACKNOWLEDGMENTS

The author would like to thank Dr. Samuel Easterling for the opportunity to conduct this research and for his guidance and patience in seeing it through to completion. She would also like to thank Dr. Thomas Murray and Dr. Richard Barker for serving on her committee. A special thank you is extended to all the graduate students and the lab technicians, Brett Farmer and Dennis Huffman, who helped with construction and testing. The author sincerely appreciates the funding for this research provided by the Steel Deck Institute and the American Iron and Steel Institute. A very special thanks goes to Frank Terry and Bill and Shirley Sellars for their endless support.

CONTENTS

LIST OF FIGURES

LIST OF TABLES

LIST OF SYMBOLS

A_{bf} = area of deck bottom flange per foot of width

A_c = concrete area able to resist vertical shear

A_p = area of deck per unit width (Appendix B)

A_s = area of deck per foot of width

A_{sc} = area of shear stud

A_{webs} = area of deck webs per foot of width

a = depth of concrete compressive block

B_t = width of top flange

B_b = width of bottom flange

b = unit width of slab

b_r = effective width of slip block

C = compressive force in concrete

C_n = bending coefficient for positive moment, n = 1 to 3

D_w = width of web

d = distance from top of slab to centroid of steel deck

d_d = depth of deck

E = steel modulus of elasticity

E_c = concrete modulus of elasticity

F = required anchorage force per foot of width

F_u = specified minimum tensile stress of shear stud

F_y = specified minimum yield stress of deck

f_c = casting stress in deck

f_{cm} = compressive strength of concrete (Appendix B)

f'_c = specified compressive strength of concrete

f_L = live load stress in deck

$f_{sy.sh}$ = yield stress of deck (Appendix B)

f_{yc} = corrected steel yield stress

H_{rib} = force per unit length resisted by the web

H_s = length of stud after welding

h = depth of composite slab from top of concrete to bottom of deck

h_r = nominal rib height

I_{avg} = average moment of inertial of the transformed section

K = $k_3 / (k_1 + k_2)$

k = ordinate intercept of reduced experimental shear bond line

k_1 = relaxation factor for embossment height relative to web dimensions

k_2 = relaxation factor for stiffness of total slab relative to deck thickness

k_3 = relaxation factor for number of corrugations

k_4 = relaxation factor for shear span and steel depth

L = length of clear span

L_c = length of cantilever

L_s = length of shear span (Appendix B)

ℓ' = length of shear span

M_a = moment capacity due to end anchorage

M_c = total moment capacity of the composite slab

M_{et} = predicted first-yield moment

M_f' = relaxed ideal ultimate moment capacity

M_f = ideal ultimate moment capacity

M_n = predicted nominal moment

M_s = moment capacity due to shear bond (Eq. 2-7)

M_s = shoring removal moment (Eq. 2-4)

M_t = observed test moment

M_t = theoretical available moment (Eq. 2-5)

m = slope of reduced experimental shear bond line

N_b = length of embossment along its base

N_r = number of studs or welds per rib

N_t = length of embossment along its top

n = modular ratio

P_n = nominal puddle weld strength

p_h = embossment depth

Q_n = nominal shear stud strength

R = stud spacing reduction factor

r = reduction factor for moment capacity due to end anchorage

S' = shear span reduction

S_p = positive deck section modulus

S_c = positive composite section modulus

s = spacing of shear transfer devices

T = tensile force in the deck

t = steel deck thickness

V = shear force at edge of clear span (Eq. 4-13)

V = shear force in slab adjacent to the load (Appendix B)

V_{dsf} = force necessary to cause a vertical shear failure

V_e = maximum experimental shear

V_m = shear force for flexural failure in reinforced concrete

V_n = nominal required shear bond strength

V_s = shear force for vertical shear failure in reinforced concrete

V_u = factored required shear bond strength (Eq. 2-1)

V_u = vertical reaction at a support when ultimate strength is reached (Eq. 2-8)

v = concrete shear stress

W_1 = weight of concrete and deck

W_b = width of embossment across its base

W_t = width of embossment across its top

W_D = weight of concrete, deck, and superimposed dead load

W_L = uniform service live load

w = applied uniform load

w_r = average width of concrete rib

x = distance to a slab cross section measured from the support

y_{cc} = distance from neutral axis of composite section to top of slab

Δ = midspan deflection

ϕ = reduction factor

γ = coefficient for proportion of dead load added upon removal of shore

μ = coefficient of friction

ρ = reinforcement ratio

σ_t = concrete tensile stress

Chapter 1

INTRODUCTION

1.1 GENERAL

Composite slabs, which are used in virtually all steel framed buildings, consist of two main components, cold-formed steel deck and concrete. They have several advantages over conventional reinforced concrete slabs. The steel deck is lightweight and easy to handle during both transport and placement. After the deck is positioned and prior to concrete placement, it serves as a platform for the work crew and their equipment. During the placement of the concrete deck, the steel deck acts as the form for the fresh concrete, eliminating the time consuming construction of costly, removable forms. After the concrete has cured and the two components become a composite system, the steel deck assumes the role of positive slab reinforcement. Composite slabs require less concrete, therefore reducing building weight which in turn reduces framing and foundation costs (Dallaire 1971). Construction time and labor costs are also reduced.

The development of the composite slab concept began in the mid 1920s. By 1938 the Fenestra Corporation was using steel-concrete floor slabs in small multistory industrial

buildings. However, these floors did not take advantage of the benefits of composite action. The deck was designed to be the sole load carrier while the concrete slab was merely a topping for a level surface. Actual composite floor slabs were first constructed in the early 1950s. Construction continued throughout the 1950s and 1960s. By 1967 several manufacturers had entered the steel deck market, designing deck based on engineering principles, producing the deck, and testing the final product. Because there was no single design standard, each manufacturing company developed its own system and was often asked by building code authorities to produce additional test data before a product could be used in construction. Suffering with the cost of extensive testing and the time consuming process of approving the metal decking, manufacturers and building code authorities, respectively, recognized the need for a design standard. In response to this need, the American Iron and Steel Institute (AISI) initiated a research project at Iowa State University (ISU) in 1967. The ultimate goal was a design criteria for composite slabs. Based on performance tests for each deck profile, strength equations developed at ISU were incorporated in the 1984 ASCE *Specifications for the Design and Construction of Composite Slabs*.

The Steel Deck Institute (SDI) sponsored research at West Virginia University (WVU) in the early 1980s and at Virginia Polytechnic Institute and State University (VPI&SU) in 1989 to study the behavior of composite floor slabs constructed as multipanel, multispan slabs with end restraint from pour stops and deck anchorage from shear studs. The test specimens were more representative of slabs actually constructed in

buildings than the majority of the specimens tested at ISU. The research at WVU and VPI&SU resulted in an analytical method for determining the strength of composite slabs. The method is based on the moment capacity of conventional reinforced concrete and elastic analysis. The method facilitates the calculation of the strength of a composite slab design without having to actually test the design. Further research was needed to prove the validity of the new method, which is presented in the SDI *Composite Deck Design Handbook* (CDDH).

1.2 OBJECTIVE AND SCOPE OF RESEARCH

The objective of this study is to provide additional test data that will either support or discourage the use of reinforced concrete models in predicting the strength of composite floor slabs. Similarly, the conclusions of this research will either recommend, possibly with modifications, or dispute the SDI method of composite floor design presented in the CDDH.

Eight three-span composite floor slabs were constructed and tested. Variables in the eight slabs were deck gage, rib height and slab thickness, span length, and degree of anchorage over supports. End restraint from pour stops and deck continuity over supports were also investigated. Each floor was tested one span at a time under a uniform load.

1.3 OVERVIEW

A brief history of composite slabs and a summary of the research that has been conducted in the area is presented in Chapter 2. The experimental research conducted in this study is described in Chapter 3. A description of the SDI CDDH Method is given in Chapter 4. An analysis of the experimental results with a comparison to the predicted CDDH results is presented in Chapter 5. A summary, and some conclusions and recommendations are given in Chapter 6. The details of each test specimen are provided in Appendix A. A review of the literature on the topic of vertical shear strength is given in Appendix B.

Chapter 2

BACKGROUND INFORMATION

2.1 HISTORICAL BACKGROUND

The development of composite slabs arose from the need for a lightweight, economic flooring system with easier installation relative to the commonly used reinforced concrete floor. James Loucks and Harry Gillet of Holorib Incorporated received a patent for their suggestion, "Holorib Deck" (U.S. Patent No. 1,574,586), in 1926. The deck was marketed by the Fenestra Corporation after the original company was sold. The product was eventually given the name "keystone beam" because of its wedge shape.

By 1938, steel deck slabs were being used in two and three story industrial buildings and apartment buildings (McDermott 1967 and Dallaire 1971). These original slabs were noncomposite. Their design did not take advantage of the strengths of both the concrete and the steel. The concrete was merely a topping for fire proofing and a means to a level surface. The deck was the only structural element designed to carry load. However, the first steel deck floor slabs did take advantage of the open channels formed by

the deck profile. Electrical wires and other building services could be run through these spaces which permitted a more flexible distribution of services than conventional reinforced concrete floors.

After World War II steel deck floor slabs were employed in high-rise structures. Engineers and designers began asking if the concrete could be allowed to carry a portion of the load. The first significant research publication on the subject was written by Bengt Friberg, a consulting engineer in St. Louis, Missouri. Friberg made economic and strength comparisons of "re-bar" slabs (concrete slabs with reinforcing bars) and "re-form" slabs (concrete slabs with steel deck). He found that moment distribution is different for re-bar slabs and re-form slabs after initial cracks have developed over the supports. Re-bar slabs crack over the supports and near the center of the span at nearly equal loads suggesting moment distribution over a uniformly stiff section. For re-form slabs increasing loads are mainly resisted by positive moments only. Sections over the supports act as "plastic hinges" (Friberg 1954).

Granco Steel Products of St. Louis marketed the first truly composite slab in 1950. The product, "Cofar", was made of high-strength steel deck with wires welded transverse to the top of the corrugations (Dallaire 1971). The wires provided a path for shear transfer between concrete and steel. By the early 1960s the concept of shear transfer had challenged other companies to develop mechanical interlocking devices. The Inland-Ryerson Company began producing embossed steel deck (Dallaire 1971). An embossment is an area of metal which protrudes into the concrete. A section of a composite slab is

illustrated in Figure 2.1. The concrete is cut away to reveal the embossed deck. Shear studs are shown and will be addressed later. The embossments performed the same function as the welded wires on the "Cofar" system but were rolled into the steel deck during its production not attached later. By using the concrete as a load carrier, designers were able to use a thinner gage deck or take advantage of longer spans.

As the popularity of composite slabs began to grow and new features such as embossments were introduced, engineers sought a better understanding of composite slab behavior. Several initiated experimental research programs to further their understanding. Since the late 1960s an extensive body of research has been conducted in the area of composite slab behavior and design.

2.2 Literature Review

Stainslaw Bryl and John McDermott published separate papers in 1967 which furthered the understanding of composite slab behavior (Bryl 1967 and McDermott 1967). Bryl presented a design recommendation based on the results of around 150 tests conducted in Switzerland, France, Germany, England, America, and the Netherlands. He concluded that a safe criteria for failure could be based on allowable bending stresses in the uncracked section. Although very conservative, it was a start to designing slabs compositely. Bryl defined three phases of behavior. In Phase I the two elements act together as a "fully effective composite section". In Phase II the strength of the bond between the steel and the concrete diminishes as the bending stress increases at the critical

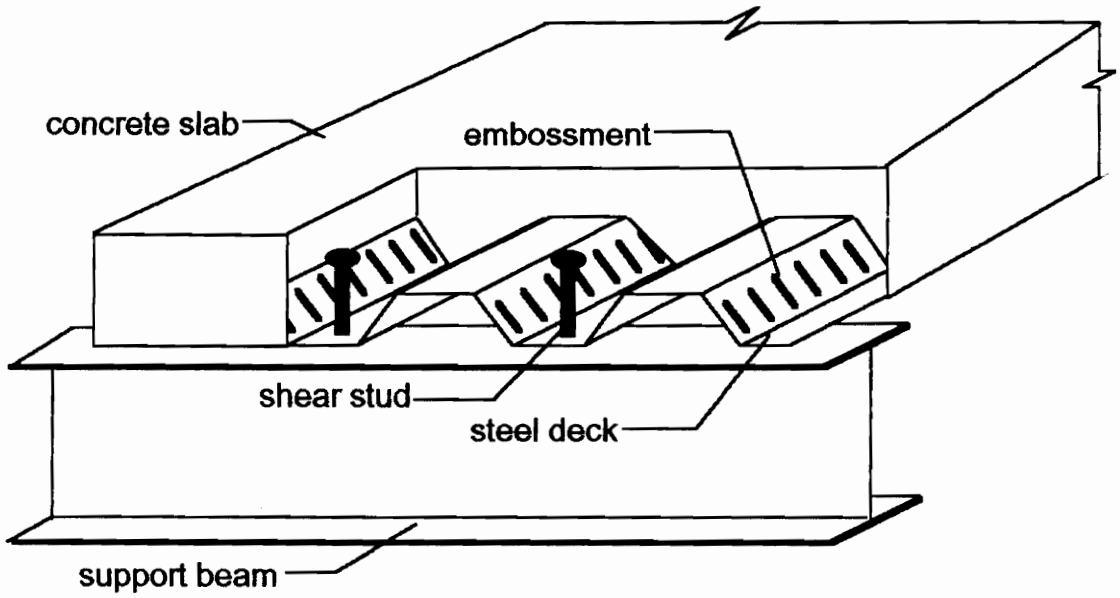

Figure 2.1 Section of Composite Floor System

section. As the strength of the bond between elements continues to diminish out from this section "this wave of bond stress arrives at the end of the plate" and slip occurs. If shear connectors are present further strength is possible, otherwise failure is certain. "Phase III is accompanied by large permanent deformation and a considerable increase in load until plastic hinges develop. Failure then generally results from the concrete crushing or the shear connectors collapsing" (Bryl 1967).

McDermott tested three specimens. The deck profile differed from the popular keystone and Cofar systems. The system consisted of a horizontal pan and vertical web which interlocked with an adjacent identical section. A circular arch snapped in between two adjacent webs. Perforations in the vertical webs which filled with concrete during placement provided mechanical interlock between the concrete and the steel. McDermott concluded that the chemical bond and the mechanical interlock of the web perforations provided sufficient resistance to slip in the practical design range for spans longer than 8.5 ft. (McDermott 1967).

As mentioned in the introduction, by 1967 several manufacturers had entered the steel deck market, designing deck based on engineering principles, producing the deck, and testing the final product for lack of a reliable analytical model. Manufacturing companies were often asked by building code authorities to produce additional test data before a product could be used in construction. Suffering with the cost of extensive testing and the time consuming process of approving the metal decking, manufacturers and building code authorities, respectively, recognized the need for a design standard. In response to this

need, the American Iron and Steel Institute (AISI) initiated a research project at Iowa State University (ISU) in 1967 directed by Carl Ekberg. The objectives were to investigate the behavior of composite floor slabs and to ultimately develop a design criteria for composite slabs.

The ISU researchers set out to develop a design method based on ultimate strength design rather than the working stress approach previously employed. The researchers determined three failure modes for composite slabs: 1) under-reinforced flexural failure, 2) over-reinforced flexural failure, and 3) shear bond failure. The latter was identified as the most common. Approximately 353 tests were eventually performed at ISU over a ten year period.

Research was also conducted at the University of Waterloo in Canada by Schuster, a former graduate student who performed many of the tests at ISU. Most were single-span, single-panel width specimens. A variety of tests were performed including repeated load tests, uniform load tests, behavioral pushout tests, and full-scale tests of one-way and two-way slabs. Multiple span slabs, slabs with welded wire fabric, slabs with shear connectors over the supports, and slabs with corrugations in the less common, transverse direction (parallel to the support beams) were also investigated.

The work directed by Ekberg, Schuster, and Porter is extensive and is best summarized in a chronological list of important findings.

(1) A steel deck profile must provide resistance to horizontal shear as well as vertical separation to achieve necessary composite action (Schuster 1976).

(2) Tests of short shear spans exhibit considerable stiffness with little nonlinearity whereas long shear spans are more ductile and are considerably nonlinear with increasing load. Load capacity decreases with increasing shear span and span length (Porter and Ekberg 1976).

(3) Ultimate load decreases with decreasing gage thickness. Nonlinearity increases with decreasing gage thickness (Porter and Ekberg 1976).

(4) Welded wire fabric influences ultimate strength (Porter and Ekberg 1977).

(5) Concerning two-way simply supported slabs, 97 percent of load at ultimate is carried by the deck in the "strong" direction, parallel to corrugations (Porter and Ekberg 1977).

(6) The ultimate load of a composite slab tested under uniform load is 3 to 19 percent higher than the same slab tested under concentrated line loads (Porter and Ekberg 1978).

(7) Shear studs, illustrated in Figure 2.1, connecting the deck to the support beam increased flexural load capacity 10 to 30 percent. Studded specimens ultimately failed by tearing of the deck near the stud. "The effect of the stud was negligible until measurable interfacial slip occurred at the end of the span (end-slip). As the concrete within the shear span attempted to override the end embossments, additional end-slip resistance was provided by the stud. Therefore, the deck-to-concrete end-slip displacement was a function of the shear-bond (interfacial) resistance, and the stud resistance" (Krupica 1979).

(8) Shear bond failure is the result of the breakdown of the mechanical interlocking capacity and frictional resistance between the deck and concrete not because of excessive principal tension stresses in the concrete (Schuster and Ling 1980).

(9) Concerning repeated loading on composite slabs, the fatigue limit of single spans is 55 percent of the ultimate static failure load, and 60 percent for double spans (McCuaig and Schuster 1988).

The research at ISU resulted in design recommendations for composite floor slabs for the limit states of shear bond, under-reinforced flexure, and over-reinforced flexure. These last two limit states are less likely to control because according to the recommendations the entire steel deck cross section must yield which was rarely exhibited in the tests. However, the recommendations for all three failure modes were incorporated in the 1984 ASCE *Specifications for the Design and Construction of Composite Slabs.*

"The characterization of a shear bond failure was identified by the formation of an approximate diagonal crack under or near one of the concentrated [line] loads, resulting in a brittle type of failure at ultimate load" (Schuster 1972). It was discovered that shear bond failure may or may not be preceded by deck yielding of the extreme fibers but not over the entire depth. The strength expression based on the shear bond limit state is given by:

$$V_u \le \phi \left[\frac{b\,d}{s} \left(\frac{m\,\rho\,d}{\ell'} + k\sqrt{f'_c} \right) + \frac{\gamma\, W_1 L}{2} \right] \qquad (2\text{-}1)$$

where,

V_u = factored required shear bond strength, lbs. per foot width

ϕ = strength reduction factor

b = unit width of slab, 12 in.

d = effective slab depth, in.

s = spacing of shear transfer devices, in.

m = slope of reduced experimental shear bond line

ρ = reinforcement ratio of steel deck area to concrete area, A_s/bd

ℓ' = length of shear span, in.

k = ordinate intercept of reduced experimental shear bond line

f'_c = specified compressive strength of concrete, psi

γ = coefficient for proportion of dead load added upon removal of shore

W_1 = weight of slab, steel deck and concrete, psf

L = clear span length, ft.

This expression was selected after the evaluation of three similar equations, one developed by Schuster, the second of the form in the ACI Building Code, and the third developed by Zsutty using dimensional analysis (Porter, et al. 1976). Schuster's equation and the familiar ACI Building Code expression predicted composite slab behavior very closely. These expressions differ in their placement of variables representing concrete strength and percentage of steel. Therefore, it was concluded that these two factors were not significantly influential in the prediction of composite slab strength.

To use the expression, a series of performance tests are required for each steel deck configuration. The researches have suggested that the important terms to vary during these tests are shear span and overall slab depth. A linear regression analysis is then performed on the data as illustrated in Figure 2.2 with the expression rearranged in the form of:

$$\frac{V_e\, s}{b\, d\sqrt{f'_c}} = m\,\frac{\rho\, d}{\ell'\sqrt{f'_c}} + k \qquad (2\text{-}2)$$

where V_e is the maximum experimental shear typically applied just prior to cracking under a load point. The terms m and k are slope and intercept values from a line reduced 15 percent from the best fit line through the experimental data. The reduction accounts for any minor variations in laboratory test specimens. Once m and k have been determined the design shear from Eq. 1 can be calculated and in turn be used to calculate the allowable superimposed live load. The last term in Eq. 1 is a correction for shoring. "Performance tests are necessary since each steel deck has its own unique shear transferring mechanism" (Porter and Ekberg 1976). For a particular profile, if the gage, the surface coating, and the type of concrete remain the same the regression line applies to any slab depth and shear span. Further research confirmed that the shear bond regression analysis was reasonably valid for uniformly loaded specimens with ℓ' = L/4 (Klaiber and Porter 1981).

In addition to its incorporation into the ASCE *Specification for the Design and Construction of Composite Slabs*, the shear bond approach was incorporated in the European Recommendations for Composite Structures (1981), the British Standards Institution (1982), and the Commission of the European Communities, Eurocode 4 (1984).

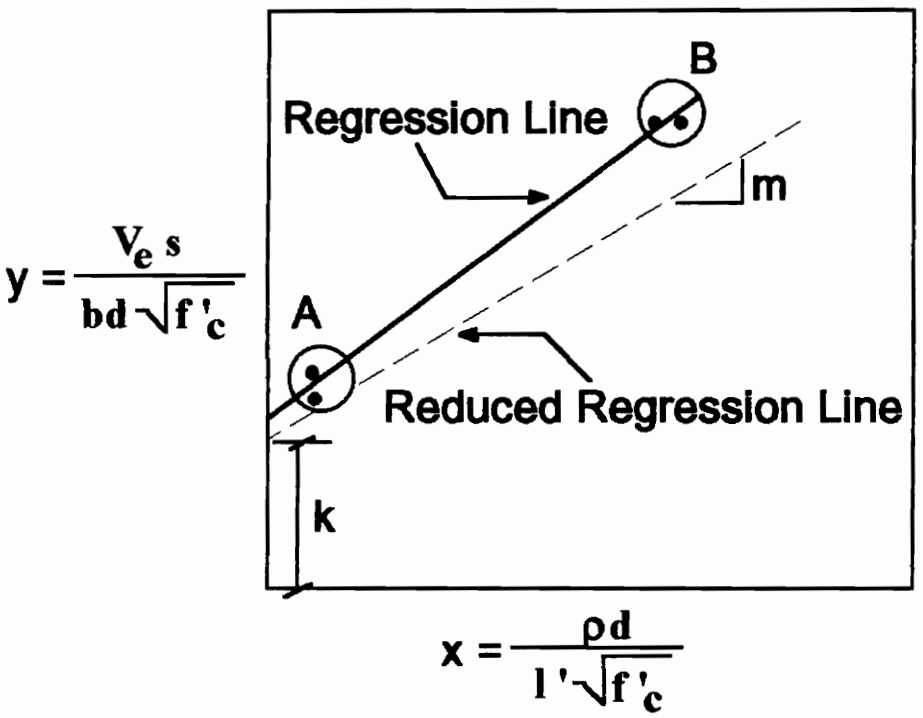

Figure 2.2 Shear Bond Regression Plot (*Standard for* 1993)

Another significant body of work on the subject of composite slab strength was conducted at West Virginia University (WVU) under the direction of Larry Luttrell. Early work at WVU included a series of 25 tests performed on one and two span slabs constructed with embossed deck. Some slabs were a single panel wide and others were two panels wide. The steel deck was the only reinforcement (Luttrell and Davison 1973). The test setup was essentially the same as the setup used at ISU and adopted for use in the ASCE *Specification for the Design and Construction of Composite Slabs*. The evaluation procedure was based on the limitation of flexural stresses at extreme fibers and shear stresses at the concrete-steel interface. Luttrell and Davison suggested that the onset of slip did not constitute failure of composite slabs with embossed deck, and that failure was not sudden. The stiffness of the deck webs affected horizontal shear capacity. Embossed webs are stiffer than plain webs and resist lateral displacement during concrete override. Subsequent research at WVU focused on this shear transfer mechanism.

"During the loading sequences for composite and essentially one-way slabs, the response may be quite unlike that of bar-reinforced one-way flat slabs. The difference rests totally within the anchorage development for the tensile reinforcement or, more specifically, in the transfer of forces between the concrete and steel through shear stresses along the interface" (Luttrell and Prasannan 1984). Whereas a reinforcing bar is bonded to the concrete over its entire surface area, steel deck is only bonded on one surface. The embossments on this surface, their shape, size and orientation, are therefore critical to anchorage development of the deck. A moment capacity computed using a simple

transformed area concept is the basis of the model, see Figure 2.3. The ideal ultimate moment capacity, M_f, is given by:

$$M_f = T_1 y_1 + T_2 y_2 + T_3 y_3 + C y_4 \quad (2\text{-}3)$$

The location of tension forces, T, and compression force, C, are shown in Figure 2.3. The ideal capacity was "relaxed" to account for shoring removal, shear span, and properties of the deck profile, all of which had been shown through statistical analysis to influence slab strength. The relaxed ideal capacity, M_f', is given by:

$$M_f' = M_f - M_s \quad (2\text{-}4)$$

where M_s is the shoring removal moment. The theoretical available moment, M_t, is given by:

$$M_t = K M_f' - k_4 S' \quad (2\text{-}5)$$

where S' is the shear span reduction (S' = L/2 - ℓ') and K = $k_3/(k_1 + k_2)$. The complex equations for relaxation factors k_1, k_2, k_3, and k_4 are a measure of the influence of:

k_1 = embossment height relative to web dimension

k_2 = stiffness of total slab relative to deck thickness

k_3 = number of corrugations

k_4 = shear span and steel depth

Although the calculation of the relaxation factors requires significant effort, this method of analysis yielded two important benefits. First, performance tests are not required with this method. Second, this method allows deck manufacturers to predict the

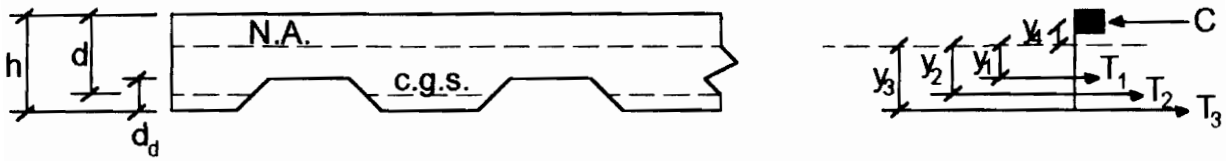

Figure 2.3 Deck Cross Section and Force Locations (Luttrell and Prasannan 1984)

strength of a new deck profile analytically without having to go to the expense of actually rolling a section to test.

Other findings at WVU were:

(1) The deeper the deck profile the more susceptible it is to lateral displacement during concrete override (Luttrell and Davison 1973).

(2) Continuous deck panels developed adequate resisting moment over intermediate supports in the absence of reinforcing steel (Luttrell and Davison 1973).

(3) Vertical embossments were 48 percent stronger than horizontal embossments. Vertical embossments, designated as Type I in Figure 2.4, act as stiffeners for the web and present a larger surface area for the concrete to override. Horizontal embossments, Type II in Figure 2.4, although ineffective in resisting horizontal slip still prevent vertical separation (Luttrell and Prasannan 1984, Luttrell 1987).

(4) "There are three phases of slip resistance: a) adhesive bond, b) mechanical bond from embossments and, c) shear studs if present. The three contributions are not additive in any direct fashion. They resist in the priority order listed and may succumb in the same listed order while trying to pass their forces off to the next system. If the next system is inadequate, failure results" (Luttrell 1987).

Another significant research study was conducted by Charles Roeder at the University of Washington (Roeder 1981). Roeder tested to failure three multispan specimens. Two were single panel width slabs (3 ft. wide), and one was nearly 10 ft. wide.

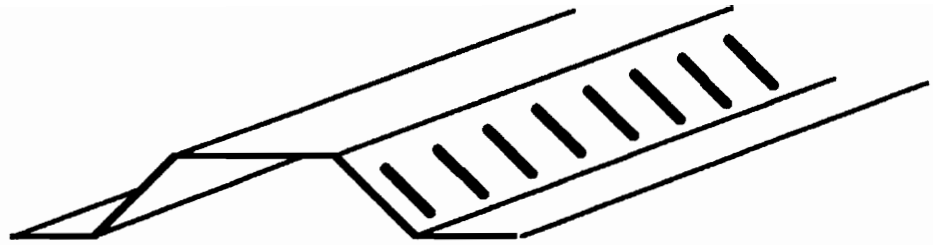

Type I Embossment

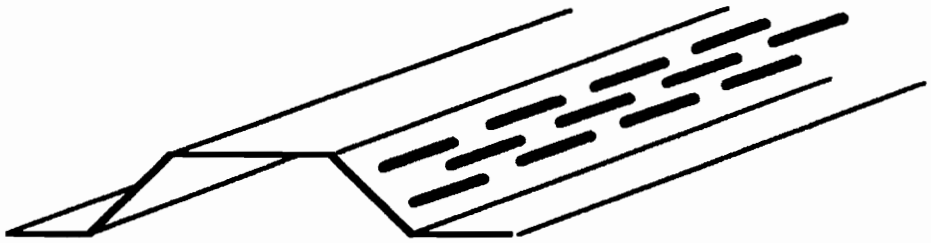

Type II Embossment

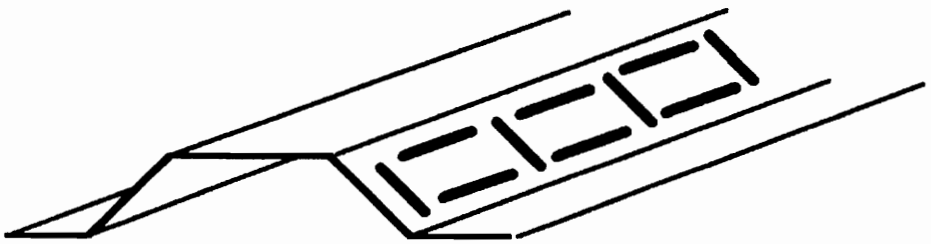

Type III Embossment

Figure 2.4 Embossment Classifications

Shear studs were used to anchor the deck to the supports. Of the two single panel width specimens, one had continuous deck and wire over the supports, while the other had spliced deck and wire. The continuous deck caused a 40 to 50 percent increase in shear bond capacity over the spliced deck. Roeder compared the results of his study to some of Porter's experimental data from simple span slabs without studs. He discovered a 50 to 100 percent increase in capacity with spliced deck and stud restraint and a 100 to 150 percent increase with continuous deck and stud restraint.

Roeder also investigated the effect of concentrated loads on the behavior of multipanel composite slabs. He found that only 50 percent of the applied load is supported by the loaded panel. The rest is distributed to adjacent panels. The continuity of the slab restricts deformation which "tends to distribute the deflections, bending stress, and shear stress across the weak direction of the floor to adjacent deck panels" (Roeder 1981). Roeder does not present a design method in his study, and he acknowledges that his findings are limited to a single deck type, stud size, span length, and concrete depth. However, his efforts drew attention to the conservativeness of existing methods. The specimens Roeder tested were more in line with actual field construction than the simple span, single panel tests which were the basis of current design methods.

The Steel Deck Institute (SDI), representing several steel deck manufacturers around the country, recognized the need for research into the behavior of slabs more representative of those typically constructed in buildings. The SDI sponsored an experimental study at Virginia Polytechnic Institute and State University (VPI&SU) in

1989 (Young 1990, Easterling and Young 1992). The research at VPI&SU focused on the influences of multiple spans, multiple panel widths, and typical field details at supports and end spans.

An analytical method for determining the strength and stiffness of composite slabs was presented. The method uses some of the same expressions used to determine the strength of traditional reinforced concrete slabs; therefore, suggesting that failure is controlled by flexure rather than shear bond. Typical construction details over the supports and at the end of a slab were found to significantly reduce the slip associated with the shear bond limit state.

The design procedure presented does not require any empirical coefficients and was therefore, independent of laboratory testing. The procedure will not be described here, but rather because it is the goal of the current study to verify the procedure, it is described in detail in Chapter 4.

The popularity of composite slab design has not grown in the United States alone. Extensive research has been conducted in the Netherlands, Switzerland, the United Kingdom, Germany, and Australia as the popularity of composite slabs has grown in these countries. Stark published a paper in 1978 describing the results of tests performed on the Dutch embossed deck product "Prins-floor" (Stark 1978). Stark discussed three failure limits: 1) vertical shear capacity, 2) moment capacity, and 3) longitudinal shear capacity. Vertical shear failure occurs at the supports and is not critical except in the case of deep slabs, short spans, and high loads. The moment capacity at midspan depends on the

magnitude of the longitudinal shear force between concrete and steel. If this force is greater than the tensile force in the steel then the connection at the interface is "complete", there is no end slip, and moment capacity controls failure. However, if this force is less than the tensile force in the steel then the connection is "incomplete" and longitudinal shear capacity controls the failure load.

Stark suggests that if the concrete is uncracked then the shear stress at the interface can be calculated by the familiar expression

$$\tau = \frac{V\,Q}{I\,b} \tag{2-6}$$

where,

τ = shear stress at section

V = shear force at section

Q = first moment with respect to the neutral axis of the area beyond the point at which the shear stress is desired

I = moment of inertia about the neutral axis

b = unit width

Accordingly, slip should start at the ends where the shear stress is a maximum. Tests showed that the slip started at the section of maximum moment. Stark explains that before cracking occurs horizontal shear stresses at the interface are small. When cracking occurs the steel stresses at the crack increase as do shear stresses between the steel and concrete. When these shear stresses reach the bond stress limit, slip occurs at the interface. Friction forces develop and the shear stress is transmitted to areas further away from the location of

the crack. As the shear forces in these subsequent areas reach the bond stress limit the process is continued until the entire bond is diminished and the slab fails. Stark predicted that flexural failure, not shear failure, will control in very long spans.

Crisinel and Daniels of Ecole Polytechnique Federale de Lausanne, Switzerland investigated the ductility of composite slabs and the influence of actual construction practices. They concluded, in agreement with Luttrell and Prasannan (1984), that vertical embossments (Type I) prevent deck-concrete separation better than horizontal embossments (Type II) and lead to a ductile failure mode as opposed to the brittle behavior of horizontal embossments (Crisinel, et al. 1986).

In another study investigating actual construction practices, simple span, one-way slabs were compared to multispan, two-way slabs having anchorage over the supports. Horizontal debonding was found to control failure only in exterior spans of multispan slabs without anchorage (Daniels, et al. 1990).

Crisinel and Daniels have recently developed a numerical model for analyzing one-way single or continuous span composite slabs (Crisinel, et al. 1992). The model uses finite element analysis to estimate the behavior of a composite slab and its load-carrying capacity. Elemental tests are required to determine the influence of embossments and end anchorage on shear bond, but full-scale testing is eliminated. The model allows for changes in deck geometry and materials.

Several researchers from the United Kingdom have published research on composite slabs including O'Leary, El-Dharat, Duffy, Jolly, Zubair, Wright, and Evans.

O'Leary, El-Dharat, and Duffy concluded in a 1987 report on end-anchored composite slabs that "There is no evidence of complete shear bond failure. The mode of failure exhibited indicates that it is dependent on the combined flexural and longitudinal shear capacities of the section" (O'Leary, et al. 1987).

Jolly and Zubair focused their research on the efficiency of embossments in providing shear bond interlock (Jolly and Zubair 1987). Embossments on the compression flange of the deck profile created initial deformations that buckled under the compressive load of wet concrete. Embossments on the tension flange tended to straighten under load and lead to excessive deformations. The shape and orientation of the embossment was found to affect the shear bond characteristics of the deck. Vertical embossments performed more effectively than horizontal or inclined embossments. They concluded that the width of an embossment should be kept at a minimum, the height at a maximum without affecting corner stiffness, and the depth at a maximum without tearing the deck.

Recent research by Jolly and Lawson has recommended that shear bond, from embossments and chemical bond, and end anchorage effects on moment capacity are directly additive (Jolly and Lawson 1992). Although independent, the two contributions to moment capacity are not activated at the same time or degree of slip. Therefore, the authors recommend that the moment capacity of a slab with combined shear bond and end anchorage is given by:

$$M_c = M_s + r\, M_a \qquad (2\text{-}7)$$

where,

M_c = total moment capacity of the composite slab

M_s = moment capacity due to shear bond

M_a = moment capacity due to end anchorage

r = reduction factor in the range of 0.3 to 0.6

The reduction factor, r, accounts for the fact that the contribution of shear bond reaches its maximum at about the same time the contribution of end anchorage is at half its maximum strength.

Wright and Evans suggested a method of analysis for the strength of composite slabs based on plastic collapse (Wright and Evans 1990). The plastic collapse method requires one empirical coefficient derived from three tests. The coefficient is representative of shear bond and is used to evaluate moment capacity. The method is based on the theory of plasticity, and assumes a hinge forms at the shear span. The energy applied to the slab to deform the hinge is equated to the energy resisting rotation of the hinge.

A new design method gaining popularity in Europe is the partial interaction or partial shear connection strength model. Extensive research has been conducted separately by Bode and colleagues of Germany and Patrick of Australia. Bode describes the method as a "simple but useful alternative to the well-known m and k method, associated with the names of Ekberg, Porter, and Schuster and others. We feel that this method leads to a better understanding of forces and their distribution over the whole length and total cross section with slip at the steel concrete interface" (Bode, et al. 1988).

The assumption behind partial interaction theory is that "the building materials, concrete and steel, as well as the connection have to show sufficient ductility and plastic deformation without brittle failure" (Bode and Storck 1990). The partial interaction model is based on the development of a plastic stress block at the maximum moment position along the slab. If there is no connection the moment capacity of the slab is the plastic moment capacity of the deck alone. The relationship between moment capacity and shear connection strength is illustrated in Figure 2.5. The partial interaction method has several advantages over the m and k method. (1) Fewer tests are required to determine the necessary empirical coefficient. Also, the coefficient has an explicit meaning: the degree of interaction or connection. (2) The method is based on a mechanical model. The influence of deviations from laboratory test conditions is difficult to quantify if a procedure is not based on a mechanical model (Bode and Storck 1990). (3) The partial interaction model can be used for any loading condition, and for slabs with end anchorage and/or conventional reinforcement (Patrick 1990).

The model developed by Patrick requires information about the strength of the shear connection derived from a slip block test shown in Figure 2.6. This test on a small segment of a composite slab determines critical information about the adhesion bond, the mechanical interlock, and the frictional resistance of a deck profile (Patrick and Poh 1990).

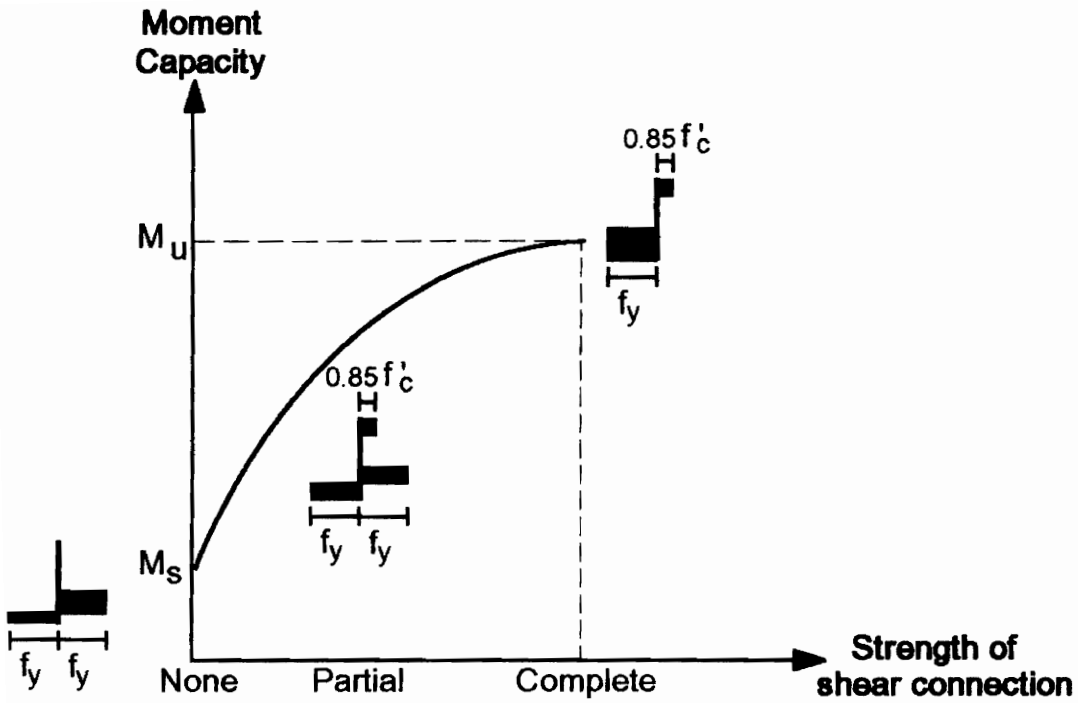

Figure 2.5 Moment Capacity vs. Strength of Shear Connection (Patrick 1990)

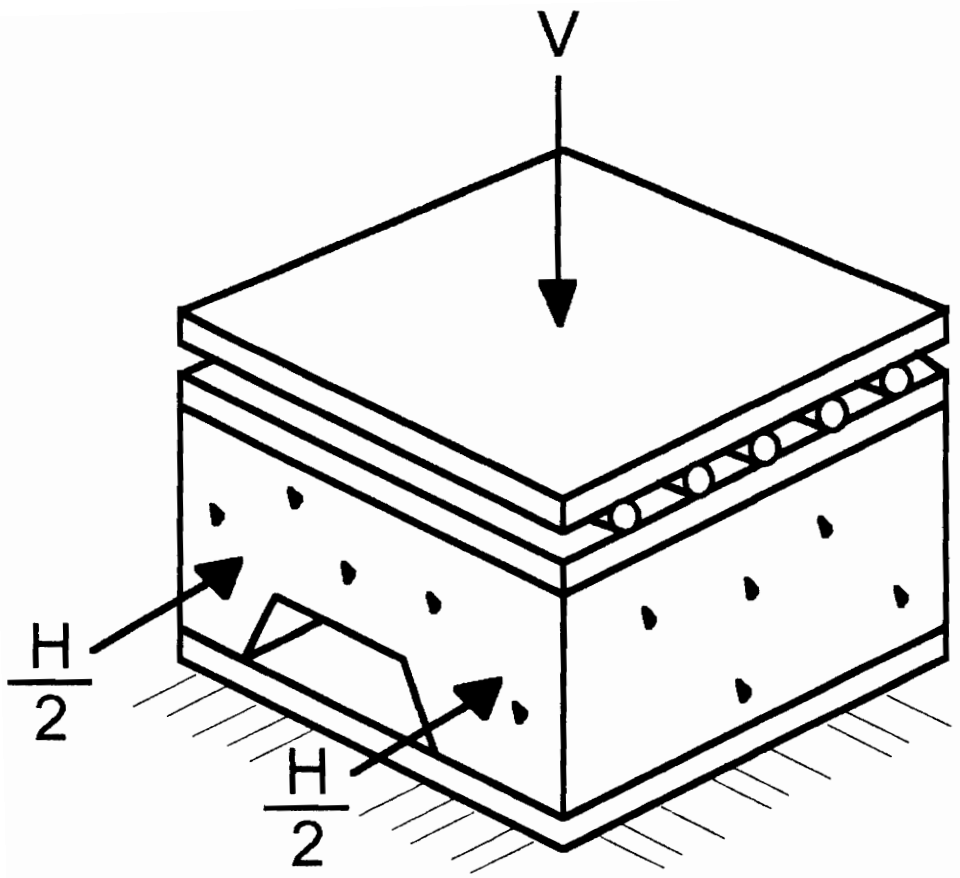

Figure 2.6 Slip Block Test (Patrick and Poh 1990)

The force per unit length resisted by the web, H_{rib}, and the coefficient of friction, μ, are derived from the slip block test. The resultant tensile force in the steel deck is computed by the expression

$$T = x \left(\frac{H_{rib}}{b_r} + \mu \frac{V_u}{b} \right) \tag{2-8}$$

where,

T = resultant tensile force in deck at a slab cross section

x = distance to a slab cross section measured from the support

b_r = effective width of slip block

V_u = vertical reaction at a support when ultimate strength is reached

b = width of slab

The difference between the model proposed by Bode and the one proposed by Patrick is the development of the tensile force in the deck. In Patrick's model "the maximum tensile force that can be developed at a cross-section is dependent on the magnitude of the shear force or reaction force that acts at the end of the slab" (Patrick 1990).

Chapter 3

EXPERIMENTAL PROGRAM

3.1 TEST PARAMETERS

Eight three-span composite floor slabs were constructed on which a total of twenty tests were performed. Variables in the eight castings were deck gage, 18 or 20; rib height, 2 in. or 3 in.; slab thickness, 4.5 in. or 5.5 in.; span length, 9 ft. or 10 ft.; and degree of anchorage over supports, studs or welds, as illustrated in Figure 3.1a and 3.1b. End restraint from a cold-formed angle was also investigated, as illustrated in Figure 3.1c. The effects of deck continuity over supports were considered. This detail is illustrated in Figure 3.2. All specimens were two panels, or approximately 6 ft., wide.

Test designations are of the form SDI-*i*/*j*-*k*-*l*. The *i*/*j* provides information about the steel deck (rib height / gage). The next character, *k*, indicates the type of anchorage over the supports of the test span. A single digit indicates an end span with the same number of shear studs over both supports. A double digit is used for center spans with studs. In general the same number of studs was not present on both supports, therefore

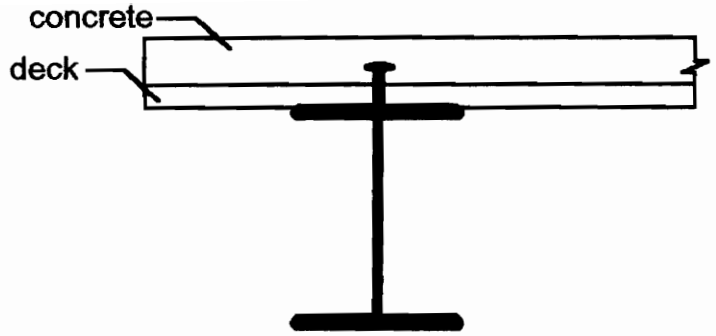

a) Shear Stud

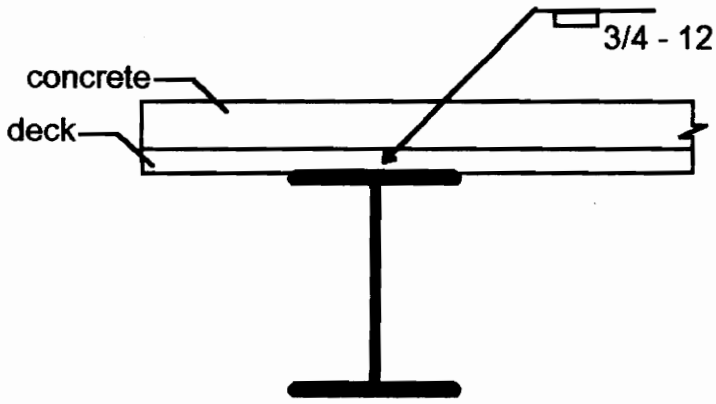

b) Arc Spot Weld

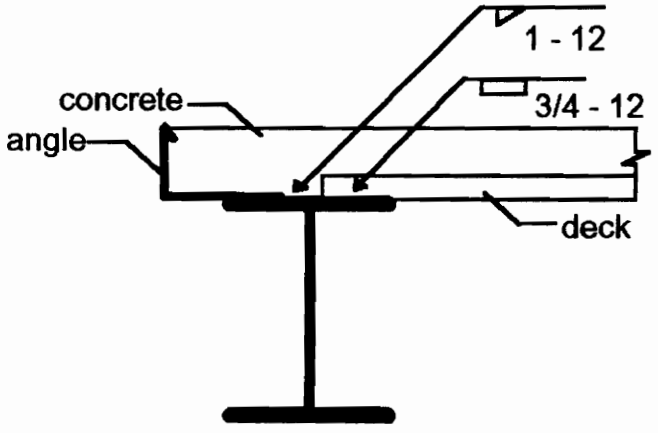

c) Arc Spot Weld
and Cold-Formed Angle with Lip

Figure 3.1 End Span Details--Exterior Support

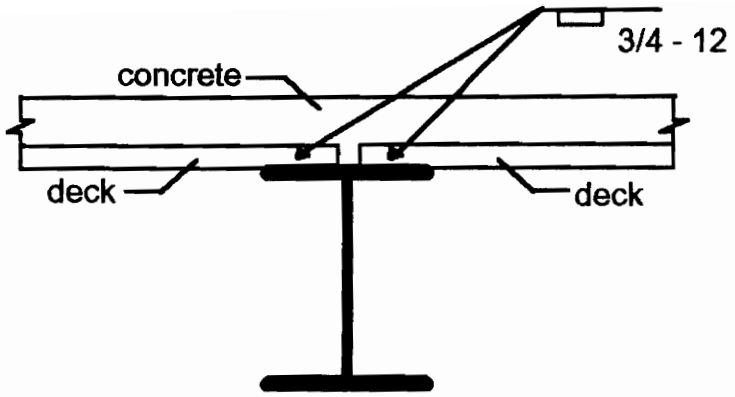

a) Deck Joint with Arc Spot Weld

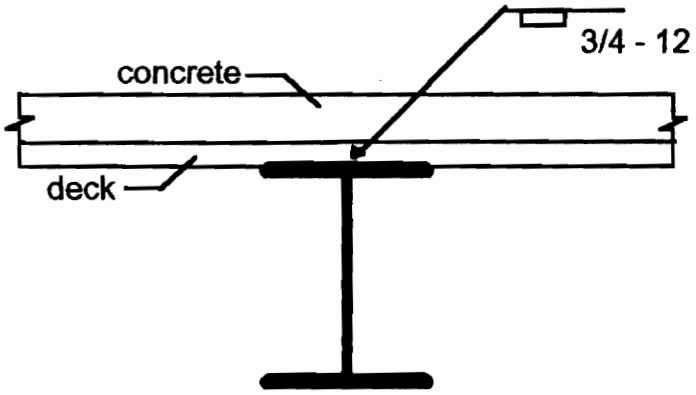

b) Continuous Deck with Arc Spot Weld

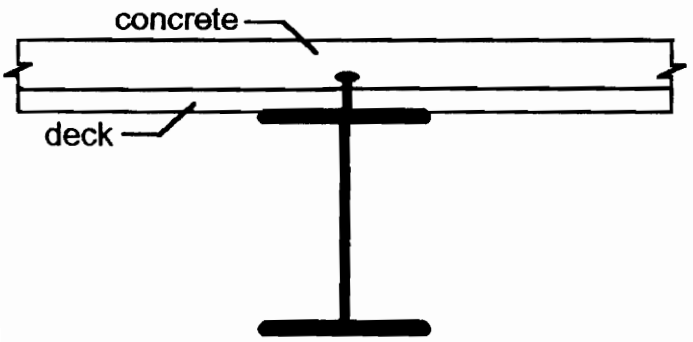

c) Continuous Deck with Shear Stud

Figure 3.2 End Span Details--Interior Support

two digits are used to indicate the number of studs on each support. A P designation indicates the presence of arc spot welds over the supports. A PX designation indicates arc spot welds as well as a butted deck joint, i.e., the deck was not continuous over the interior support. The number on the P and PX designations, for example, P1 and PX1, indicates the span. Spans one and three are end spans, and span two is the center span. The last character, *l*, of each test designation is the span length, center-to-center of supports.

For example, the test designation for the first test was SDI-2/20-4-9. The steel deck was two inches deep with a 20 gage thickness. The span was and end span, and four studs provided anchorage over the supports. The span length was nine feet. Table 3.1 summarizes the details of each specimen. A complete list of all details for each floor is given in Appendix A.

Specimen seven was different from the other specimens in that two different deck profiles were used. Span one was constructed with a 3-in. deck, and span three was constructed with a 2-in. deck. The height difference resulted in a 1-in. "step" in the center span, which was not tested. This odd construction was used in order to obtain two data points in one casting instead of two.

Each specimen was constructed similarly. The deck was cut to the appropriate length, or lengths if there were butted deck joints over the supports. Strain gages were attached on the underside of the deck sheets at several locations. The sheets were then placed on the supports, and the seams were aligned. The two panels were fastened together by button punching (crimping) on 18-in. centers. The deck was positioned on the

Table 3.1 Specimen Details

Specimen Number	Test Number	Test Designation	Span	End Details	Support Anchorage
1	1	SDI-2/20-4-9	end	1 ft. cantilever	4 studs
	2	SDI-2/20-5-9	end	1 ft. cantilever	5 studs
2	3	SDI-2/20-2-9	end	1 ft. cantilever	2 studs
	4	SDI-2/20-23-9	center	N/A	2 studs/3 studs
	5	SDI-2/20-3-9	end	1 ft. cantilever	3 studs
3	6	SDI-2/20-PI-9	end	1 ft. cantilever	arc spot weld
	7	SDI-2/20-P2-9	center	N/A	arc spot weld
	8	SDI-2/20-P3-9	end	angle with lip	arc spot weld
4	9	SDI-2/20-PX1-9	end	1 ft. cantilever, int. sup. deck joint	arc spot weld
	10	SDI-2/20-PX2-9	center	deck joints	arc spot weld
	11	SDI-2/20-PX3-9	end	angle with lip, int. sup. deck joint	arc spot weld
5	12	SDI-2/18-3-9	end	1 ft. cantilever	3 studs
	13	SDI-2/18-35-9	center	N/A	3 studs/5 studs
	14	SDI-2/18-5-9	end	1 ft. cantilever	5 studs
6	15	SDI-3/20-3-10	end	1 ft. cantilever	3 studs
	16	SDI-3/20-35-10	center	N/A	3 studs/5 studs
	17	SDI-3/20-5-10	end	1 ft. cantilever	5 studs
7	18	SDI-3/20-PX1-10	end	1 ft. cantilever, int. sup. deck joint	arc spot weld
	19	SDI-2/18-PX3-9	end	1 ft. cantilever, int. sup. deck joint	arc spot weld
8	20	SDI-3/20-33-10	center	N/A	3 studs

supports and attached with either shear studs or arc spot welds. Pour stops were screwed to the deck and wire mesh (WWF 6x6-W1.4 x W1.4) was placed inside the form and allowed to rest on the top flange of the deck. No other reinforcement was used.

Each composite slab was cast with a normal weight, 3,000 psi mix concrete, vibrated, and screeded. Steel deck strains and displacements due to casting were recorded. Slabs were covered with plastic and moist cured for seven days. On the seventh day the plastic and the pour stops were removed, with the exception of specimens three and four. The cold-formed angle on one end of both specimens had a return lip into the slab and was left on during testing to evaluate end restraint capability. Each composite slab was cured for a minimum of 21 days. Concrete cylinders were cast with each slab.

Three deck profiles from three different manufacturers were evaluated. All three profiles were galvanized trapezoidal sections with web embossments.

3.2 INSTRUMENTATION

Each specimen was instrumented with strain gages on the steel deck and the concrete. Transducers were used to measure vertical displacement. Potentiometers or dial gages were used to measure end slip. A pressure transducer was used to measure the load applied to the specimen.

Strain gages were placed on the underside of the steel deck in four major groups. A series of gages was placed nine inches inside the centerline of both the interior and exterior supports of all end spans tested. A third series of gages was placed at the location

of maximum moment, which was calculated assuming a three span configuration with the load placed only on the span under consideration. The last series of gages was placed along the span at one foot intervals. In each series of gages along a cross section of the deck, gages measured strain in the top flange and the bottom flange of the deck. Strain was also measured in the web of the deck near the exterior support and at the location of maximum moment. Strain gages were placed on the top of the cured composite slab to measure the compressive strains in the concrete. Two gages were placed at the location of maximum moment on each span tested. A sketch of the location of all strain gages for each slab is presented in Appendix A.

Two transducers were used to measure the vertical displacement at midspan of the loaded span. Potentiometers or dial gages were used to measure the horizontal slip between the steel deck and the concrete at the end of the specimen during an end span test. Measurements of end slip were taken at several locations along the specimen cross section, including both top and bottom flanges of the deck.

Uniform load was applied using an airbag, as will be described in the next section. The air bag was designed with two valves, one for the input of air and the other for measuring the pressure in the bag. A calibrated pressure transducer was connected to this second valve and the pressure was recorded by a data acquisition system.

3.3 TEST SETUP

The test setup, illustrated in Figure 3.3, consisted of two W21x68 column frames, bolted to the laboratory floor outside the supports of the span being tested. Two W12x26 beams were bolted horizontally between the columns, parallel to the composite slab. A rubber press bag with a 6 ft. x 10 ft. bearing surface was placed on the slab. Sheets of 3/4-in. plywood were placed on top of the bag. Two holes in the plywood allowed access to the valves in the bag. For nine foot spans, five W8x24 beams were bolted to the bottoms of the W12x26 beams, perpendicular to the composite slab. The frame was extended to seven perpendicular beams for ten foot spans. The regulated air source and the pressure transducer were attached to the valves in the bag. All instrumentation was then connected to a data acquisition system.

3.4 TEST PROCEDURE

The test procedure was the same for all tests. The test span was first preloaded to 0.35 psi to seat the structure and insure that all instrumentation was functioning properly. The bag was then emptied through a valve in the input line.

The span was loaded in 0.35 psi increments at a rate of approximately 0.3 psi per minute. At each load increment the air flow was stopped, and the system was allowed to stabilize for two minutes before any measurements were recorded. This process continued until a crack appeared over the interior support and a plot of load versus displacement

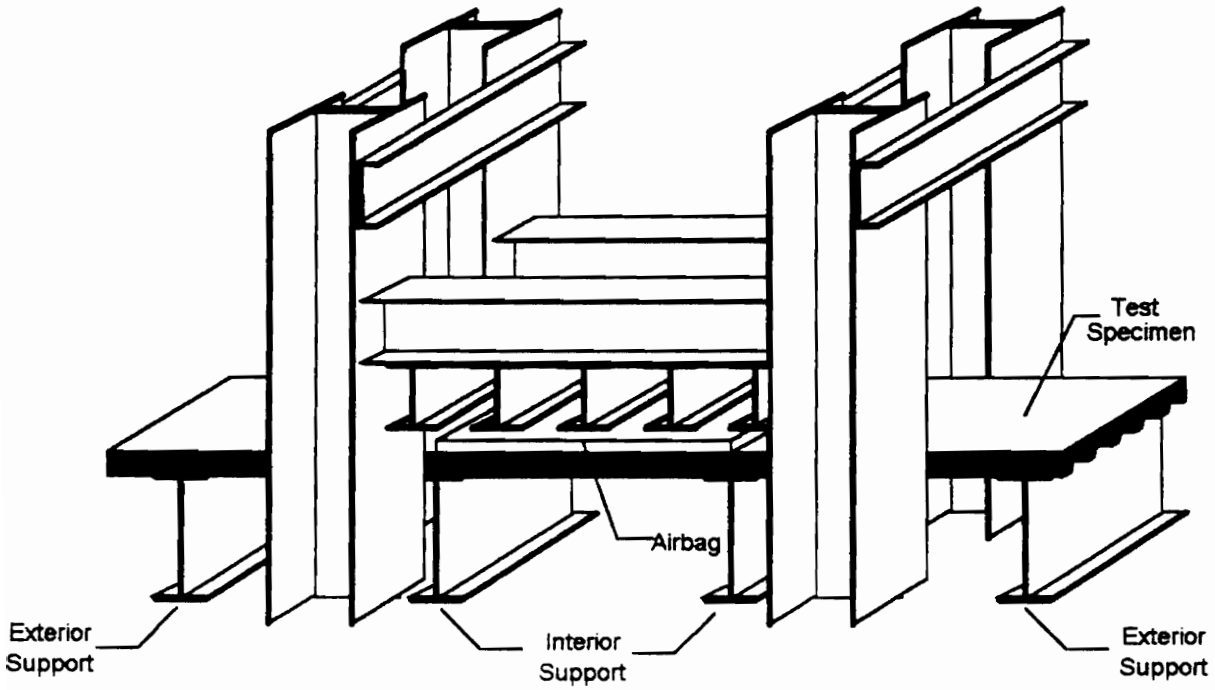

Figure 3.3 Test Setup

showed that the slab would have some permanent set when unloaded. The bag was again emptied.

The span was loaded again in 0.35 psi increments. Pressure, steel and concrete strains, midspan deflection, and end slip were recorded. Any cracks along the sides of the span were noted at each load increment. Loading was stopped between increments and measurements were taken if significant slip, debonding, or cracking occurred before the next load level was reached. As the midspan displacement increased in later stages of the test, displacement increments were used instead of load increments. Measurements were taken at 0.5-in. displacement increments. If a plot of load versus displacement showed that the maximum load had been reached and that further loading only increased the midspan displacement and end slip with a decrease in load resistance, the input valve was shut and the bag was emptied.

After the test frame and bag were removed, cracks on the surface of the floor were noted. Areas where the steel deck had debonded from the concrete were estimated by tapping the bottom of the slab. During the removal of the slab, the steel deck surrounding a shear stud was examined for buckling.

All three spans were tested on specimens two through six. Both end spans were tested before the center span. It was believed that only the initial stiffness of the center span would be adversely affected by the cracks over the supports resulting from the end span tests.

3.5 COMPONENT TESTS

Tensile coupons were tested from each of the three profiles. The yield strength of the steel deck and the compressive strength of the concrete at the time of test based on cylinder tests are given in Table 3.2.

3.6 RESULTS

A similar series of events occurred during each test. The first visible effect of the applied load was the formation of a vertical crack in the concrete over the interior support. Subsequent load caused the formation of cracks in the positive moment region. These were vertical cracks that propagated transversely across the slab, typically described by and associated with flexural cracking in reinforced concrete slabs. With increased load the deck began to debond from the concrete near the location of the cracks. Debonding was often accompanied by an increase in the steel deck strain and sometimes a sudden drop in load. As the load continued to increase new cracks formed in the positive moment region and existing cracks propagated through the depth of the concrete slab. The bottom flange of the steel deck in the positive bending region yielded, and midspan displacement increased significantly. Cracks formed longitudinally along the slab over the deck seam connecting the two panels. Near the end of the test, midspan displacement and end slip increased significantly with only slight increases in load. The test was stopped when the maximum load had been reached and the midspan displacement was three inches or more.

Load versus displacement curves for specimens with shear studs for anchorage showed a gradual increase in displacement with increased load as illustrated in Figure 3.4. On the other hand, specimens with arc spot welds for anchorage over the supports had more irregular load versus displacement curves as illustrated in Figure 3.5. Peaks and plateaus mark sudden drops in load with increased displacement that accompany debonding, loss of deck anchorage, etc.

Test results are summarized in Table 3.2. A few general observations can be made. The strengths of specimens with shear studs for deck anchorage were higher than the strengths of specimens without shear studs. The highest loads were obtained with the 2-in., 18 gage deck profile. The next highest loads were obtained with the 3-in., 20 gage deck profile. The 2-in., 20 gage deck profile supported the lowest maximum load of the three decks. The strengths increased somewhat in proportion to the cross-sectional area of the deck. The bottom deck flange in the positive bending region yielded in every specimen. The strain in the deck at the exterior supports was below the yield strain in the specimens without studs, but above the yield strain in the specimens with studs.

The largest end slips occurred in the specimens without shear studs for anchorage, specimens three and seven. This is expected because the mechanical interlocking ability of the embossments alone does not compare to the ability of shear studs to resist slip. The midspan displacements at maximum load for the specimens with deck joints, specimens four and seven, were smaller than the displacements of specimens with continuous deck

Table 3.2 Experimental Results

Specimen Number	Test Number	Test Designation	f'c (psi)	Fy (ksi)	Maximum Load (psf)	Deflection at Max. Load (in)	End Slip at Max. Load (in)
1	1	SDI-2/20-4-9	3,180	45	703	2.70	0.15
	2	SDI-2/20-5-9	3,180	45	729	2.61	0.11
2	3	SDI-2/20-2-9	5,170	45	597	2.55	0.06
	4	SDI-2/20-23-9	5,170	45	598	3.17	N/A
	5	SDI-2/20-3-9	5,170	45	602	2.35	0.12
3	6	SDI-2/20-PI-9	3,340	45	492	1.76	0.16
	7	SDI-2/20-P2-9	3,340	45	598	2.74	N/A
	8	SDI-2/20-P3-9	3,340	45	590	1.69	0.00
4	9	SDI-2/20-PX1-9	3,770	45	369	1.59	0.10
	10	SDI-2/20-PX2-9	3,770	45	344	1.82	N/A
	11	SDI-2/20-PX3-9	3,770	45	488	1.77	0.00
5	12	SDI-2/18-3-9	5,300	47	903	2.50	0.17
	13	SDI-2/18-35-9	5,300	47	891	3.10	N/A
	14	SDI-2/18-5-9	5,300	47	912	2.70	0.21
6	15	SDI-3/20-3-10	3,750	50	743	2.58	0.12
	16	SDI-3/20-35-10	3,750	50	787	3.83	N/A
	17	SDI-3/20-5-10	3,750	50	891	3.49	0.12
7	18	SDI-3/20-PX1-10	3,370	50	478	0.60	0.00
	19	SDI-2/18-PX1-9	3,400	47	499	1.57	0.16
8	20	SDI-3/20-33-10	3,220	50	911	3.33	N/A

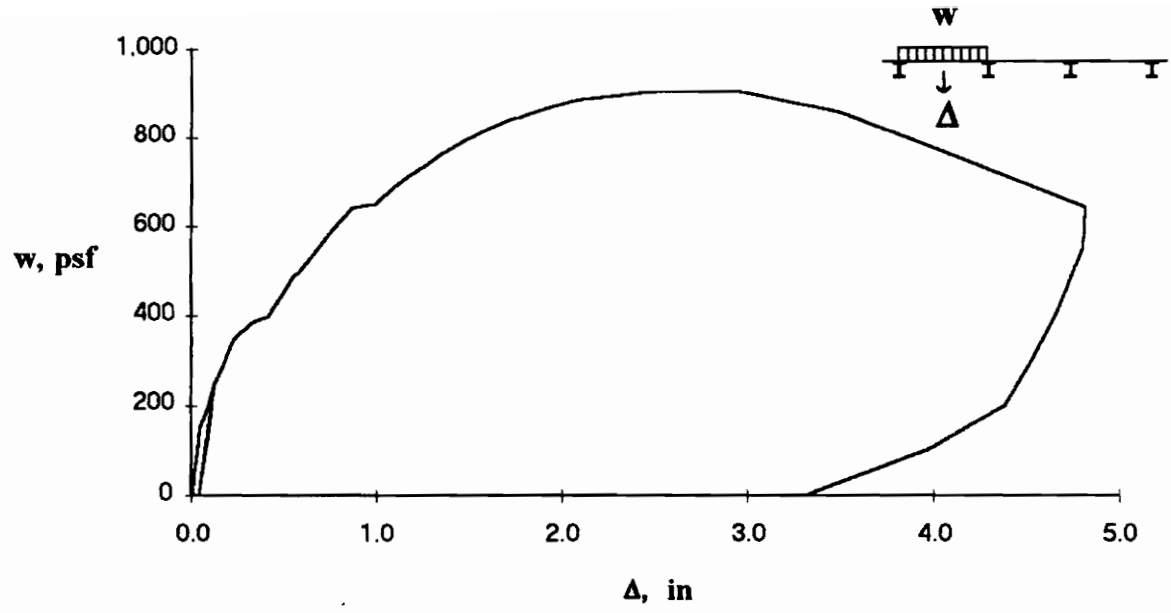

Figure 3.4 SDI-2/18-3-9 Load vs. Deflection

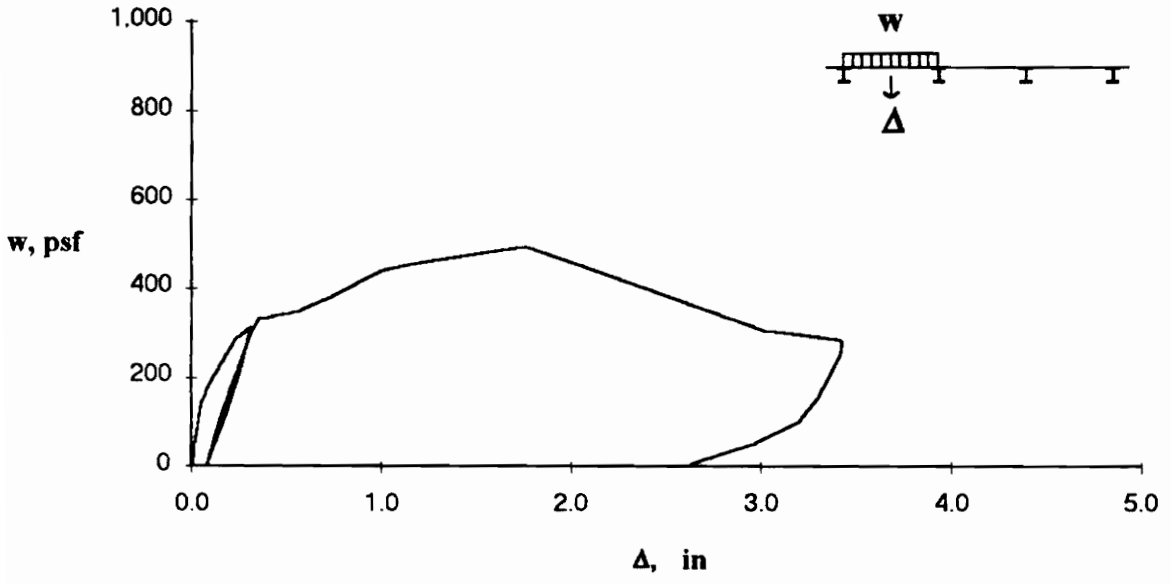

Figure 3.5 SDI-2/20-P1-9 Load vs. Deflection

over the supports. These specimens were less ductile than specimens with continuous deck.

The cold-formed angle with the return lip significantly increased the strength of specimens three and four. The end restraint provided by the angle increased the capacity of SDI-2/20-P3-9 by 20 percent over the comparable span without the angle. Similarly for SDI-2/20-PX3-9, maximum capacity was increased 32 percent.

A detailed discussion of each test follows. Note that the two lines in the following figures labeled *First Yield* and *Ultimate* are limits used in the CDDH procedure which is explained in the next chapter. Figure 3.6 through Figure 3.26 are referred to again in Chapter 5 when these limits are discussed.

3.6.1 SDI-2/20-4-9

SDI-2/20-4-9 was an end span test with four shear studs over both supports. The maximum load was 703 psf. The load at initial slip was 398 psf. The slip at maximum load was 0.15 in., and the maximum slip at the termination of the test was 0.26 in. The midspan deflection at maximum load was 2.70 in., and the maximum deflection at the termination of the test was 3.54 in. See Figure 3.6. (Note: End slip is magnified five times.) A load of 326 psf caused cracking over the interior support, and a load of 345 psf caused cracking in the positive bending region. A longitudinal crack occurred over the seam between deck panels. The concrete strain was 0.0049 in/in at maximum load. The bottom flange of the deck yielded in positive bending and at the exterior support. The top

flange of the deck yielded at the interior support. During concrete removal, deck buckling was detected behind the shear studs on the exterior support as illustrated in Figure 3.7.

3.6.2 SDI-2/20-5-9

SDI-2/20-5-9 was an end span test with five shear studs over both supports. The maximum load was 729 psf. The load at initial slip was 435 psf. The slip at maximum load was 0.11 in., and the maximum slip at the termination of the test was 0.52 in. The midspan deflection at maximum load was 2.61 in., and the maximum deflection at the termination of the test was 5.11 in. See Figure 3.8. (Note: End slip is magnified five times.) A load of 337 psf caused cracking over the interior support, and a load of 375 psf caused cracking in the positive bending region. A longitudinal crack occurred over the seam between deck panels. The concrete strain was 0.0031 in/in at maximum load. The bottom flange of the deck yielded in positive bending and at the exterior support. The top flange of the deck yielded at the interior support. Post test inspection revealed that approximately 80% of the deck surface area was debonded from the concrete. During concrete removal, deck buckling was detected behind the shear studs on the exterior support.

3.6.3 SDI-2/20-2-9

SDI-2/20-2-9 was an end span test with two shear studs over both supports. The maximum load was 597 psf. The load at initial slip was 551 psf. The slip at maximum

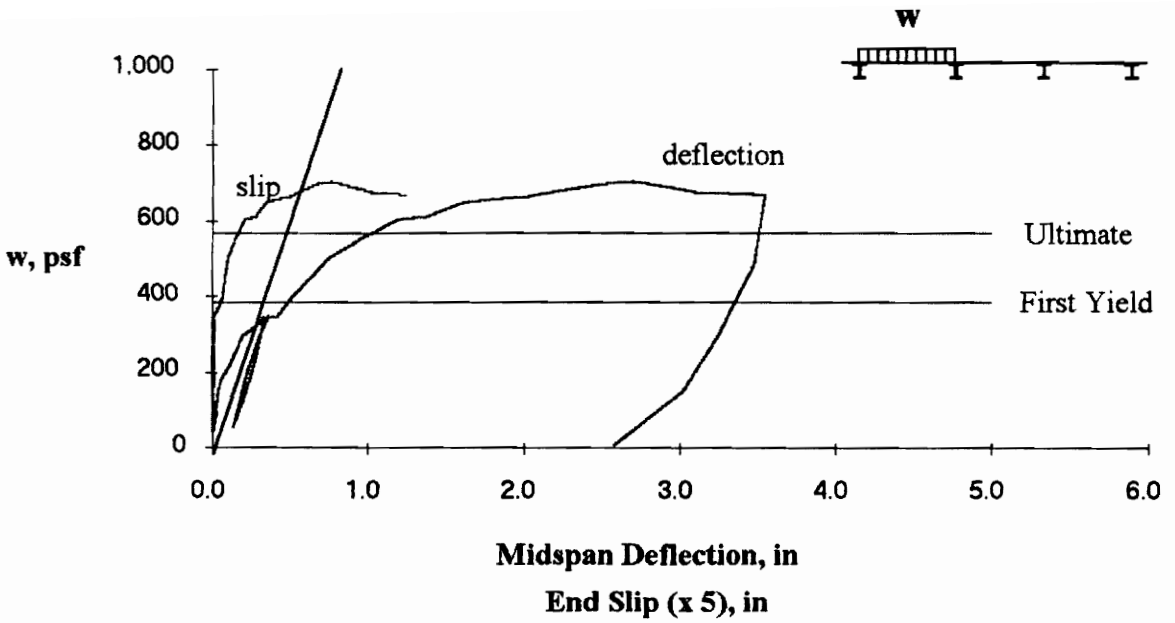

Figure 3.6 SDI-2/20-4-9 Load vs. Deflection and End Slip

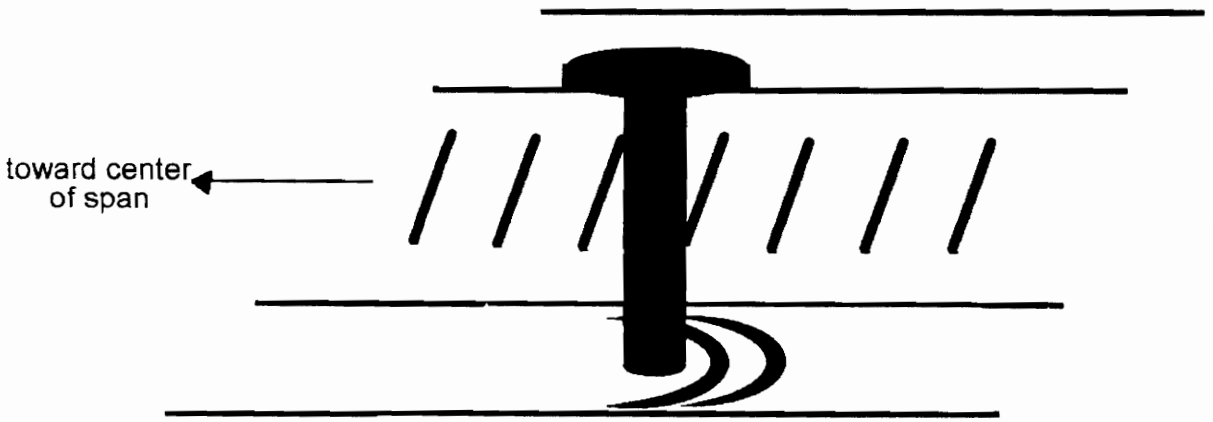

Figure 3.7 Deck Buckling Behind Stud

load was 0.06 in., and the maximum slip at the termination of the test was 0.39 in. The midspan deflection at maximum load was 2.55 in., and the maximum deflection at the termination of the test was 4.69 in. See Figure 3.9. (Note: End slip is magnified five times.) A load of 214 psf caused cracking over the interior support, and a load of 230 psf caused cracking in the positive bending region. The major crack in positive bending occurred at 3.7 ft. from the exterior support. A longitudinal crack occurred over the seam between deck panels. The concrete strain was 0.0028 in/in at maximum load. The bottom flange of the deck yielded in positive bending and at the exterior support. The top flange of the deck yielded at the interior support. During concrete removal, deck buckling was detected behind the shear studs on the exterior support.

3.6.4 SDI-2/20-23-9

SDI-2/20-23-9 was a center span test with two shear studs over one support and three shear studs over the other support. The maximum load was 598 psf. The midspan deflection at maximum load was 3.17 in., and the maximum deflection at the termination of the test was 4.58 in. See Figure 3.10. Cracks over the supports were present from prior end span tests. A load of 226 psf caused cracking in the positive bending region. The major crack in positive bending occurred at 4.6 ft. from the support.

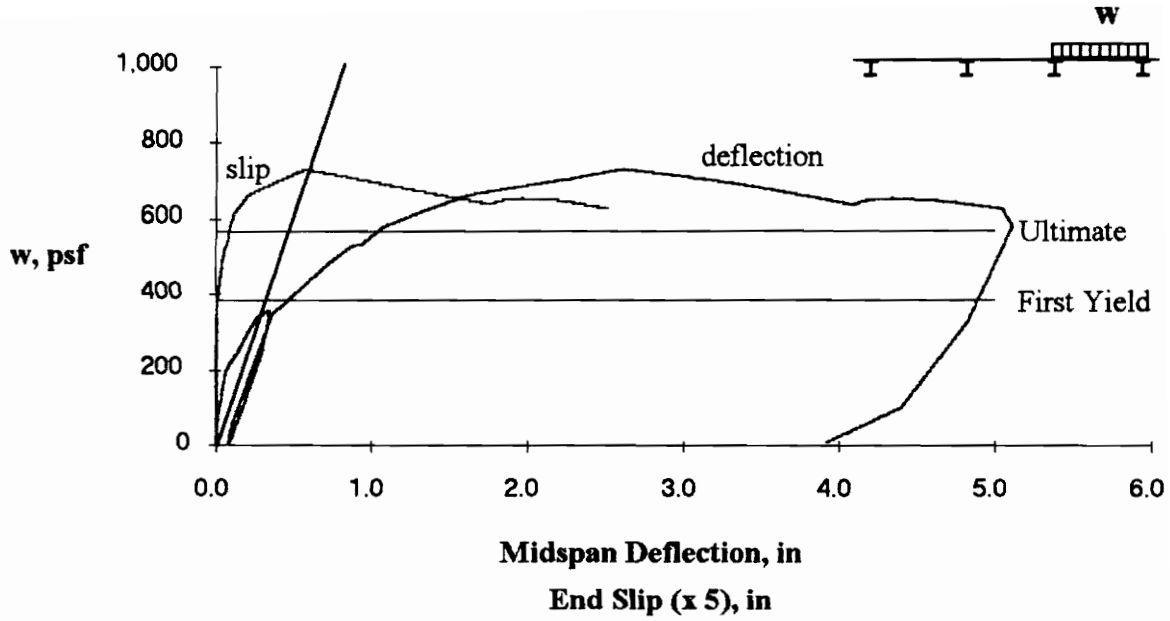

Figure 3.8 SDI-2/20-5-9 Load vs. Deflection and End Slip

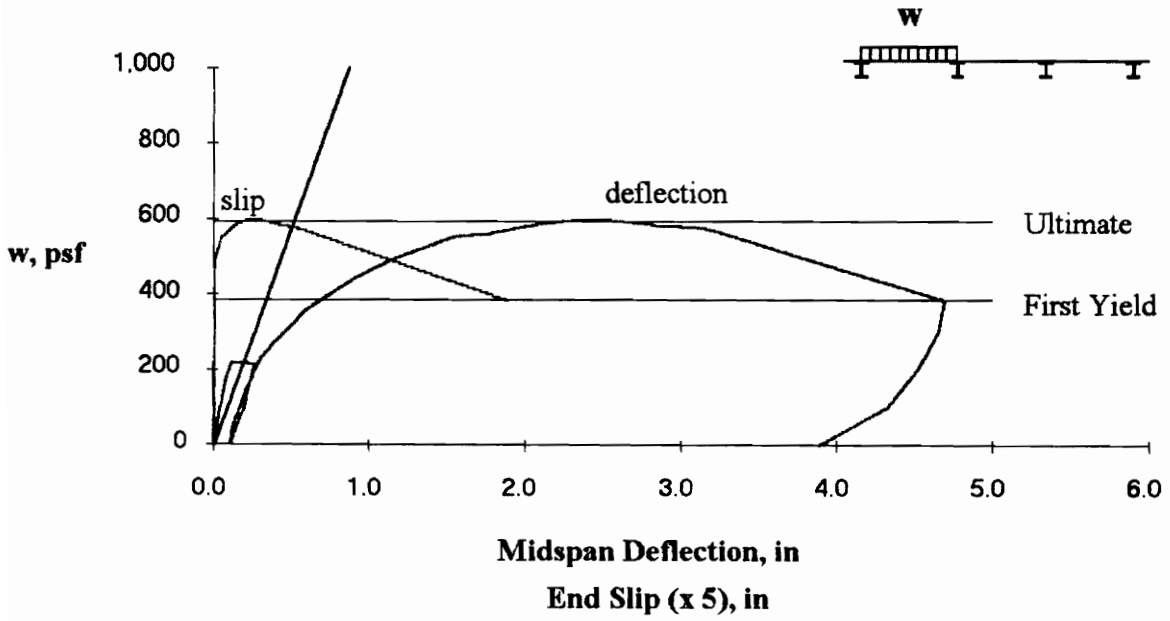

Figure 3.9 SDI-2/20-2-9 Load vs. Deflection and End Slip

3.6.5 SDI-2/20-3-9

SDI-2/20-3-9 was an end span test with three shear studs over both supports. The maximum load was 602 psf. The load at initial slip was 455 psf. The slip at maximum load was 0.12 in., and the maximum slip at the termination of the test was 0.51 in. The midspan deflection at maximum load was 2.35 in., and the maximum deflection at the termination of the test was 4.24 in. See Figure 3.11. (Note: End slip is magnified five times.) A load of 251 psf caused cracking over the interior support, and a load of 267 psf caused cracking in the positive bending region. A longitudinal crack occurred over the seam between deck panels. The concrete strain was 0.0021 in/in at maximum load. The bottom flange of the deck yielded in positive bending and at the exterior support. The top flange of the deck yielded at the interior support. During concrete removal, deck buckling was detected behind the shear studs on the exterior support.

3.6.6 SDI-2/20-P1-9

SDI-2/20-P1-9 was an end span test with arc spot welds over both supports. The maximum load was 492 psf. The load at initial slip was 349 psf. The slip at maximum load was 0.16 in., and the maximum slip at the termination of the test was 0.73 in. The midspan deflection at maximum load was 1.76 in., and the maximum deflection at the termination of the test was 3.43 in. See Figure 3.12. (Note: End slip is magnified five times.) A load of 313 psf caused cracking over the interior support, and a load of 332 psf caused cracking in the positive bending region. The major crack in positive bending

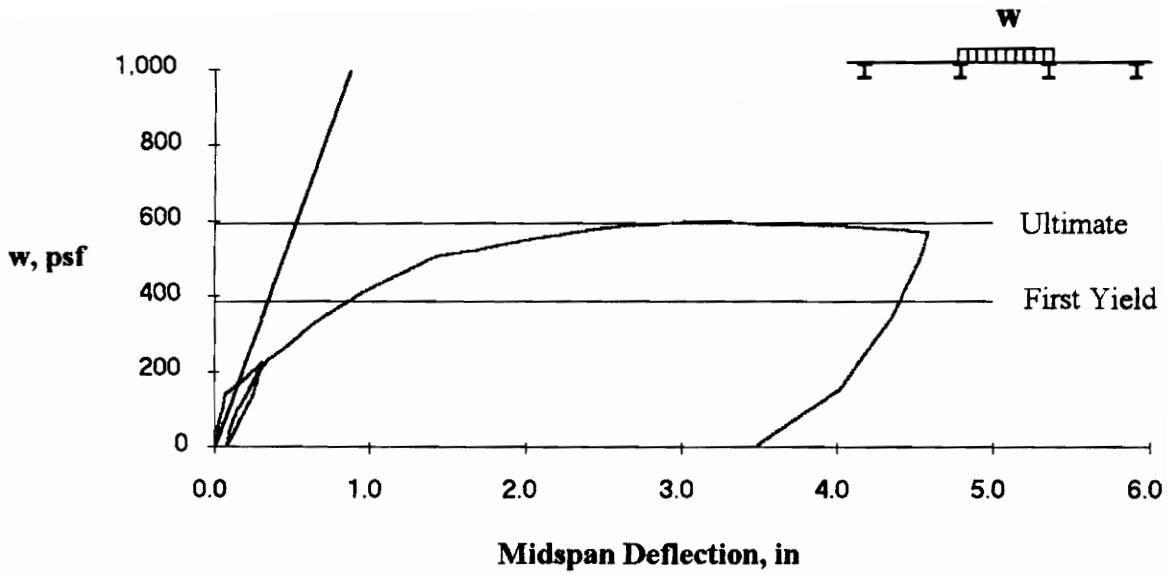

Figure 3.10 SDI-2/20-23-9 Load vs. Deflection

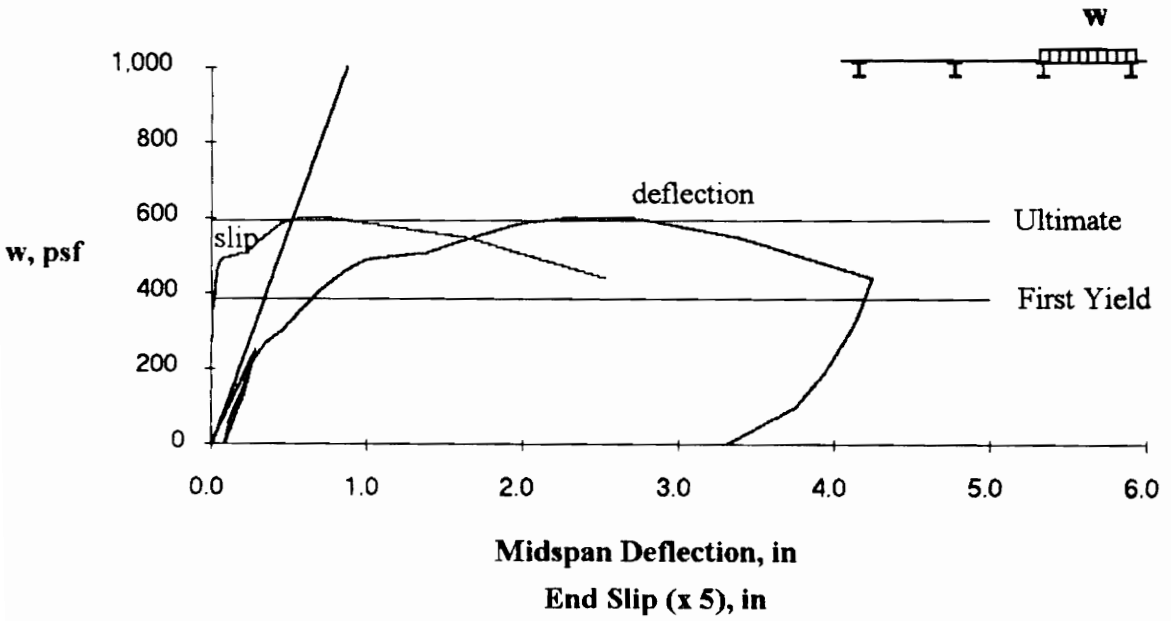

Figure 3.11 SDI-2/20-3-9 Load vs. Deflection and End Slip

occurred at 2.8 ft. from the exterior support. A longitudinal crack occurred over the seam between deck panels. The concrete strain was 0.0009 in/in at maximum load. The bottom flange of the deck yielded in positive bending. The top flange of the deck yielded at the interior support. Post test inspection revealed that approximately 85% of the deck surface area was debonded from the concrete.

3.6.7 SDI-2/20-P2-9

SDI-2/20-P2-9 was a center span test with arc spot welds over both supports. The maximum load was 598 psf. The midspan deflection at maximum load was 2.74 in., and the maximum deflection at the termination of the test was 4.32 in. See Figure 3.13. Cracks over the supports were present from prior end span tests. A load of 245 psf caused cracking in the positive bending region. The major crack in positive bending occurred at 5.0 ft. from the support. The concrete strain was 0.0022 in/in at maximum load. The bottom flange of the deck yielded in positive bending. Post test inspection revealed that approximately 85% of the deck surface area was debonded from the concrete.

3.6.8 SDI-2/20-P3-9

SDI-2/20-P3-9 was an end span test with arc spot welds over both supports and a cold-formed angle with a lip on the exterior support. The maximum load was 590 psf. The midspan deflection at maximum load was 1.69 in., and the maximum deflection at the termination of the test was 4.71 in. See Figure 3.14. A load of 234 psf caused cracking

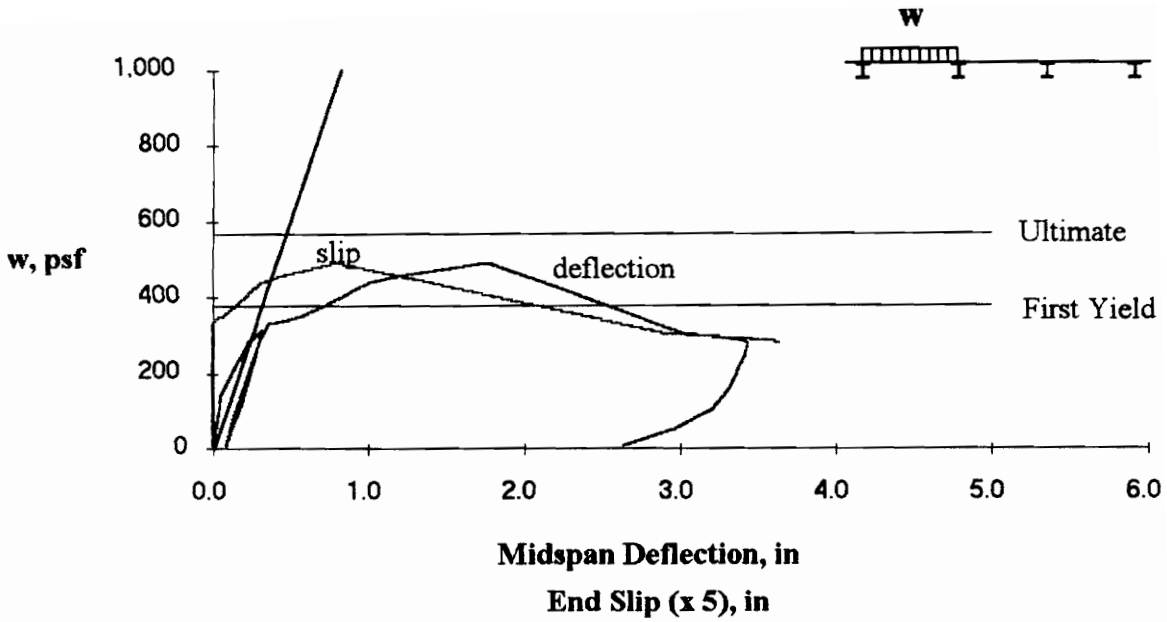

Figure 3.12 SDI-2/20-P1-9 Load vs. Deflection and End Slip

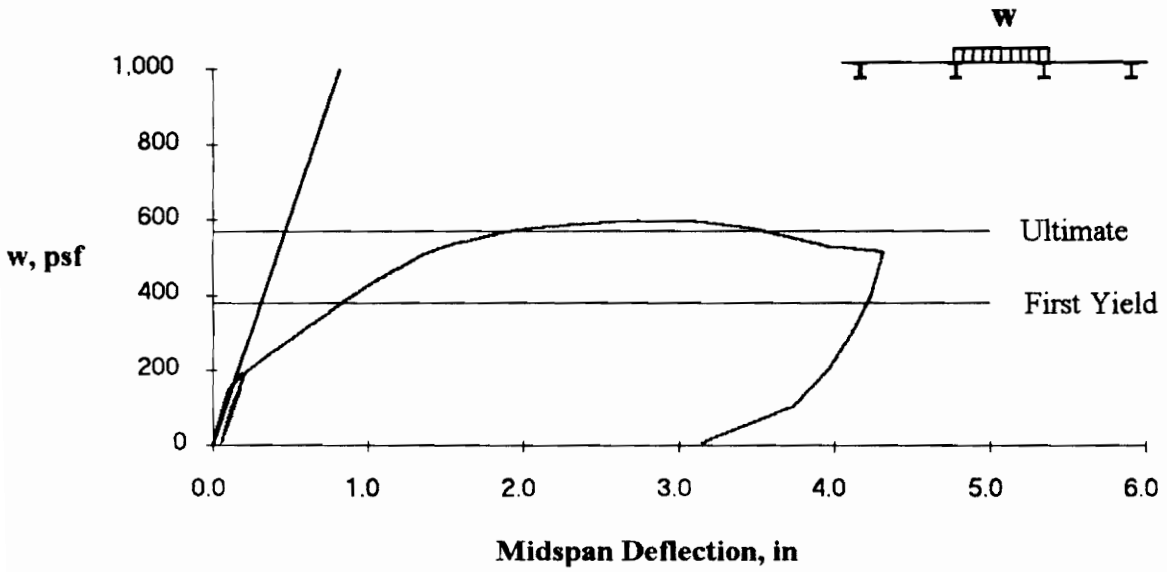

Figure 3.13 SDI-2/20-P2-9 Load vs. Deflection

over the interior support, and a load of 431 psf caused cracking in the positive bending region. The major crack in positive bending occurred at 3.6 ft. from the exterior support. The concrete strain was 0.0022 in/in at maximum load. The bottom flange of the deck yielded in positive bending. The top flange of the deck yielded at the interior support. Just prior to maximum load the horizontal leg of the cold-formed angle separated from the concrete. At 2.25 in. of deflection the welds attaching the cold-formed angle to the support failed suddenly. Midspan deflection immediately increased to over 4.0 in of deflection. Post test inspection revealed that 100% of the deck surface area was debonded from the concrete.

3.6.9 SDI-2/20-PX1-9

SDI-2/20-PX1-9 was an end span test with arc spot welds over both supports and a deck joint over the interior support. The maximum load was 369 psf. The load at initial slip was 323 psf. The slip at maximum load was 0.10 in., and the maximum slip at the termination of the test was 0.43 in. The midspan deflection at maximum load was 1.59 in., and the maximum deflection at the termination of the test was 3.13 in. See Figure 3.15. (Note: End slip is magnified five times.) A load of 239 psf caused cracking over the interior support, and a load of 318 psf caused cracking in the positive bending region. The major crack in positive bending occurred at 4.0 ft. from the exterior support. A longitudinal crack occurred over the seam between deck panels. The concrete strain was 0.0018 in/in at maximum load. The bottom flange of the deck yielded in positive bending.

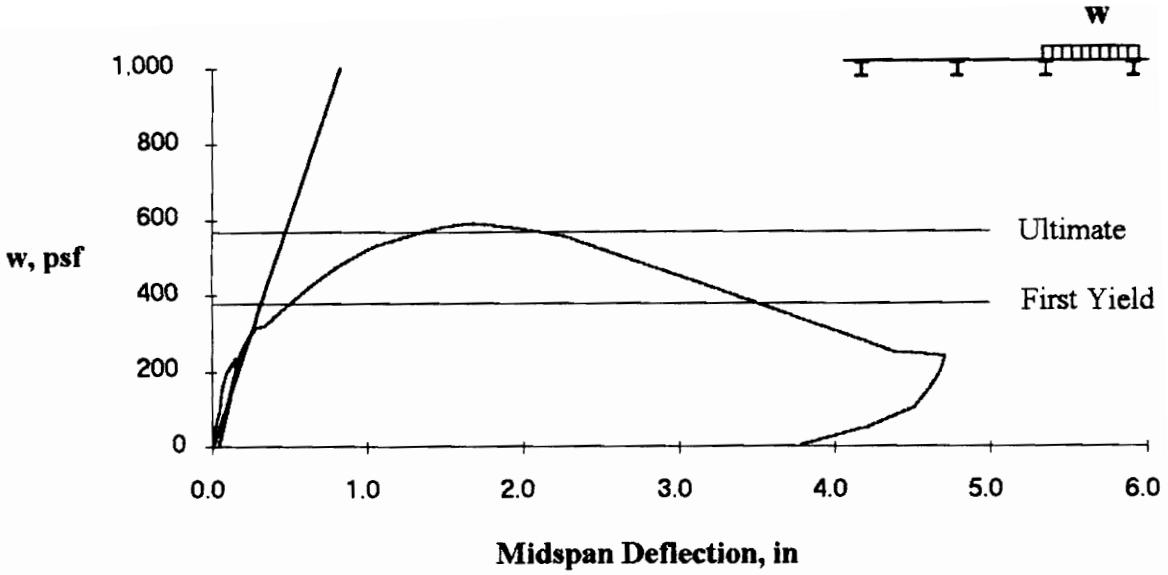

Figure 3.14 SDI-2/20-P3-9 Load vs. Deflection

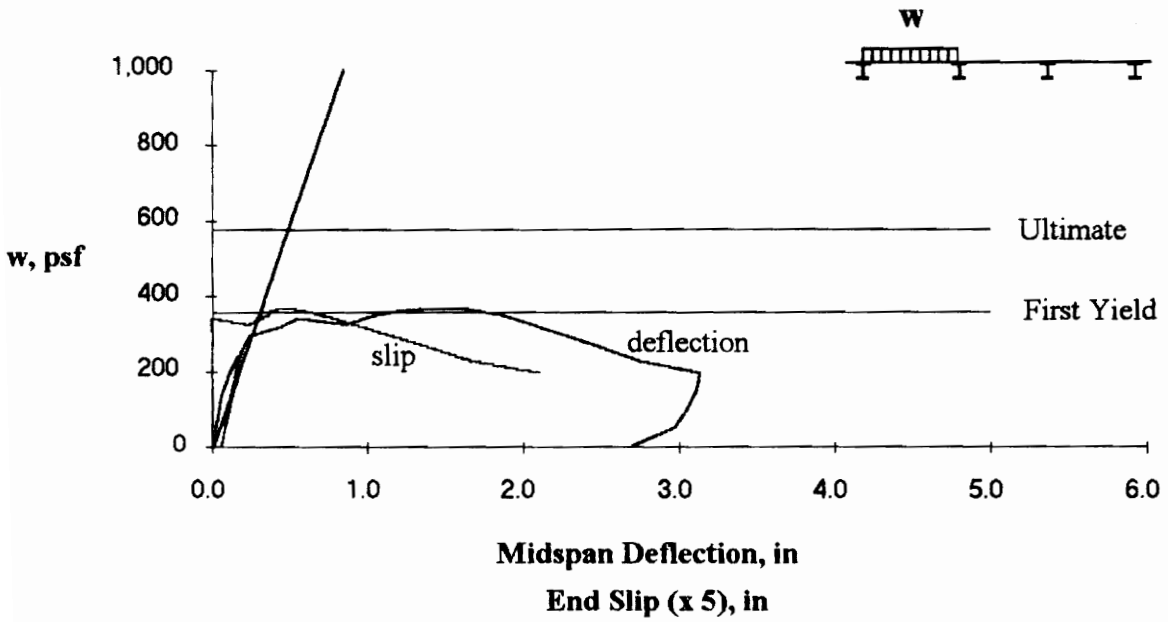

Figure 3.15 SDI-2/20-PX1-9 Load vs. Deflection and End Slip

Post test inspection revealed that approximately 75% of the deck surface area was debonded from the concrete.

3.6.10 SDI-2/20-PX2-9

SDI-2/20-PX2-9 was a center span test with arc spot welds and deck joints over both supports. The maximum load was 344 psf. The midspan deflection at maximum load was 1.82 in., and the maximum deflection at the termination of the test was 2.31 in. See Figure 3.16. Cracks over the supports were present from prior end span tests. A load of 211 psf caused cracking in the positive bending region. The major crack in positive bending occurred at 4.6 ft. from the support. The concrete strain was 0.0005 in/in at maximum load. The bottom flange of the deck yielded in positive bending. Post test inspection revealed that 100% of the deck surface area was debonded from the concrete.

3.6.11 SDI-2/20-PX3-9

SDI-2/20-PX3-9 was an end span test with arc spot welds over both supports, a deck joint over the interior support, and a cold-formed angle with a lip on the exterior support. The maximum load was 488 psf. The midspan deflection at maximum load was 1.77 in., and the maximum deflection at the termination of the test was 3.91 in. See Figure 3.17. A load of 267 psf caused cracking over the interior support, and a load of 340 psf caused cracking in the positive bending region. The major crack in positive bending occurred at 4.6 ft. from the exterior support. The concrete strain was 0.0019 in/in at

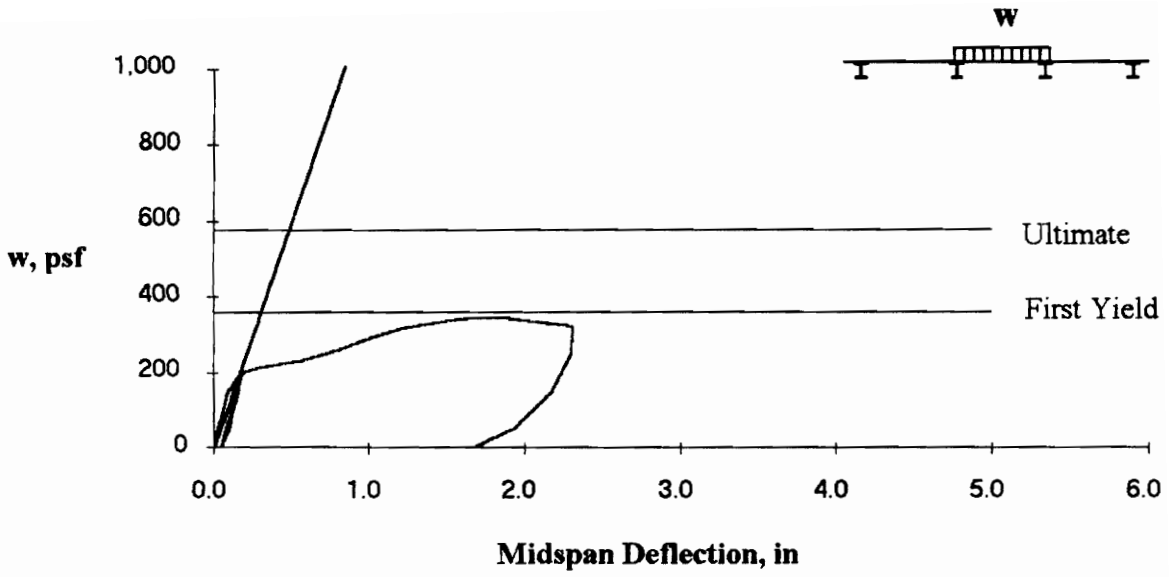

Figure 3.16 SDI-2/20-PX2-9 Load vs. Deflection

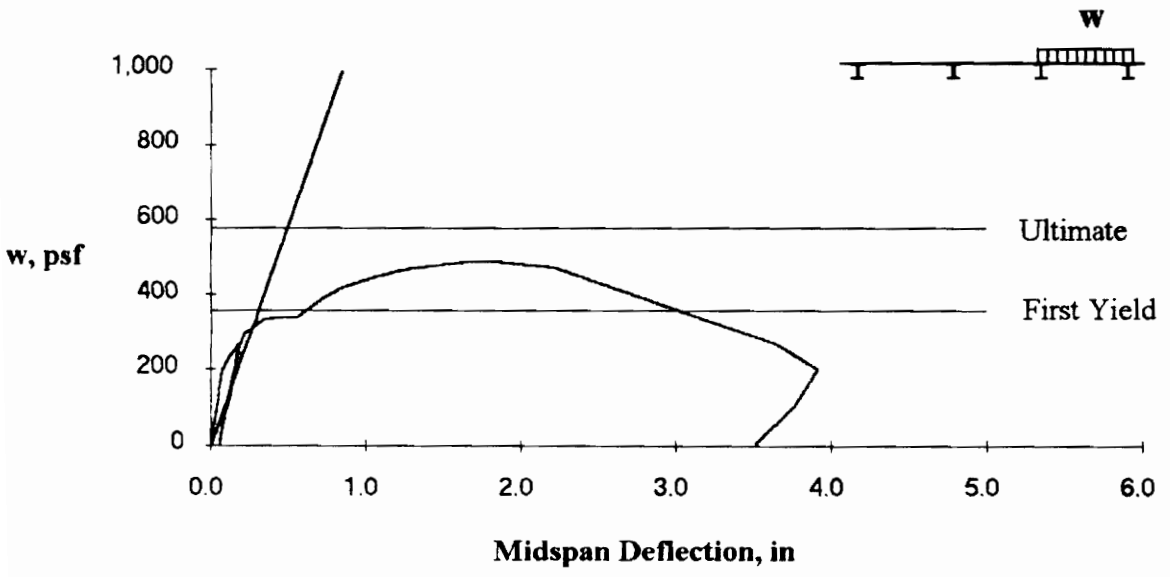

Figure 3.17 SDI-2/20-PX3-9 Load vs. Deflection

maximum load. The bottom flange of the deck yielded in positive bending. At 3.65 in. of deflection the welds attaching the cold-formed angle to the support failed. Post test inspection revealed that approximately 80% of the deck surface area was debonded from the concrete.

3.6.12 SDI-2/18-3-9

SDI-2/18-3-9 was an end span test with three shear studs over both supports. The maximum load was 903 psf. The load at initial slip was 398 psf. The slip at maximum load was 0.17 in., and the maximum slip at the termination of the test was 0.68 in. The midspan deflection at maximum load was 2.50 in., and the maximum deflection at the termination of the test was 4.82 in. See Figure 3.18. (Note: End slip is magnified five times.) A load of 197 psf caused cracking over the interior support, and a load of 383 psf caused cracking in the positive bending region. The major crack in positive bending occurred at 3.2 ft. from the exterior support. A longitudinal crack occurred over the seam between deck panels. The concrete strain was 0.0023 in/in at maximum load. The bottom flange of the deck yielded in positive bending and at the exterior support. The top flange of the deck yielded at the interior support. Post test inspection revealed that 100% of the deck surface area was debonded from the concrete. During concrete removal, deck buckling was detected behind the shear studs on the exterior support.

3.6.13 SDI-2/18-35-9

SDI-2/18-35-9 was a center span test with three shear studs over one support and five shear studs over the other. The maximum load was 891 psf. The midspan deflection at maximum load was 3.10 in., and the maximum deflection at the termination of the test was 3.95 in. See Figure 3.19. Cracks over the supports were present from prior end span tests. A load of 195 psf caused cracking in the positive bending region. The concrete strain was 0.0024 in/in at maximum load. The bottom flange of the deck yielded in positive bending. Post test inspection revealed that 100% of the deck surface area was debonded from the concrete.

3.6.14 SDI-2/18-5-9

SDI-2/18-5-9 was an end span test with five shear studs over both supports. The maximum load was 912 psf. The load at initial slip was 463 psf. The slip at maximum load was 0.21 in., and the maximum slip at the termination of the test was 0.35 in. The midspan deflection at maximum load was 2.70 in., and the maximum deflection at the termination of the test was 3.50 in. See Figure 3.20. (Note: End slip is magnified five times.) A load of 385 psf caused cracking over the interior support, and a load of 422 psf caused cracking in the positive bending region. The major crack in positive bending occurred at 3.3 ft. from the exterior support. The concrete strain was 0.0022 in/in at maximum load. The bottom flange of the deck yielded in positive bending and at the exterior support. The top flange of the deck yielded at the interior support. Post test

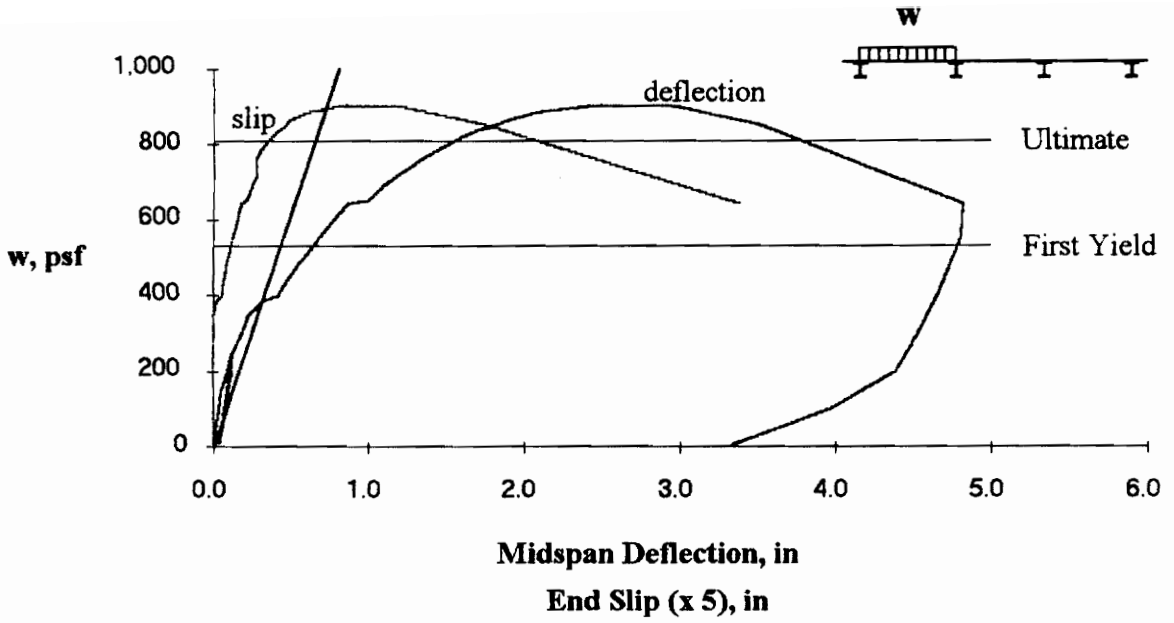

Figure 3.18 SDI-2/18-3-9 Load vs. Deflection and End Slip

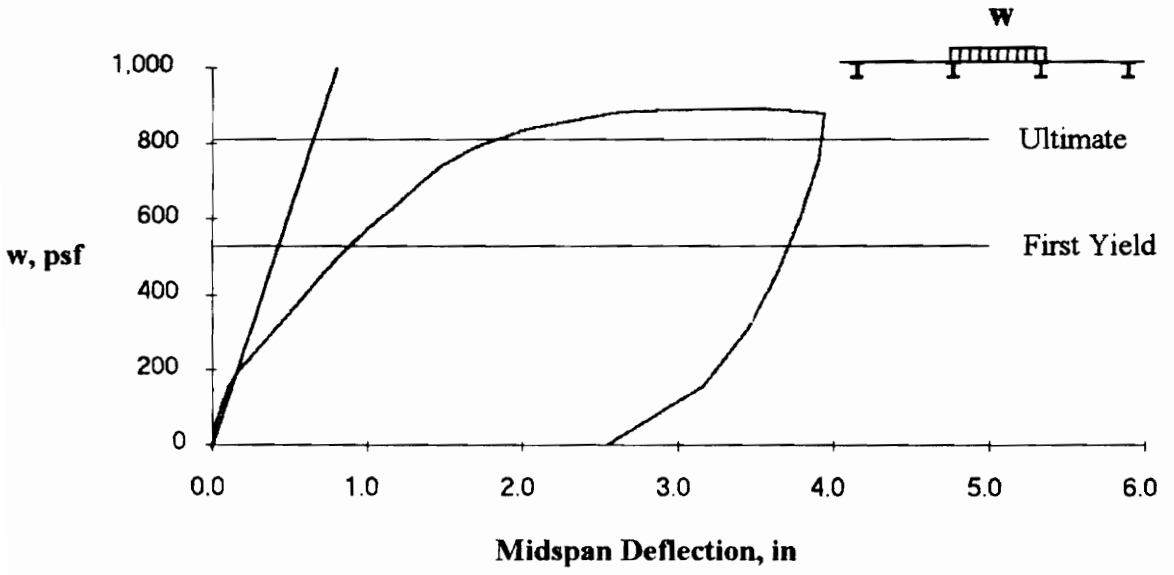

Figure 3.19 SDI-2/18-35-9 Load vs. Deflection

inspection revealed that 100% of the deck surface area was debonded from the concrete. During concrete removal, deck buckling was detected behind the shear studs on the exterior support.

3.6.15 SDI-3/20-3-10

SDI-3/20-3-10 was an end span test with three shear studs over both supports. The maximum load was 743 psf. The load at initial slip was 489 psf. The slip at maximum load was 0.12 in., and the maximum slip at the termination of the test was 0.24 in. The midspan deflection at maximum load was 2.58 in., and the maximum deflection at the termination of the test was 3.57 in. See Figure 3.21. (Note: End slip is magnified five times.) A load of 190 psf caused cracking over the interior support, and a load of 379 psf caused cracking in the positive bending region. The major crack in positive bending occurred at 3.4 ft. from the exterior support. A longitudinal crack occurred over the seam between deck panels. The concrete strain was 0.0022 in/in at maximum load. The bottom flange of the deck yielded in positive bending and at the exterior support. The top flange of the deck yielded at the interior support. Post test inspection revealed that approximately 90% of the deck surface area was debonded from the concrete. During concrete removal, deck buckling was detected behind the shear studs on the exterior support.

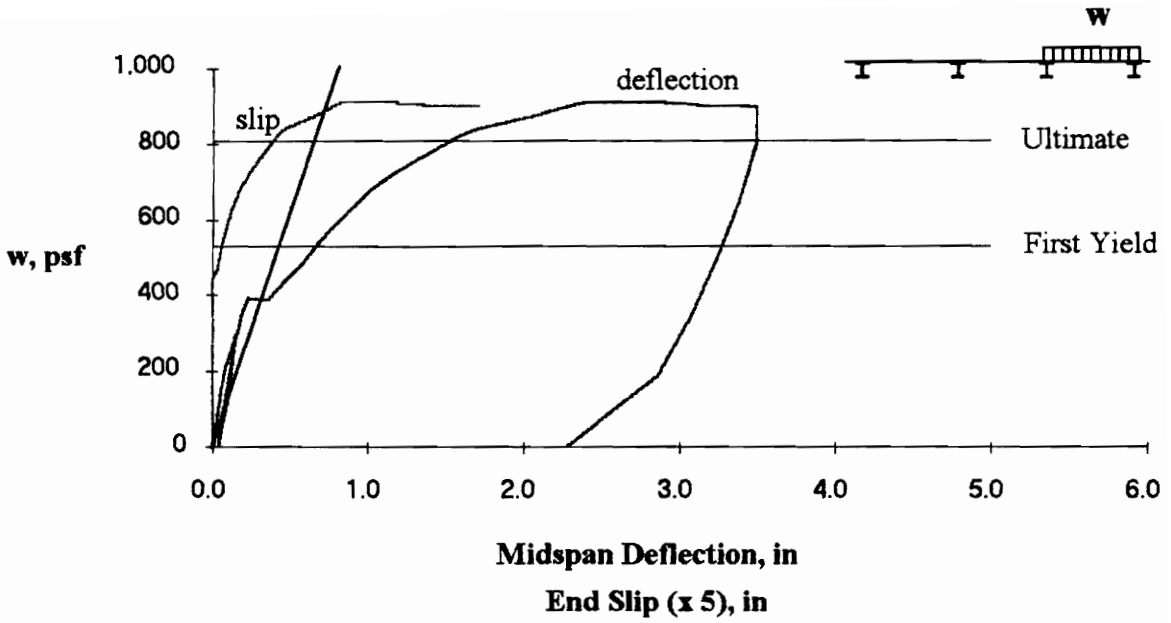

Figure 3.20 SDI-2/18-5-9 Load vs. Deflection and End Slip

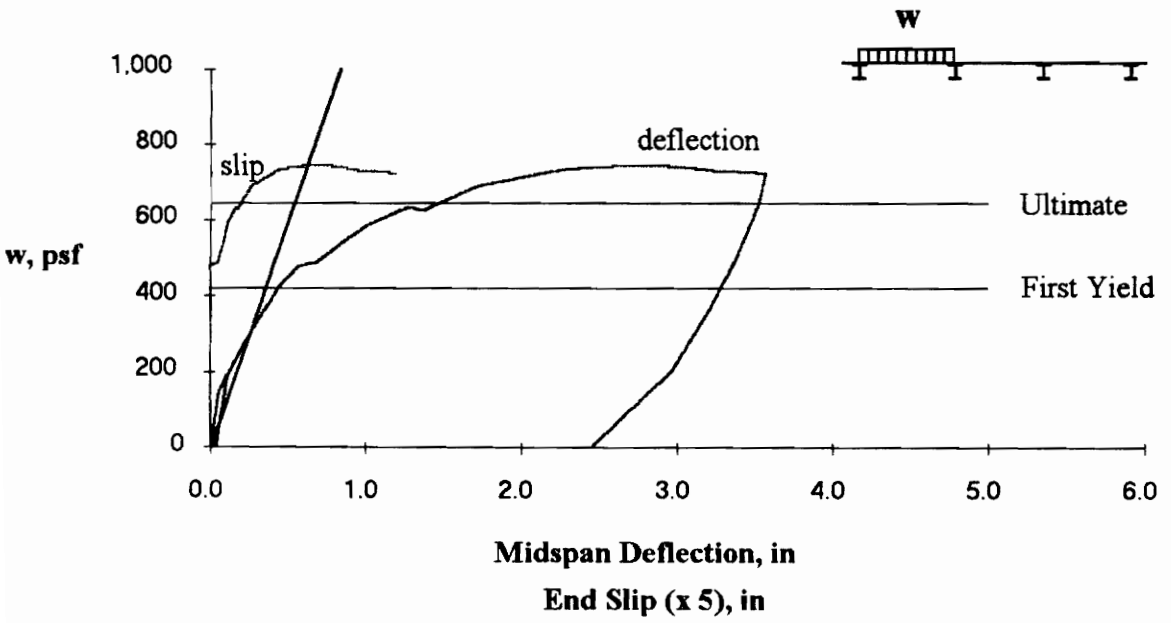

Figure 3.21 SDI-3/20-3-10 Load vs. Deflection and End Slip

3.6.16 SDI-3/20-35-10

SDI-3/20-35-10 was a center span test with three shear studs over one support and five shear studs over the other support. The maximum load was 787 psf. The midspan deflection at maximum load was 3.83 in., and the maximum deflection at the termination of the test was 4.17 in. See Figure 3.22. Cracks over the supports were present from prior end span tests. A load of 342 psf caused cracking in the positive bending region. The major crack in positive bending occurred at 5.6 ft. from the support. The concrete strain was 0.0034 in/in at maximum load. The bottom flange of the deck yielded in positive bending. Post test inspection revealed that 100% of the deck surface area was debonded from the concrete.

3.6.17 SDI-3/20-5-10

SDI-3/20-5-10 was an end span test with five shear studs over both supports. The maximum load was 891 psf. The load at initial slip was 629 psf. The slip at maximum load was 0.12 in., and the maximum slip at the termination of the test was 0.21 in. The midspan deflection at maximum load was 3.49 in., and the maximum deflection at the termination of the test was 4.24 in. See Figure 3.23. (Note: End slip is magnified five times.) A load of 285 psf caused cracking over the interior support, and a load of 494 psf caused cracking in the positive bending region. The major crack in positive bending occurred at 3.7 ft. from the exterior support. A longitudinal crack occurred over the seam between deck panels. The concrete strain was 0.0041 in/in at maximum load. The bottom

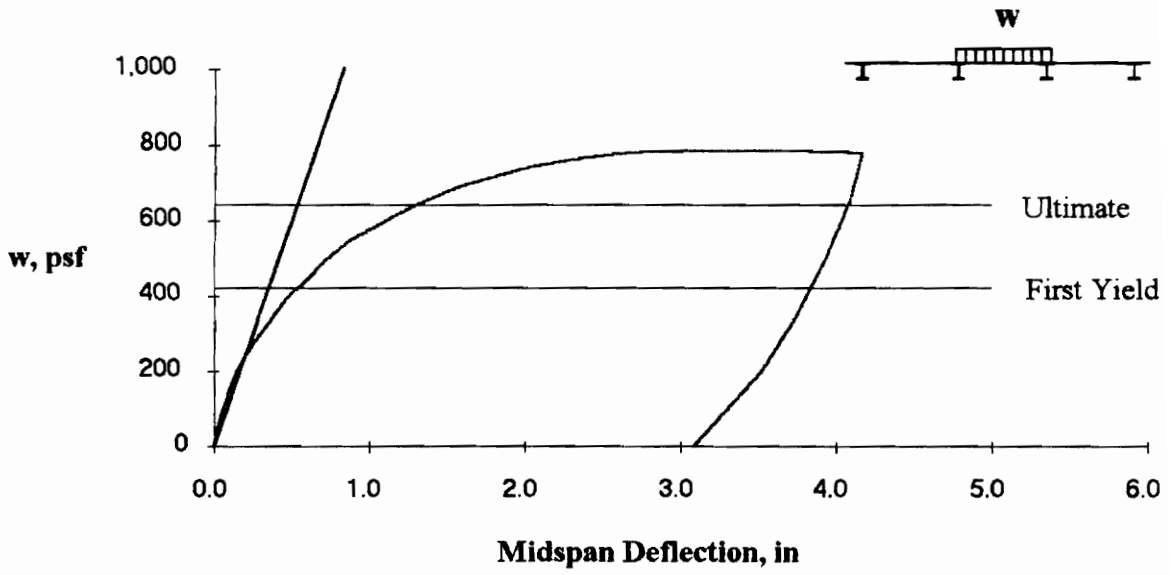

Figure 3.22 SDI-3/20-35-10 Load vs. Deflection

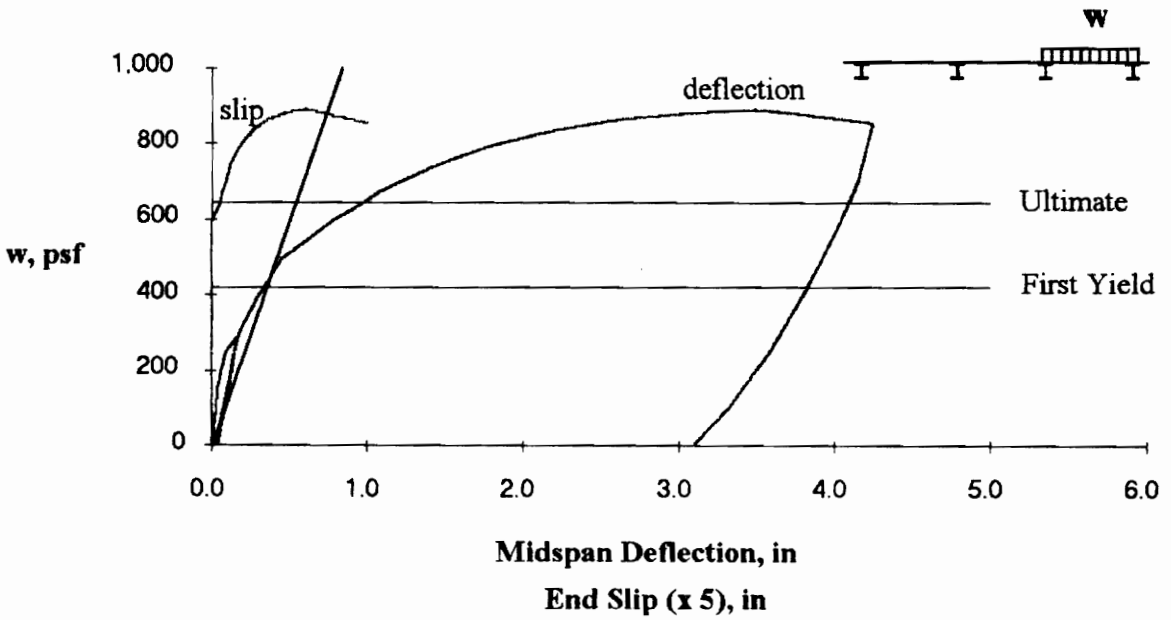

Figure 3.23 SDI-3/20-5-10 Load vs. Deflection and End Slip

flange of the deck yielded in positive bending and at the exterior support. The top flange of the deck yielded at the interior support. Post test inspection revealed that 100% of the deck surface area was debonded from the concrete. During concrete removal deck buckling was detected behind the shear studs on the exterior support.

3.6.18 SDI-3/20-PX1-10

SDI-3/20-PX1-10 was an end span test with arc spot welds over both supports and a deck joint over the interior support. The maximum load was 478 psf. Initial slip occurred at maximum load, and the maximum slip at the termination of the test was 0.56 in. The midspan deflection at maximum load was 0.60 in., and the maximum deflection at the termination of the test was 2.95 in. See Figure 3.24. (Note: End slip is magnified five times.) A load of 323 psf caused cracking over the interior support, and a load of 419 psf caused cracking in the positive bending region. The major crack in positive bending occurred at 4.3 ft. from the exterior support. The concrete strain was 0.0007 in/in at maximum load. The bottom flange of the deck yielded in positive bending. Post test inspection revealed that 100% of the deck surface area was debonded from the concrete.

3.6.19 SDI-2/18-PX3-9

SDI-2/18-PX3-9 was an end span test with arc spot welds over both supports and a deck joint over the exterior support. The maximum load was 499 psf. The load at initial slip was 412 psf. The slip at maximum load was 0.16 in., and the maximum slip at the

termination of the test was 0.72 in. The midspan deflection at maximum load was 1.57 in., and the maximum deflection at the termination of the test was 3.11 in. See Figure 3.25. (Note: End slip is magnified five times.) A load of 342 psf caused cracking over the interior support, and a load of 390 psf caused cracking in the positive bending region. The major crack in positive bending occurred at 2.5 ft. from the exterior support. A longitudinal crack occurred over the seam between deck panels. The concrete strain was 0.0013 in/in at maximum load. The bottom flange of the deck yielded in positive bending. Post test inspection revealed that 100% of the deck surface area was debonded from the concrete.

3.6.20 SDI-3/20-33-10

SDI-3/20-33-10 was a center span test with three shear studs over both supports. The maximum load was 911 psf. The midspan deflection at maximum load was 3.33 in., and the maximum deflection at the termination of the test was 4.29 in. See Figure 3.26. A load of 295 psf caused cracking over the supports, and a load of 494 psf caused cracking in the positive bending region. The major crack in positive bending occurred at 5.7 ft. from the support. The concrete strain was 0.0032 in/in at maximum load. The bottom flange of the deck yielded in positive bending. The top flange of the deck yielded at the supports. Post test inspection revealed that 100% of the deck surface area was debonded from the concrete.

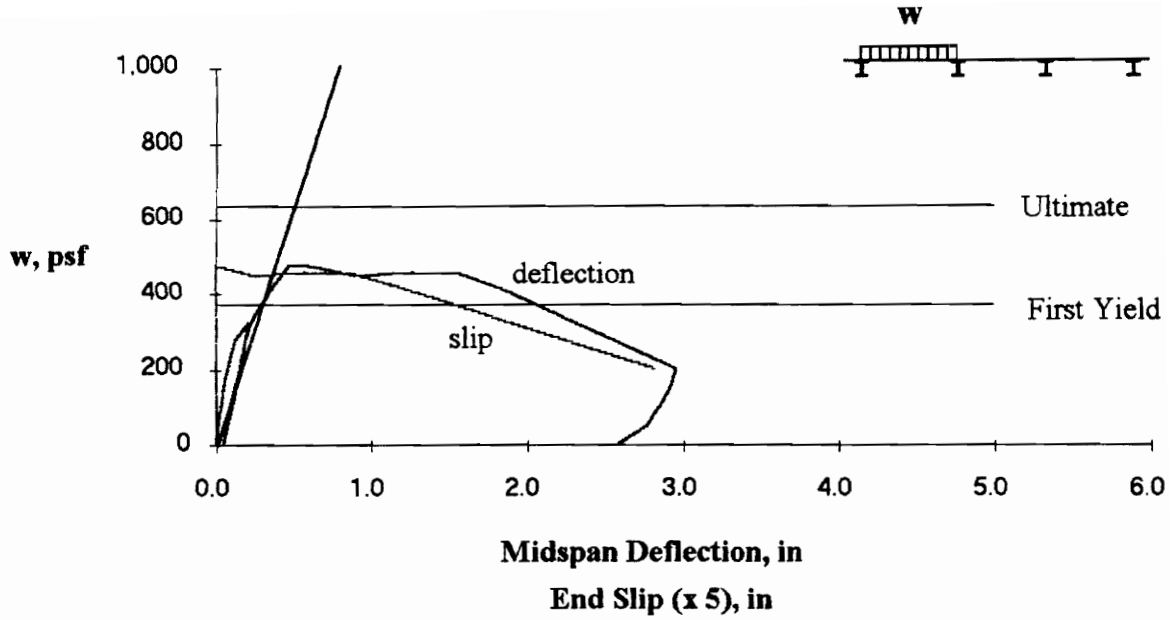

Figure 3.24 SDI-3/20-PX1-10 Load vs. Deflection and End Slip

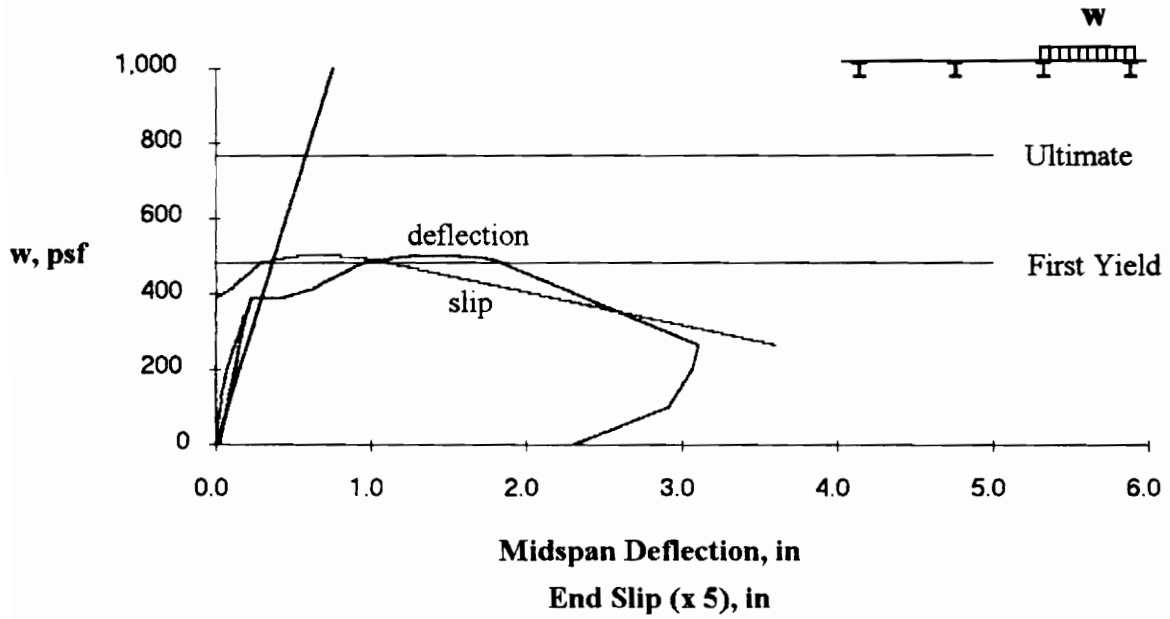

Figure 3.25 SDI-2/18-PX3-9 Load vs. Deflection and End Slip

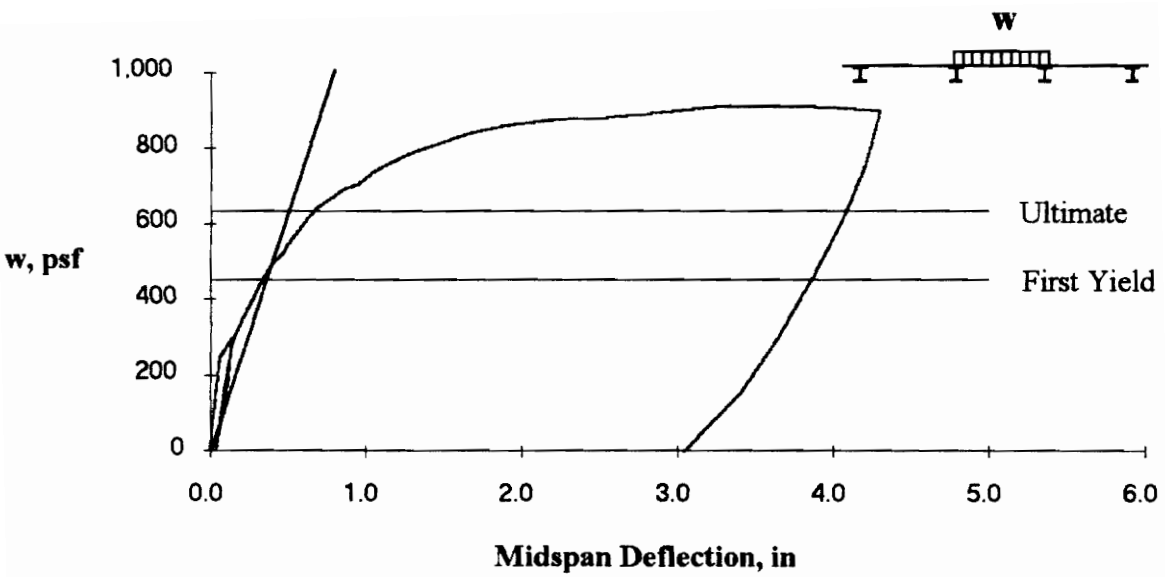

Figure 3.26 SDI-3/20-33-10 Load vs. Deflection

Chapter 4

SDI CDDH PROCEDURE

4.1 GENERAL

The Steel Deck Institute *Composite Deck Design Handbook* (SDI CDDH) (Heagler, et al. 1991) contains expressions for calculating the strength of composite slabs based on two flexural limit states, the moment at first yield of the extreme fiber and the ultimate moment capacity, assuming an under-reinforced concrete section. The CDDH is currently divided into two sections, composite slabs with and without shear studs. The following discussion of the CDDH flexural limit states will likewise be divided into these two cases.

However, the limits on maximum unshored span, allowable concrete shear stress, and maximum live load deflection are the same for slabs with studs and without studs. These limits are presented first.

The maximum unshored span is the least of:

(1) the span whose bending stress caused by concrete weight and construction loads is 0.6 times the yield strength, F_y.

(2) the span whose deflection under the uniform loading of concrete plus deck weight is span/180 or 3/4 in.

(3) the span whose support reaction is large enough to cause web crippling at the support.

Concrete shear stress is given by:

$$v = \frac{V}{A_c} \tag{4-13}$$

$v \leq 60$ psi for normal weight concrete

$v \leq 45$ psi for light weight concrete

where,

v = concrete shear stress

V = shear force at edge of clear span

A_c = concrete area able to resist vertical shear

Live load deflection is given by:

$$\Delta = \frac{0.0130 W_L L^4}{E I_{avg}} \leq \frac{span}{360} \tag{4-14}$$

where,

Δ = midspan deflection

E = modulus of elasticity of steel

I_{avg} = average of the cracked and uncracked moments of inertia of the transformed section

Live load deflection is calculated using a single span configuration even if the configuration is more than one span because negative bending reinforcement is assumed absent.

4.2 COMPOSITE SLABS WITHOUT SHEAR STUDS

The limit state for this case is the initiation of yielding at the extreme fiber of the deck bottom flange. Casting stresses in the deck due to fresh concrete are computed, accounting for deck continuity over supports where applicable, as given by:

$$f_c = \frac{C_n W_D L^2}{S_p} \qquad (4\text{-}1)$$

where,

f_c = casting stress in deck

C_n = bending coefficient for positive moment, n number of spans

C_1 = 0.018 shored

= 0.125 unshored

C_2 = 0.020 shored

= 0.070 unshored

C_3 = 0.020 shored

= 0.080 unshored

W_D = concrete and deck weight and any superimposed dead load

L = clear span between permanent supports

S_p = positive deck section modulus

The maximum superimposed live load is the least of the live loads limited by concrete shear stress, deflection, or live load stress, the latter of which is given by:

$$f_L = 0.6 F_y - f_c \tag{4-2}$$

$$f_L = \frac{0.125 W_L L^2}{S_c} \tag{4-3}$$

where,

f_L = live load stress in deck

W_L = superimposed live load

S_c = positive composite section modulus

The above stress is calculated using a single span configuration (C = 0.125) even if the configuration is more than one span because negative bending reinforcement is assumed absent.

The calculation of first-yield moment is based on a cracked section analysis. The calculations are as follows:

$$M_{et} = \left(T_1 e_1 + T_2 e_2 + T_3 e_3\right) \tag{4-4}$$

$$e_1 = e_3 - d_d \tag{4-5}$$

$$e_2 = e_3 - \frac{d_d}{2} \tag{4-6}$$

$$e_3 = h - \frac{y_{cc}}{3} \tag{4-7}$$

$$T_1 = f_{yc}\left(B_t\ t\right)\left[\frac{h - y_{cc} - d_d}{h - y_{cc}}\right] \tag{4-8}$$

$$T_2 = f_{yc}\left(2\,D_w\ t\right)\left[\frac{h - y_{cc} - \frac{d_d}{2}}{h - y_{cc}}\right] \tag{4-9}$$

$$T_3 = f_{yc}\left(B_b\ t\right) \tag{4-10}$$

$$f_{yc} = F_y - f_c \tag{4-11}$$

$$y_{cc} = d\left\{\left[2\,\rho n + \left(\rho n\right)^2\right]^{0.5} - \rho n\right\} \tag{4-12}$$

where,

M_{et} = first yield moment per unit width

f_{yc} = yield stress corrected for stresses due to casting

f_c = casting stress in deck

ρ = reinforcement ratio, $A_s/(bd)$

n = modular ratio, E_s/E_c

All other variables are forces and dimensions illustrated in Figure 4.1. Based on prior test observations there is a 10 percent increase in capacity permitted if welded wire fabric is present in the slab (*Standard for* 1993, Porter and Ekberg 1977).

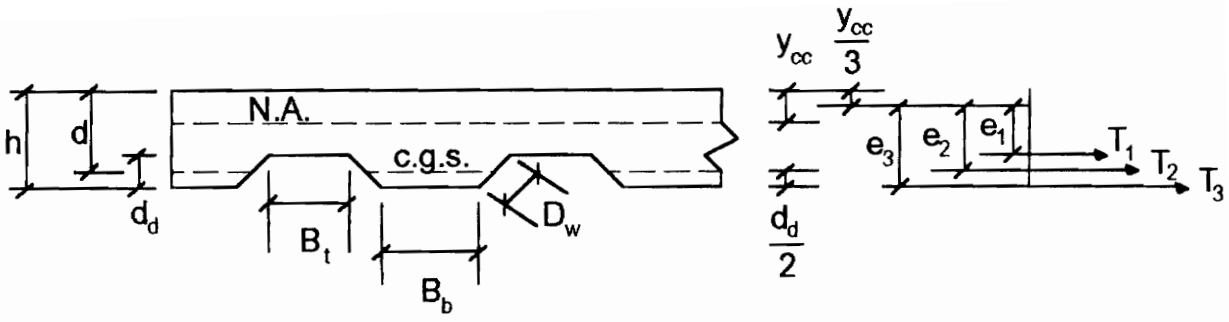

Figure 4.1 Deck Cross Section and Force Locations (*Standard for* 1993)

4.3 COMPOSITE SLABS WITH SHEAR STUDS

The limit state for this case is yielding of the entire deck cross section. The factored ultimate moment capacity per unit width of slab is calculated by the following expression:

$$\phi M_n = \phi A_s F_y (d - \frac{a}{2}) \qquad (4\text{-}15)$$

where,

ϕ = reduction factor, 0.85

M_n = nominal moment capacity per unit width

A_s = steel deck area per unit width

F_y = steel yield stress

d = distance from top of slab to centroid of steel deck

a = depth of compressive stress block, $A_sF_y/(0.85f'_cb)$

The maximum superimposed live load is the least of the live loads limited by concrete shear stress, deflection, or ultimate moment capacity, the latter of which is given by:

$$\phi M_n = 0.125 (1.6 W_L + 1.2 W_D) L^2 \quad (4\text{-}16)$$

where,

W_L = superimposed live load

W_D = concrete and deck weight and any superimposed dead load

L = clear span between permanent supports

A 10 percent increase in capacity is permitted if welded wire fabric is present in the slab.

If the anchorage force provided by the shear studs is adequate the deck cross section will yield and the superimposed live load is computed according to Eq. 4-16. The required anchorage force per unit width is computed by:

$$F = F_y \left(A_s - \frac{A_{webs}}{2} - A_{bf} \right) \quad (4\text{-}17)$$

where,

F = required anchorage force per unit width

A_{webs} = area of deck webs per unit width

A_{bf} = area of deck bottom flange per unit width

The available anchorage force per stud is given by Eq. I5-1 in the American Institute of Steel Construction Specification (*Load and* 1993) for nominal stud strength:

$$Q_n = 0.5 A_{sc} \sqrt{f'_c E_c} \leq A_{sc} F_u \quad (4\text{-}18)$$

where,

Q_n = nominal stud strength

A_{sc} = cross sectional area of shear stud

f'_c = compressive strength of concrete

E_c = modulus of elasticity of concrete

F_u = tensile stress of shear stud material

A strength reduction factor, Eq. I3-1 (*Load* and 1993), is applied to Q_n if the following equation applies (for deck ribs oriented perpendicular to beams):

$$\frac{0.85}{\sqrt{N_r}}\left(\frac{w_r}{h_r}\right)\left[\left(\frac{H_s}{h_r}\right) - 1.0\right] \leq 1.0 \qquad (4\text{-}19)$$

where,

N_r = number of studs in one rib

w_r = average width of concrete rib

h_r = nominal rib height

H_s = length of stud after welding

The following reduction factor, R, is applied to the nominal moment capacity of Eq 4-16 if the available anchorage force (Eq. 4-18) is less than the required (Eq. 4-17):

$$R = \frac{N_r Q_n}{F} \leq 1.0 \qquad (4\text{-}20)$$

The lower limit on this reduction is the moment calculated at first yield given in Eq. 4-4. R is essentially a measure of the degree of composite action.

Figure 4.2 graphically illustrates the limit states considered in the SDI CDDH. Line $\overline{AB}$ represents the limit state for slabs without studs, the first yield moment. Line $\overline{CE}$ represents the limit state for slabs with studs. The line $\overline{CD}$ illustrates the use of the reduction factor, R, for partial anchorage. The line $\overline{DE}$ is the nominal moment capacity for a composite slab with full anchorage.

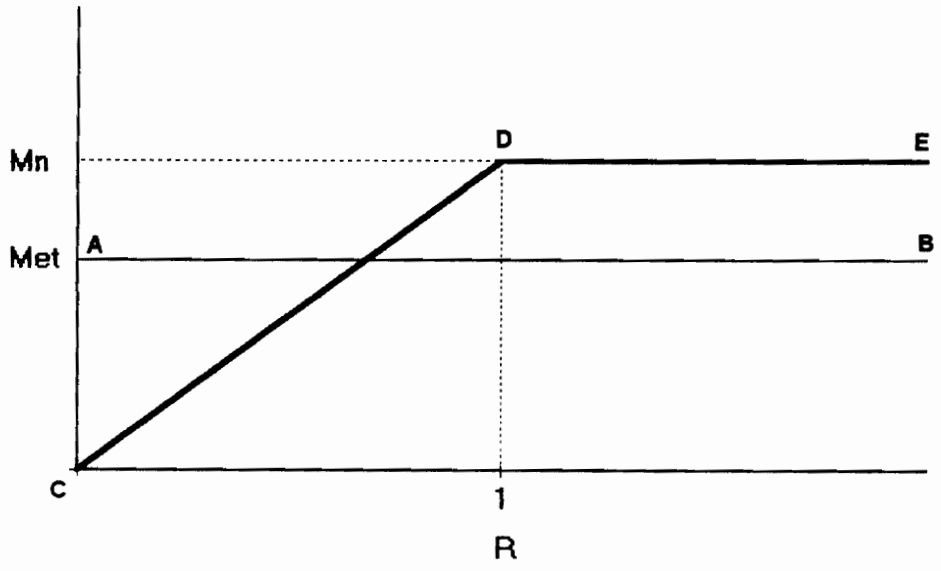

Figure 4.2 SDI CDDH Limit States

Chapter 5

EVALUATION OF RESULTS

5.1 COMPARISON OF EXPERIMENTAL DATA WITH CDDH PROCEDURE

In this chapter, the test results presented in Chapter 3 will be analyzed and compared to the results predicted using the CDDH procedure. A comparison of observed strengths and predicted strengths is given in Table 5.1 and illustrated in Figure 5.1. Strengths of the composite slabs are given in terms of the maximum moment produced at midspan assuming simple supports. The observed test moment is given as M_t. The predicted first-yield moment is given as M_{el}, and the predicted moment based on the under-reinforced flexural strength of the section is given as M_n. (Note that all calculations are based on measured material properties for comparisons with test results.) The calculation of M_n assumes the entire cross section of the steel deck at the location of maximum moment has yielded. These calculations are described in Chapter 4.

Figure 5.1 is normalized to the predicted moment, M_n, which varies for each specimen according to deck geometry, steel yield strain, and concrete strength. The two

Table 5.1 Comparison of Experimental and Analytical Results

Test Number	Test Designation	Mt (ft-k)	Met (ft-k)	Mn (ft-k)	Mt / Met	Mt / Mn
1	SDI-2/20-4-9	42.7	23.2	34.4		1.24
2	SDI-2/20-5-9	44.3	23.2	34.4		1.29
3	SDI-2/20-2-9	36.3	23.6	36.0		1.01
4	SDI-2/20-23-9	36.3	23.6	36.0		1.01
5	SDI-2/20-3-9	36.6	23.6	36.0		1.01
6	SDI-2/20-PI-9	29.9	22.9	34.6	1.30	
7	SDI-2/20-P2-9	36.3	22.9	34.6	1.58	1.05
8	SDI-2/20-P3-9	35.8	22.9	34.6	1.56	1.04
9	SDI-2/20-PX1-9	22.4	21.8	35.1	1.03	
10	SDI-2/20-PX2-9	20.9	21.8	35.1	0.96	
11	SDI-2/20-PX3-9	29.7	21.8	35.1	1.36	
12	SDI-2/18-3-9	54.9	32.2	49.2		1.11
13	SDI-2/18-35-9	54.1	32.2	49.2		1.10
14	SDI-2/18-5-9	55.4	32.2	49.2		1.13
15	SDI-3/20-3-10	55.7	31.7	48.3		1.15
16	SDI-3/20-35-10	59.0	31.7	48.3		1.22
17	SDI-3/20-5-10	66.8	31.7	48.3		1.38
18	SDI-3/20-PX1-10	35.9	27.9	47.7	1.29	
19	SDI-2/18-PX3-9	30.3	29.3	46.5	1.03	
20	SDI-3/20-33-10	68.3	33.8	47.4		1.44

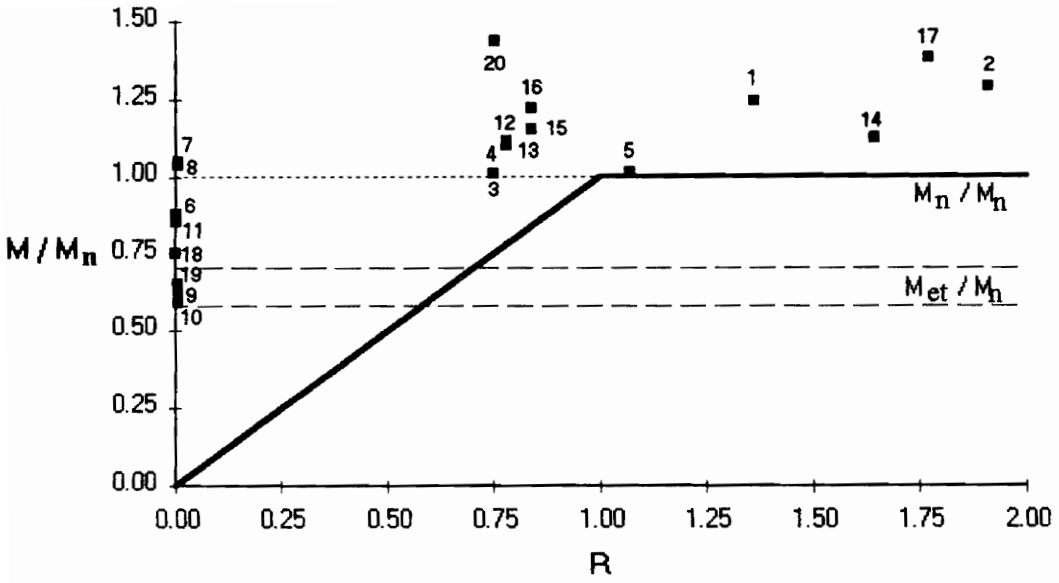

Figure 5.1 Comparison of Experimental and Analytical Results

dashed lines indicate the range of first-yield moment ratios for all specimens. The ratio of M_{et} to M_n varies between 0.58 and 0.71. Moment ratios are plotted versus the stud reduction factor, R, for the test. For specimens without studs R = 0. Under the current SDI CDDH procedure the line from the origin to the intersection of M_n represents the predicted strength of composite slabs with less than 100 percent anchorage ($R \leq 1$).

The test moment, M_t, for specimens without studs exceeded the first-yield moment in all but one case, SDI-2/20-PX2-9. The M_t to M_{et} ratio for this test was 0.96. If this span had been tested first rather than after the two end spans it is believed that this ratio would have been above 1.0. This conclusion is based on the comparison of tests 16 and 20. Essentially the same specimen, with the exception of two additional studs on one support of test 16, test 20 supported approximately 15 percent more load than test 16. This increase is attributed to the fact that test 20 was not tested subsequent to end span tests. SDI-2/20-P2-9, a center span, and SDI-2/20-P3-9, which has end restraint from a cold-formed angle with the return lip, slightly exceeded the moment M_n as well.

The test moment, M_t, exceeded the calculated moment M_n in all the tests where studs were present, tests 1-5, 12-17, and 20. However, the entire cross section of the steel deck did not yield in any of the tests as is assumed in the computation of the nominal moment, M_n. This suggests that the shear studs as well as the continuity of the deck over the supports provided some rotational restraint at the supports, and the assumption of simply supported boundary conditions was not entirely accurate.

A series of strain gages was placed close to the exterior and interior supports in order to estimate the force in the deck at the supports. Plots of all the strain data collected during testing are provided in Appendix A. The strains in the top and the bottom flange of the deck were averaged to eliminate the effects of bending. From this average strain across the deck, the stress and the resultant axial force in the deck were calculated. These forces are given in Table 5.2 through Table 5.5. The tests are not considered all together but rather in groups as the table headings suggest.

The forces in the deck of end span tests with shear studs are given in Table 5.2. The CDDH required anchorage force, F, is also given. The CDDH equation for F is based on the assumption that the mechanical interlocking capability of the deck profile and the deck anchorage provided by welds are sufficient to achieve the first-yield moment of the composite slab. The required anchorage force is the force that must be developed in the deck by the studs in order for the slab to achieve the ultimate moment strength, M_n.

The required anchorage force and the existing force in the deck can not be compared directly. Knowledge of the shear connection performance of each profile is necessary to evaluate the anchorage provided solely by the stud. Such information could be obtained from elemental tests, for example, the slip block test. Therefore, only general observations will be made concerning the forces in the deck at the supports.

(1) Shear studs significantly increase the force developed in the deck at the supports of end spans and center spans.

Table 5.2 Deck Forces in End Spans

Test Designation	Support Anchorage	Axial Force in Deck: Exterior Support (k / ft)	Axial Force in Deck: Interior Support (k / ft)	F (k / ft)	Mt / Mn
SDI-2/20-PI-9	welds	4.8	9.0	11.8	0.86
SDI-2/20-2-9	2 studs	13.8	13.8	11.8	1.01
SDI-2/20-3-9	3 studs	12.9	14.5	11.8	1.01
SDI-2/18-3-9	3 studs	16.2	19.4	16.2	1.11
SDI-3/20-3-10	3 studs	14.8	17.1	14.3	1.15
SDI-2/20-4-9	4 studs	16.1	15.1	11.8	1.24
SDI-2/20-5-9	5 studs	20.0	19.2	11.8	1.29
SDI-2/18-5-9	5 studs	23.0	17.1	16.2	1.13
SDI-3/20-5-10	5 studs	25.0	24.5	14.3	1.38

Table 5.3 Deck Forces in Center Spans

Test Designation	Support Anchorage: Left	Support Anchorage: Right	Deck	Axial Force in Deck: Left Support (k / ft)	Axial Force in Deck: Right Support (k / ft)
SDI-2/20-PX2-9	welds	welds	butted	2.1	1.7
SDI-2/20-P2-9	welds	welds	continuous	5.8	5.8
SDI-2/18-35-9	3 studs	5 studs	continuous	8.0	5.9
SDI-3/20-35-10	3 studs	5 studs	continuous	12.1	11.9
SDI-3/20-33-10	3 studs	3 studs	continuous	25.9	25.9

Table 5.4 Deck Forces in Slabs with Butted Deck

Test Designation	Deck	Axial Force in Deck	
		Exterior Support (k / ft)	Interior Support (k / ft)
SDI-2/20-PI-9	continuous	4.8	9.0
SDI-2/20-PXI-9	butted	3.0	4.7
SDI-2/18-PX3-9	butted	4.5	8.2
SDI-3/20-PX1-10	butted	4.3	6.5

Table 5.5 Deck Forces in Slabs with Angles

Test Designation	Deck	Axial Force in Deck	
		Exterior Support (k / ft)	Interior Support (k / ft)
SDI-2/20-PI-9	continuous	4.8	9.0
SDI-2/20-P3-9	continuous	8.0	11.2
SDI-2/20-PX1-9	butted	3.0	4.7
SDI-2/20-PX3-9	butted	7.3	6.2

(2) The forces in the deck of slabs with butted joints are less than the forces in the deck of slabs with continuous deck.

(3) The cold-formed angle with a lip significantly increased the force in the deck at the exterior support.

5.2 Suggested Modifications to CDDH Procedure

The results of this study support the use of simple reinforced concrete models for determining the strength of composite floor slabs. The results also suggest that a single unified method can be developed to predict the strength of composite floors regardless of the type or degree of anchorage. Figure 5.1 illustrates the current SDI approach to predicting the strength of floors with less than 100% anchorage. The reduction factor, R, applied to the nominal moment capacity, M_n, results in a line from the origin to the intersection of the nominal moment line at R = 1. The test results from this study are well above this line.

In order to have a single unified method for predicting strength, regardless of the type of anchorage over the supports, an available anchorage force per arc spot weld must be calculated as is done for each stud in slabs with studs. An arc spot weld strength, P_n, can be calculated using Eqs. E2.2-1 through E2.2-4 in the American Iron and Steel Institute Cold-Formed LRFD Specification (*Load and* 1991). The anchorage force provided by the arc spot welds is less than the force needed to develop the moment, M_n.

Therefore, a reduction factor, R, is computed similar to Eq. 4-20

$$R = \frac{N_r P_n}{F} \leq 1.0 \qquad (5\text{-}1)$$

where N_r = number of welds per rib. The values of R plotted on the x-axis of Figure 5.2 are given in Table 5.6 along with the required anchorage forces, F, and the anchorage provided per stud, Q_n, or per weld, P_n used to compute R.

Figure 5.2 illustrates the suggested modifications to the CDDH method. Test results suggest that floors with studs that provide less than 100 percent anchorage and floors with arc spot welds over the supports have a strength at least equal to the strength required to develop the first-yield moment of the slab. Therefore, the line predicting the strength of slabs with less than 100 percent anchorage should be shifted from the origin, or the point of zero moment, to the first-yield moment. In Figure 5.2 the two lines from the vertical axis to the intersection of the nominal moment line at R = 1 indicate a range for all specimens tested.

Three tests fell outside this range (9, 10, and 19). These specimens had butted joints and arc spot welds over the supports essentially resembling a single span rather than a multispan configuration. If the suggested reduction factor, $\phi = 0.50$, (*Load and* 1991) is applied to the arc spot weld strength, P_n, these data points shift to the left, and fall within or very close to the allowable range. However, it is recommended that M_{ct} be used as the maximum strength for single span deck configurations even if the calculation procedure predicts a slightly higher strength.

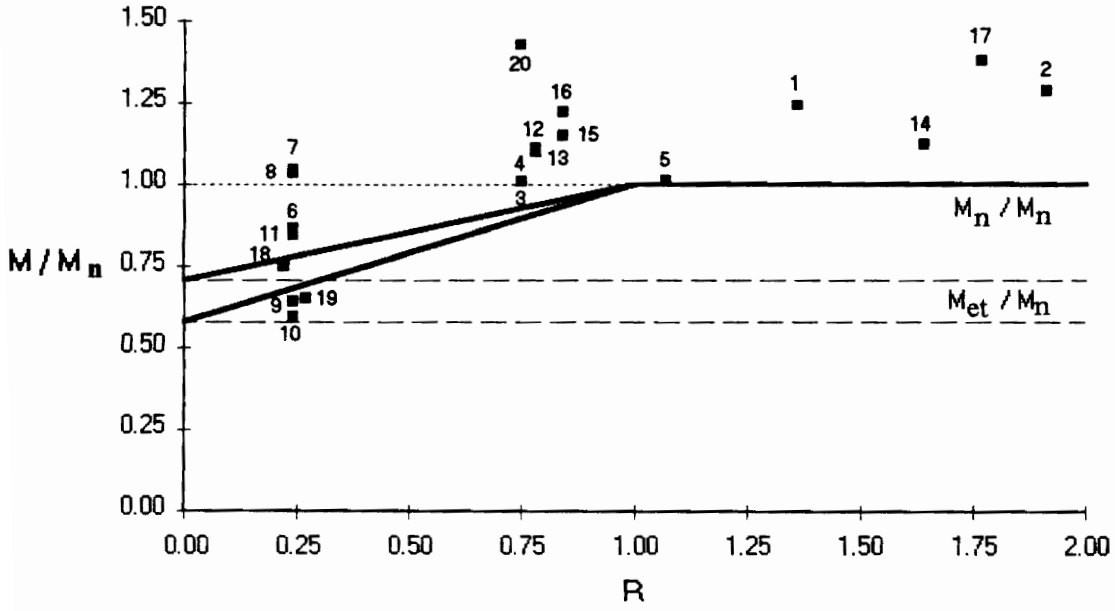

Figure 5.2 Comparison of Experimental and Modified Analytical Results

Table 5.6 Moment Reduction Factors

Test Number	Test Designation	F (k / ft)	Qn or Pn (k)	Nr (ancorage / ft)	R
1	SDI-2/20-4-9	11.8	22.5	0.71	1.36
2	SDI-2/20-5-9	11.8	22.5	1.00	1.91
3	SDI-2/20-2-9	11.8	26.5	0.33	0.75
4	SDI-2/20-23-9	11.8	26.5	0.33	0.75
5	SDI-2/20-3-9	11.8	26.5	0.48	1.07
6	SDI-2/20-PI-9	11.8	2.9	1.00	0.24
7	SDI-2/20-P2-9	11.8	2.9	1.00	0.24
8	SDI-2/20-P3-9	11.8	2.9	1.00	0.24
9	SDI-2/20-PX1-9	11.8	2.9	1.00	0.24
10	SDI-2/20-PX2-9	11.8	2.9	1.00	0.24
11	SDI-2/20-PX3-9	11.8	2.9	1.00	0.24
12	SDI-2/18-3-9	16.2	26.5	0.48	0.78
13	SDI-2/18-35-9	16.2	26.5	0.48	0.78
14	SDI-2/18-5-9	16.2	26.5	1.00	1.64
15	SDI-3/20-3-10	14.3	25.4	0.48	0.84
16	SDI-3/20-35-10	14.3	25.4	0.48	0.84
17	SDI-3/20-5-10	14.3	25.4	1.00	1.77
18	SDI-3/20-PX1-10	14.3	3.1	1.00	0.22
19	SDI-2/18-PX3-9	16.2	4.4	1.00	0.27
20	SDI-3/20-33-10	14.3	22.7	0.48	0.75

Chapter 6

SUMMARY, CONCLUSIONS AND RECOMMENDATIONS

6.1 SUMMARY

This study describes the results of research conducted at Virginia Polytechnic Institute and State University on the subject of composite slabs. This study investigates the effects of typical construction details at supports on the strength of steel deck reinforced concrete slabs. The test specimens were representative of slabs actually constructed in buildings. The effects of multiple spans, multiple panels, end restraint from cold-formed angles, and deck anchorage from shear studs were investigated. Each slab was subjected to a uniform load. These specimens differed significantly from the standard single span, single panel specimens subjected to concentrated line loads that have dominated much of the research conducted to date.

The results of this study were analyzed using methods given in the Steel Deck Institute *Composite Deck Design Handbook* (CDDH). The methods were developed by researchers at West Virginia University and Virginia Polytechnic Institute and State University and by members of the Steel Deck Institute. Two flexural limit states are

considered in the CDDH, the moment at first-yield of the extreme fiber and the ultimate strength. One of the primary objectives of this study was to generate additional data to support the CDDH procedure. Another was to modify the method such that a single procedure applies to all slabs regardless of the type or degree of anchorage over the supports. Currently, the procedure is divided into a method for slabs with studs and one for slabs without studs.

Eight three-span composite floor slabs were constructed and twenty uniform load tests were performed. Variables in the eight slabs were deck gage, rib height, slab thickness, span length, degree of anchorage, and deck continuity over supports.

6.2 CONCLUSIONS

From the results of this study, the following conclusions are drawn:

(1) The strength of composite slabs, regardless of the type of deck anchorage, welds or studs, were conservatively predicted based on the under-reinforced flexural limit state as presented in the CDDH. An anchorage value for arc spot welds was calculated similar to the anchorage capacity of a shear stud. The calculated ultimate strength was reduced for slabs in which the ends of the deck were not sufficiently anchored to develop the required tensile force in the deck necessary to achieve ultimate moment capacity. This condition is referred to as partial composite action.

(2) The lower-bound strength was calculated based on first-yield of the extreme fibers of the deck.

(3) The strength of simply supported slabs or multispan slabs in which the deck is not continuous over the supports was accurately predicted assuming the lower-bound strength.

(4) Shear studs and deck continuity provided rotational restraint at the supports. Therefore by basing calculations on a simply supported condition as was done in using the CDDH procedure the calculated capacities for slabs with studs and continuous deck were conservative.

(5) Pour stops significantly increased the strength of the composite slabs.

6.3 RECOMMENDATIONS

From the results of this study, the following recommendations are made for determining the strength of composite slabs:

(1) The strength of a composite slab, employing either welds or studs for deck anchorage, can be calculated based on the under-reinforced flexural limit state. A linear reduction between ultimate strength and first-yield must be made for slabs with only partial composite action.

(2) The strength of simply supported slabs or multispan slabs in which the deck is not continuous over the supports should be taken as the lower-bound strength based on first-yield.

6.4 FURTHER RESEARCH

An analytical method of predicting the additional capacity contributed by pour stops needs to be established. Research in the area of vertical shear strength is needed as well. A review of the existing literature is given in Appendix B. The concrete is currently considered to be the sole load carrier for live load shear forces. A model is needed to analyze the load carrying capacity of the deck.

REFERENCES

Bode, H., Kunzel, R. and Schanzenbach, J. (1988). "Profiled Steel Sheeting and Composite Action," *Proceedings of the Ninth International Specialty Conference on Cold-Formed Steel Structures*, University of Missouri-Rolla, pp. 343-359.

Bode, H. and Storck, I. (1990). "Hintergrundbericht zu Eurocode 4, Abschnitte 7 und 12.3: Verbunddecken" Bericht Nr.: RS ll2-674102-8817, Kaiserslautern, June.

Bode, H. and Sauerborn, I. (1992). "Modern Design Concept for Composite Slabs with Ductile Behavior," *Proceedings of an Engineering Foundation Conference on Composite Construction in Steel and Concrete*, ASCE, June, pp. 125-141.

Bryl, S. (1967). "The Composite Effect of Profiled Steel Plate and Concrete in Deck Slabs," *Acier Stahl Steel*, October, pp. 448-454.

Crisinel, M., Fidler, M. and Daniels, B. (1986). "Behaviour of Steel Deck Reinforced Composite Floors," *International Association for Bridge and Structural Engineering Colloquium*, Stockholm, pp. 279-290.

Crisinel, M., Daniels, B. and Ren, P. (1992). "Numerical Analysis of Composite Slab Behavior," *Proceedings of an Engineering Foundation Conference on Composite Construction in Steel and Concrete*, ASCE, June, pp. 798-808.

Dallaire, E. E. (1971). "Cellular Steel Floors Mature," *Civil Engineering*, ASCE, July, pp. 70-74.

Daniels, B. and Crisinel, M. (1987). *Composite Slabs with Profiled Sheeting*, ICOM Publication No. 180, Ecole Polytechnique Federale De Lausanne.

Daniels, B., O'Leary, D. and Crisinel, M. (1990). "Prediction of the Behavior and Strength of Composite Slabs," *International Association for Bridge and Structural Engineering Symposium*, Brussels, pp. 155-160.

Easterling, W. S. and Young, C. S. (1992). "Strength of Composite Slabs," *Journal of Structural Engineering*, ASCE, Vol. 118, No. 9, pp. 2370-2389.

Friberg, B. F. (1954). "Combined Form and Reinforcement for Concrete Slabs," *Journal of the American Concrete Institute*, Vol. 50, May, pp. 697-716.

Heagler, R. B., Luttrell, L. D. and Easterling, W. S. (1991). *Composite Deck Design Handbook*, Steel Deck Institute, Canton, Ohio.

Jolly, C. K. and Zubair, A. K. M. (1987). "The Efficiency of Shear-Bond Interlock Between Profiled Steel Sheeting and Concrete," *Composite Steel Structures--Advances, Design, and Construction*, Elsevier Science Publishing Co., Inc., pp. 127-136.

Jolly, C. K. and Lawson, R. M. (1992). "End Anchorage in Composite Slabs: An Increased Load Carrying Capacity," *The Structural Engineer*, Vol. 70, No. 11, pp. 202-205.

Klaiber, F. W. and Porter, M. L. (1981). "Uniform Loading for Steel-Deck-Reinforced Slabs," *Journal of the Structural Division*, ASCE, Vol. 107, No. ST11, pp. 2097-2109.

Krupica, G. L. (1979). *The Behavior and Analysis of Steel-Deck-Reinforced Concrete Slabs with End-Span Studs*, M. S. Thesis, Iowa State University, Ames, Iowa.

Load and Resistance Factor Design Cold-Formed Steel Design Specification (1991). American Iron and Steel Institute, Washington, D.C.

Load and Resistance Factor Design Specification for Structural Steel Buildings (1993). American Institute of Steel Construction, Chicago.

Luttrell, L. D. and Davison, J. H. (1973). "Composite Slabs with Steel Deck Panels," *Proceedings of the Second International Specialty Conference on Cold-Formed Steel Structures*, University of Missouri-Rolla, pp. 573-603.

Luttrell, L. D. and Prassanan, S. (1984). "Strength Formulations for Composite Slabs," *Proceedings of the Seventh International Specialty Conference on Cold-Formed Steel Structures*, University of Missouri-Rolla, pp. 306-325.

Luttrell, L. D. (1987). "Flexural Strength of Composite Slabs," *Composite Steel Structures--Advances, Design, and Construction*, Elsevier Science Publishing Co., Inc., pp. 106-116.

McCuaig, L. A. and Schuster, R. M. (1988). "Repeated Point Loading on Composite Slabs," *Proceedings of the Ninth International Specialty Conference on Cold-Formed Steel Structures*, University of Missouri-Rolla, pp. 361-385.

McDermott, J. F. (1967). "Structural Tests on a Composite Floor System," *Journal of the Structural Division*, ASCE, Vol. 93, No. ST1, pp. 255-274.

O'Leary, D., El-Dharat, A. and Duffy, C. (1987). "Composite Reinforced End-Anchored Concrete Floors," *Composite Steel Structures--Advances, Design, and Construction*, Elsevier Science Publishing Co., Inc., pp. 117-126.

Patrick, M. (1989). "Design of Continuous Composite Slabs--The Issue of Ductility," *Steel Construction*, Vol. 23, No. 3, pp. 2-10.

Patrick, M. (1990). "A New Partial Shear Connection Strength Model for Composite Slabs," BHP Melbourne Research Laboratories Report MRL/PS64/90/016, March.

Patrick, M. and Bridge, R. Q. (1990). "Parameters Affecting the Design and Behaviour of Composite Slabs," *International Association for Bridge and Structural Engineering Symposium*, Brussels, pp. 221-226.

Patrick, M. and Poh, K. W. (1990). "Controlled Test for Composite Slab Design Parameters," *International Association for Bridge and Structural Engineering Symposium*, Brussels, pp. 227-231.

Patrick, M. and Bridge, R. Q. (1992). "Design of Composite Slabs for Vertical Shear," *Proceedings of an Engineering Foundation Conference on Composite Construction in Steel and Concrete*, ASCE, June, pp. 304-322.

Porter, M. L. and Ekberg, C. E. Jr. (1975). "Design vs. Test Results for Steel Deck Floor Slabs," *Proceedings of the Third International Specialty Conference on Cold-Formed Steel Structures*, University of Missouri-Rolla, pp. 793-811.

Porter, M. L. and Ekberg, C. E. Jr. (1975). "Design Recommendations for Steel Deck Floor Slabs," *Proceedings of the Third International Specialty Conference on Cold-Formed Steel Structures*, University of Missouri-Rolla, pp. 761-791.

Porter, M. L., Ekberg, C. E. Jr., Greimann, L. F. and Elleby, H. A. (1976). "Shear-Bond Analysis of Steel-Deck-Reinforced Slabs," *Journal of the Structural Division*, ASCE, Vol. 102, No. ST12, pp. 2255-2268.

Porter, M. L. and Ekberg, C. E. Jr. (1977). "Behavior of Steel-Deck-Reinforced Slabs," *Journal of the Structural Division*, ASCE, Vol. 103, No. ST3, pp. 663-677.

Porter, M. L. and Ekberg, C. E. Jr. (1978). *Compendium of ISU Research Conducted on Cold-Formed Steel-Deck-Reinforced Slab Systems*, Bulletin 200, Engineering Research Institute, Iowa State University, Ames, Iowa.

Roeder, C. W. (1981). "Point Loads on Composite Deck-Reinforced Slabs," *Journal of the Structural Division*, ASCE, Vol. 107, No. ST12, pp. 2421-2429.

Schuster, R. M. (1972). "Composite Steel Deck-Reinforced Concrete Systems Failing in Shear-Bond," *International Association for Bridge and Structural Engineering Congress Proceedings*, pp. 185-191.

Schuster, R. M. (1976). "Composite Steel-Deck Concrete Floor Systems," *Journal of the Structural Division*, ASCE, Vol. 102, No. ST5, pp. 899-917.

Schuster, R. M. and Ling, W. C. (1980). "Mechanical Interlocking Capacity of Composite Slabs," *Proceedings of the Fifth International Specialty Conference on Cold-Formed Steel Structures*, University of Missouri-Rolla, pp. 387-407.

Specifications for the Design and Construction of Composite Slabs (1993). ASCE Standard, New York.

Stark, J. (1978). "Design of Composite Floors with Profiled Steel Sheet," *Proceedings of the Fourth International Specialty Conference on Cold-Formed Steel Structures*, University of Missouri-Rolla, pp. 893-922.

Wolfel, E. (1987). "Elastic Design of Composite Slabs," *Proceedings of an Engineering Foundation Conference on Composite Construction in Steel and Concrete*, ASCE, June, pp. 680-690.

Wright, H. D. and Evans, H. R. (1990). "A Review of Composite Slab Design," *Proceedings of the Tenth International Specialty Conference on Cold-Formed Steel Structures*, University of Missouri-Rolla, pp. 27-47.

Young, C. S. (1990). *Effects of End Restraint on Steel Deck Reinforced Concrete Floor Systems*, M. S. Thesis, Virginia Polytechnic Institute and State University, Blacksburg, Virginia.

Zsutty, T. C. (1968). "Beam Shear Strength Prediction by Analysis of Existing Data," *Journal of the American Concrete Institute*, Vol. 65, No. 11.

Appendix A

TEST DATA

A complete description of each specimen and the strain data from each test are provided in this section. Strain gage designations are of the form 1A5. The first number is the span number (1 through 3). The next character, a letter, indicates the cross section. The last number is the location of the gage along the cross section. The letters A through E designate the following cross sections:

A : exterior support (left interior support for center span)
B : maximum moment
C : interior support (right interior support for center span)
D : 1 ft. intervals along the span
E : concrete gages at maximum moment

Web embossment dimensions are given for each deck profile. Dimensions are represented by the following variables:

N_b : length of embossment along its base
N_t : length of embossment along its top
W_b : width of embossment along its base
W_t : width of embossment along its top
s : horizontal distance between embossment centerline
p_h : embossment depth

Test Designation: SDI-2/20-4-9
Test Date: July 1, 1993

MATERIALS AND DIMENSIONS

General:

width:	6 ft. (2 panels)
span length:	9 ft. end span
end details:	1 ft. cantilever
deck anchorage type:	shear stud, 3-7/8 in. long, 3/4 in. dia.
average anchorage spacing:	1.4 ft.

Deck:

thickness:	0.0345 in. (20 gage)
depth:	2 in.
area:	0.519 $in.^2$/ft.
yield stress:	45.4 ksi
ultimate strength:	52.6 ksi
web embossment type:	N/A

embossment dimensions:

N_b :	1.76 in.	W_b :	0.81 in.	s :	3.07 in.
N_t :	1.19 in.	W_t :	0.58 in.	p_h :	0.15 in.

Concrete:

type:	normal weight
test strength:	3,180 psi
total depth:	4.5 in.
cover depth:	2.5 in.

RESULTS

midspan strain due to fresh concrete:	230 x 10^{-6} in./in.
maximum load:	703 psf
deflection at maximum load:	2.70 in.
deflection at termination of test:	3.54 in.
end slip at maximum load:	0.15 in.
end slip at termination of test:	0.26 in.

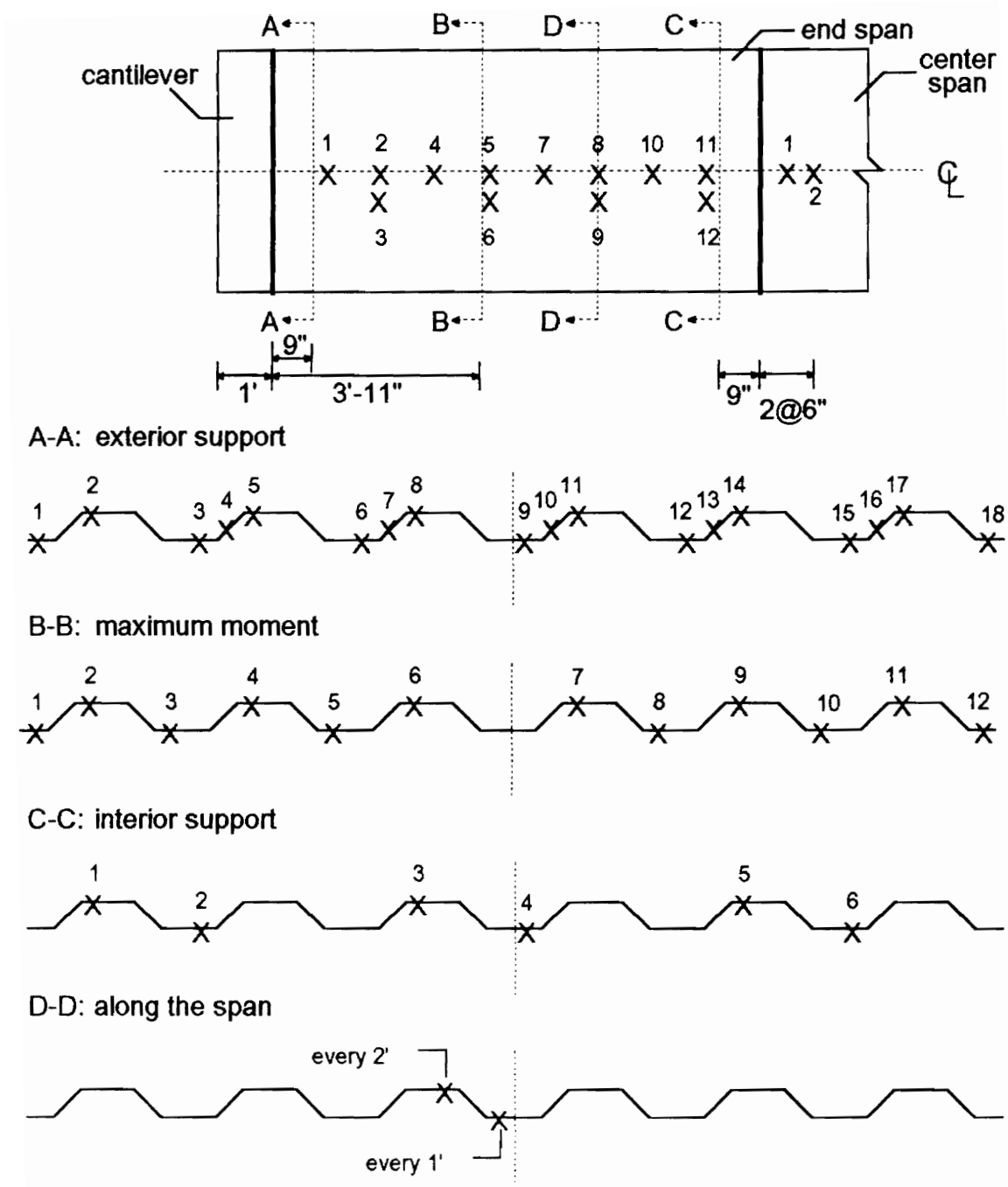

Figure A.1 SDI-2/20-4-9 Steel Deck Strain Gage Locations

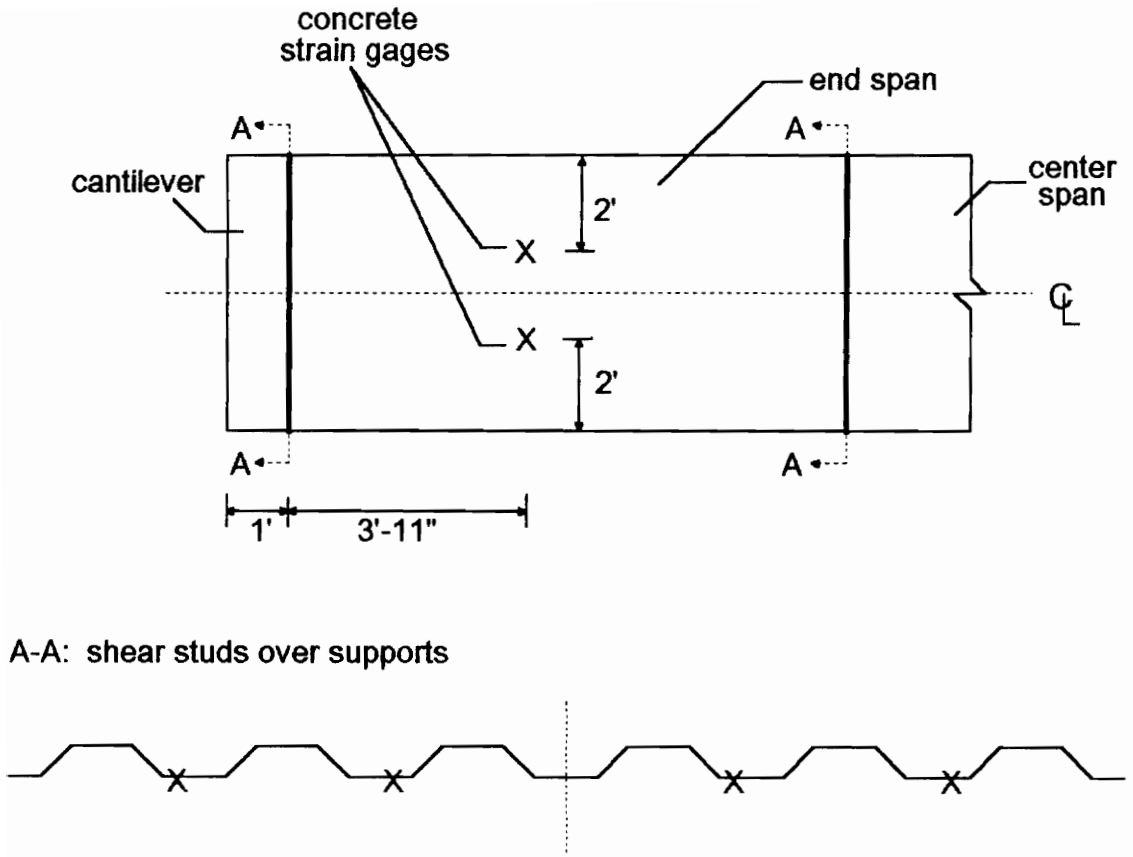

Figure A.2 SDI-2/20-4-9 Concrete Strain Gage and Shear Stud Locations

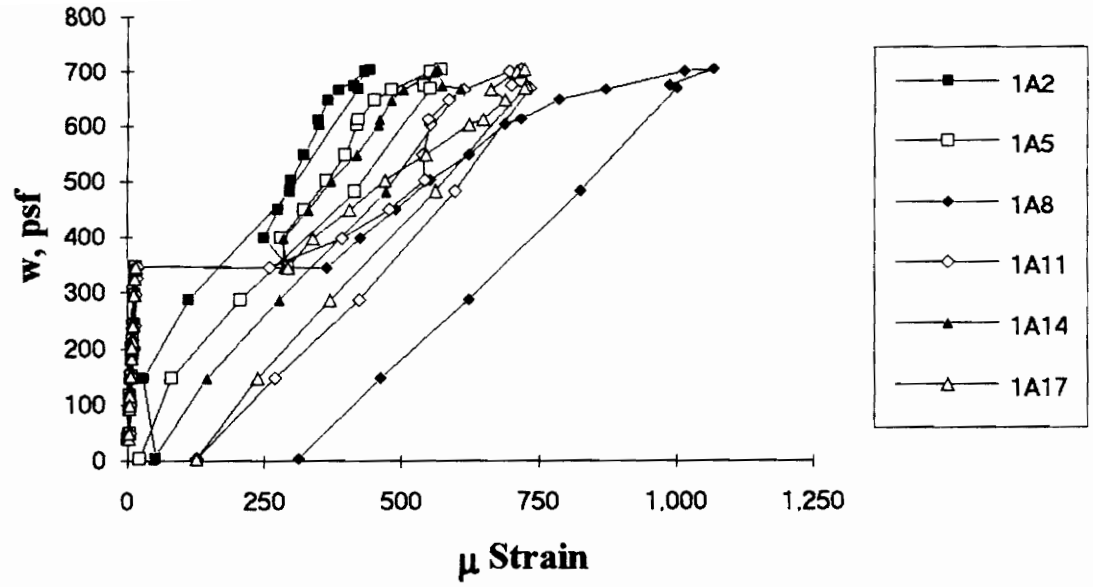

Figure A.3 SDI-2/20-4-9 Load vs. Strain in Deck Top Flange at Exterior Support

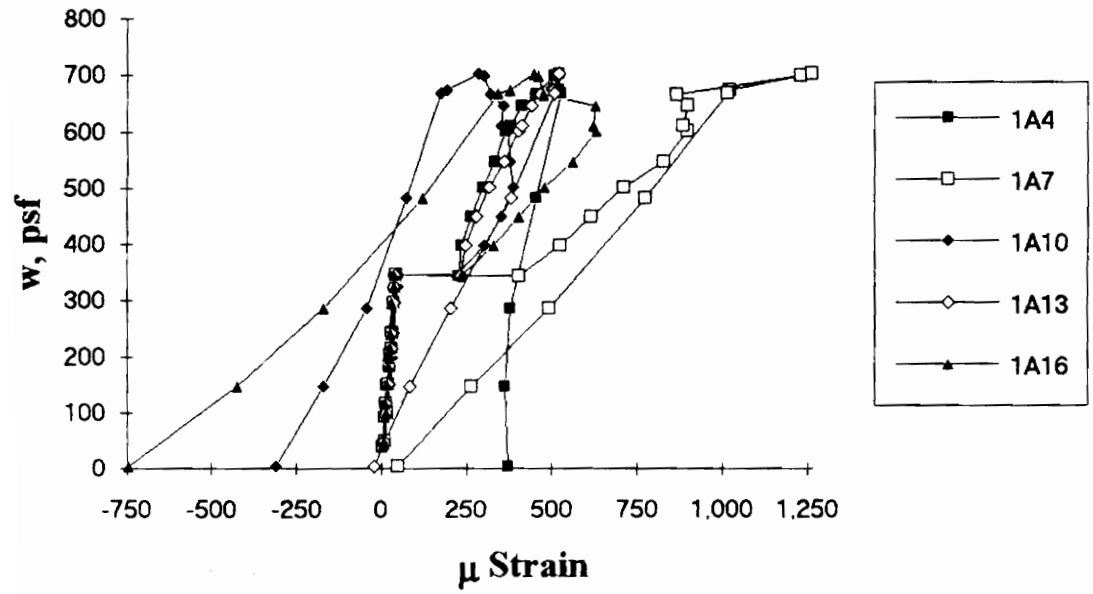

Figure A.4 SDI-2/20-4-9 Load vs. Strain in Deck Web at Exterior Support

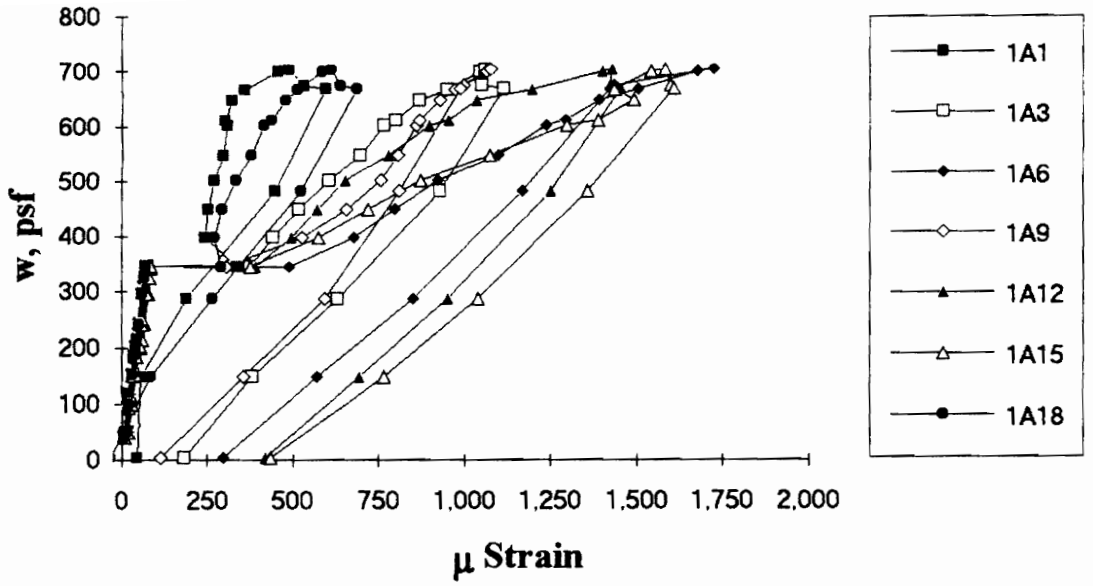

Figure A.5 SDI-2/20-4-9 Load vs. Strain in Deck Bottom Flange at Exterior Support

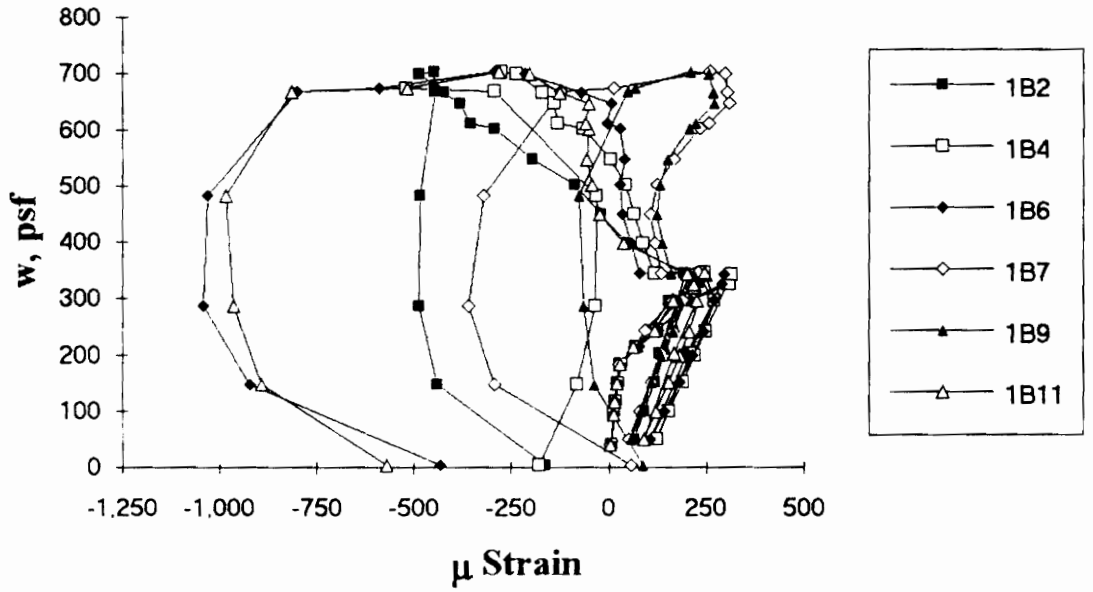

Figure A.6 SDI-2/20-4-9 Load vs. Strain in Deck Top Flange at Maximum Moment

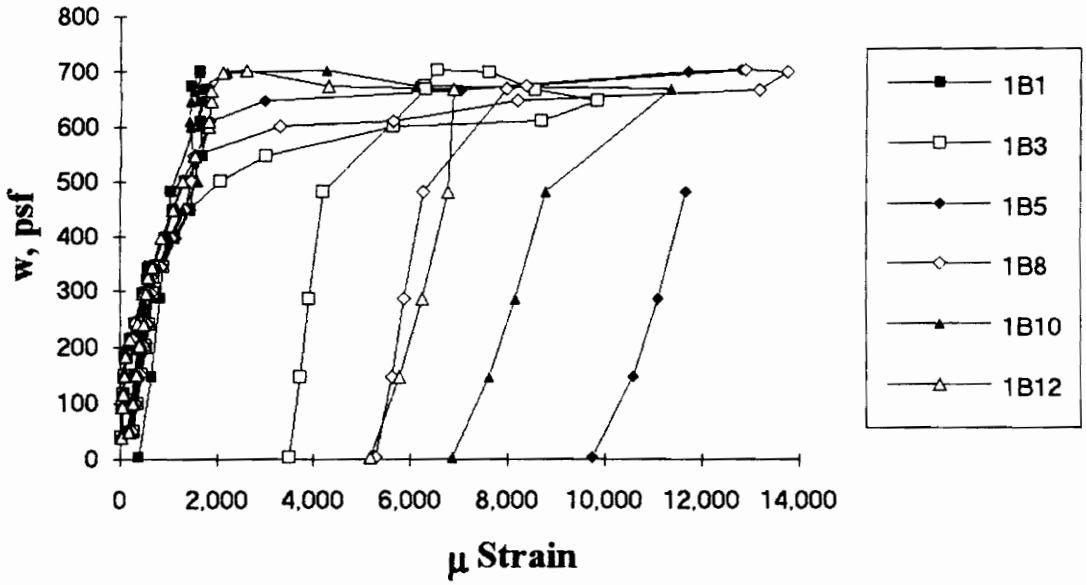

Figure A.7 SDI-2/20-4-9 Load vs. Strain in Deck Bottom Flange at Maximum Moment

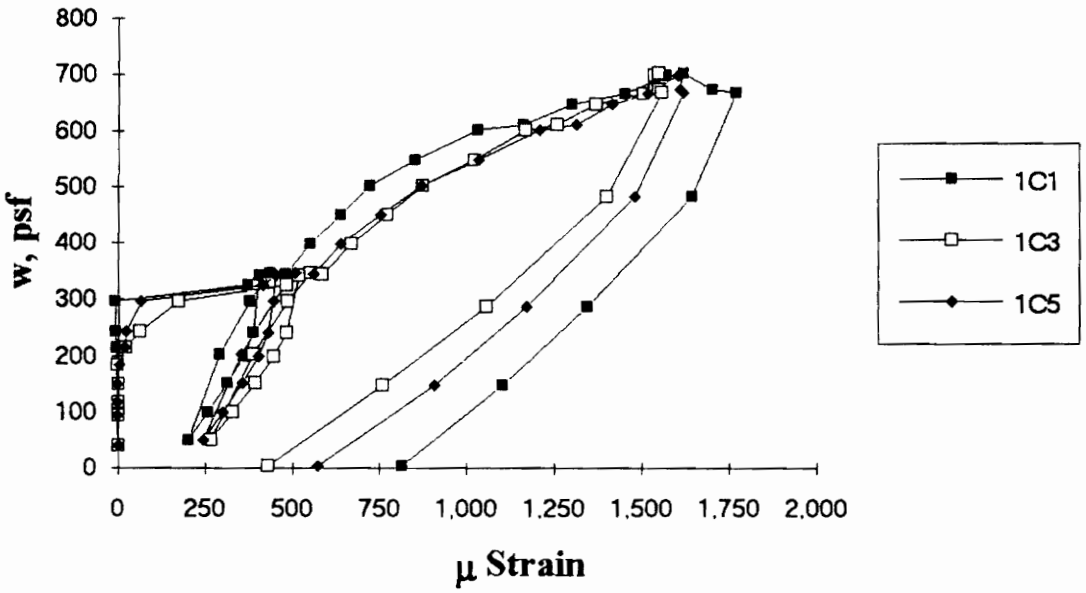

Figure A.8 SDI-2/20-4-9 Load vs. Strain in Deck Top Flange at Interior Support

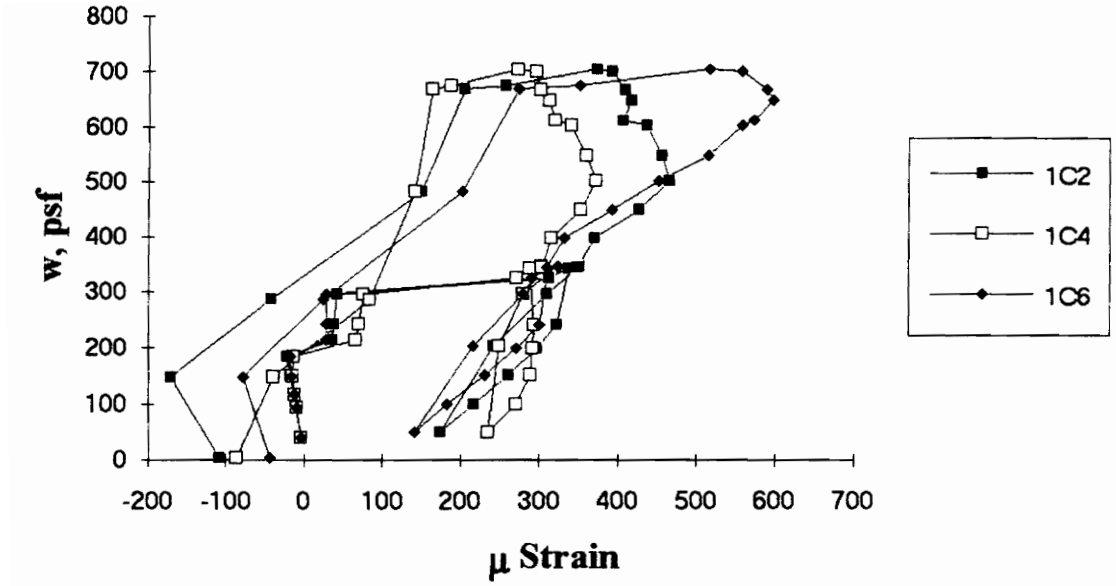

Figure A.9 SDI-2/20-4-9 Load vs. Strain in Deck Bottom Flange at Interior Support

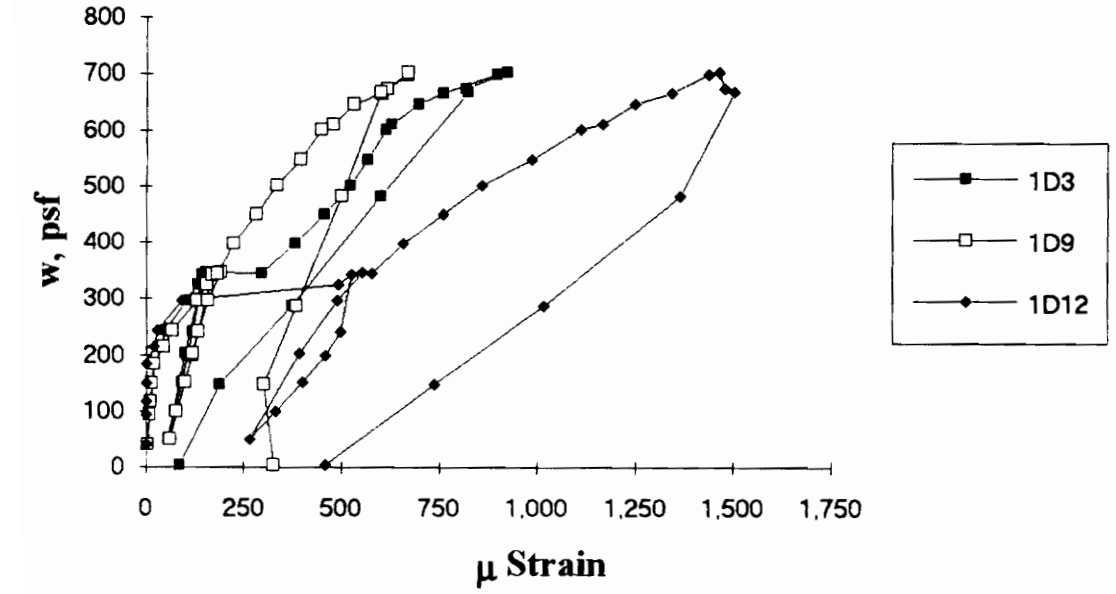

Figure A.10 SDI-2/20-4-9 Load vs. Strain in Deck Top Flange along the Span

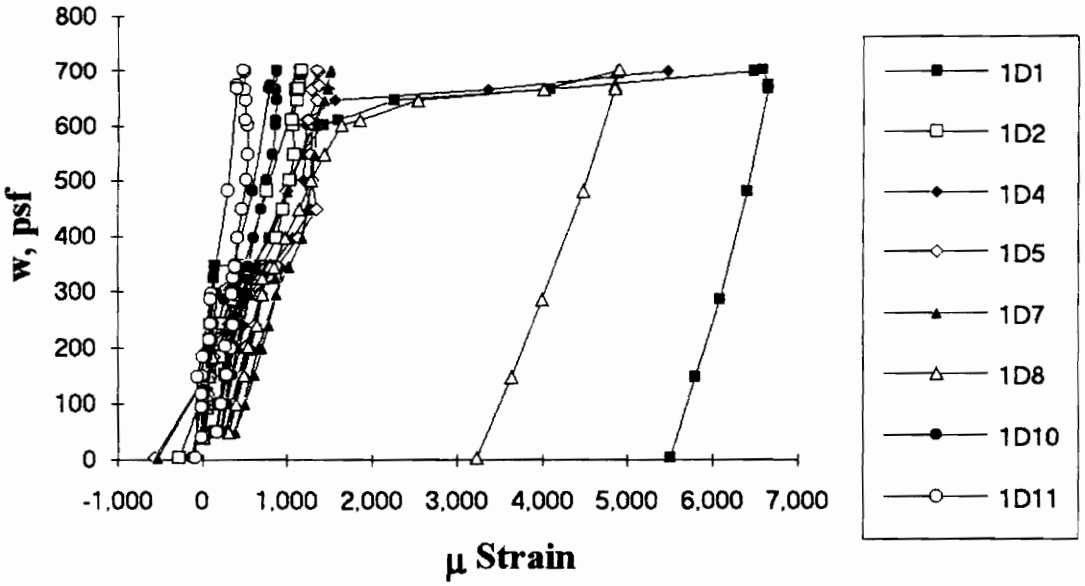

Figure A.11 SDI-2/20-4-9 Load vs. Strain in Deck Bottom Flange along the Span

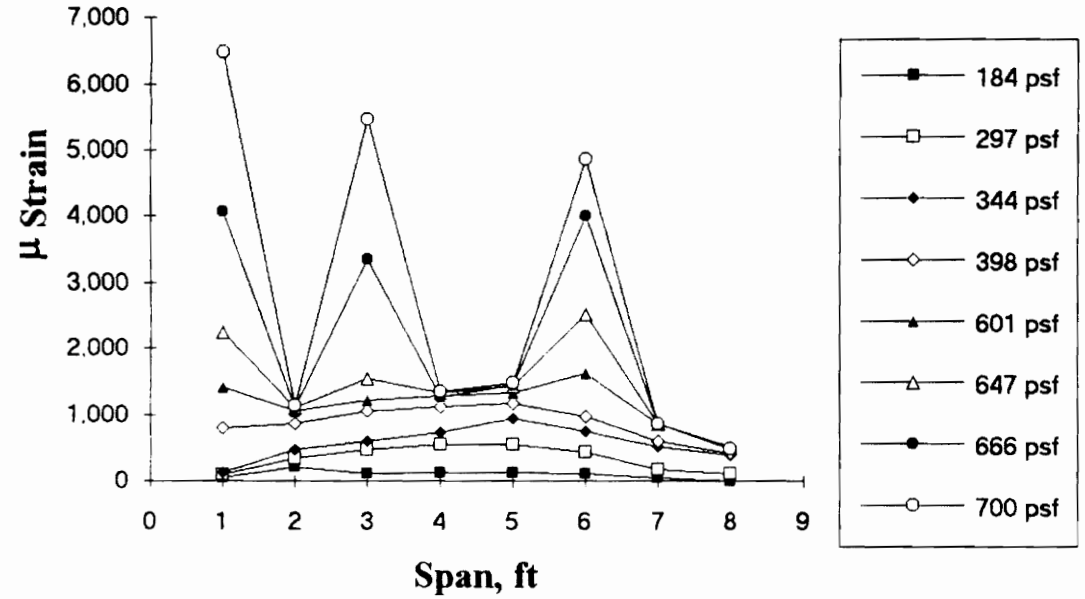

Figure A.12 SDI-2/20-4-9 Strain Variation in Deck Bottom Flange along the Span (from centerline of exterior support)

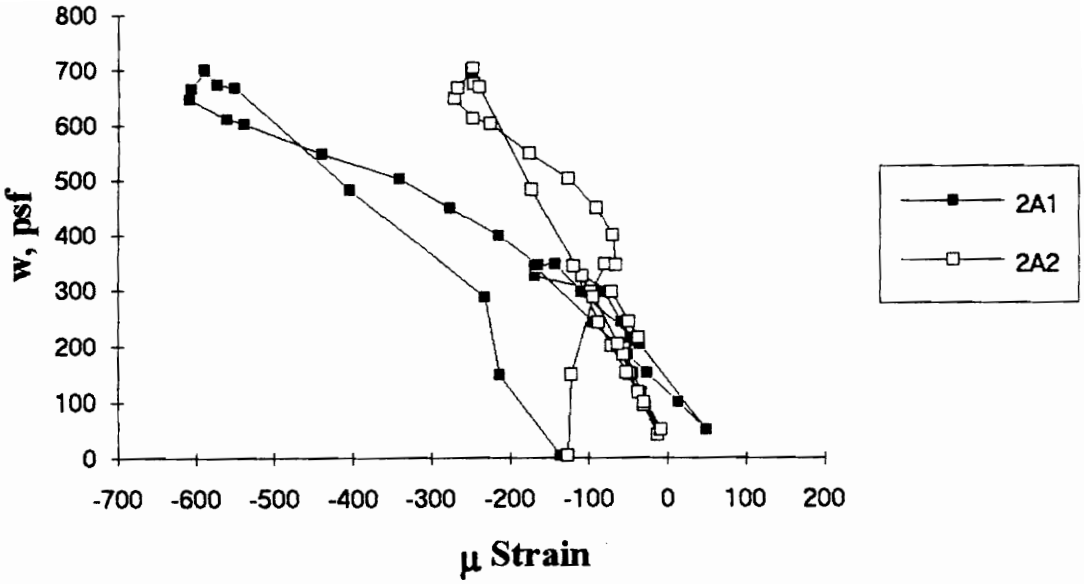

Figure A.13 SDI-2/20-4-9 Load vs. Strain in Deck Bottom Flange in Center Span

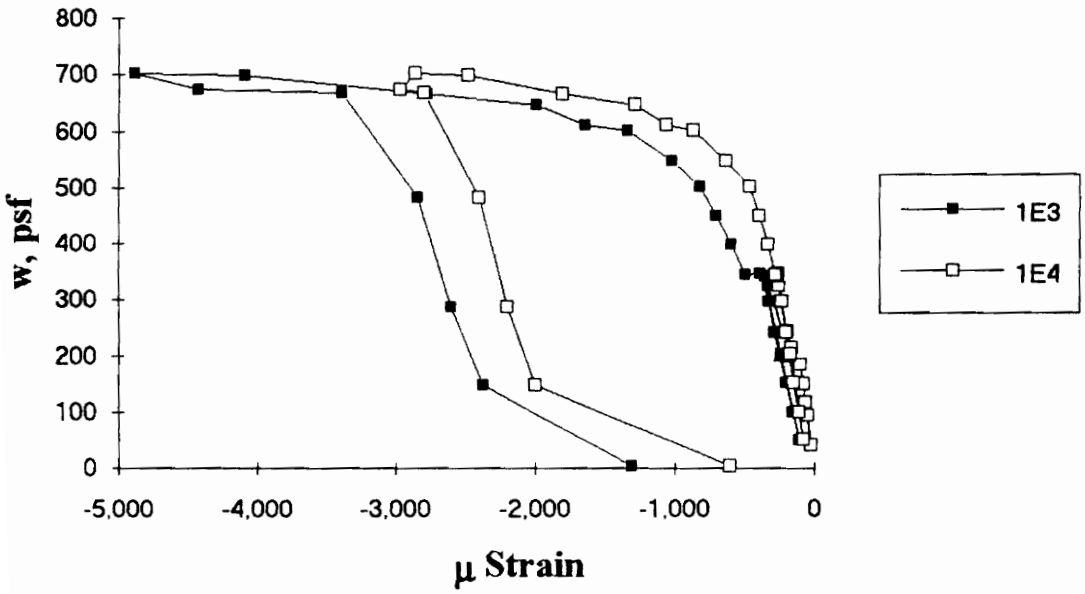

Figure A.14 SDI-2/20-4-9 Load vs. Strain in Concrete at Maximum Moment

Test Designation: SDI-2/20-5-9
Test Date: July 13, 1993

MATERIALS AND DIMENSIONS

General:

width:	6 ft. (2 panels)
span length:	9 ft. end span
end details:	1 ft. cantilever
deck anchorage type:	shear stud, 3-7/8 in. long, 3/4 in. dia.
average anchorage spacing:	1.0 ft.

Deck:

thickness:	0.0345 in. (20 gage)
depth:	2 in.
area:	0.519 in.^{2}/ft.
yield stress:	45.4 ksi
ultimate strength:	52.6 ksi
web embossment type:	N/A

embossment dimensions:

N_b :	1.76 in.	W_b :	0.81 in.	s :	3.07 in.
N_t :	1.19 in.	W_t :	0.58 in.	p_h :	0.15 in.

Concrete:

type:	normal weight
test strength:	3,180 psi
total depth:	4.5 in.
cover depth:	2.5 in.

RESULTS

midspan strain due to fresh concrete:	230 x 10^{-6} in./in.
maximum load:	729 psf
deflection at maximum load:	2.61 in.
deflection at termination of test:	5.11 in.
end slip at maximum load:	0.11 in.
end slip at termination of test:	0.52 in.

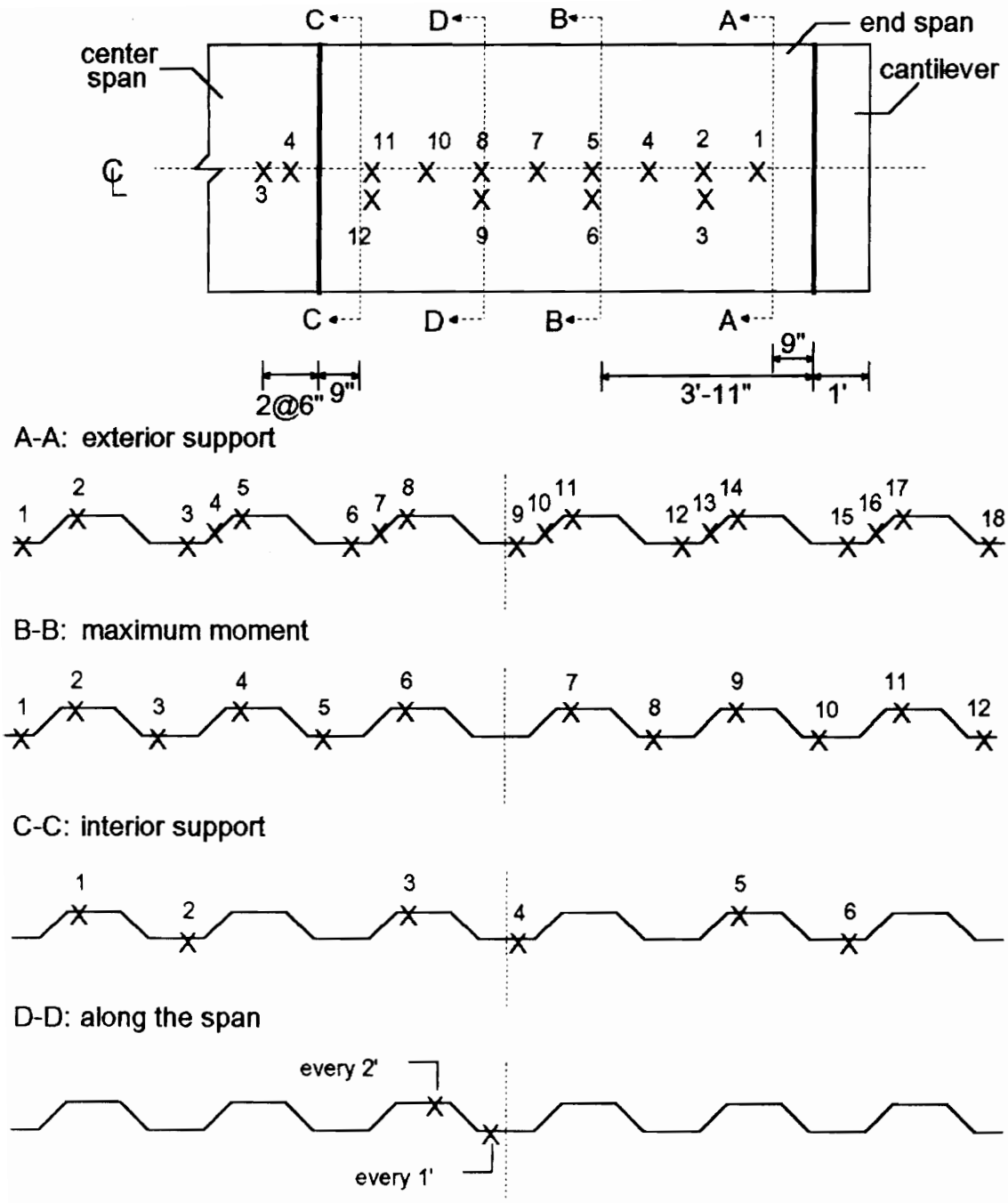

Figure A.15 SDI-2/20-5-9 Steel Deck Strain Gage Locations

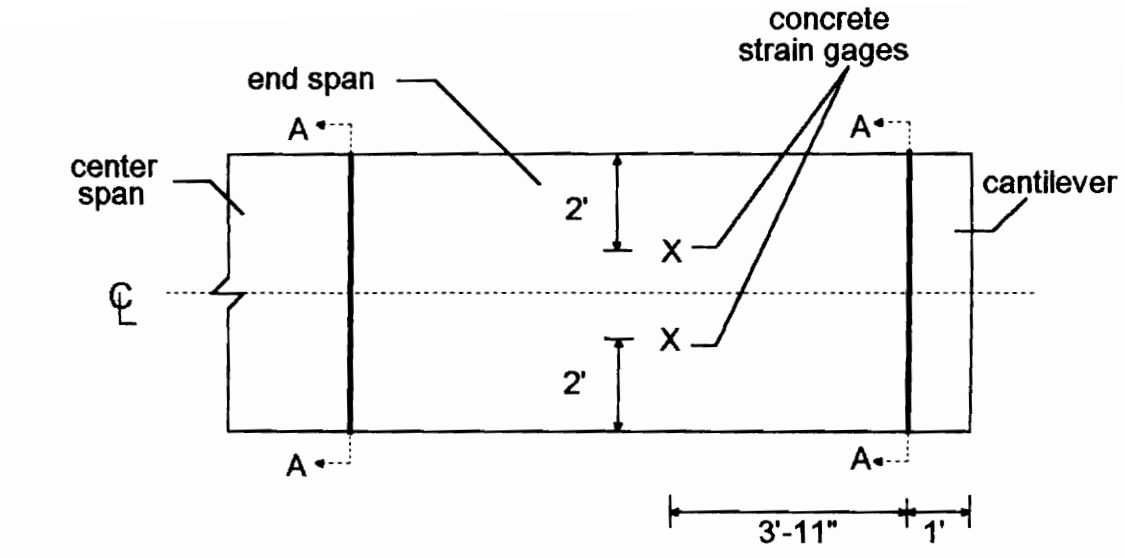

A-A: shear studs over supports

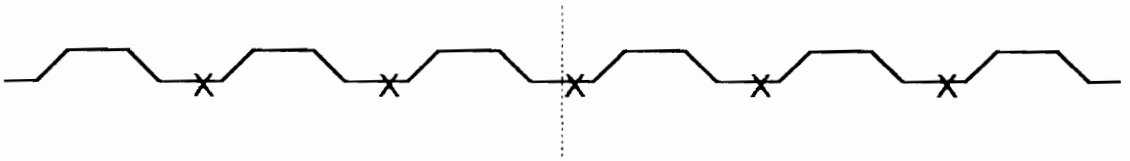

Figure A.16 SDI-2/20-5-9 Concrete Strain Gage and Shear Stud Locations

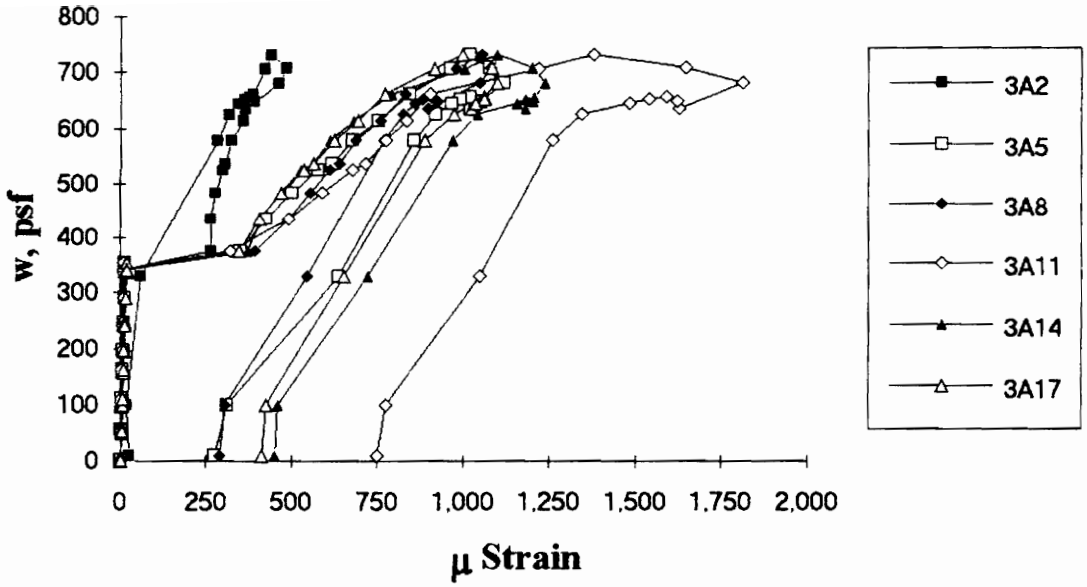

Figure A.17 SDI-2/20-5-9 Load vs. Strain in Deck Top Flange at Exterior Support

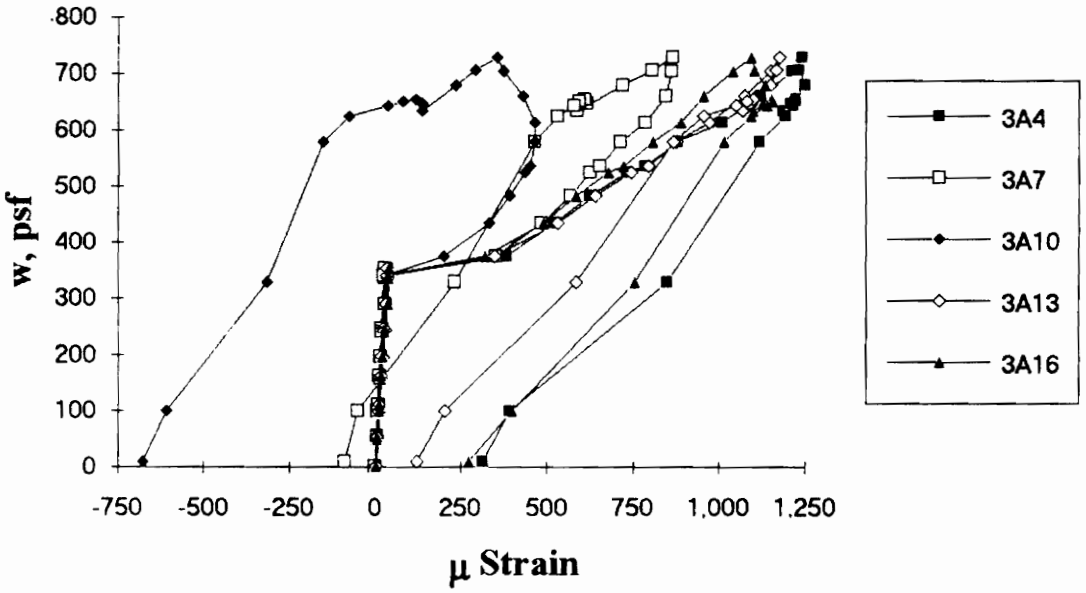

Figure A.18 SDI-2/20-5-9 Load vs. Strain in Deck Web at Exterior Support

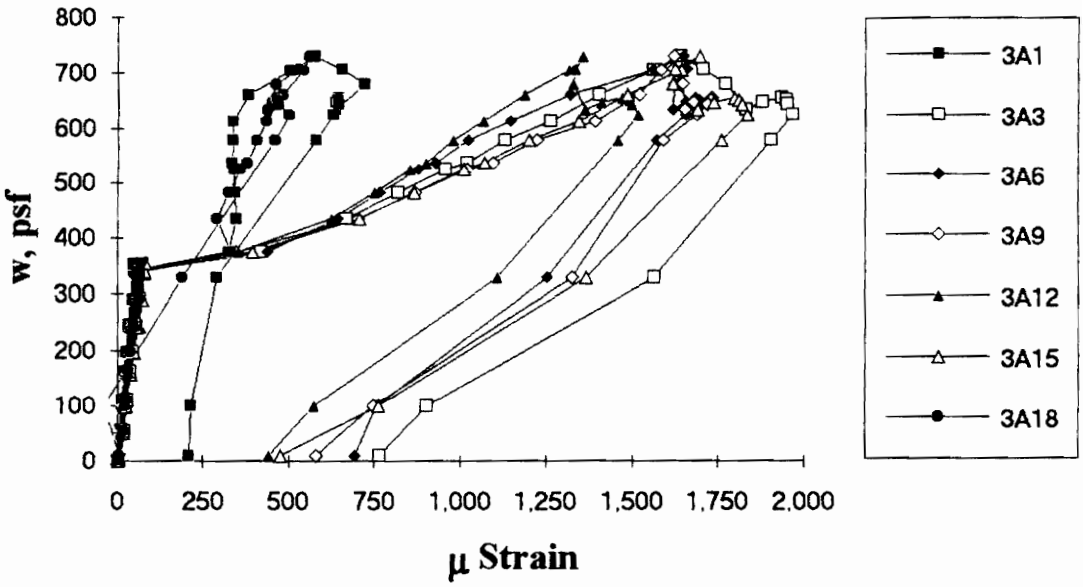

Figure A.19 SDI-2/20-5-9 Load vs. Strain in Deck Bottom Flange at Exterior Support

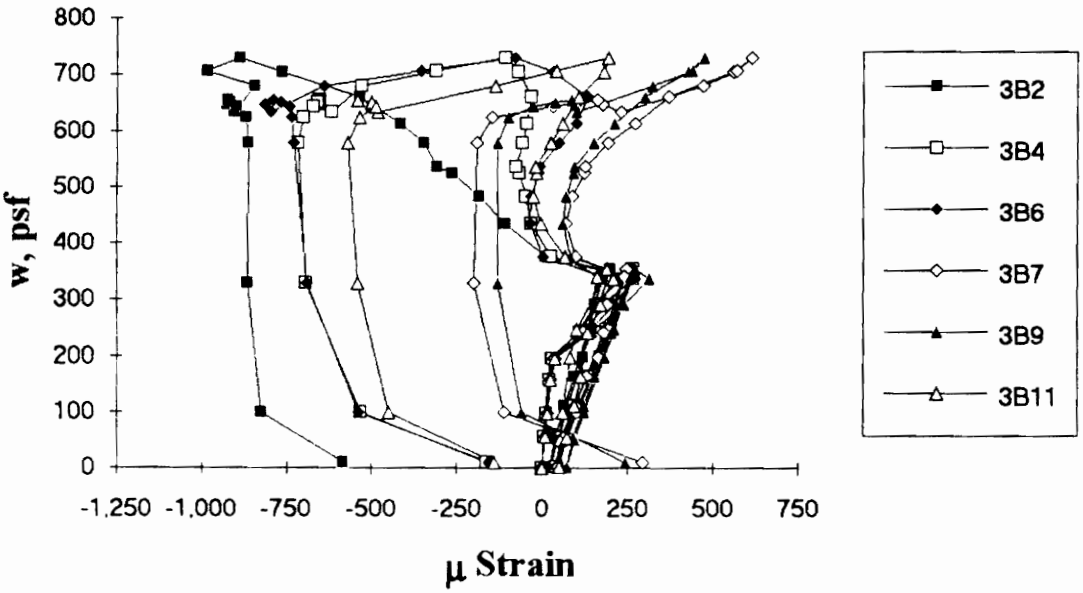

Figure A.20 SDI-2/20-5-9 Load vs. Strain in Deck Top Flange at Maximum Moment

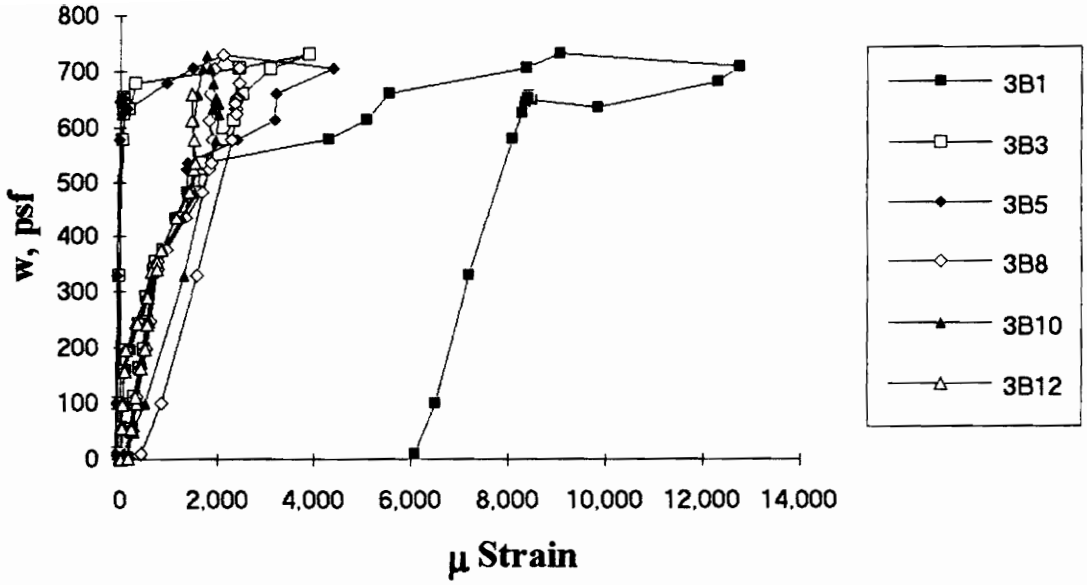

Figure A.21 SDI-2/20-5-9 Load vs. Strain in Deck Bottom Flange at Maximum Moment

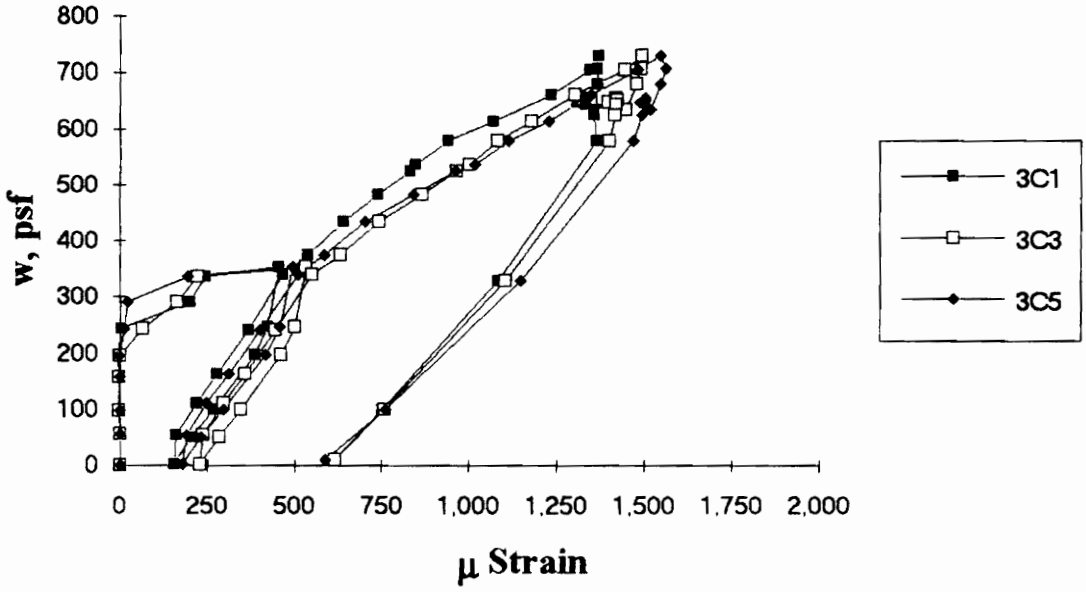

Figure A.22 SDI-2/20-5-9 Load vs. Strain in Deck Top Flange at Interior Support

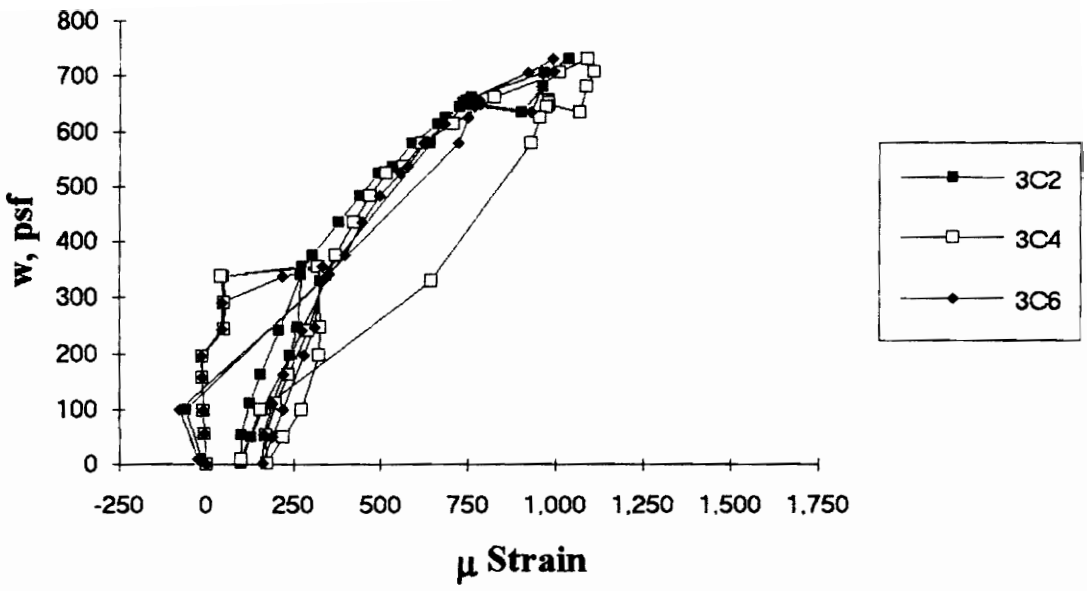

Figure A.23 SDI-2/20-5-9 Load vs. Strain in Deck Bottom Flange at Interior Support

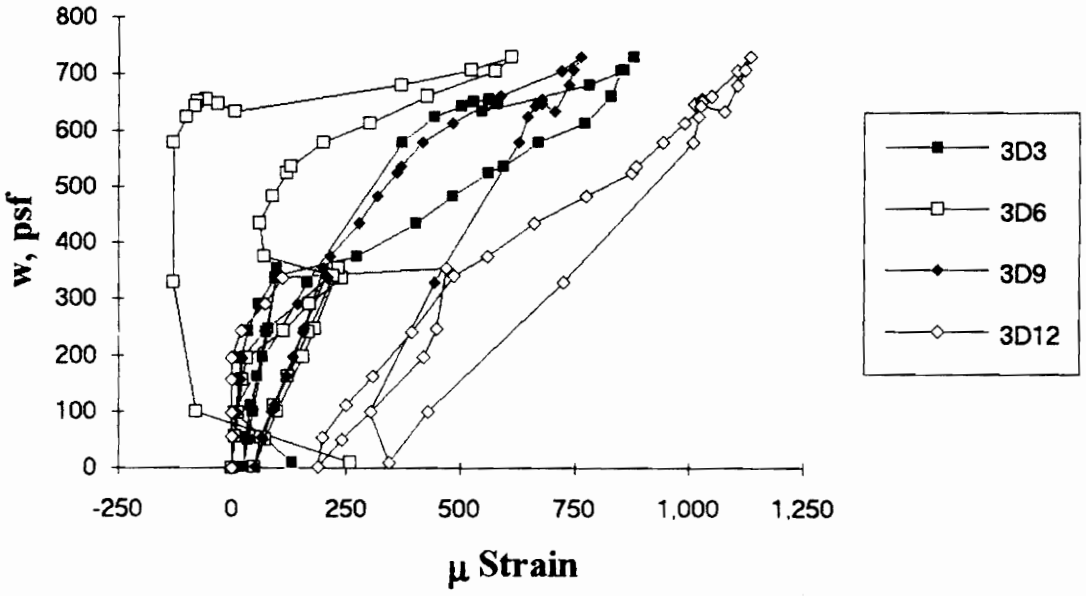

Figure A.24 SDI-2/20-5-9 Load vs. Strain in Deck Top Flange along the Span

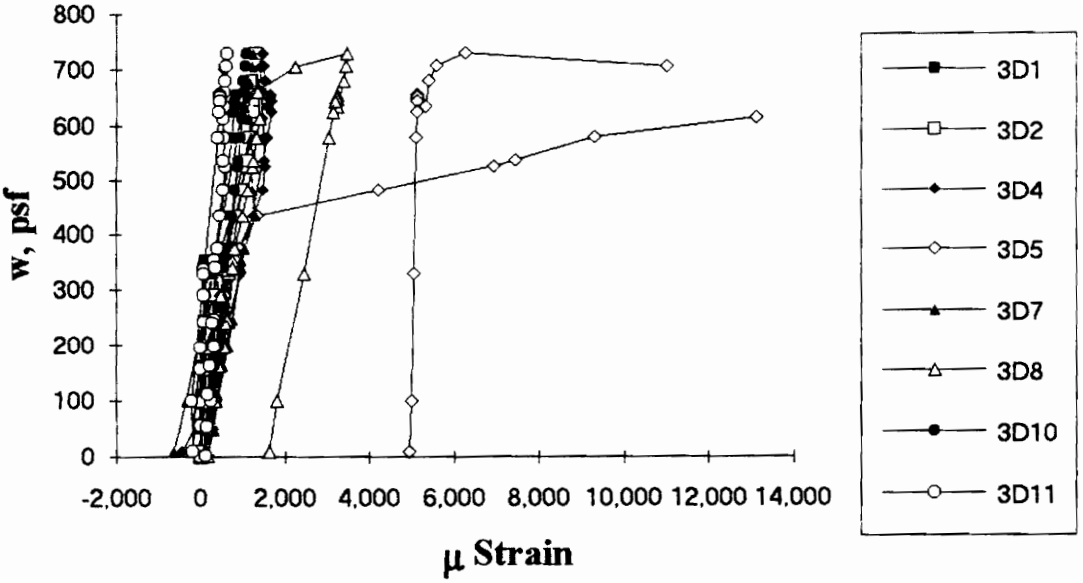

Figure A.25 SDI-2/20-5-9 Load vs. Strain in Deck Bottom Flange along the Span

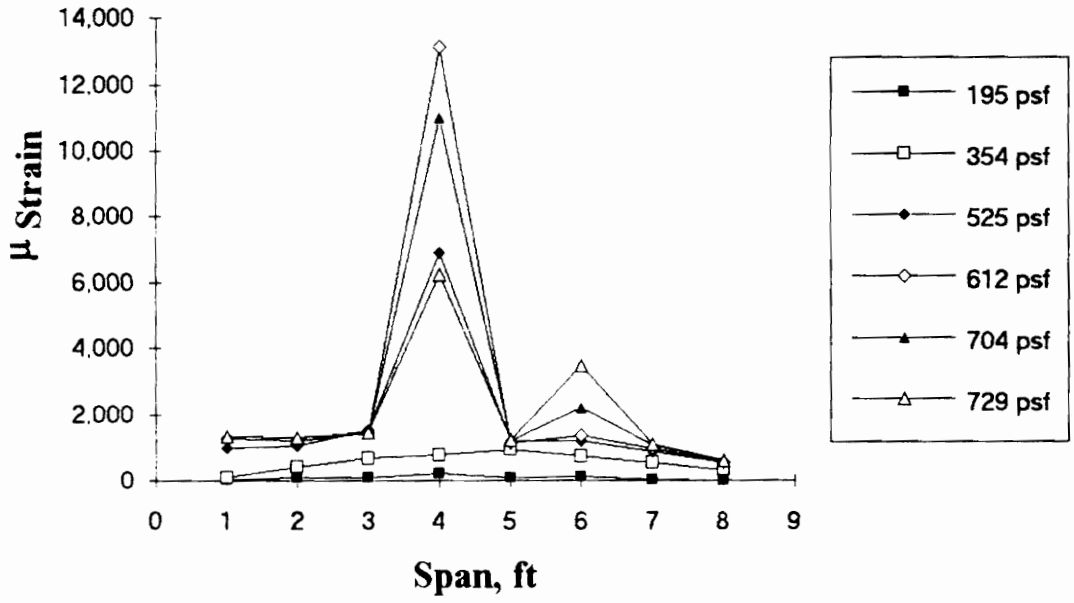

Figure A.26 SDI-2/20-5-9 Strain Variation in Deck Bottom Flange along the Span (from centerline of exterior support)

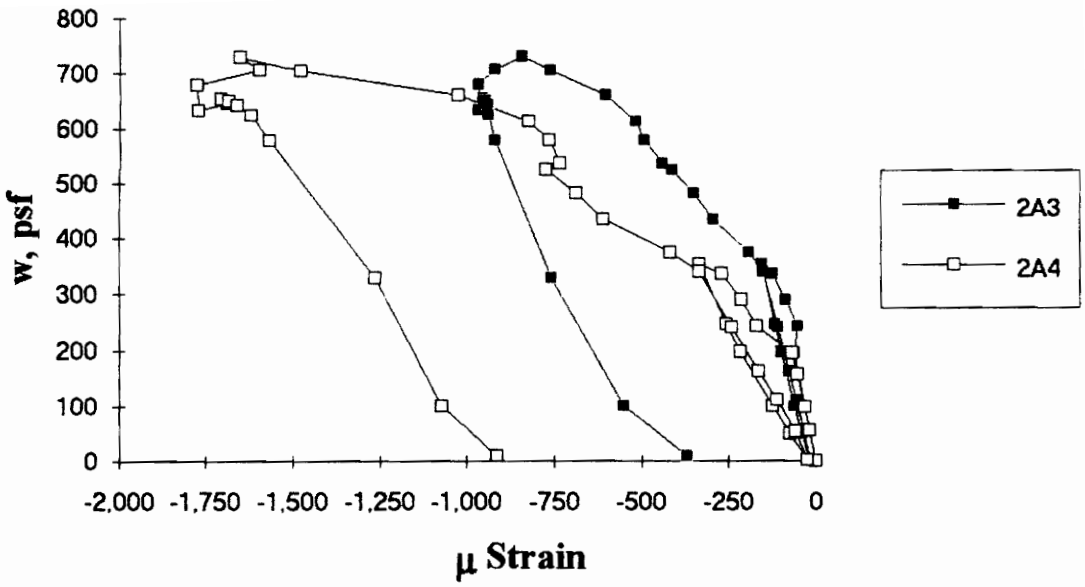

Figure A.27 SDI-2/20-5-9 Load vs. Strain in Deck Bottom Flange in Center Span

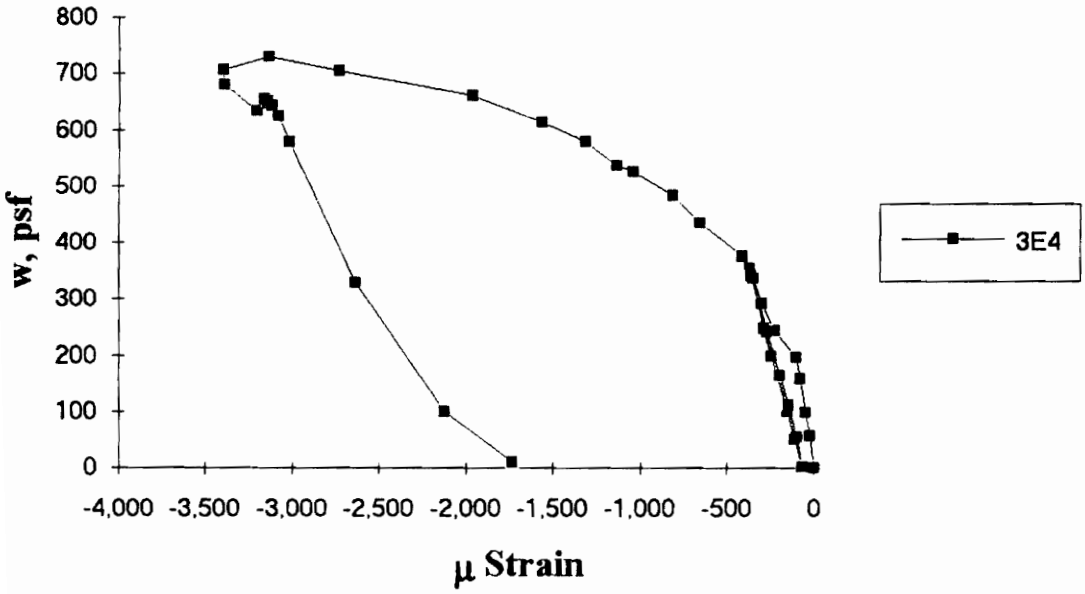

Figure A.28 SDI-2/20-5-9 Load vs. Strain in Concrete at Maximum Moment

Test Designation: SDI-2/20-2-9
Test Date: August 26, 1993

MATERIALS AND DIMENSIONS

General:

width:	6 ft. (2 panels)
span length:	9 ft. end span
end details:	1 ft. cantilever
deck anchorage type:	shear stud, 3-7/8 in. long, 3/4 in. dia.
average anchorage spacing:	3.0 ft.

Deck:

thickness:	0.0345 in. (20 gage)
depth:	2 in.
area:	0.519 in.^{2}/ft.
yield stress:	45.4 ksi
ultimate strength:	52.6 ksi
web embossment type:	N/A

embossment dimensions:

N_b : 1.76 in.	W_b : 0.81 in.	s : 3.07 in.
N_t : 1.19 in.	W_t : 0.58 in.	p_h : 0.15 in.

Concrete:

type:	normal weight
test strength:	5,170 psi
total depth:	4.5 in.
cover depth:	2.5 in.

RESULTS

midspan strain due to fresh concrete:	240 x 10^{-6} in./in.
maximum load:	597 psf
deflection at maximum load:	2.55 in.
deflection at termination of test:	4.69 in.
end slip at maximum load:	0.06 in.
end slip at termination of test:	0.39 in.

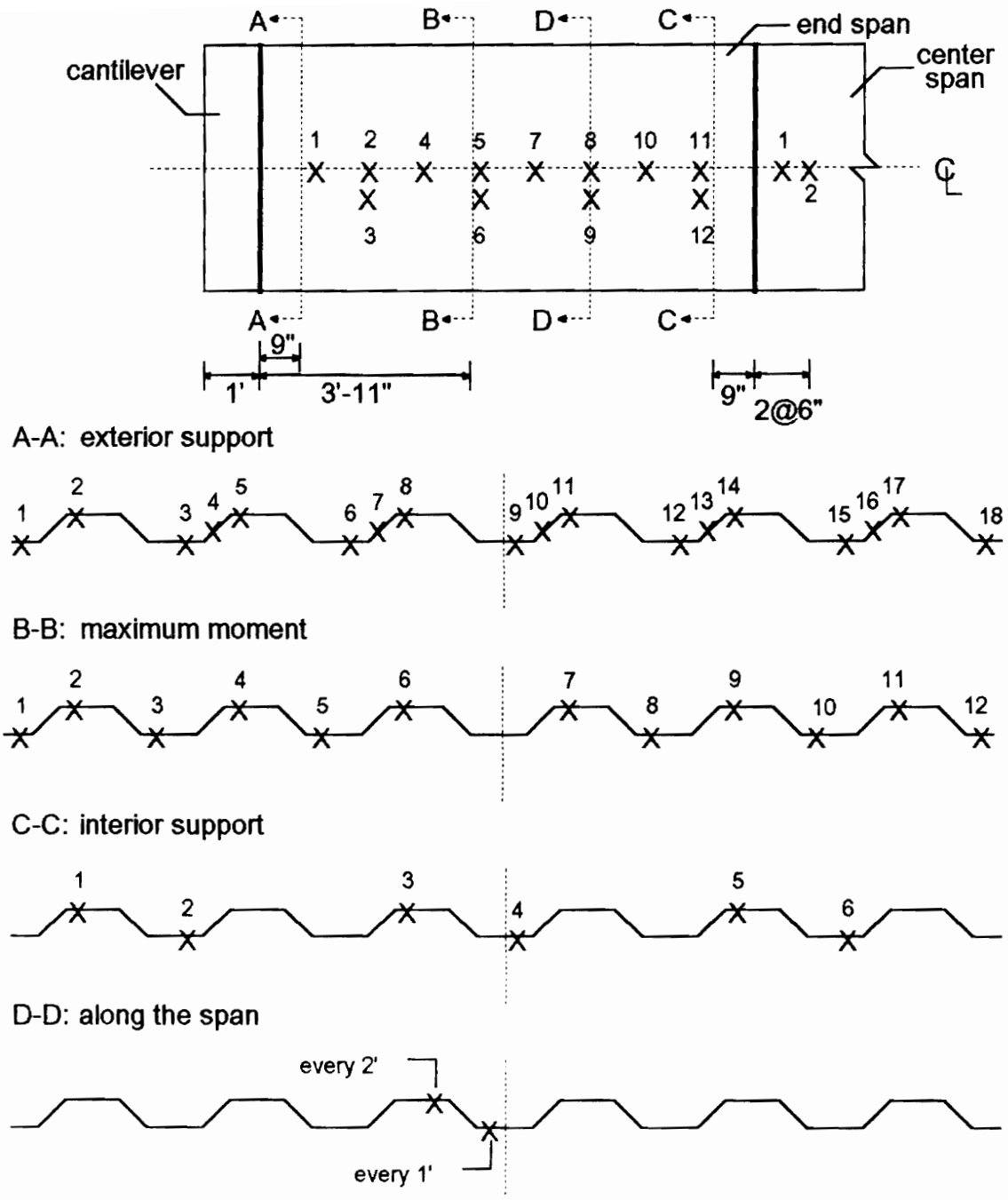

Figure A.29 SDI-2/20-2-9 Steel Deck Strain Gage Locations

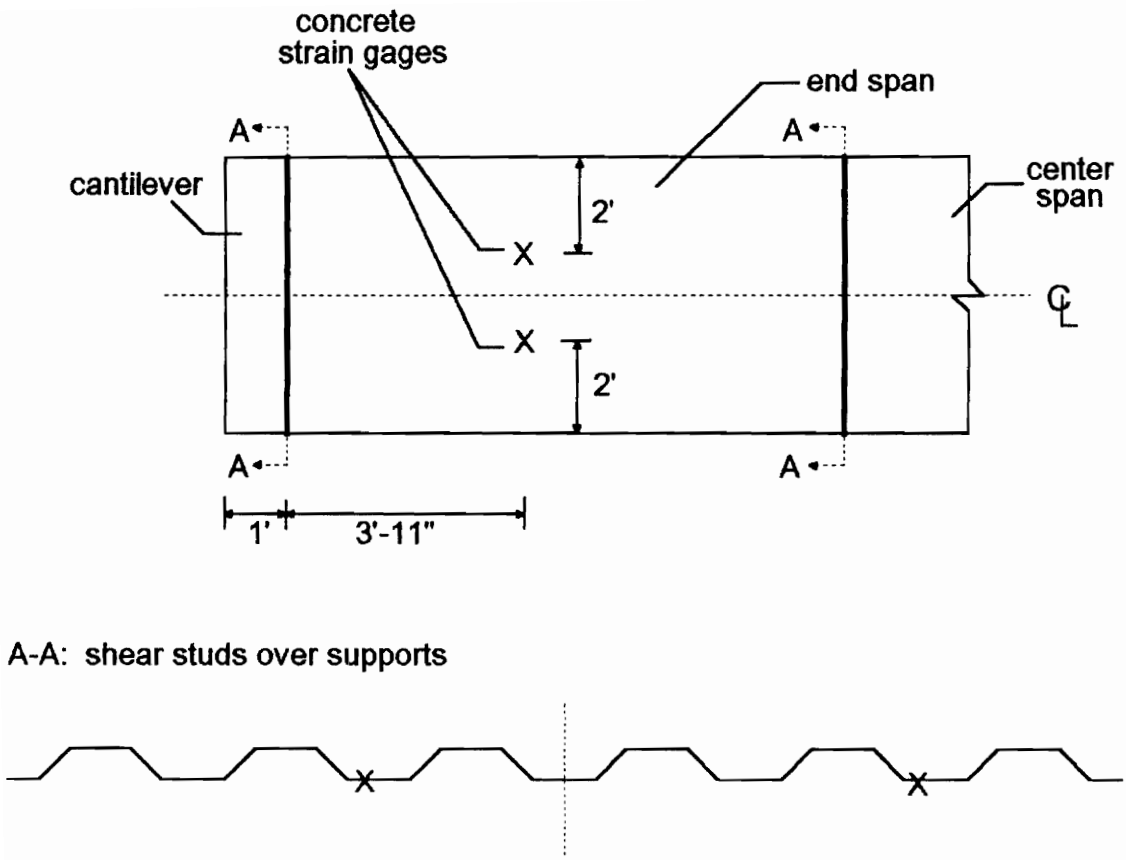

Figure A.30 SDI-2/20-2-9 Concrete Strain Gage and Shear Stud Locations

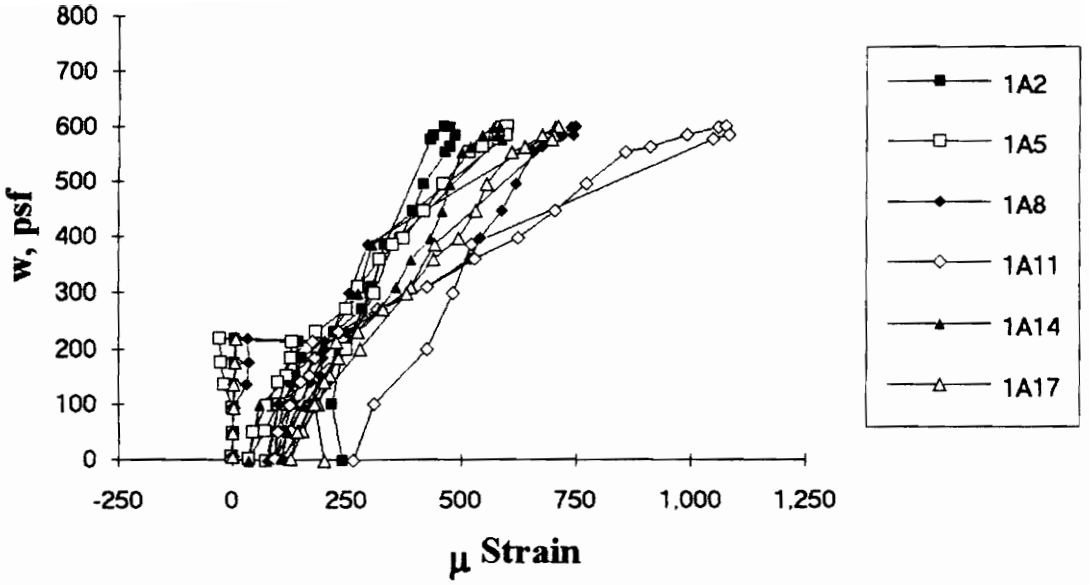

Figure A.31 SDI-2/20-2-9 Load vs. Strain in Deck Top Flange at Exterior Support

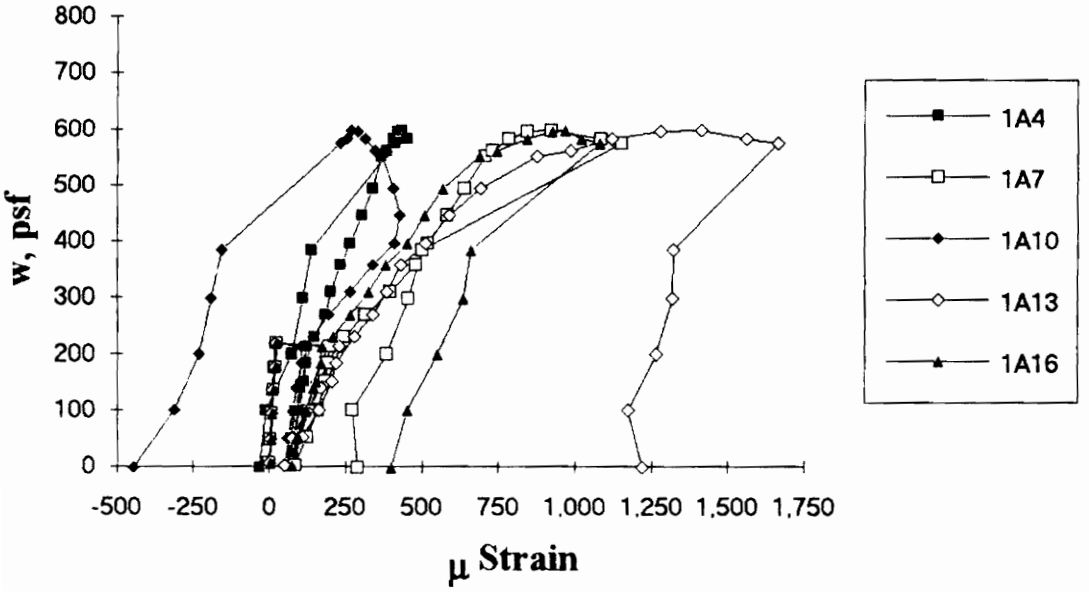

Figure A.32 SDI-2/20-2-9 Load vs. Strain in Deck Web at Exterior Support

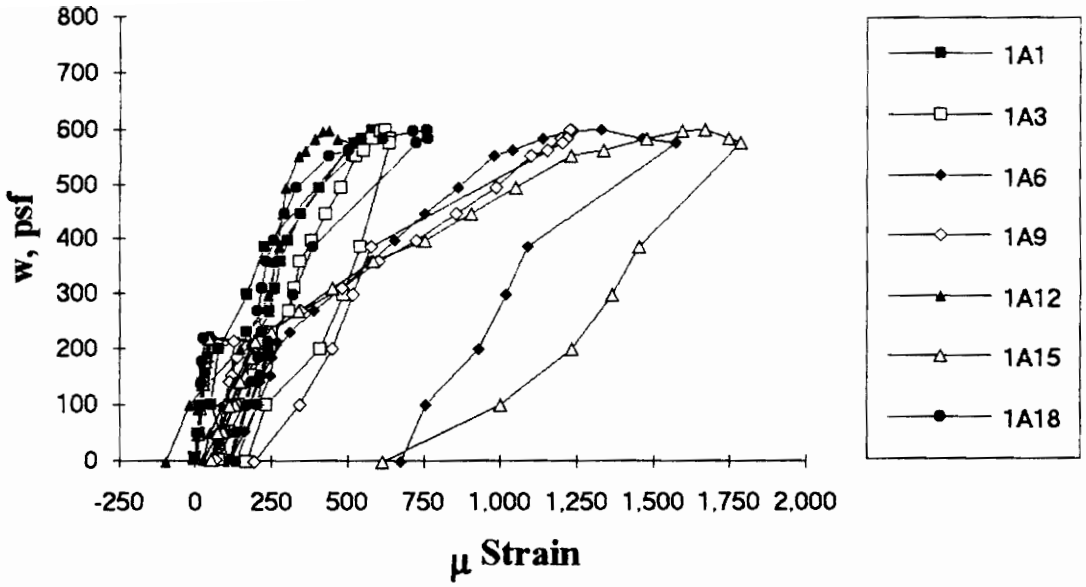

Figure A.33 SDI-2/20-2-9 Load vs. Strain in Deck Bottom Flange at Exterior Support

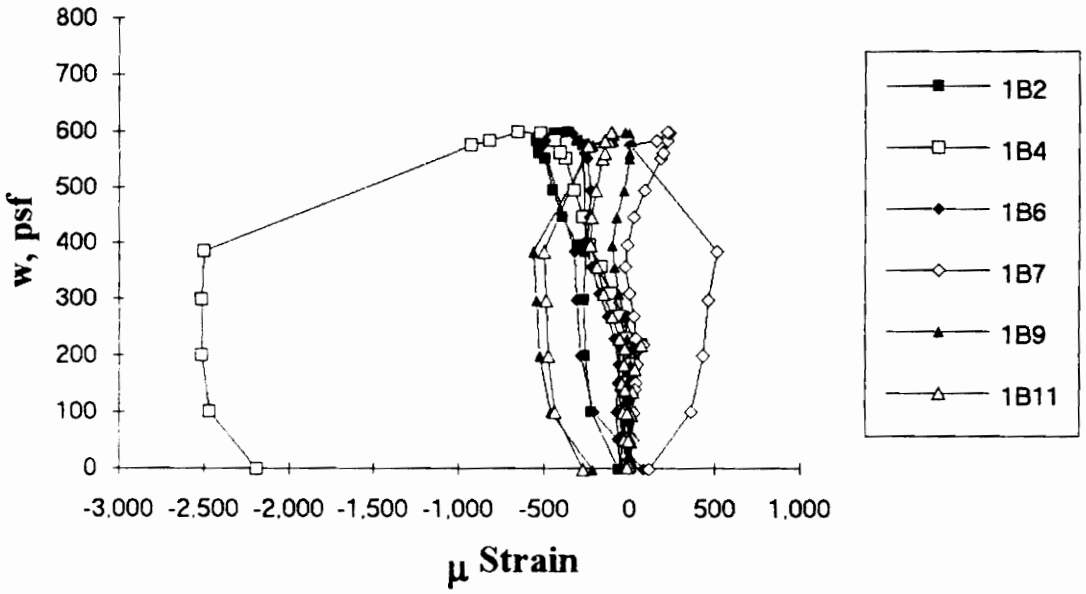

Figure A.34 SDI-2/20-2-9 Load vs. Strain in Deck Top Flange at Maximum Moment

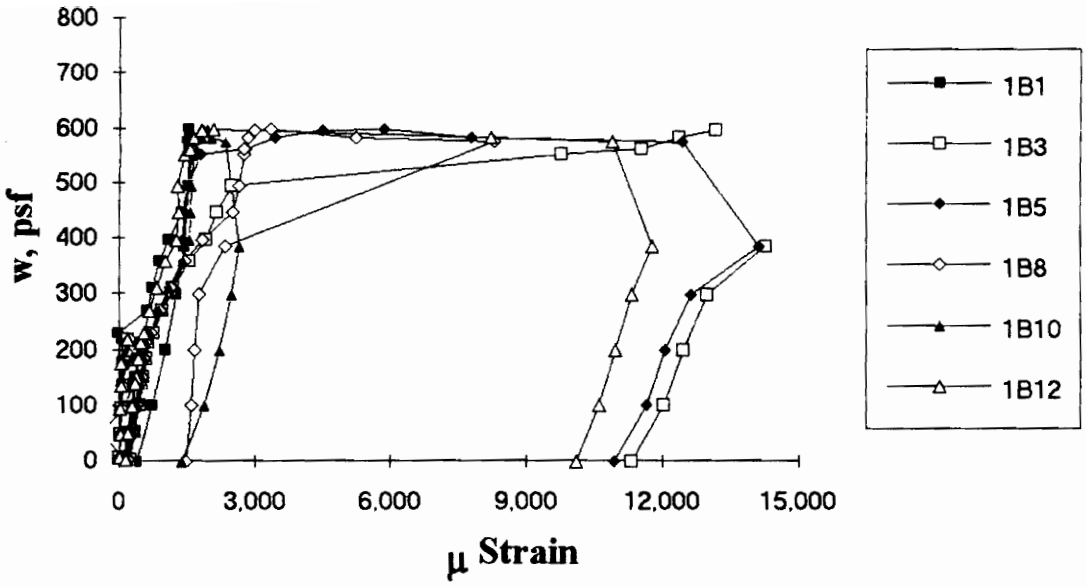

Figure A.35 SDI-2/20-2-9 Load vs. Strain in Deck Bottom Flange at Maximum Moment

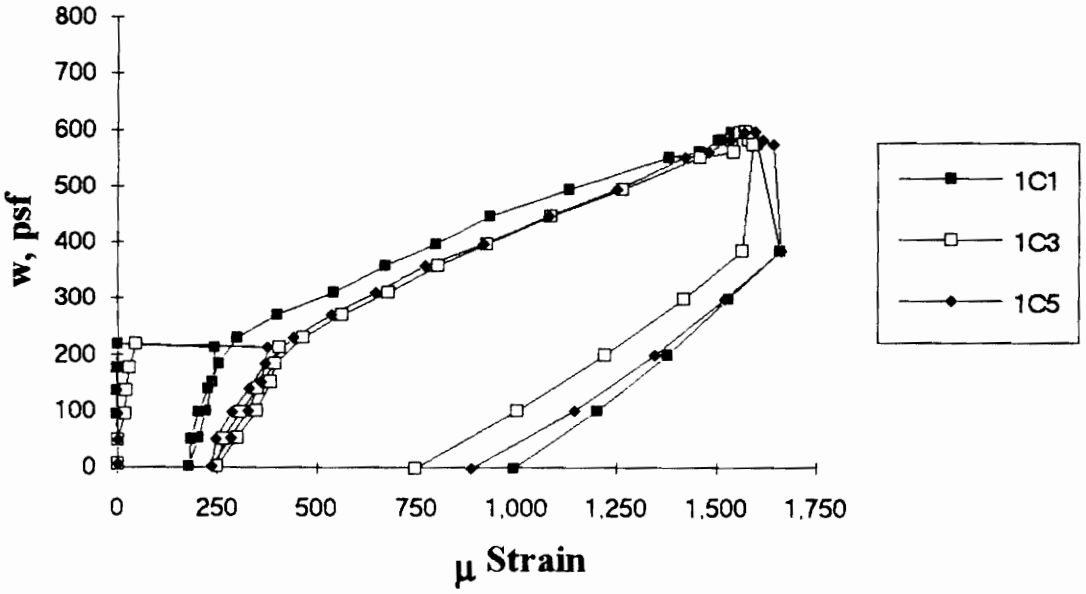

Figure A.36 SDI-2/20-2-9 Load vs. Strain in Deck Top Flange at Interior Support

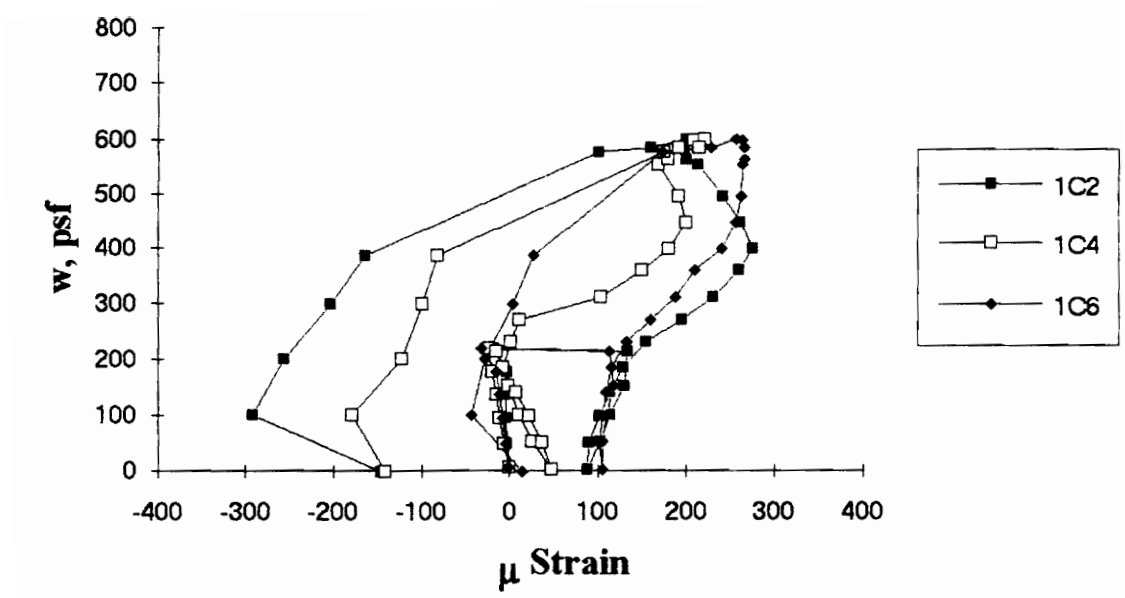

Figure A.37 SDI-2/20-2-9 Load vs. Strain in Deck Bottom Flange at Interior Support

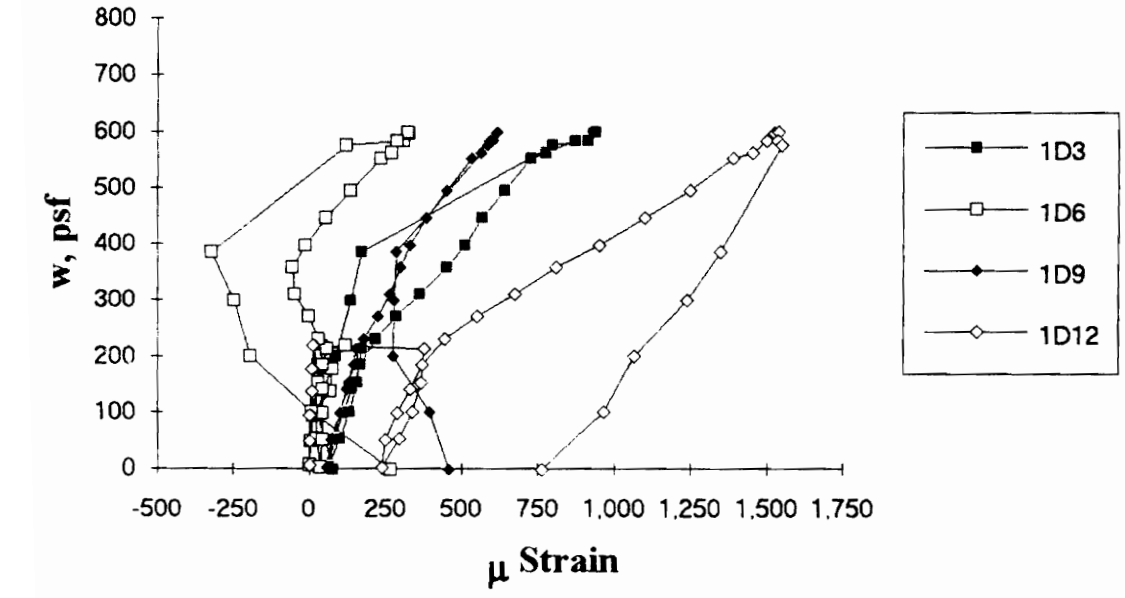

Figure A.38 SDI-2/20-2-9 Load vs. Strain in Deck Top Flange along the Span

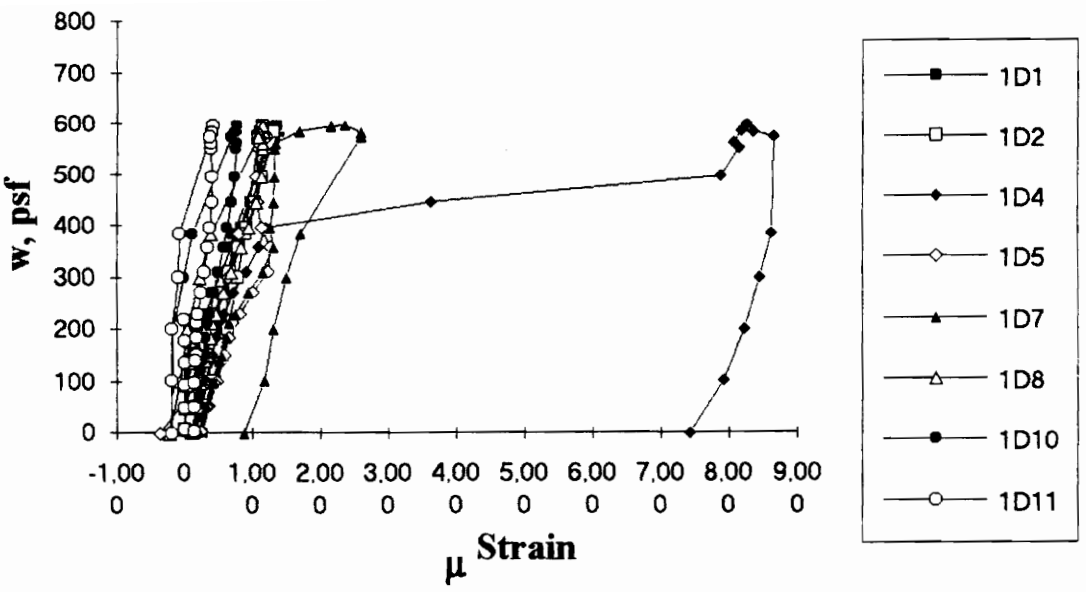

Figure A.39 SDI-2/20-2-9 Load vs. Strain in Deck Bottom Flange along the Span

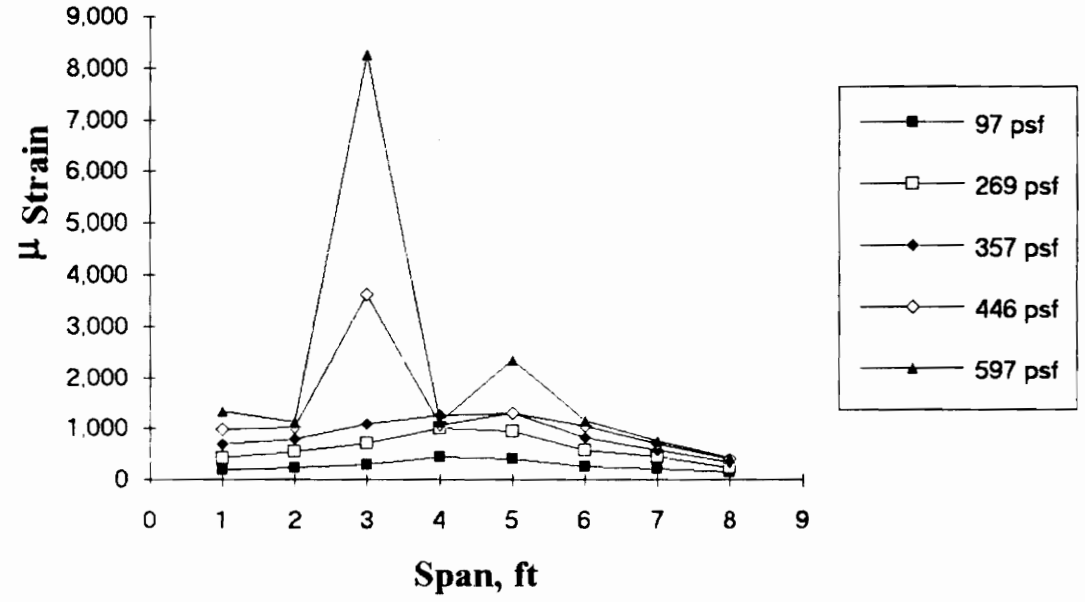

Figure A.40 SDI-2/20-2-9 Strain Variation in Deck Bottom Flange along the Span (from centerline of exterior support)

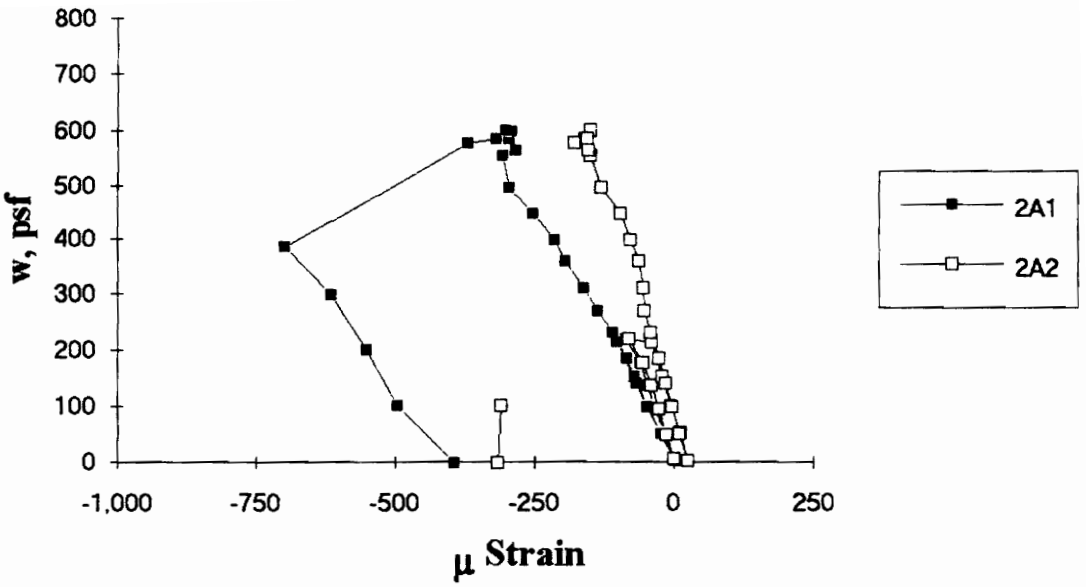

Figure A.41 SDI-2/20-2-9 Load vs. Strain in Deck Bottom Flange in Center Span

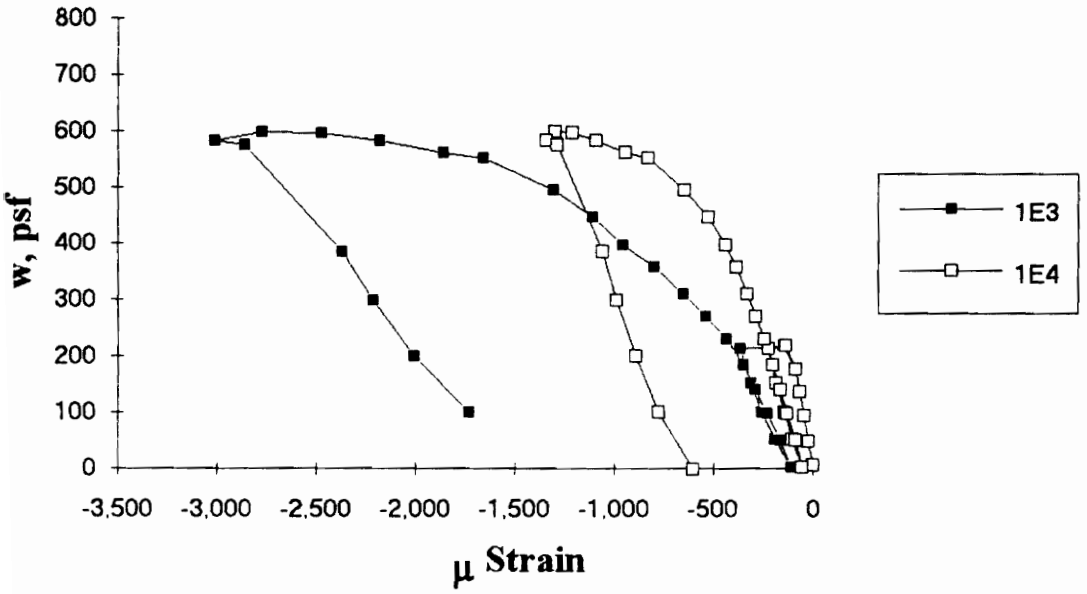

Figure A.42 SDI-2/20-2-9 Load vs. Strain in Concrete at Maximum Moment

Test Designation: SDI-2/20-23-9
Test Date: September 14, 1993

MATERIALS AND DIMENSIONS

General:

width:	6 ft. (2 panels)
span length:	9 ft. center span
end details:	N/A
deck anchorage type:	shear stud, 3-7/8 in. long, 3/4 in. dia.
average anchorage spacing:	3.0 ft. and 2.1 ft.

Deck:

thickness:	0.0345 in. (20 gage)
depth:	2 in.
area:	0.519 $in.^2$/ft.
yield stress:	45.4 ksi
ultimate strength:	52.6 ksi
web embossment type:	N/A

embossment dimensions:

N_b : 1.76 in.	W_b : 0.81 in.	s : 3.07 in.
N_t : 1.19 in.	W_t : 0.58 in.	p_h : 0.15 in.

Concrete:

type:	normal weight
test strength:	5,170 psi
total depth:	4.5 in.
cover depth:	2.5 in.

RESULTS

midspan strain due to fresh concrete:	240 x 10^{-6} in./in.
maximum load:	598 psf
deflection at maximum load:	3.17 in.
deflection at termination of test:	4.58 in.
end slip at maximum load:	N/A
end slip at termination of test:	N/A

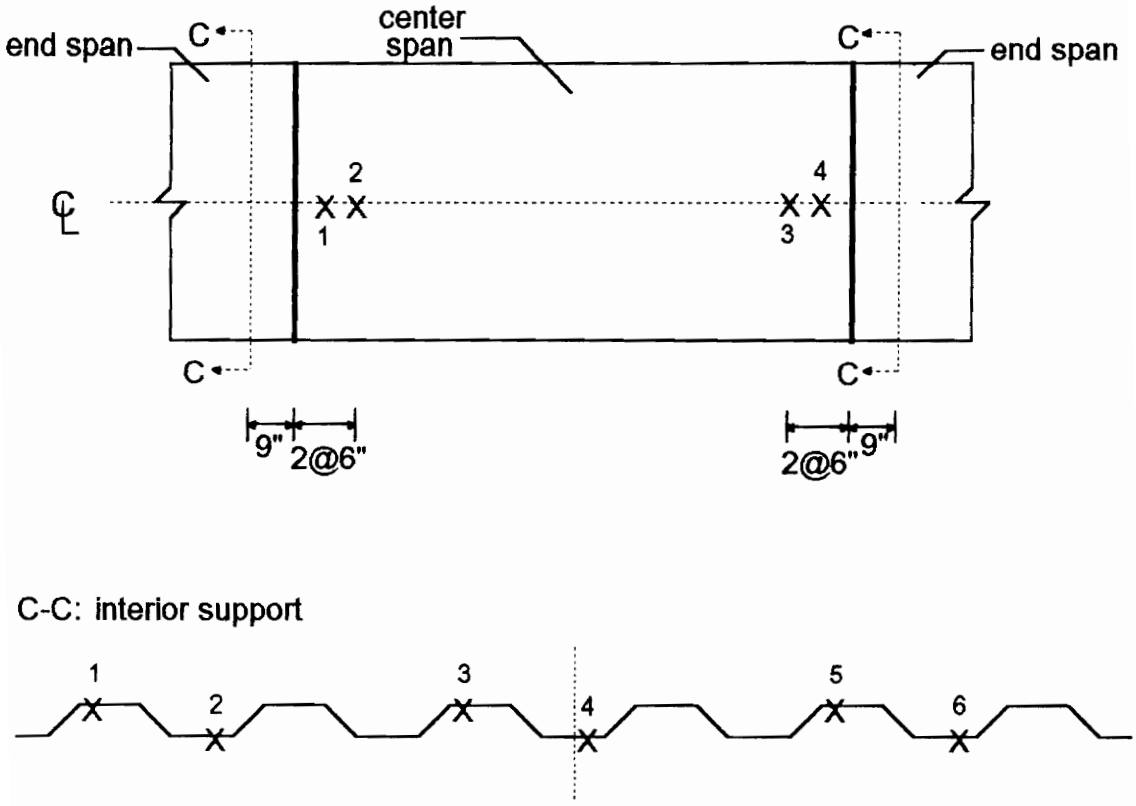

Figure A.43 SDI-2/20-23-9 Steel Deck Strain Gage Locations

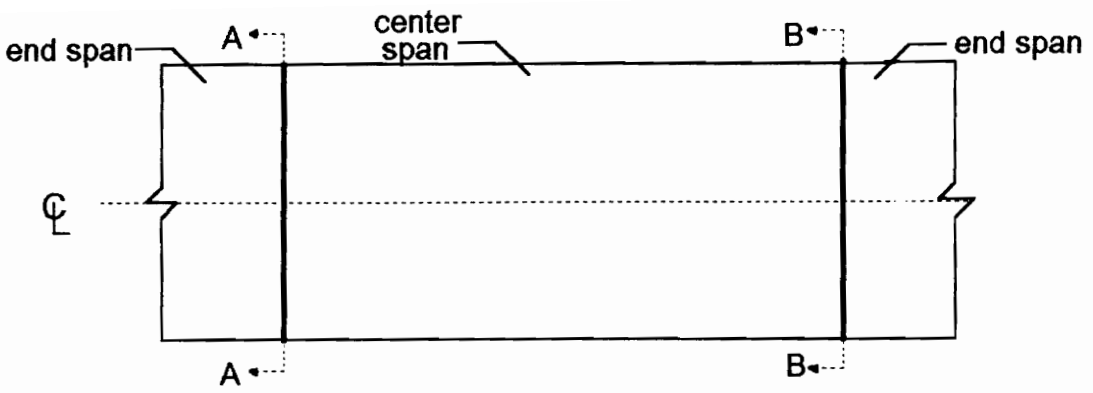

A-A: shear studs over supports

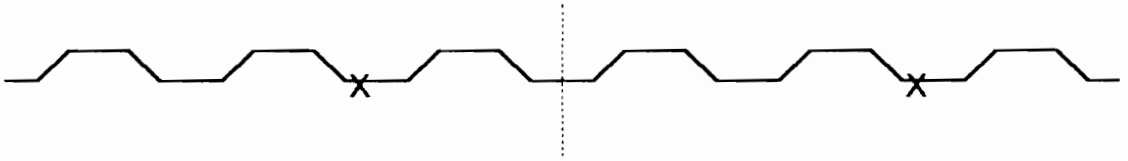

B-B: shear studs over supports

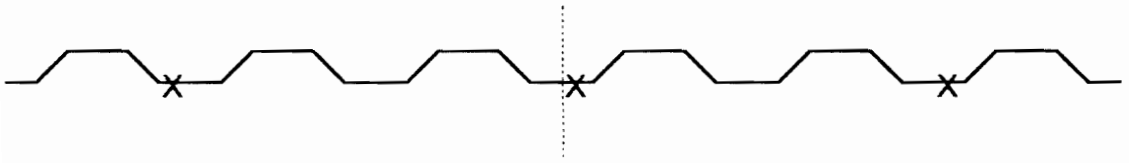

Figure A.44 SDI-2/20-23-9 Shear Stud Locations

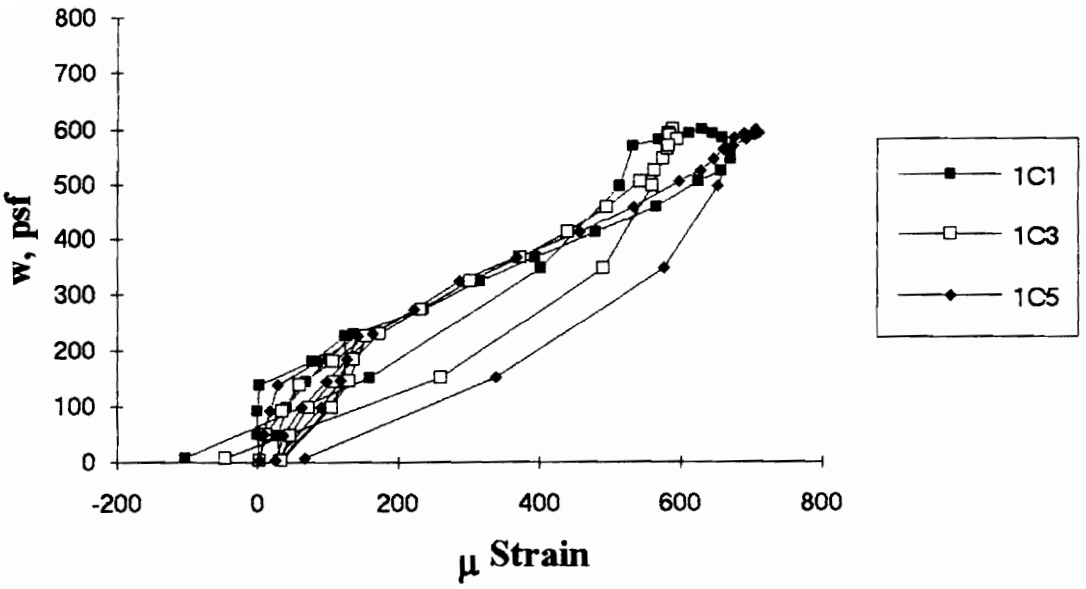

Figure A.45 SDI-2/20-23-9 Load vs. Strain in Deck Top Flange at Interior Support in End Span

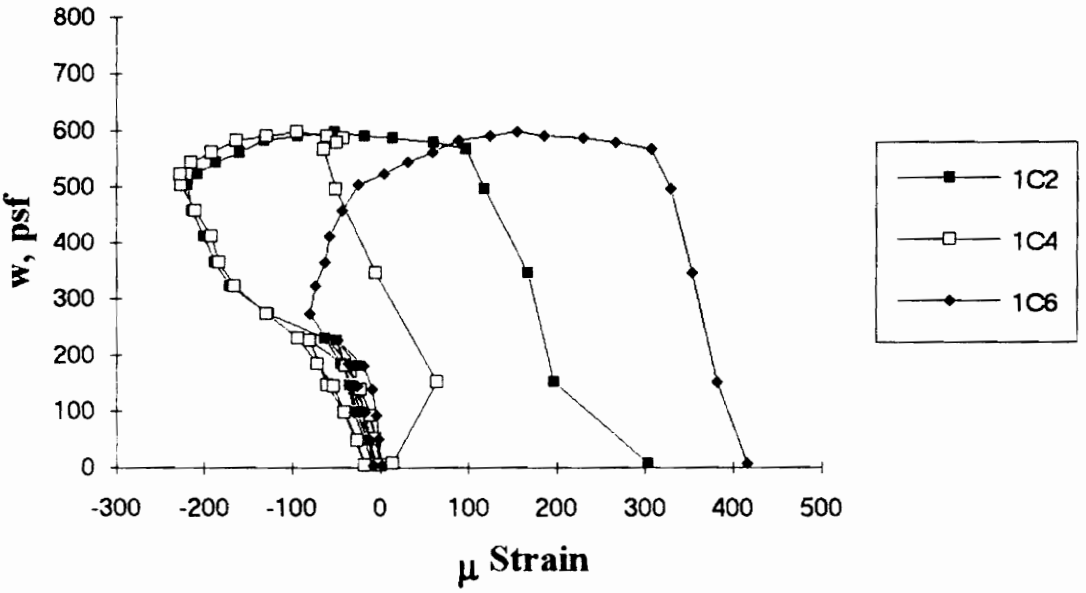

Figure A.46 SDI-2/20-23-9 Load vs. Strain in Deck Bottom Flange at Interior Support in End Span

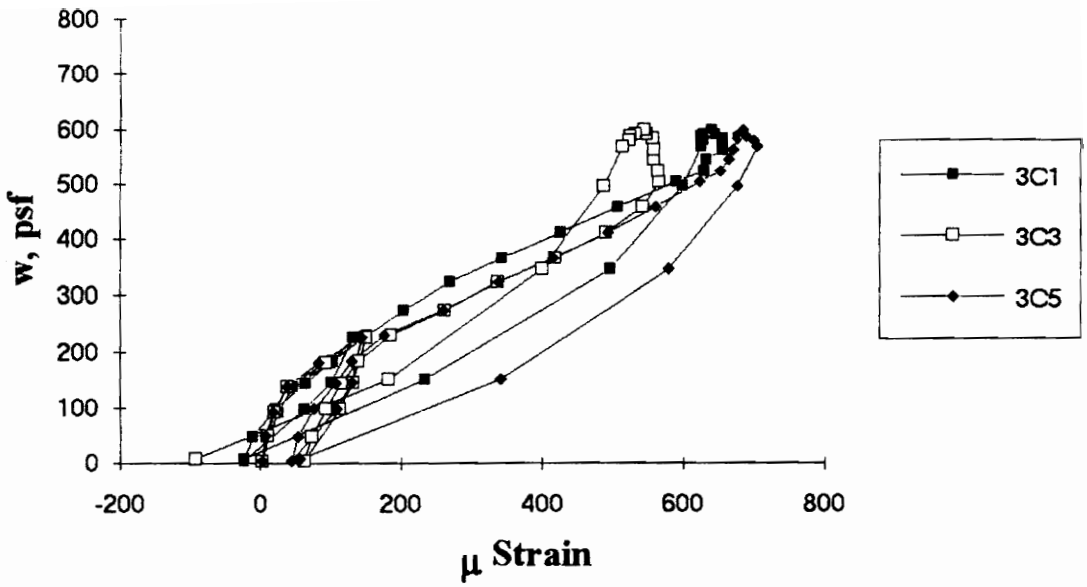

Figure A.47 SDI-2/20-23-9 Load vs. Strain in Deck Top Flange at Interior Support in End Span

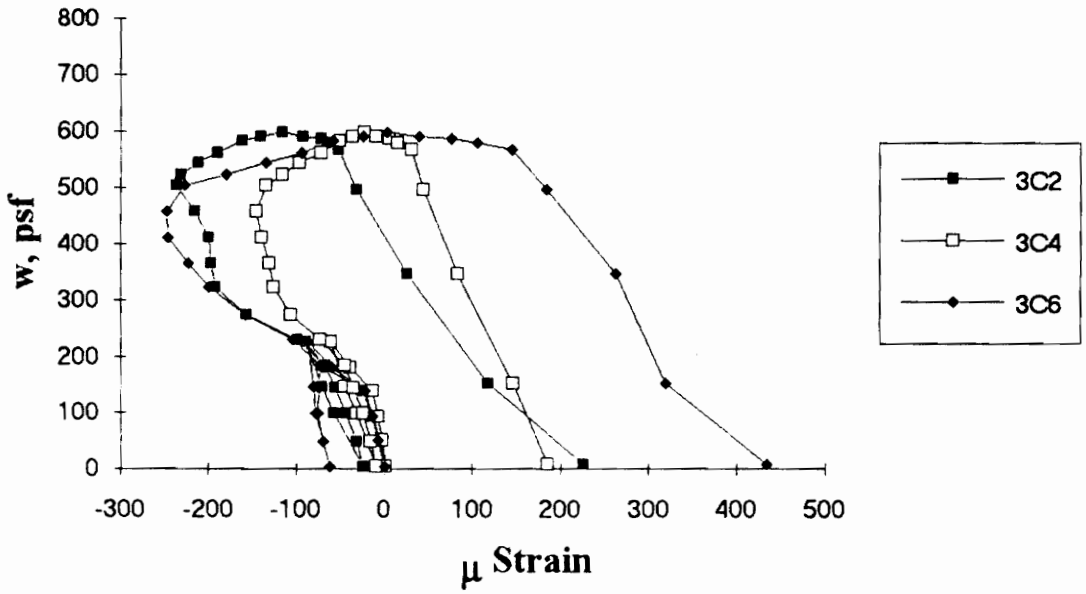

Figure A.48 SDI-2/20-23-9 Load vs. Strain in Deck Bottom Flange at Interior Support in End Span

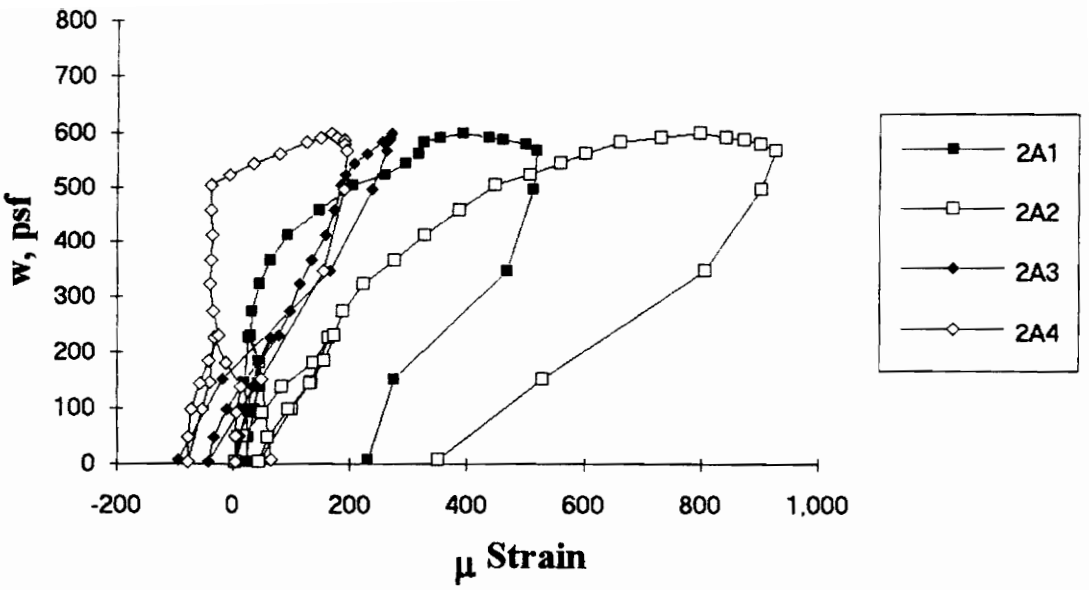

Figure A.49 SDI-2/20-23-9 Load vs. Strain in Deck Bottom Flange at Interior Support in Center Span

Test Designation: SDI-2/20-3-9
Test Date: August 9, 1993

MATERIALS AND DIMENSIONS

General:

width:	6 ft. (2 panels)
span length:	9 ft. end span
end details:	1 ft. cantilever
deck anchorage type:	shear stud, 3-7/8 in. long, 3/4 in. dia.
average anchorage spacing:	2.1 ft.

Deck:

thickness:	0.0345 in. (20 gage)
depth:	2 in.
area:	0.519 $in.^2/ft.$
yield stress:	45.4 ksi
ultimate strength:	52.6 ksi
web embossment type:	N/A

embossment dimensions:

N_b : 1.76 in.	W_b : 0.81 in.	s : 3.07 in.
N_t : 1.19 in.	W_t : 0.58 in.	p_h : 0.15 in.

Concrete:

type:	normal weight
test strength:	5,170 psi
total depth:	4.5 in.
cover depth:	2.5 in.

RESULTS

midspan strain due to fresh concrete:	240 x 10^{-6} in./in.
maximum load:	602 psf
deflection at maximum load:	2.35 in.
deflection at termination of test:	4.24 in.
end slip at maximum load:	0.12 in.
end slip at termination of test:	0.51 in.

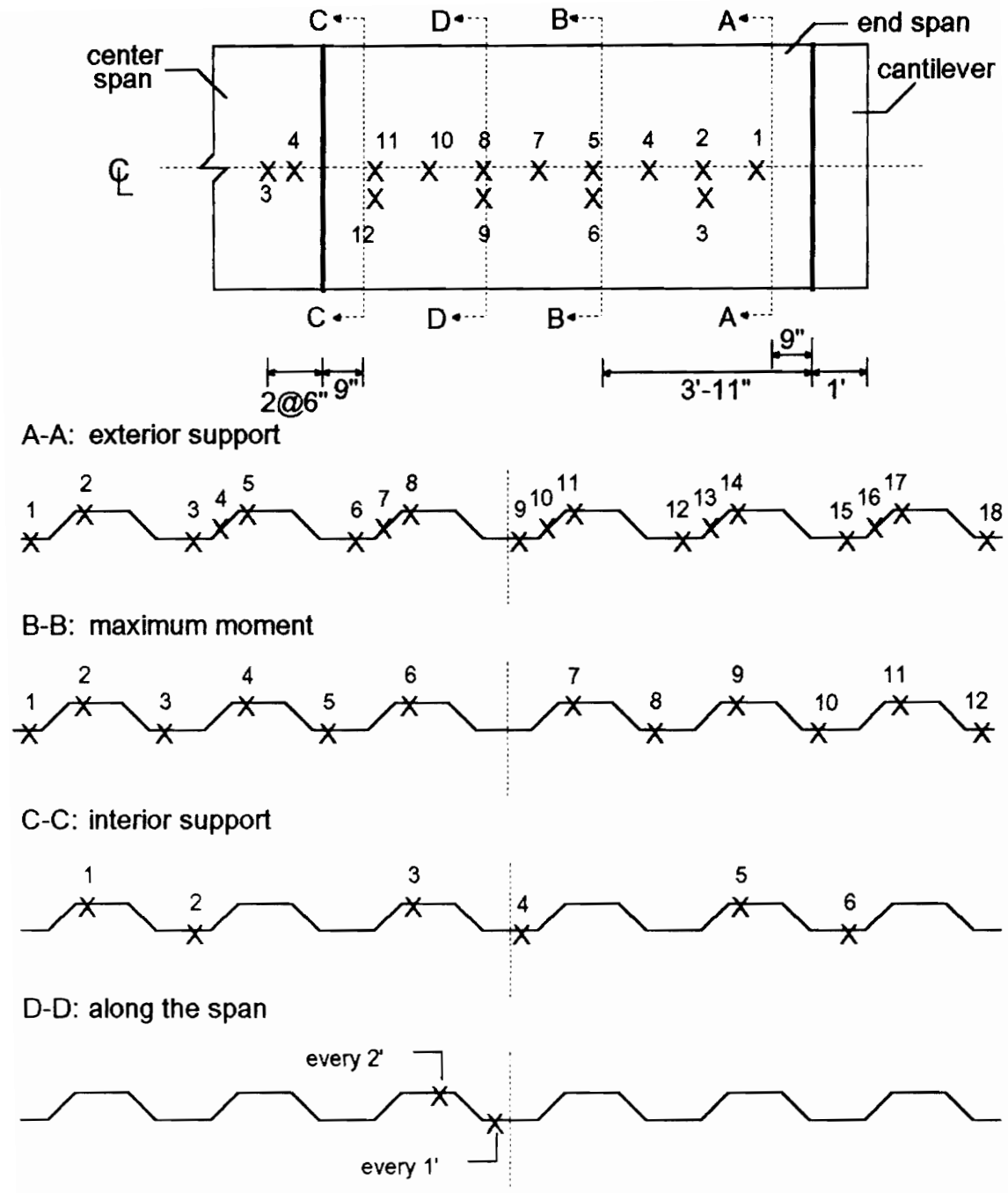

Figure A.50 SDI-2/20-3-9 Steel Deck Strain Gage Locations

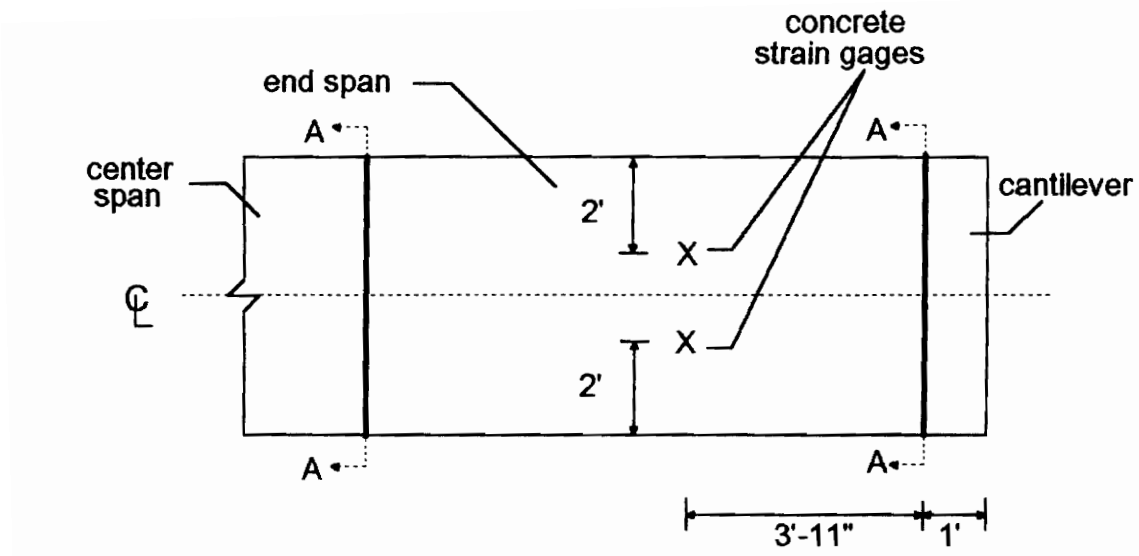

A-A: shear studs over supports

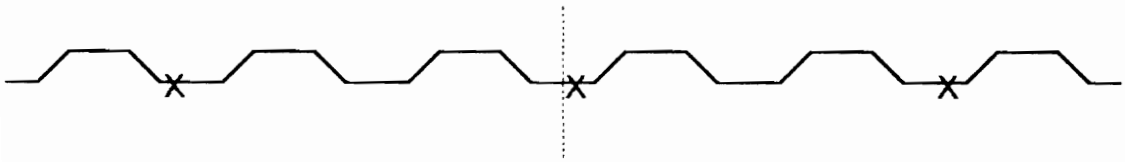

Figure A.51 SDI-2/20-3-9 Concrete Strain Gage and Shear Stud Locations

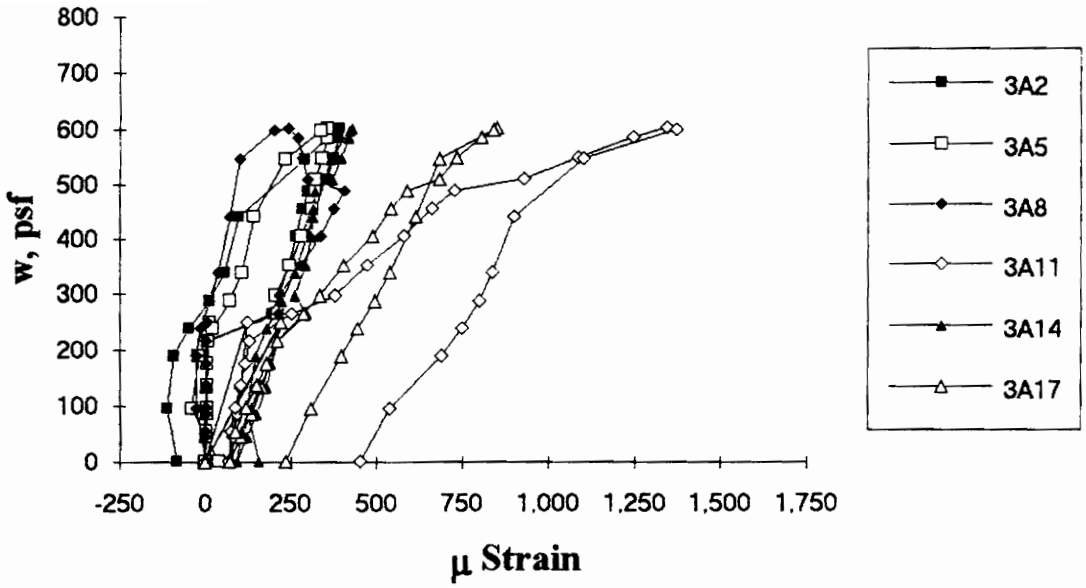

Figure A.52 SDI-2/20-3-9 Load vs. Strain in Deck Top Flange at Exterior Support

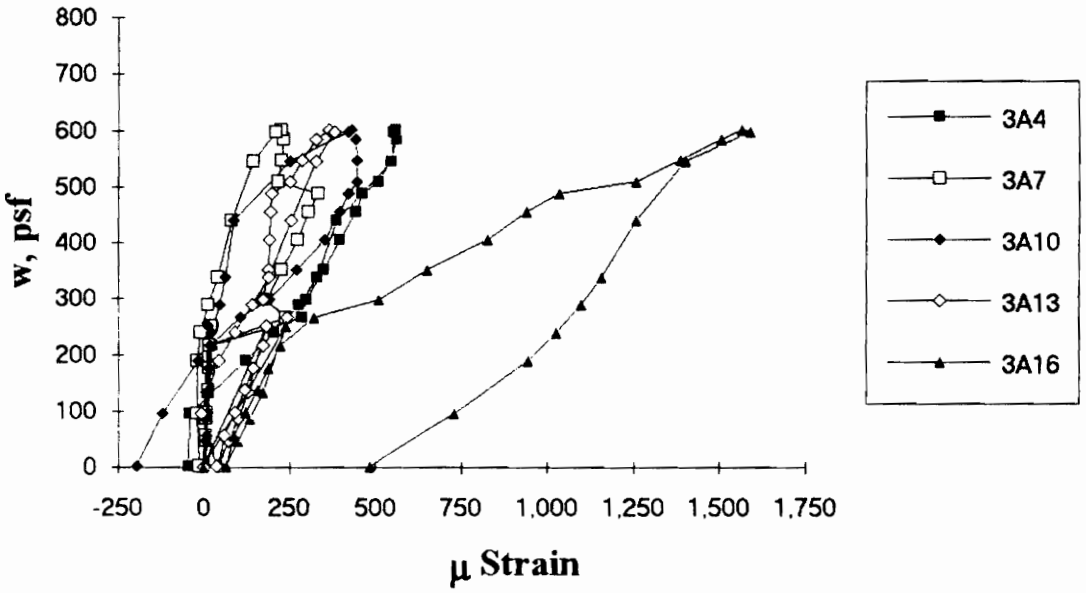

Figure A.53 SDI-2/20-3-9 Load vs. Strain in Deck Web at Exterior Support

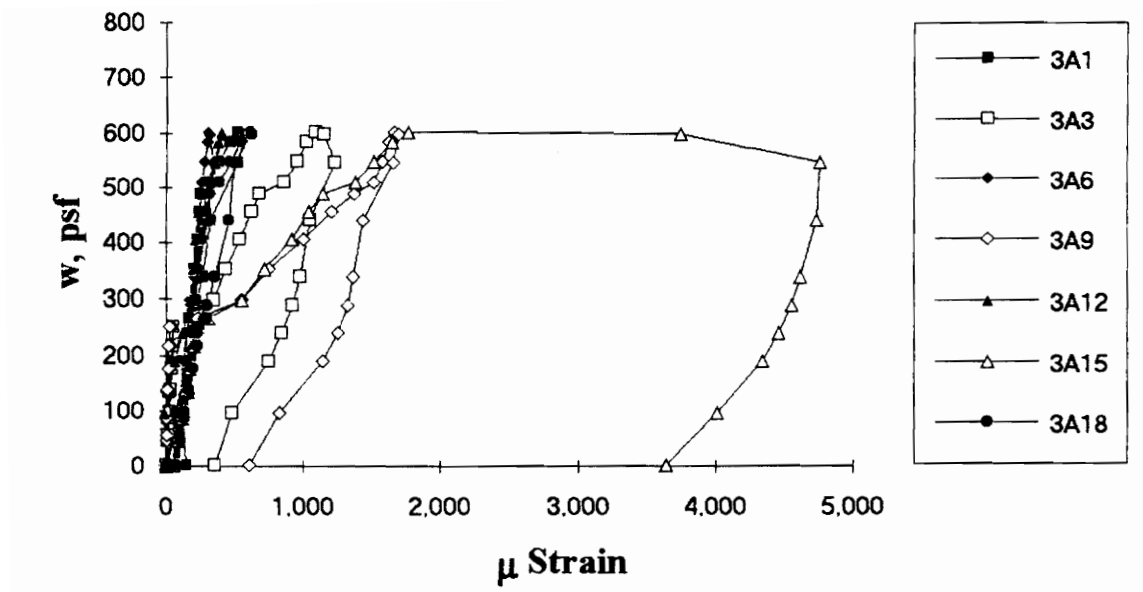

Figure A.54 SDI-2/20-3-9 Load vs. Strain in Deck Bottom Flange at Exterior Support

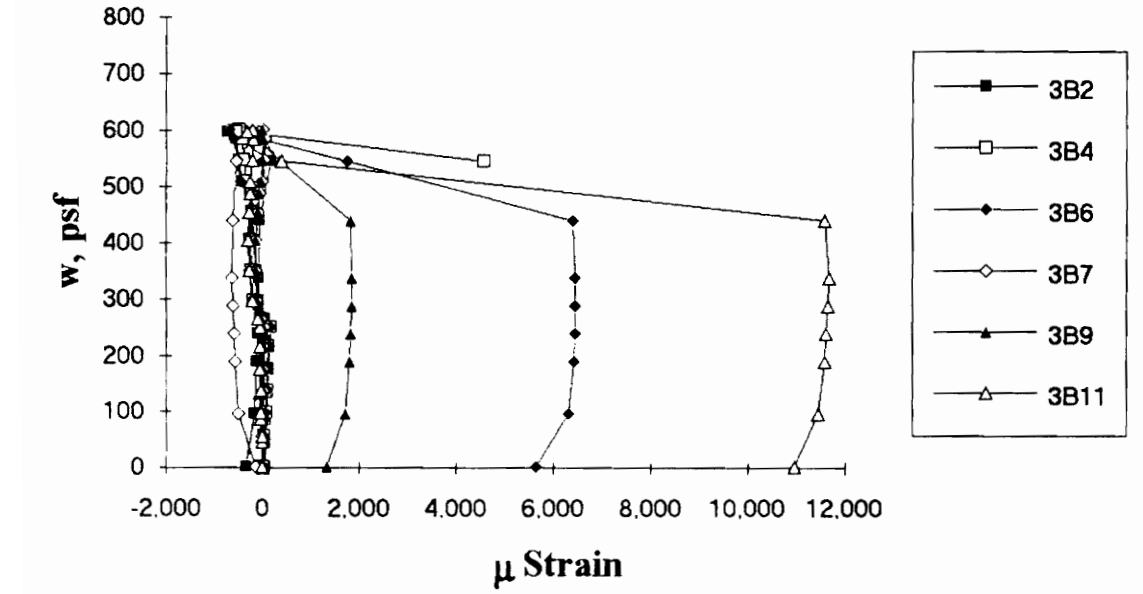

Figure A.55 SDI-2/20-3-9 Load vs. Strain in Deck Top Flange at Maximum Moment

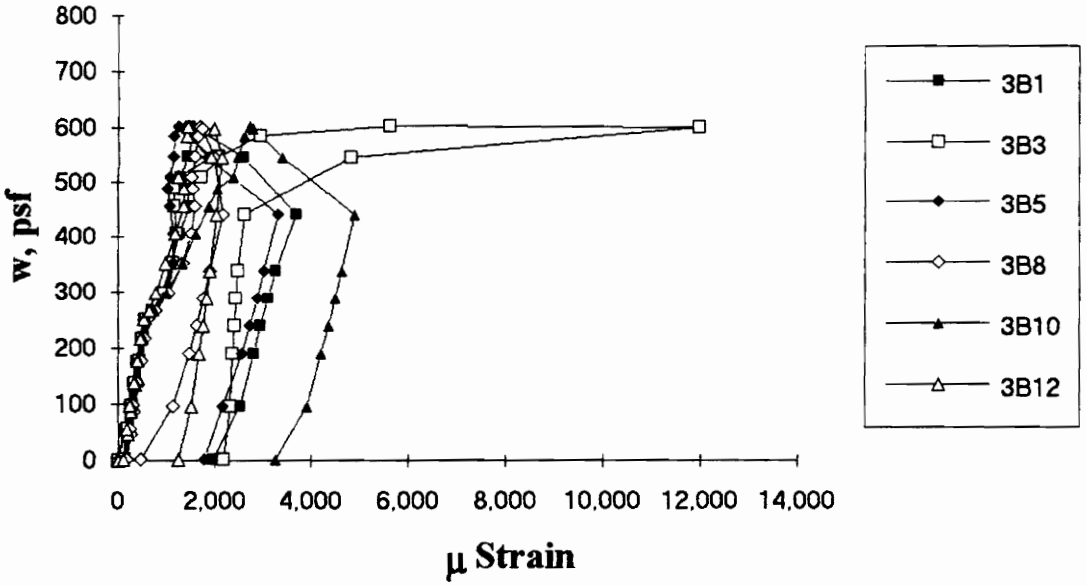

Figure A.56 SDI-2/20-3-9 Load vs. Strain in Deck Bottom Flange at Maximum Moment

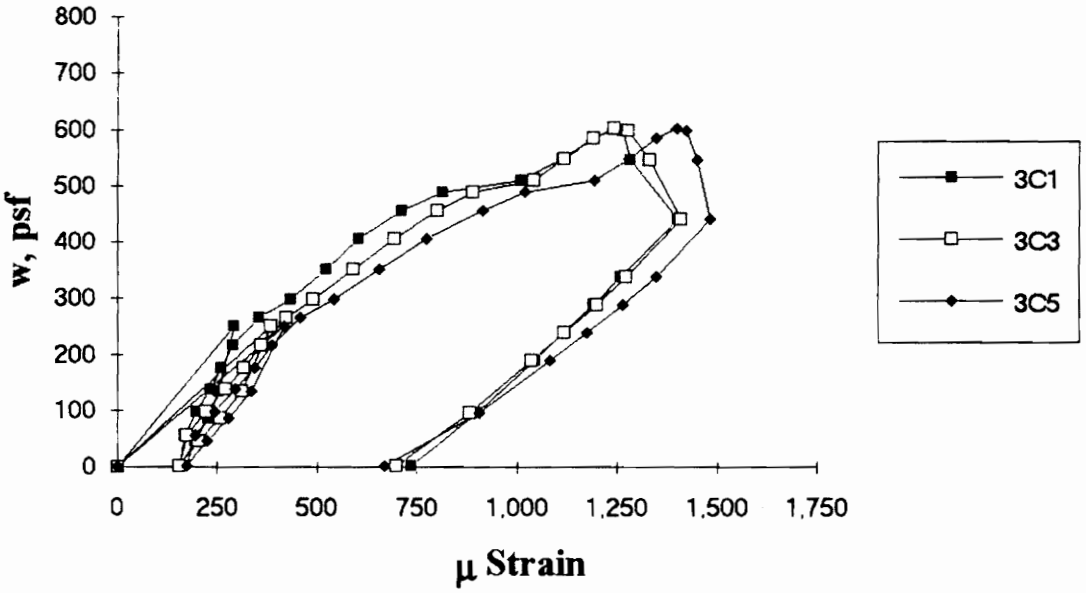

Figure A.57 SDI-2/20-3-9 Load vs. Strain in Deck Top Flange at Interior Support

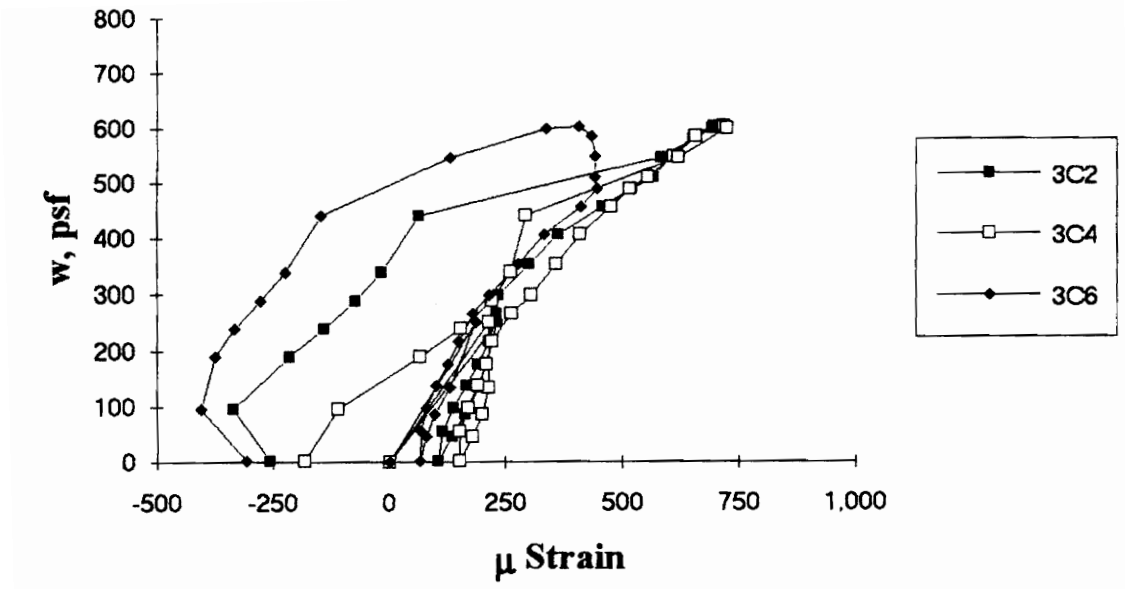

Figure A.58 SDI-2/20-3-9 Load vs. Strain in Deck Bottom Flange at Interior Support

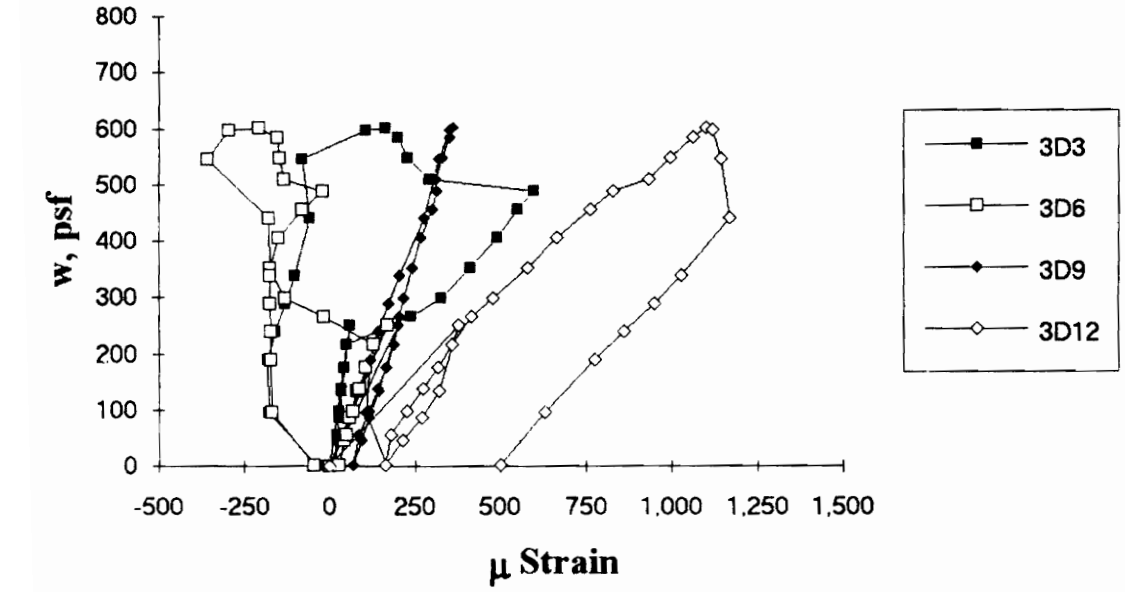

Figure A.59 SDI-2/20-3-9 Load vs. Strain in Deck Top Flange along the Span

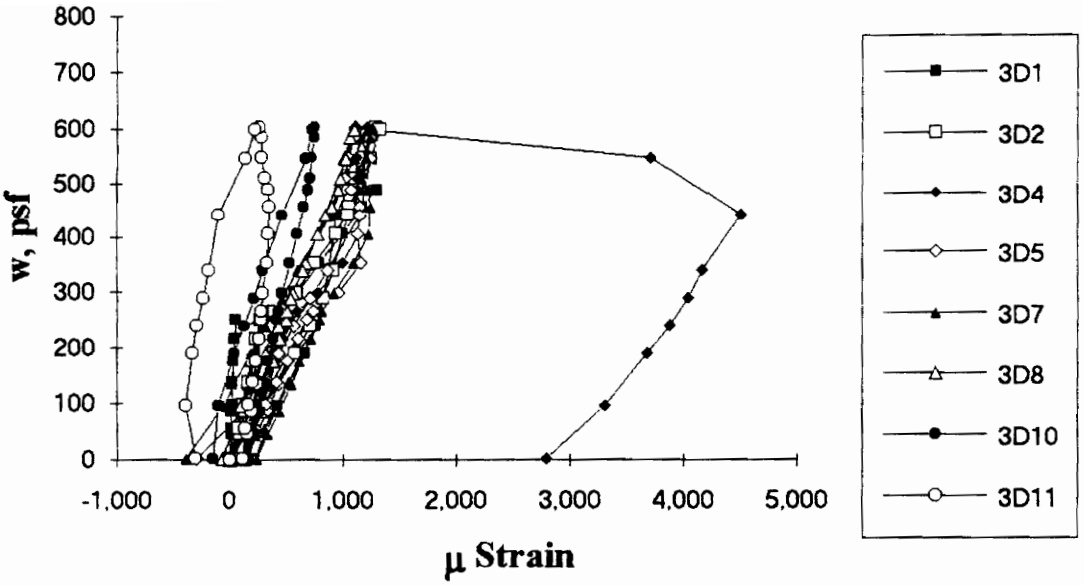

Figure A.60 SDI-2/20-3-9 Load vs. Strain in Deck Bottom Flange along the Span

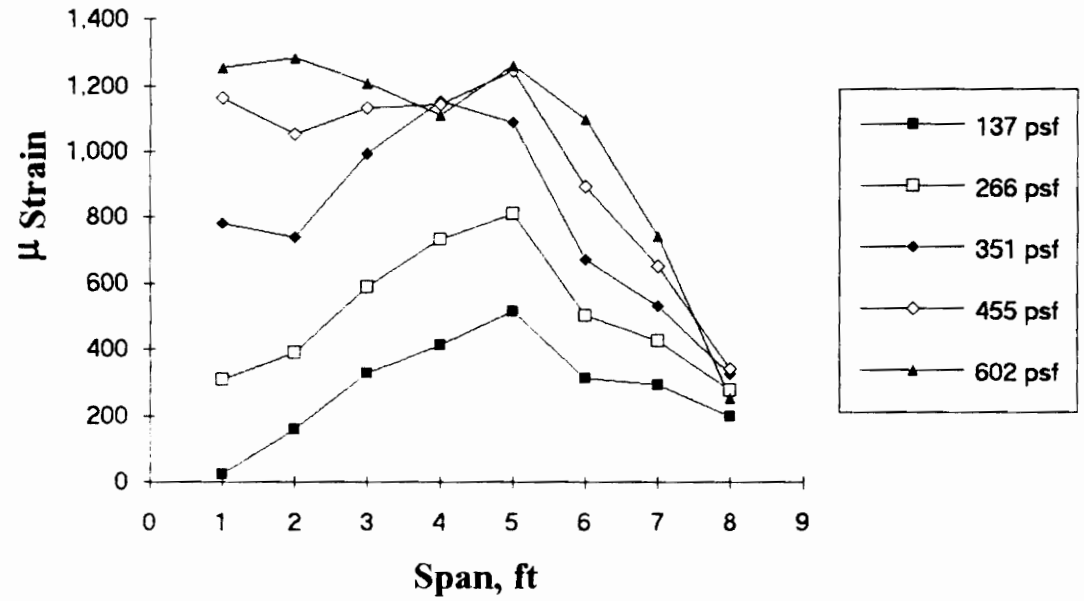

Figure A.61 SDI-2/20-3-9 Strain Variation in Deck Bottom Flange along the Span (from centerline of exterior support)

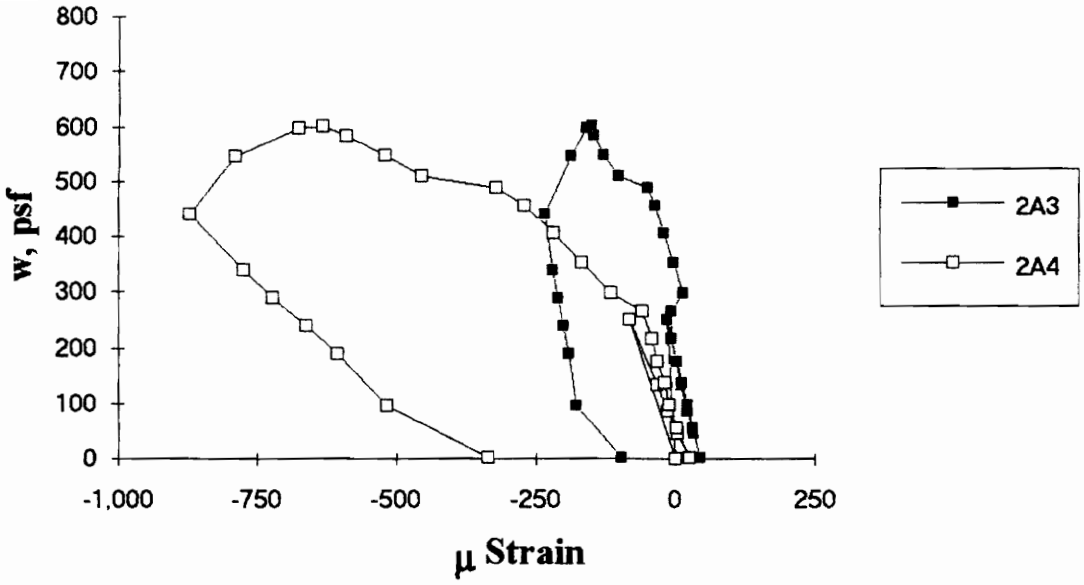

Figure A.62 SDI-2/20-3-9 Load vs. Strain in Deck Bottom Flange in Center Span

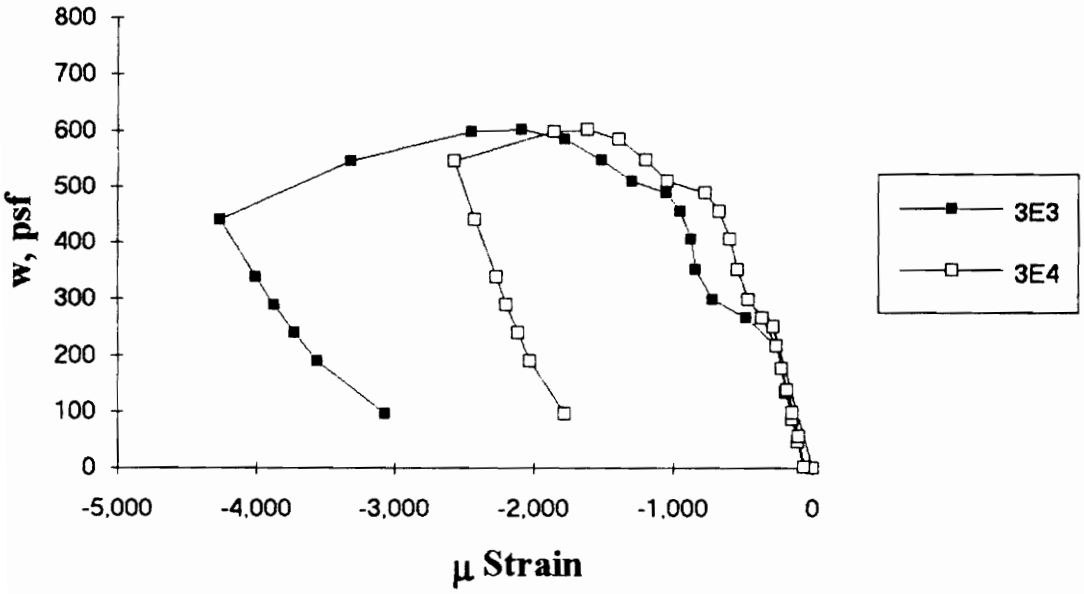

Figure A.63 SDI-2/20-3-9 Load vs. Strain in Concrete at Maximum Moment

Test Designation: SDI-2/20-P1-9
Test Date: November 11, 1993

MATERIALS AND DIMENSIONS

General:

width:	6 ft. (2 panels)
span length:	9 ft. end span
end details:	1 ft. cantilever
deck anchorage type:	arc spot weld, 3/4 in. dia.
average anchorage spacing:	1.0 ft.

Deck:

thickness:	0.0345 in. (20 gage)
depth:	2 in.
area:	0.519 $in.^2/ft.$
yield stress:	45.4 ksi
ultimate strength:	52.6 ksi
web embossment type:	N/A

embossment dimensions:

N_b :	1.76 in.	W_b :	0.81 in.	s :	3.07 in.
N_t :	1.19 in.	W_t :	0.58 in.	p_h :	0.15 in.

Concrete:

type:	normal weight
test strength:	3,340 psi
total depth:	4.5 in.
cover depth:	2.5 in.

RESULTS

midspan strain due to fresh concrete:	250 x 10^{-6} in./in.
maximum load:	492 psf
deflection at maximum load:	1.76 in.
deflection at termination of test:	3.43 in.
end slip at maximum load:	0.16 in.
end slip at termination of test:	0.73 in.

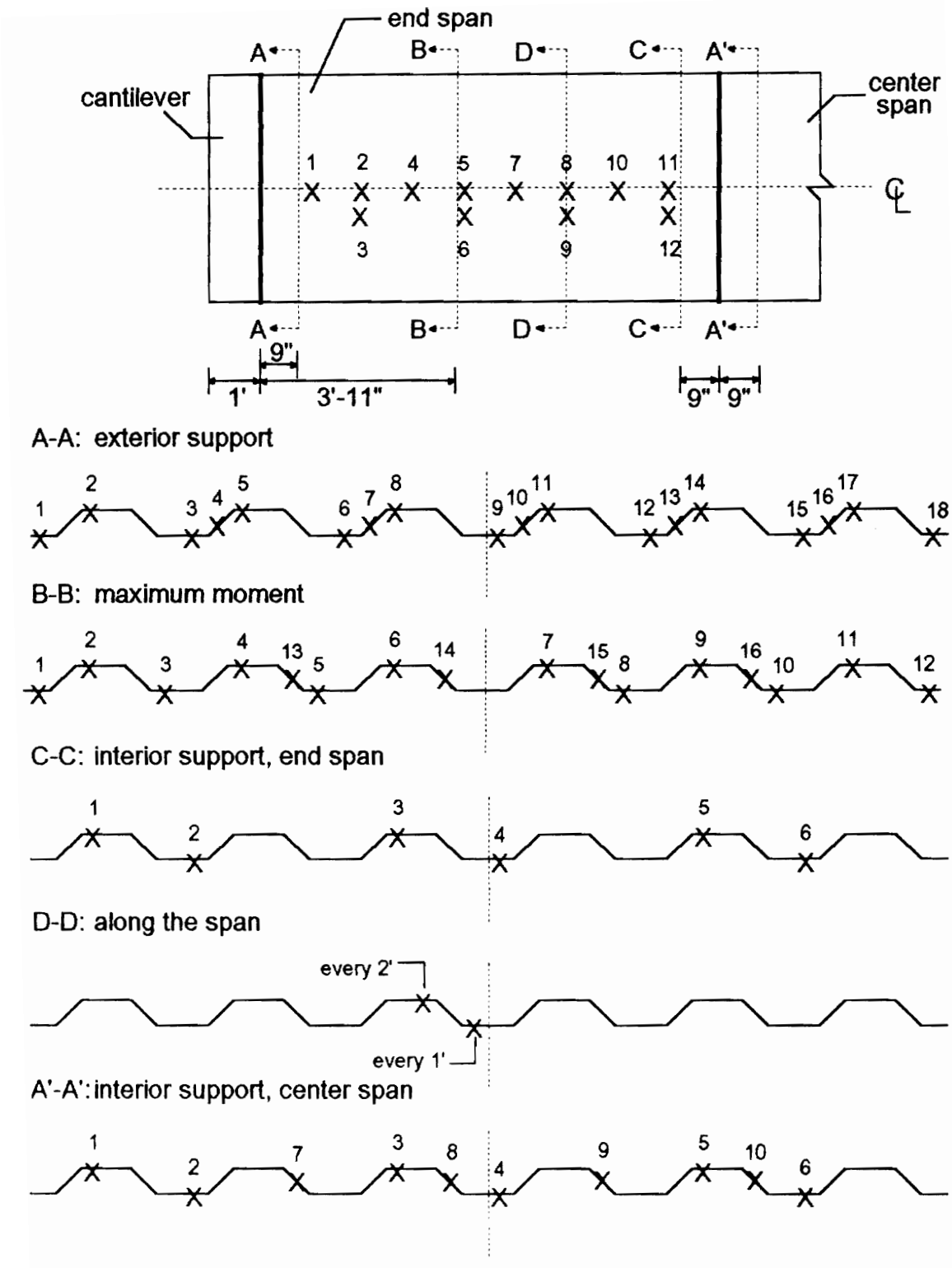

Figure A.64 SDI-2/20-P1-9 Steel Deck Strain Gage Locations

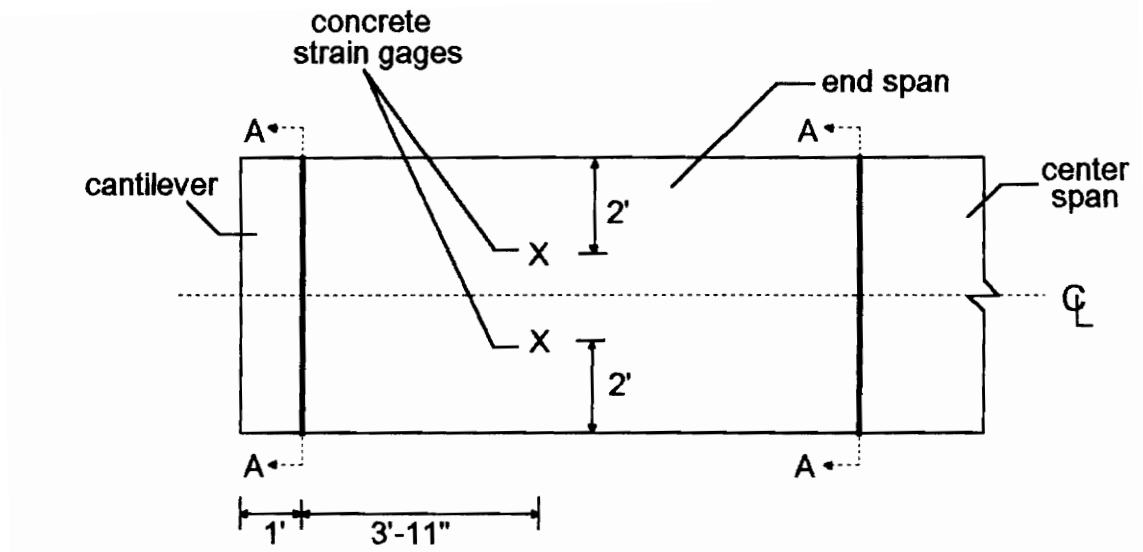

A-A: arc spot welds over supports

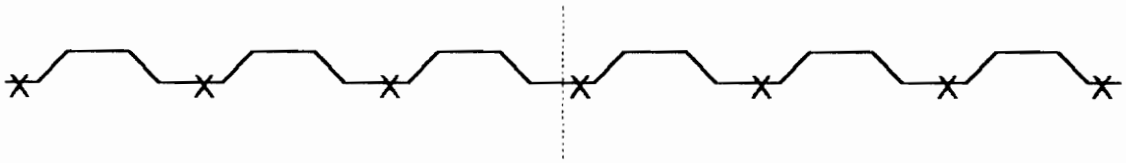

Figure A.65 SDI-2/20-P1-9 Concrete Strain Gage and Arc Spot Weld Locations

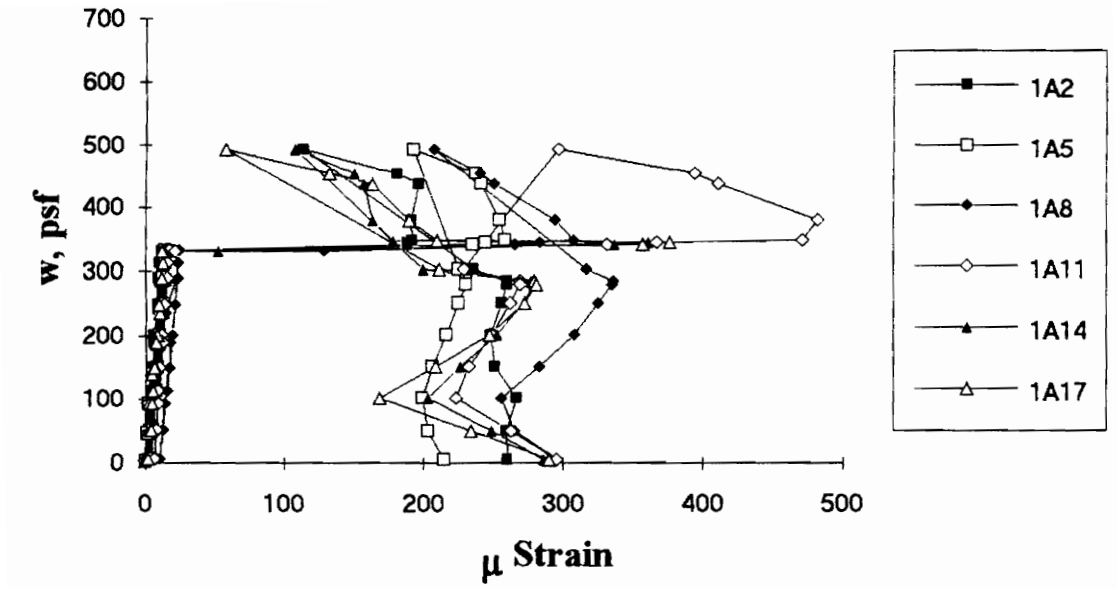

Figure A.66 SDI-2/20-P1-9 Load vs. Strain in Deck Top Flange at Exterior Support

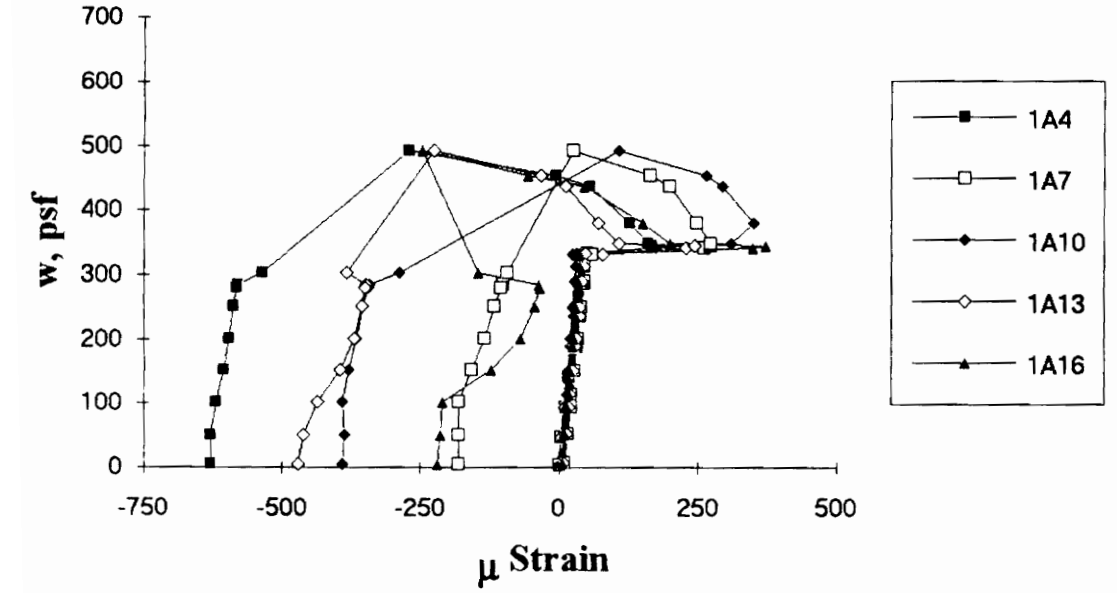

Figure A.67 SDI-2/20-P1-9 Load vs. Strain in Deck Web at Exterior Support

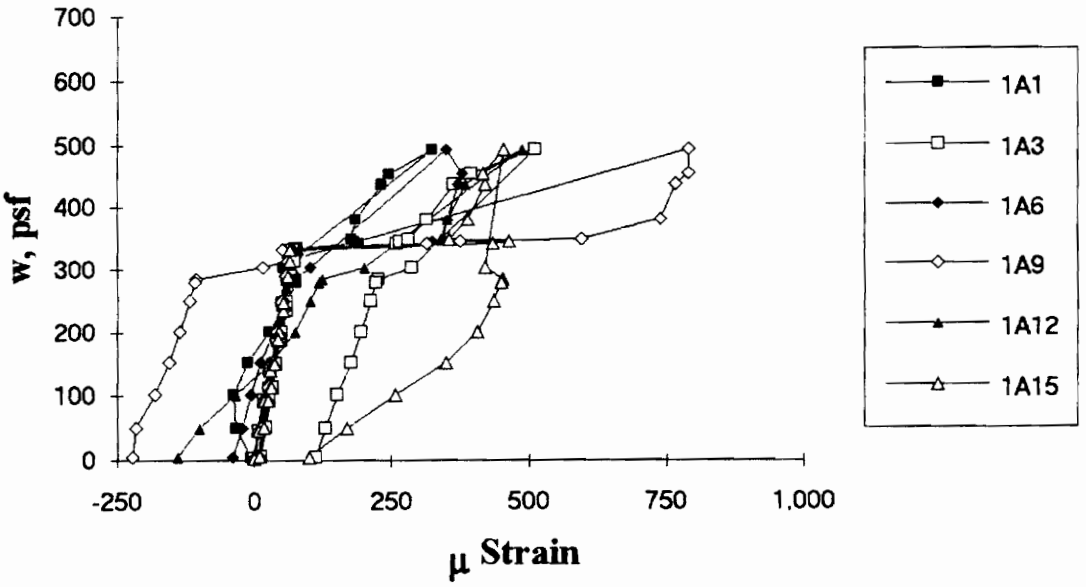

Figure A.68 SDI-2/20-P1-9 Load vs. Strain in Deck Bottom Flange at Exterior Support

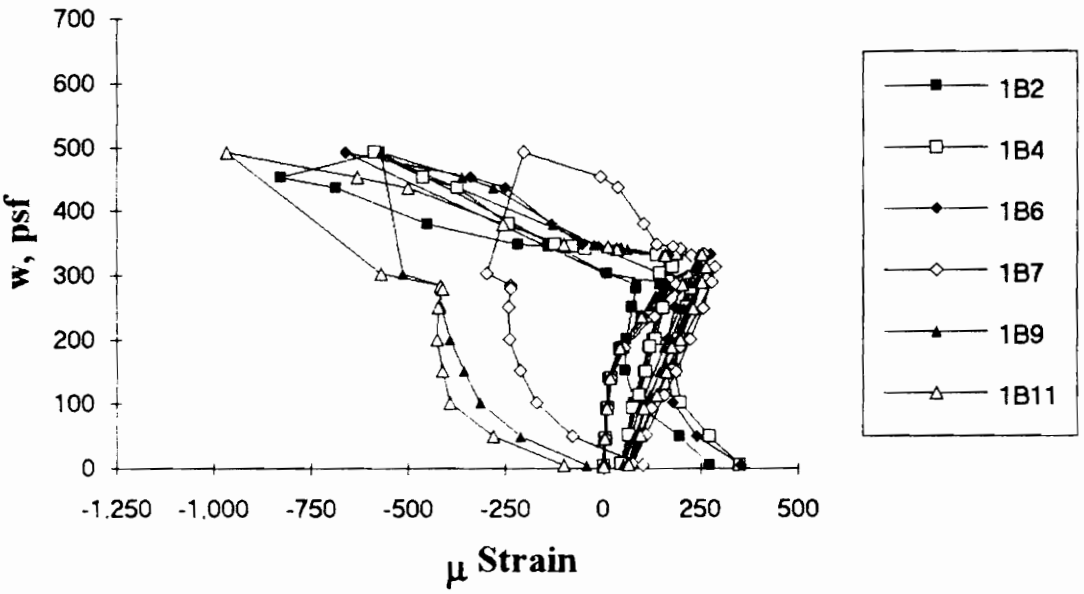

Figure A.69 SDI-2/20-P1-9 Load vs. Strain in Deck Top Flange at Maximum Moment

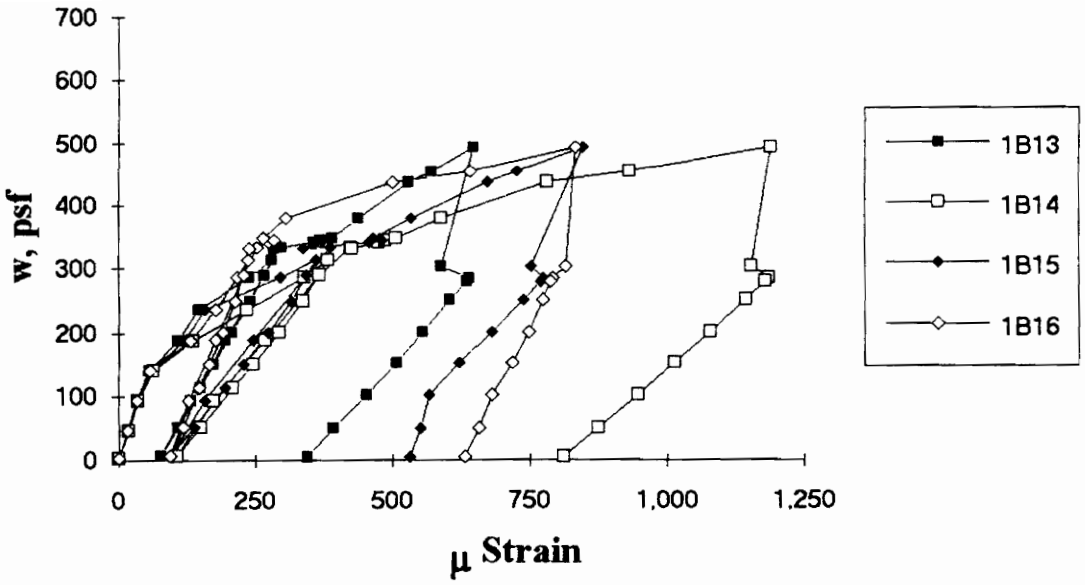

Figure A.70 SDI-2/20-P1-9 Load vs. Strain in Deck Web at Maximum Moment

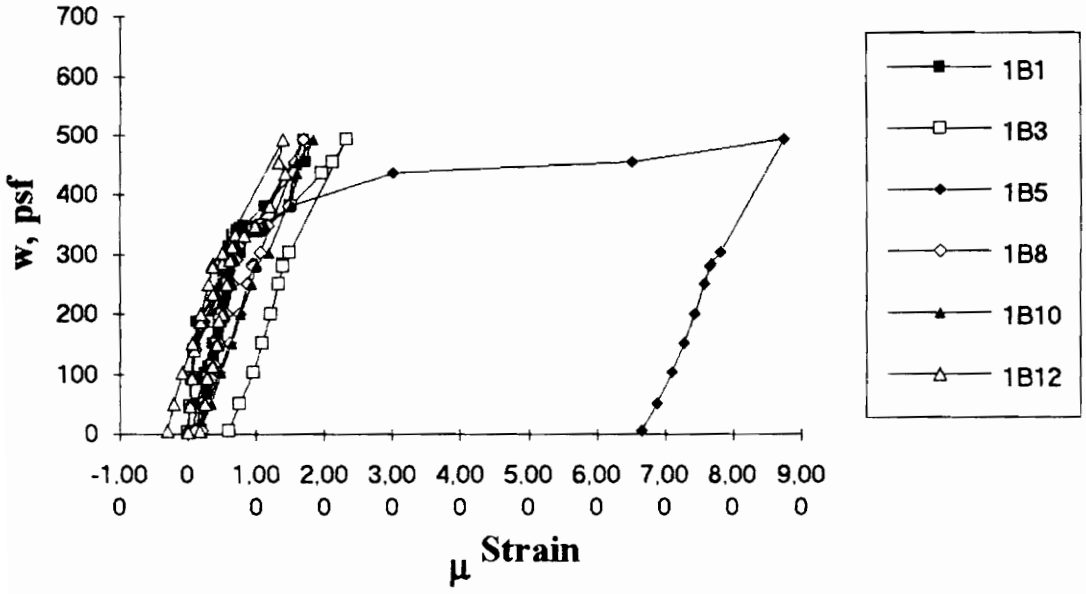

Figure A.71 SDI-2/20-P1-9 Load vs. Strain in Deck Bottom Flange at Maximum Moment

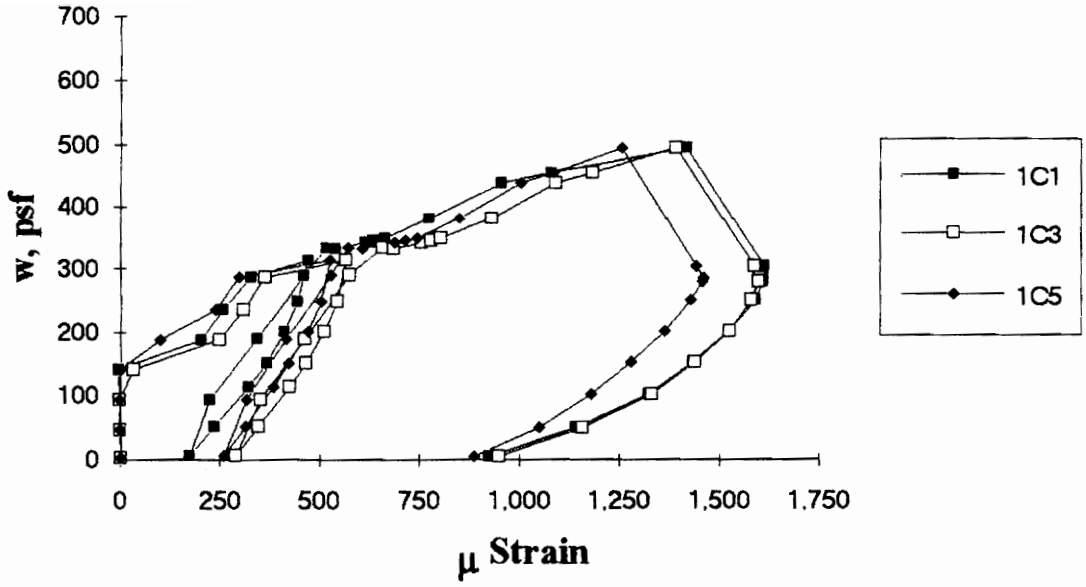

Figure A.72 SDI-2/20-P1-9 Load vs. Strain in Deck Top Flange at Interior Support

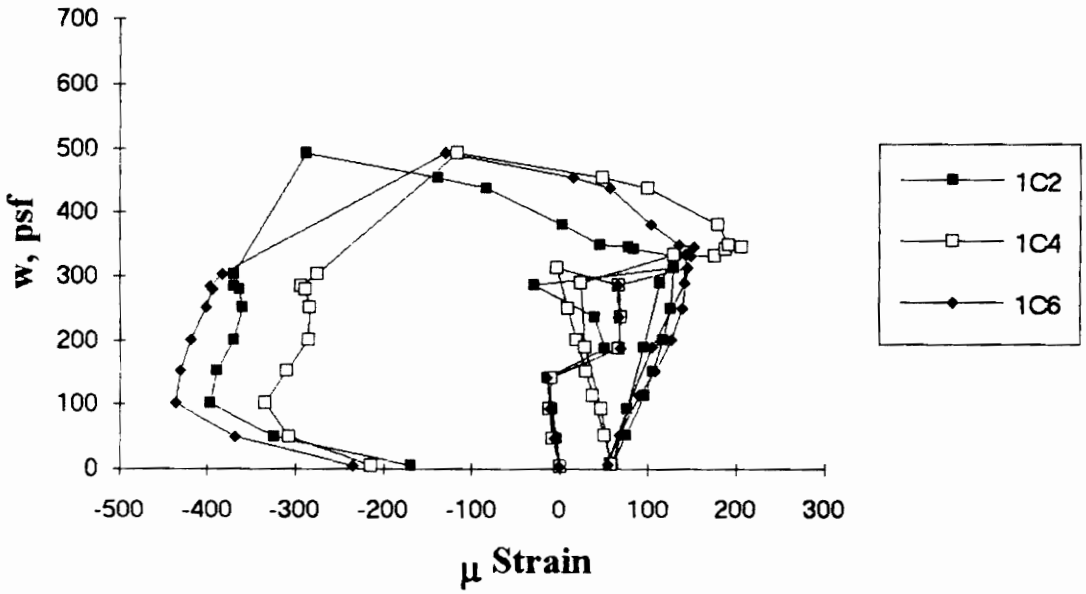

Figure A.73 SDI-2/20-P1-9 Load vs. Strain in Deck Bottom Flange at Interior Support

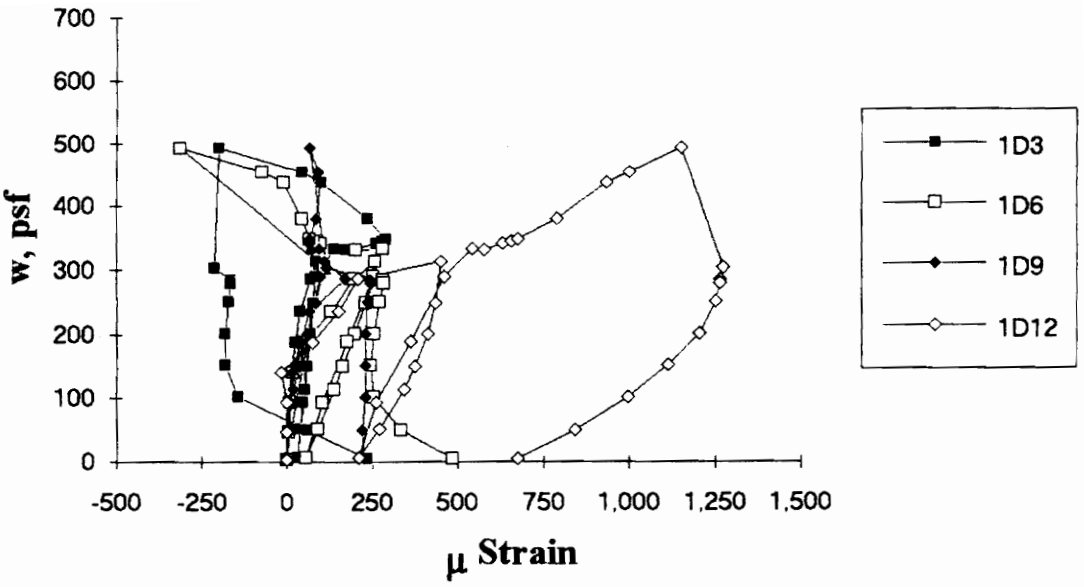

Figure A.74 SDI-2/20-P1-9 Load vs. Strain in Deck Top Flange along the Span

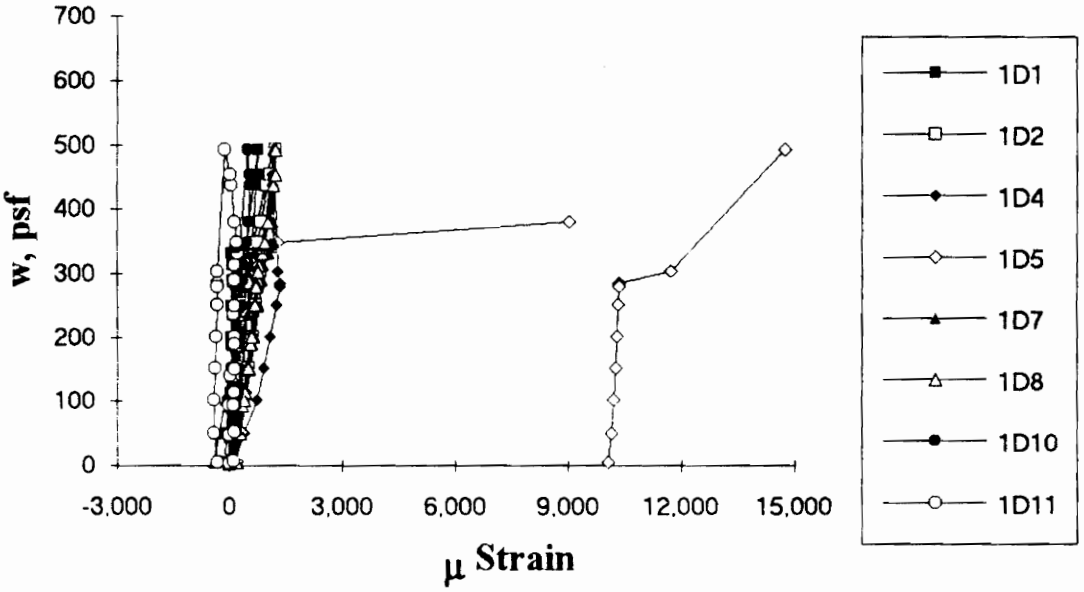

Figure A.75 SDI-2/20-P1-9 Load vs. Strain in Deck Bottom Flange along the Span

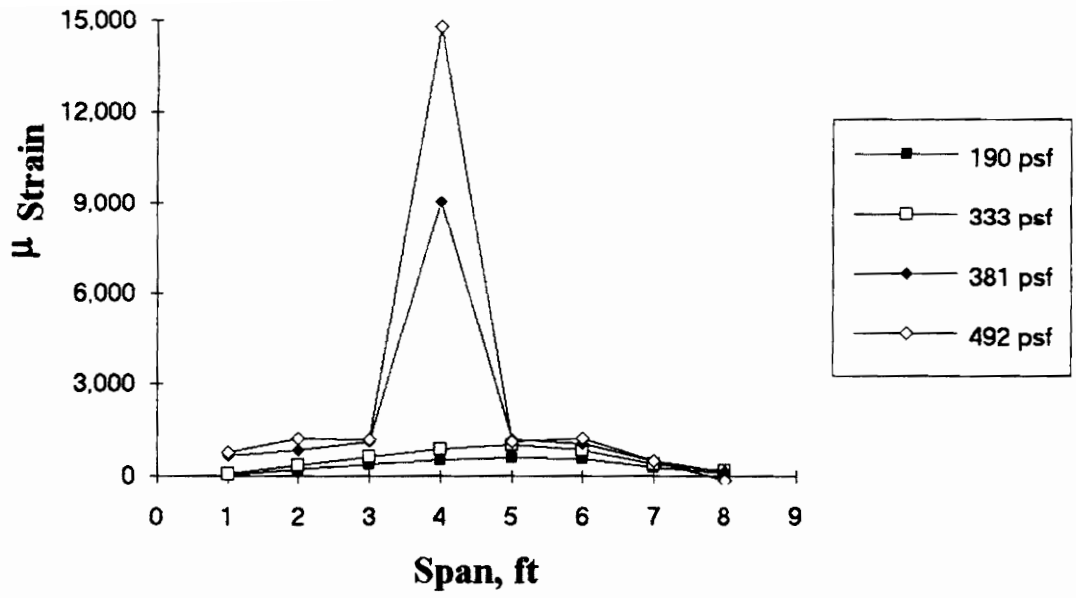

Figure A.76 SDI-2/20-P1-9 Strain Variation in Deck Bottom Flange along the Span (from centerline of exterior support)

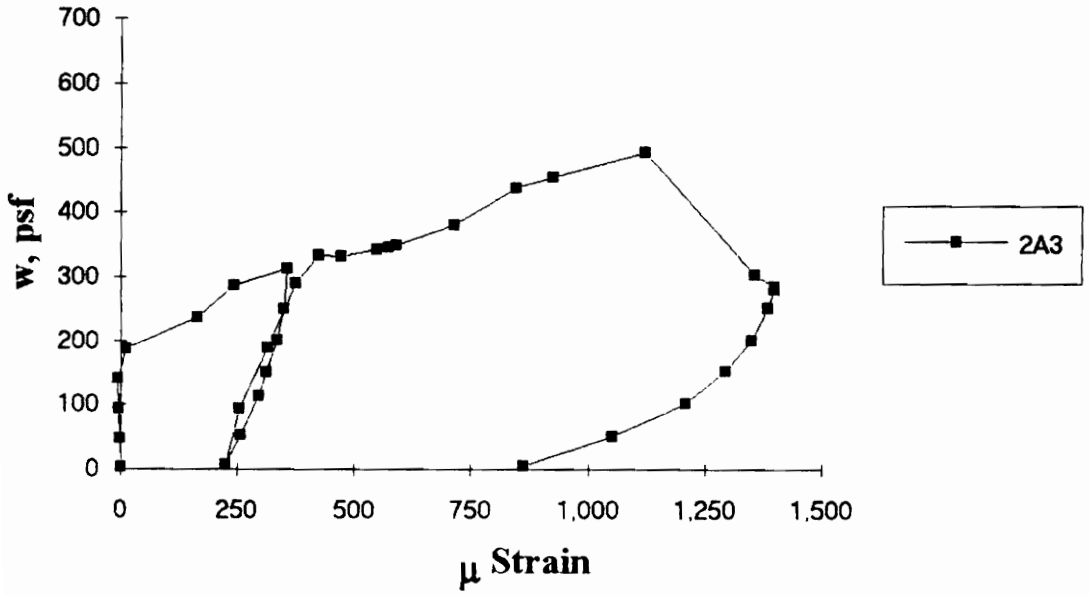

Figure A.77 SDI-2/20-P1-9 Load vs. Strain in Deck Flange in Center Span

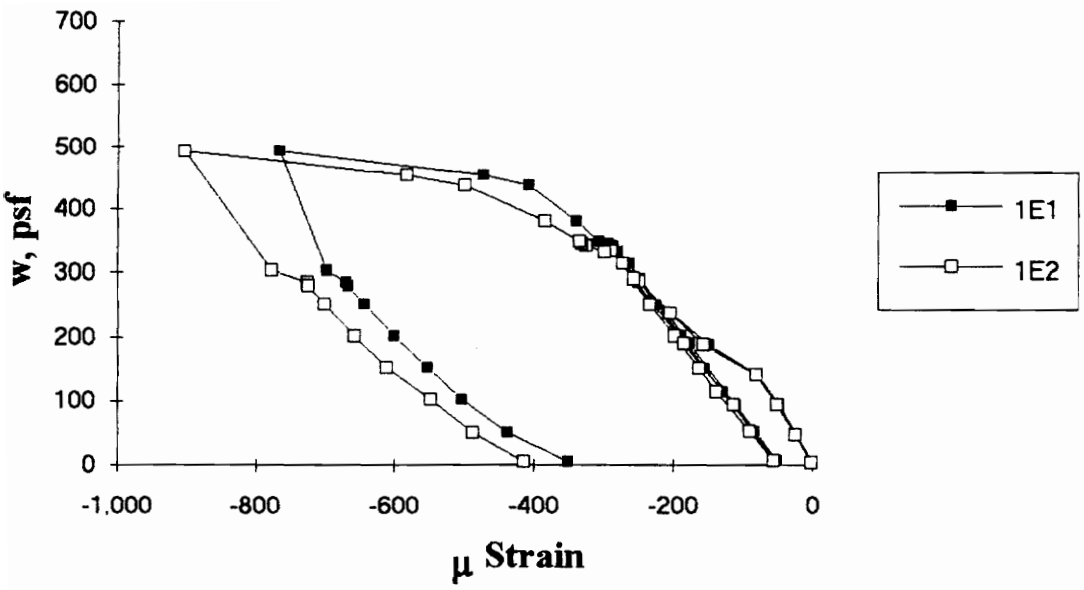

Figure A.78 SDI-2/20-P1-9 Load vs. Strain in Concrete at Maximum Moment

Test Designation: SDI-2/20-P2-9
Test Date: November 16, 1993

MATERIALS AND DIMENSIONS

General:

width:	6 ft. (2 panels)
span length:	9 ft. center span
end details:	N/A
deck anchorage type:	arc spot weld, 3/4 in. dia.
average anchorage spacing:	1.0 ft.

Deck:

thickness:	0.0345 in. (20 gage)
depth:	2 in.
area:	0.519 $in.^2/ft.$
yield stress:	45.4 ksi
ultimate strength:	52.6 ksi
web embossment type:	N/A

embossment dimensions:

N_b :	1.76 in.	W_b :	0.81 in.	s :	3.07 in.
N_t :	1.19 in.	W_t :	0.58 in.	p_h :	0.15 in.

Concrete:

type:	normal weight
test strength:	3,340 psi
total depth:	4.5 in.
cover depth:	2.5 in.

RESULTS

midspan strain due to fresh concrete:	250 x 10^{-6} in./in.
maximum load:	598 psf
deflection at maximum load:	2.74 in.
deflection at termination of test:	4.32 in.
end slip at maximum load:	N/A
end slip at termination of test:	N/A

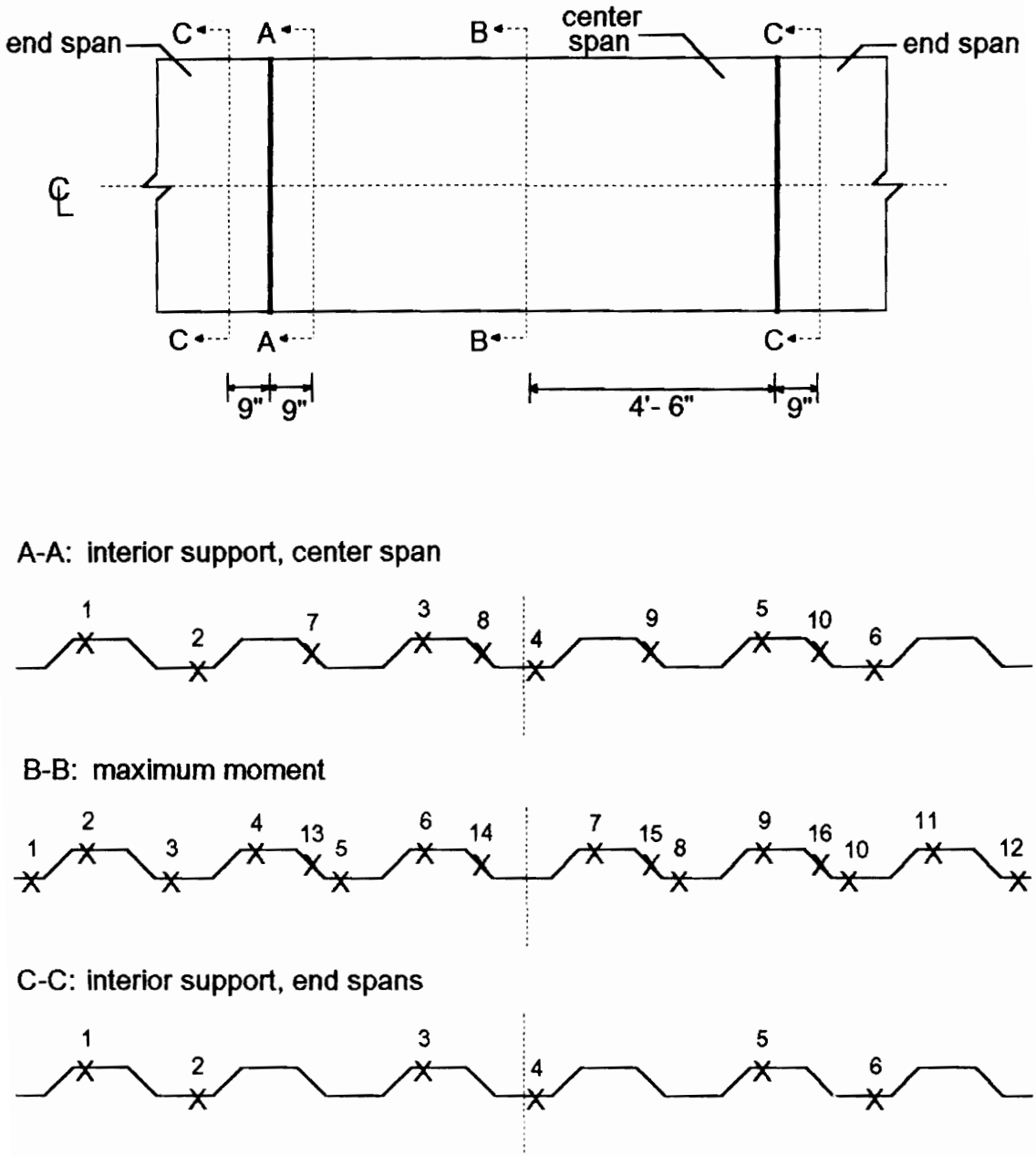

Figure A.79 SDI-2/20-P2-9 Steel Deck Strain Gage Locations

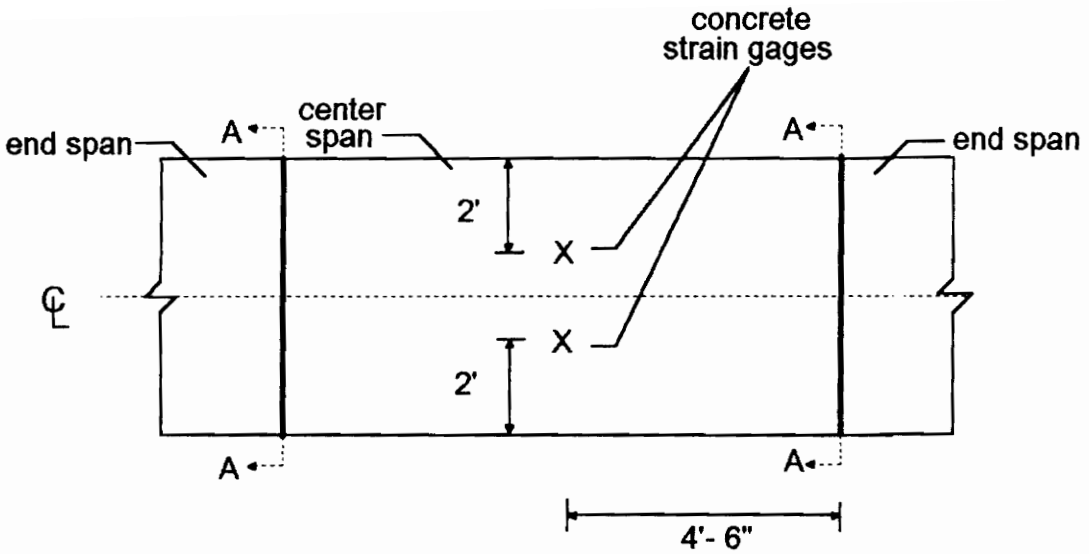

A-A: arc spot welds over supports

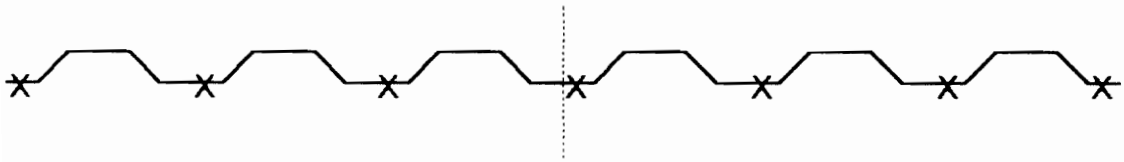

Figure A.80 SDI-2/20-P2-9 Concrete Strain Gage and Arc Spot Weld Locations

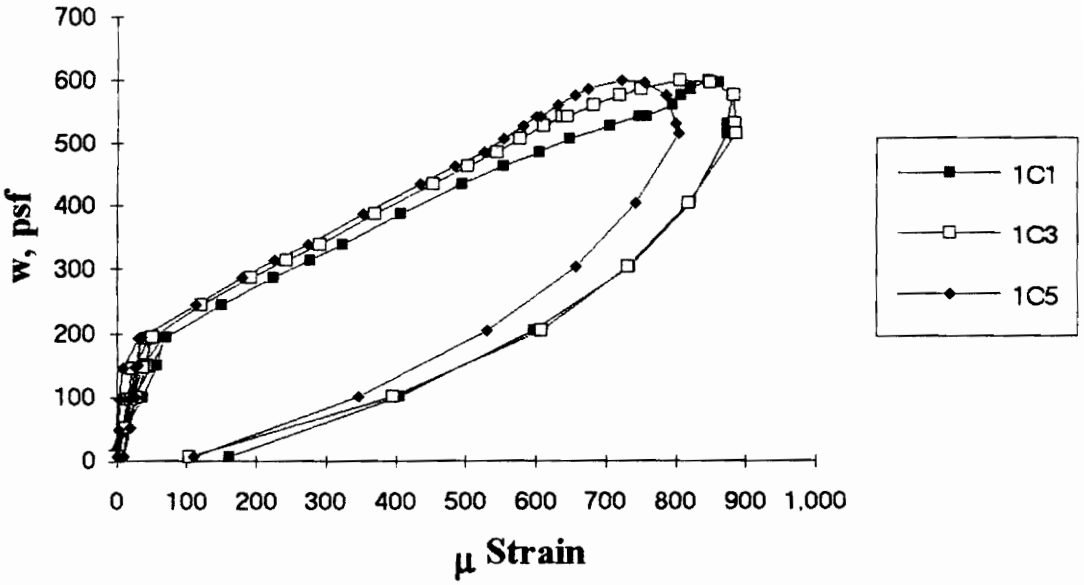

Figure A.81 SDI-2/20-P2-9 Load vs. Strain in Deck Top Flange at Interior Support in End Span

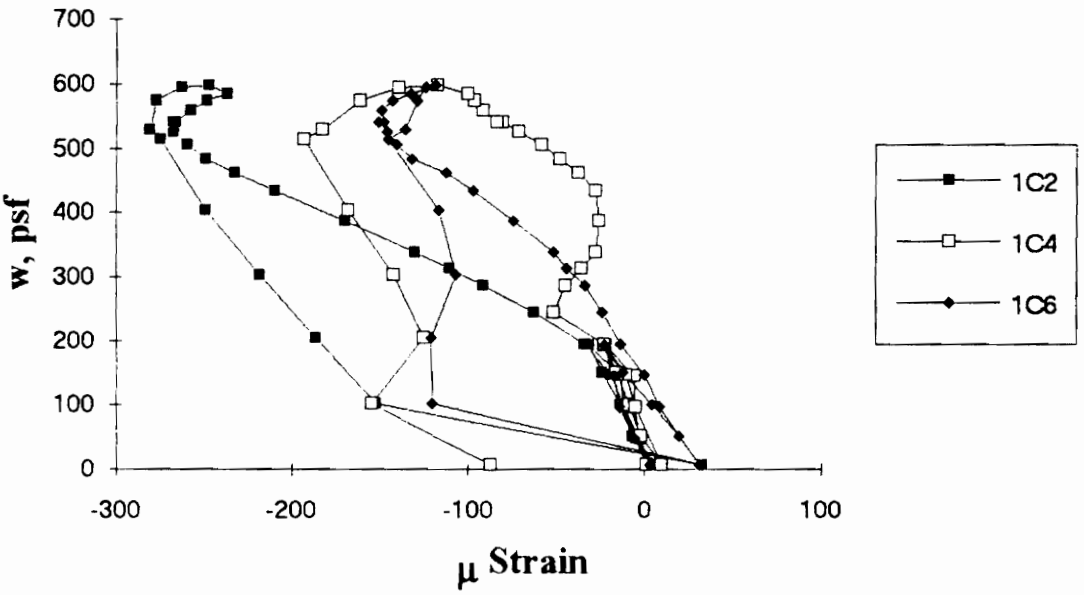

Figure A.82 SDI-2/20-P2-9 Load vs. Strain in Deck Bottom Flange at Interior Support in End Span

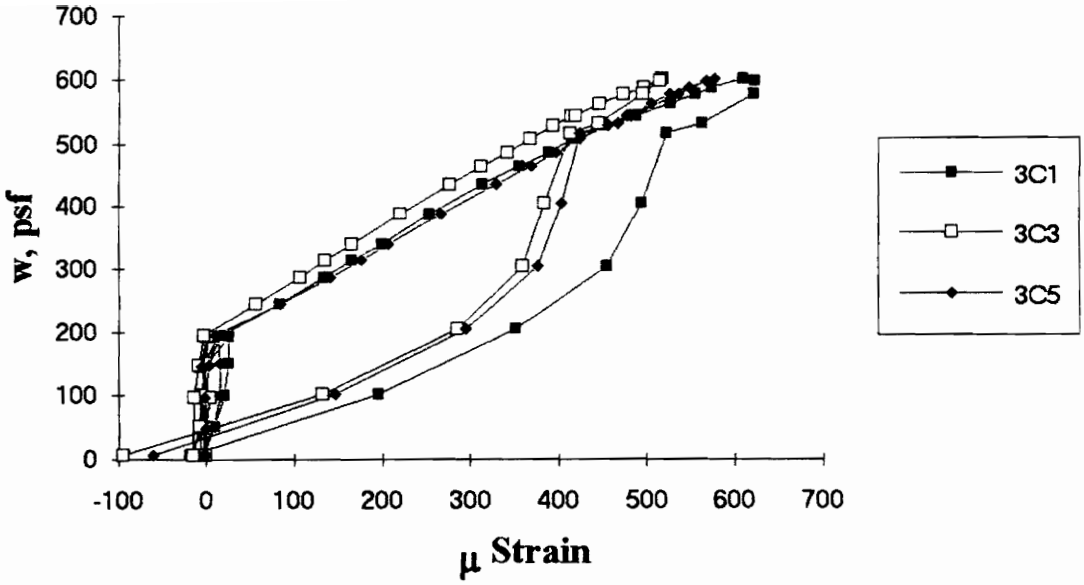

Figure A.83 SDI-2/20-P2-9 Load vs. Strain in Deck Top Flange at Interior Support in End Span

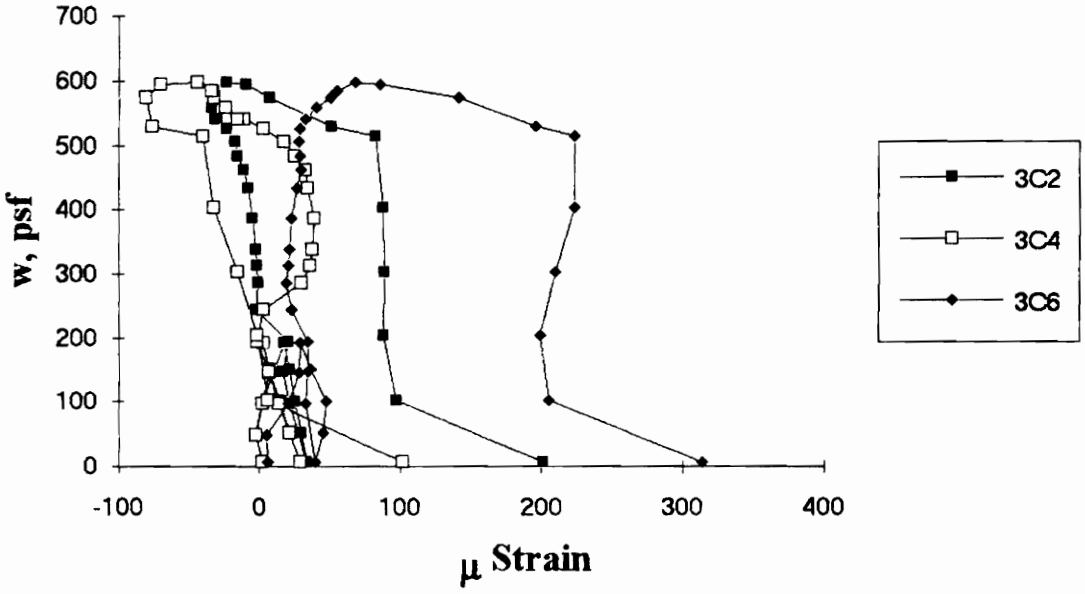

Figure A.84 SDI-2/20-P2-9 Load vs. Strain in Deck Bottom Flange at Interior Support in End Span

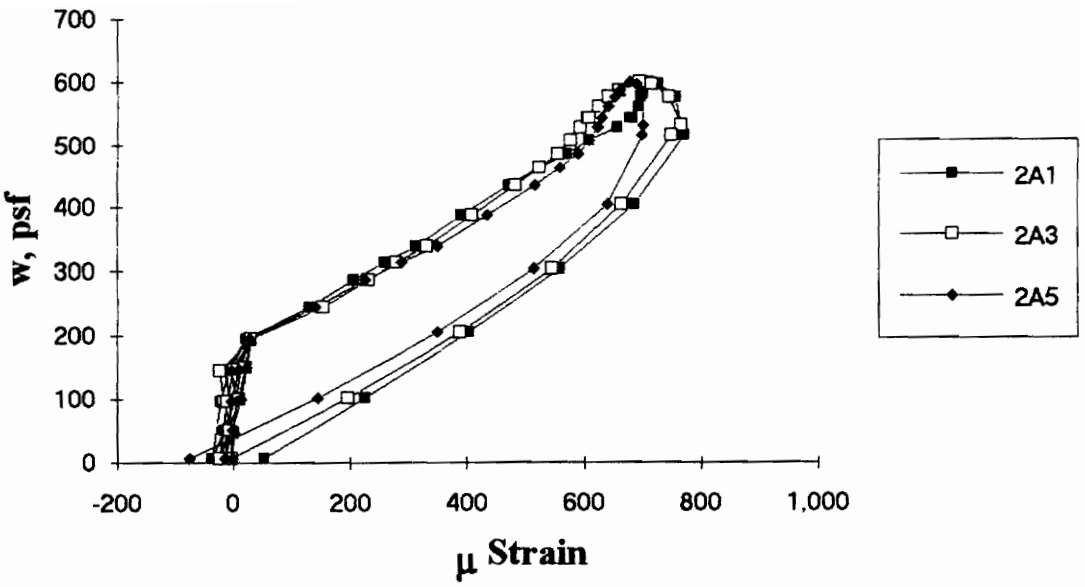

Figure A.85 SDI-2/20-P2-9 Load vs. Strain in Deck Top Flange at Interior Support in Center Span

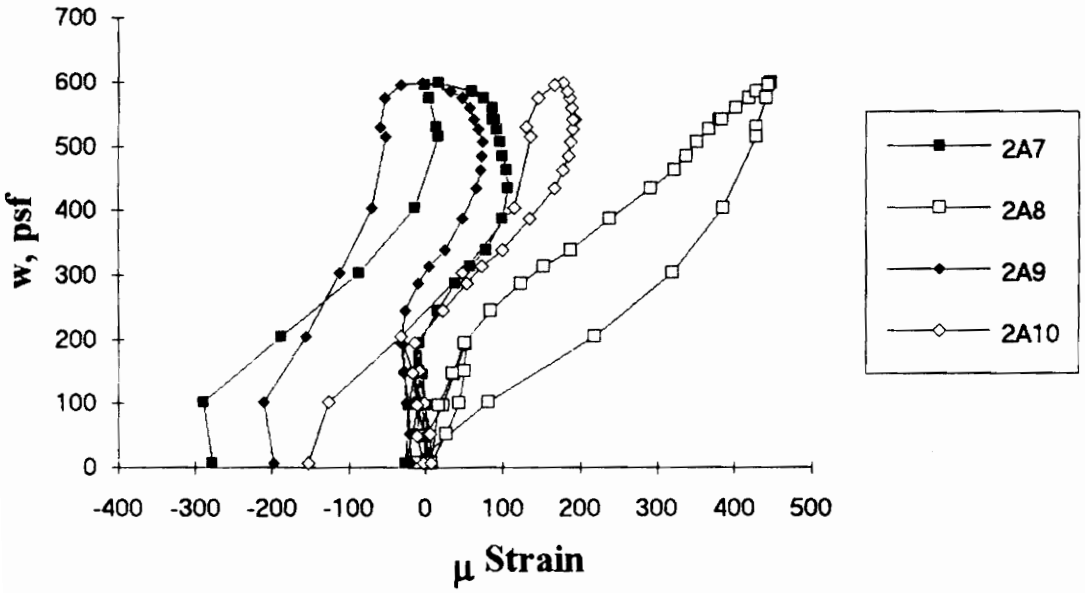

Figure A.86 SDI-2/20-P2-9 Load vs. Strain in Deck Web at Interior Support in Center Span

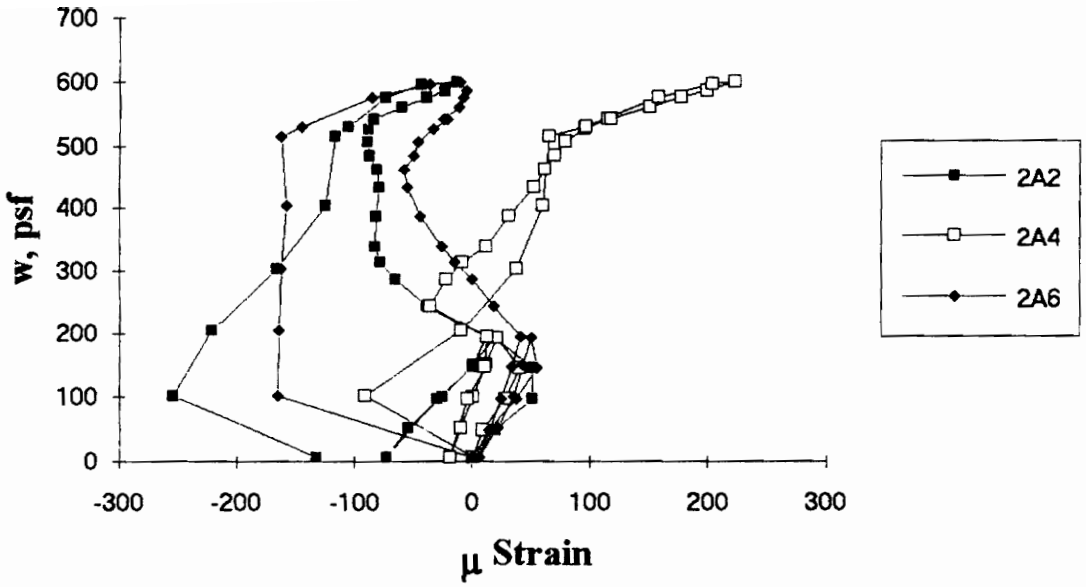

Figure A.87 SDI-2/20-P2-9 Load vs. Strain in Deck Bottom Flange at Interior Support in Center Span

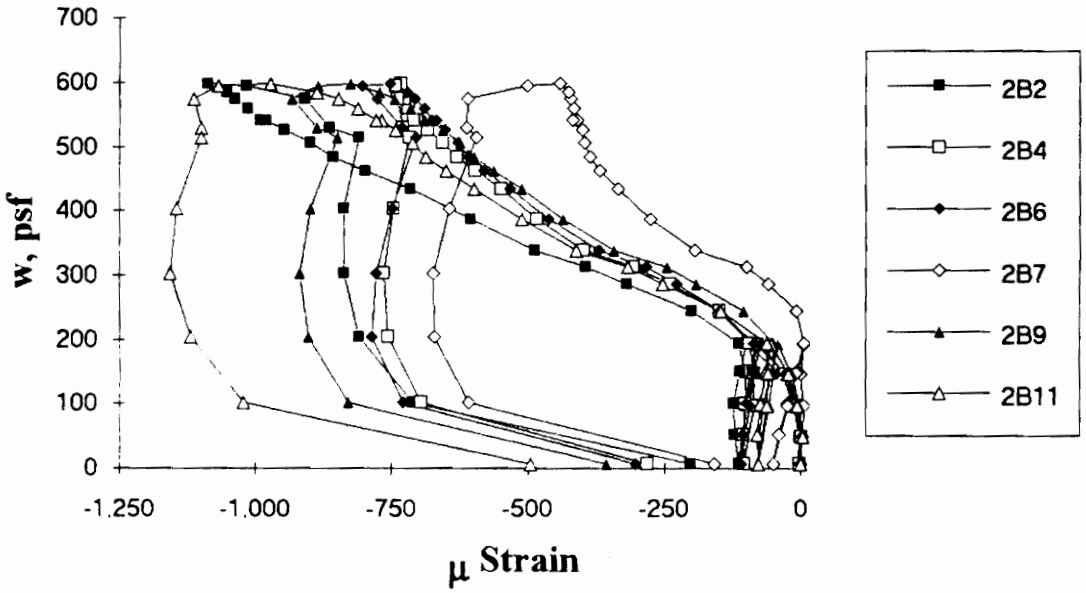

Figure A.88 SDI-2/20-P2-9 Load vs. Strain in Deck Top Flange at Maximum Moment

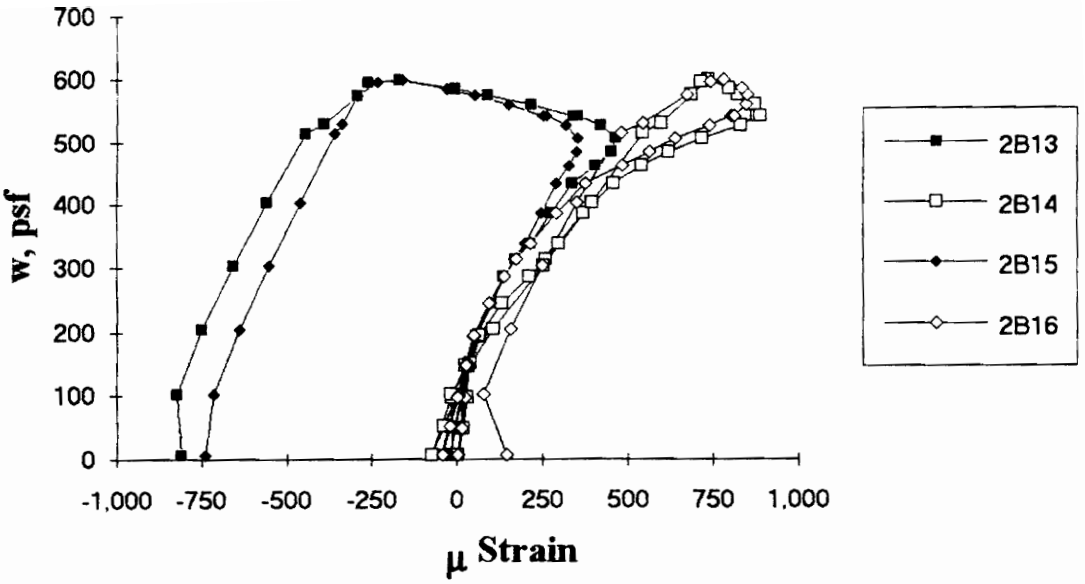

Figure A.89 SDI-2/20-P2-9 Load vs. Strain in Deck Web at Maximum Moment

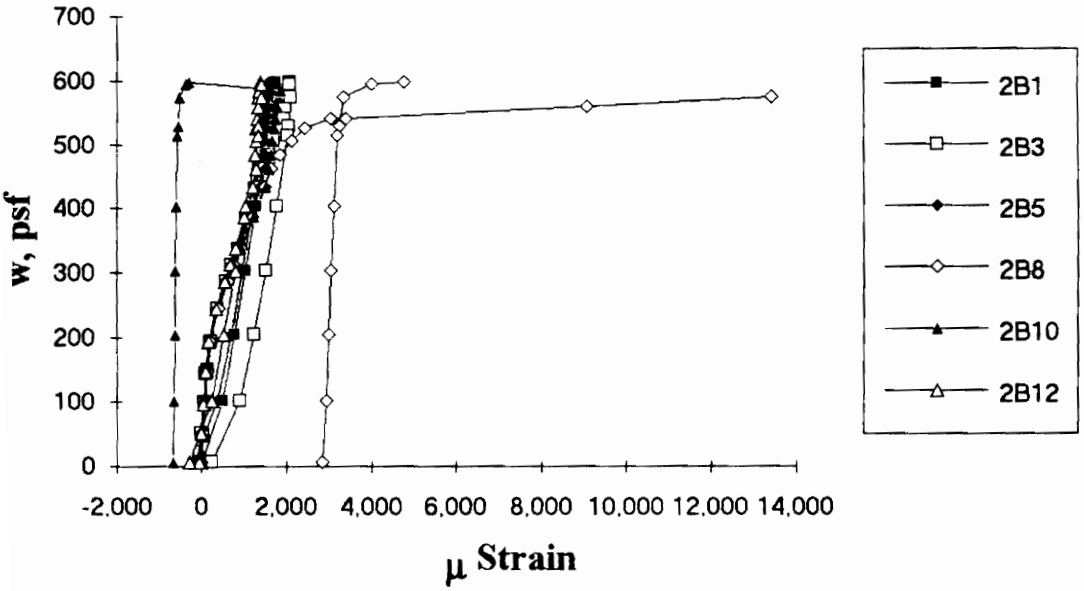

Figure A.90 SDI-2/20-P2-9 Load vs. Strain in Deck Bottom Flange at Maximum Moment

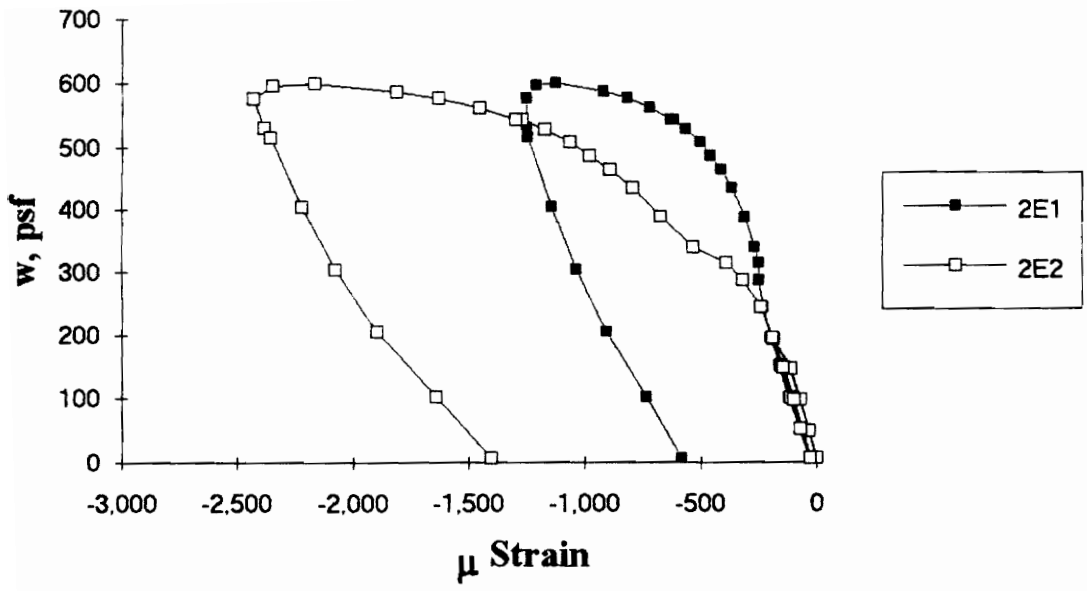

Figure A.91 SDI-2/20-P2-9 Load vs. Strain in Concrete at Maximum Moment

Test Designation: SDI-2/20-P3-9
Test Date: November 13, 1993

MATERIALS AND DIMENSIONS

General:

width:	6 ft. (2 panels)
span length:	9 ft. end span
end details:	angle with return lip
deck anchorage type:	arc spot weld, 3/4 in. dia.
average anchorage spacing:	1.0 ft.

Deck:

thickness:	0.0345 in. (20 gage)
depth:	2 in.
area:	0.519 $in.^2/ft.$
yield stress:	45.4 ksi
ultimate strength:	52.6 ksi
web embossment type:	N/A

embossment dimensions:

N_b : 1.76 in.	W_b : 0.81 in.	s : 3.07 in.
N_t : 1.19 in.	W_t : 0.58 in.	p_h : 0.15 in.

Concrete:

type:	normal weight
test strength:	3,340 psi
total depth:	4.5 in.
cover depth:	2.5 in.

RESULTS

midspan strain due to fresh concrete:	250 x 10^{-6} in./in.
maximum load:	590 psf
deflection at maximum load:	1.69 in.
deflection at termination of test:	4.71 in.
end slip at maximum load:	0.00 in.
end slip at termination of test:	0.00 in.

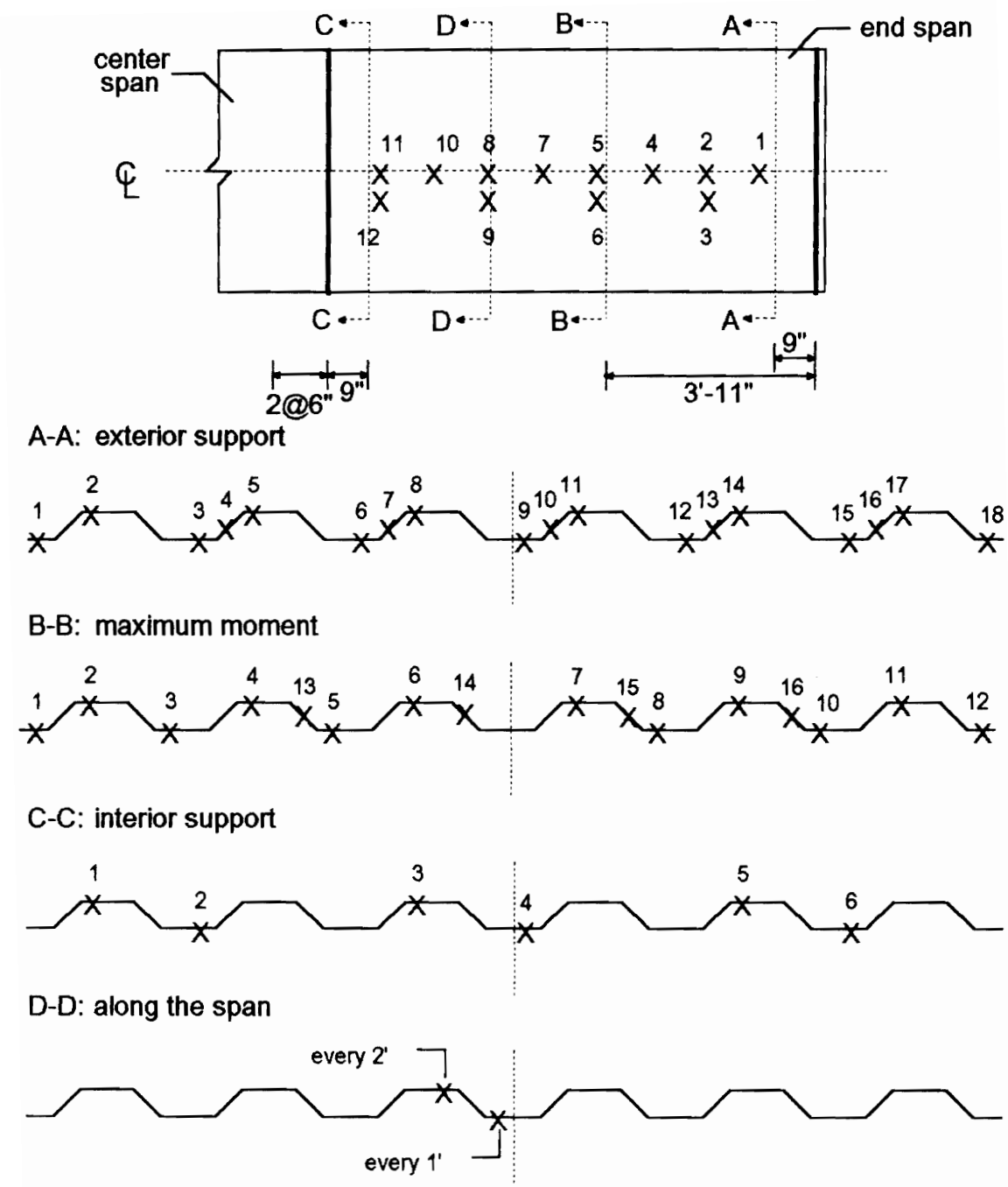

Figure A.92 SDI-2/20-P3-9 Steel Deck Strain Gage Locations

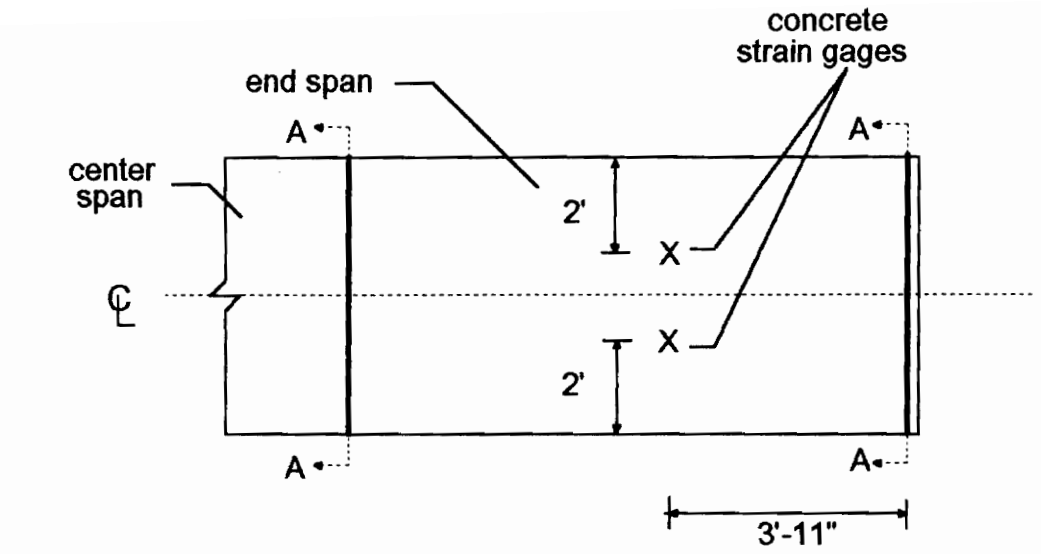

A-A: arc spot welds over supports

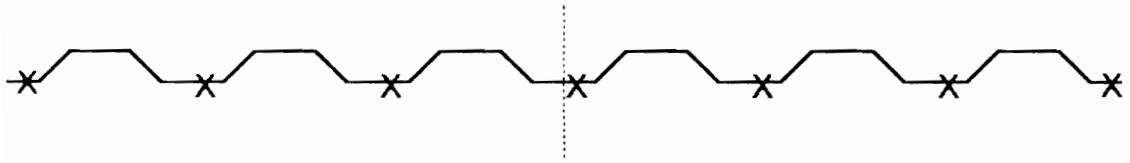

Figure A.93 SDI-2/20-P3-9 Concrete Strain Gage and Arc Spot Weld Locations

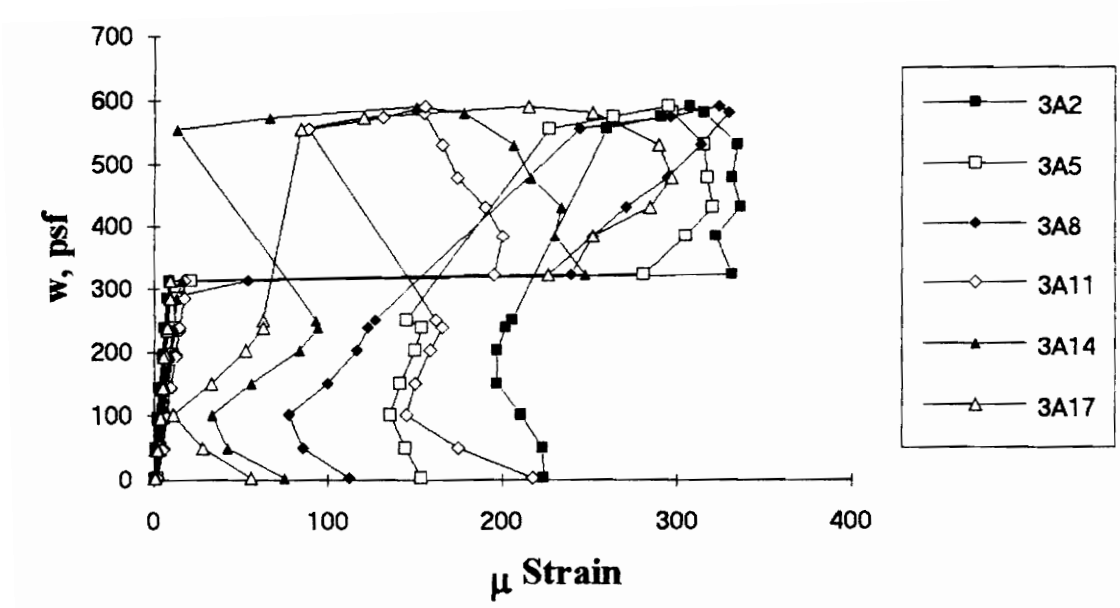

Figure A.94 SDI-2/20-P3-9 Load vs. Strain in Deck Top Flange at Exterior Support

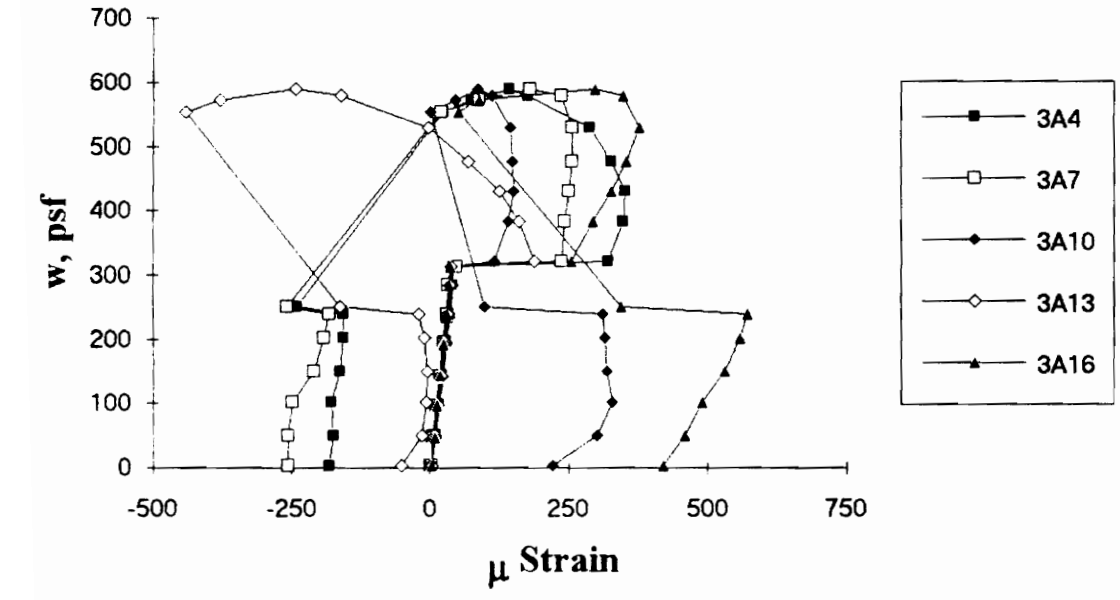

Figure A.95 SDI-2/20-P3-9 Load vs. Strain in Deck Web at Exterior Support

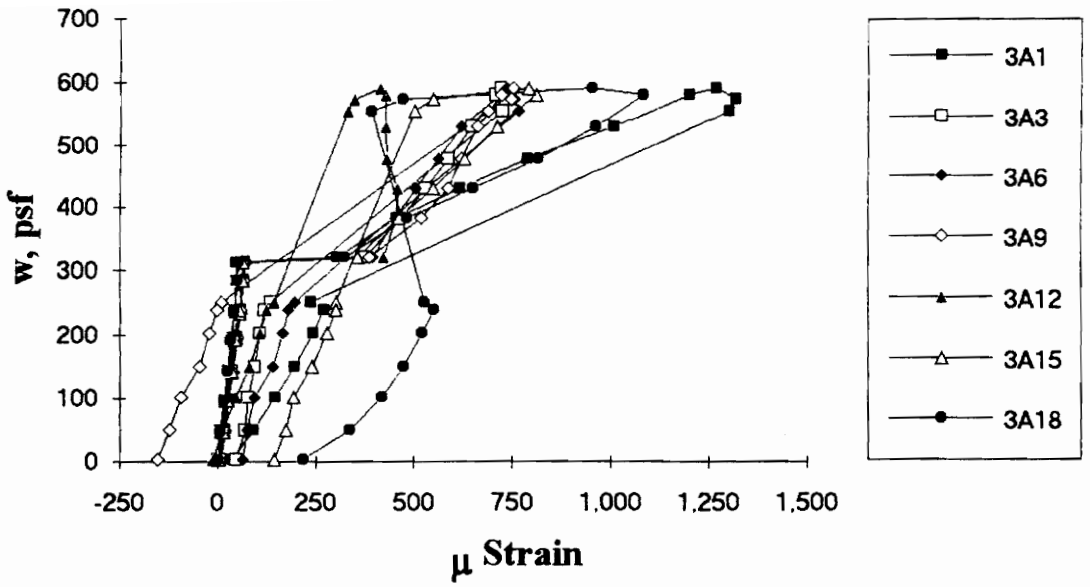

Figure A.96 SDI-2/20-P3-9 Load vs. Strain in Deck Bottom Flange at Exterior Support

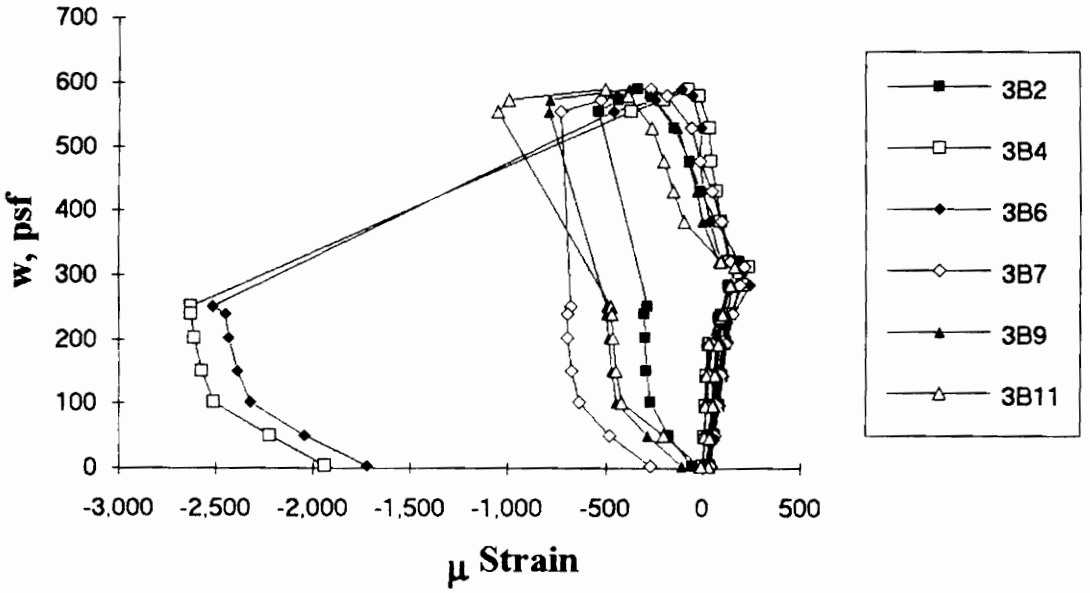

Figure A.97 SDI-2/20-P3-9 Load vs. Strain in Deck Top Flange at Maximum Moment

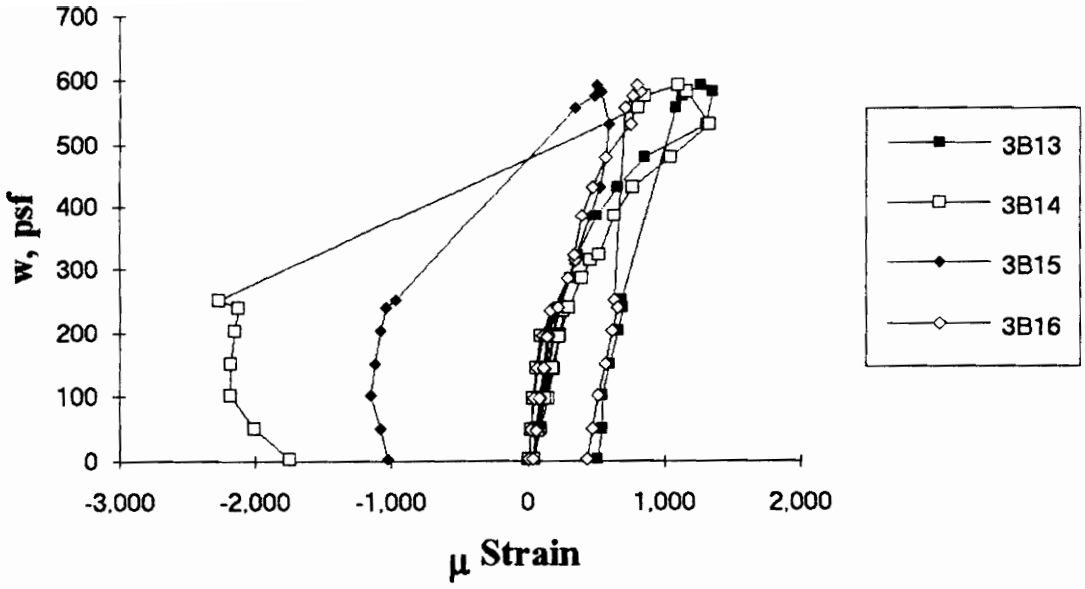

Figure A.98 SDI-2/20-P3-9 Load vs. Strain in Deck Web at Maximum Moment

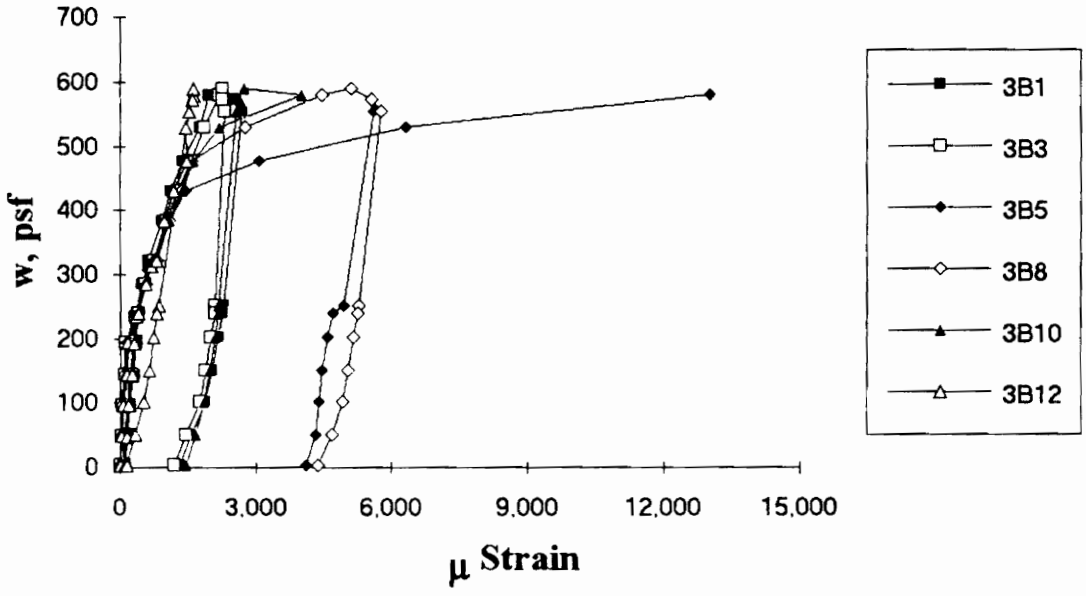

Figure A.99 SDI-2/20-P3-9 Load vs. Strain in Deck Bottom Flange at Maximum Moment

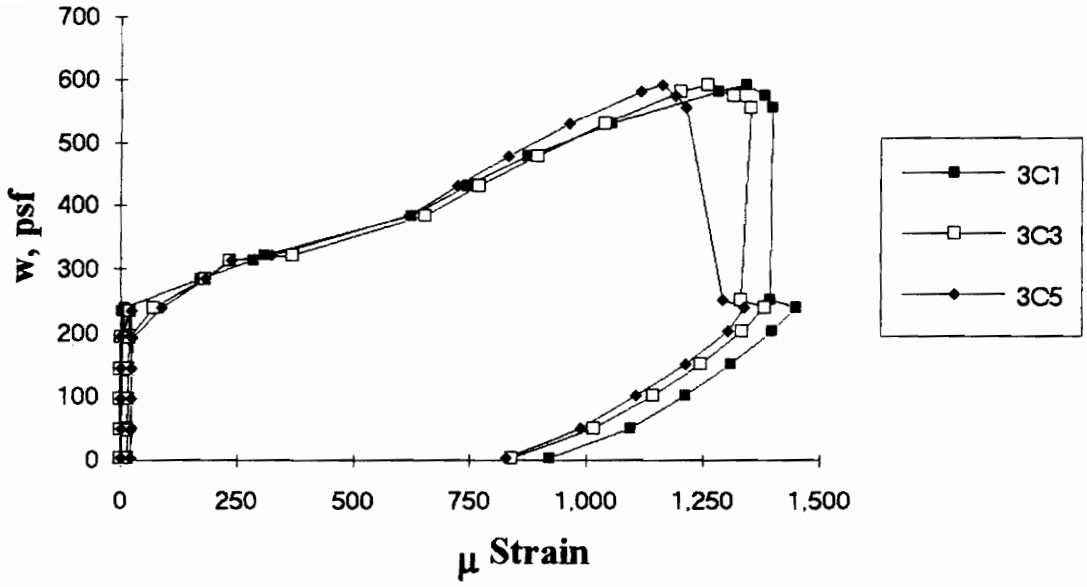

Figure A.100 SDI-2/20-P3-9 Load vs. Strain in Deck Top Flange at Interior Support

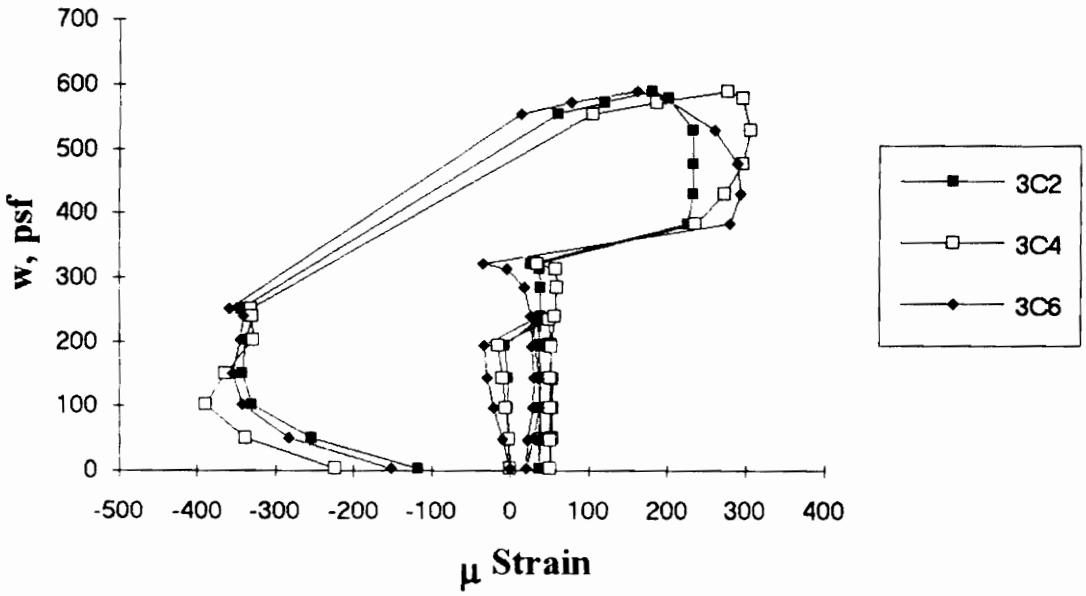

Figure A.101 SDI-2/20-P3-9 Load vs. Strain in Deck Bottom Flange at Interior Support

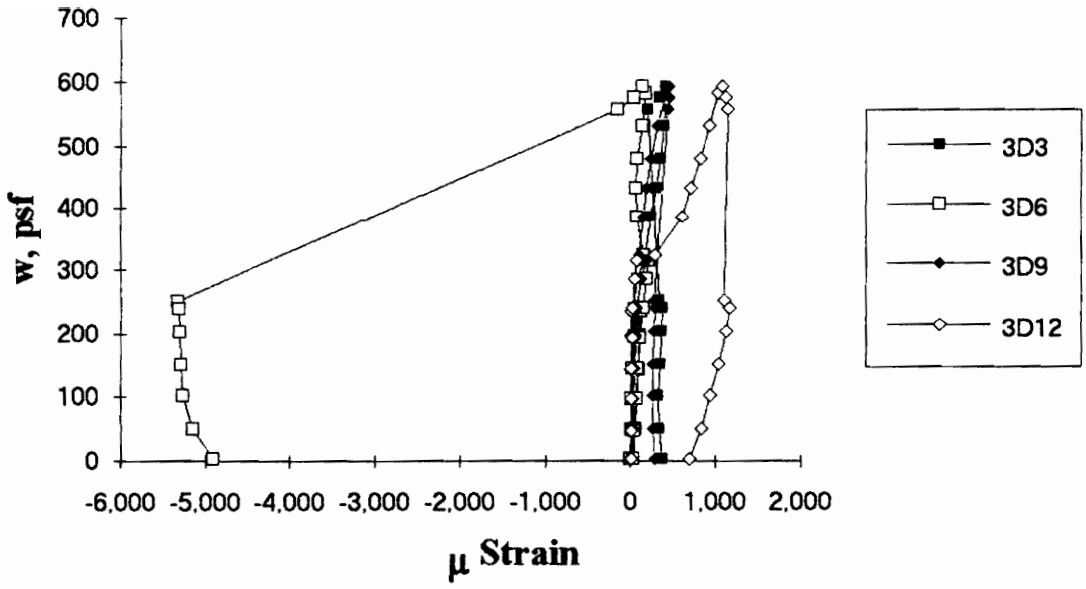

Figure A.102 SDI-2/20-P3-9 Load vs. Strain in Deck Top Flange along the Span

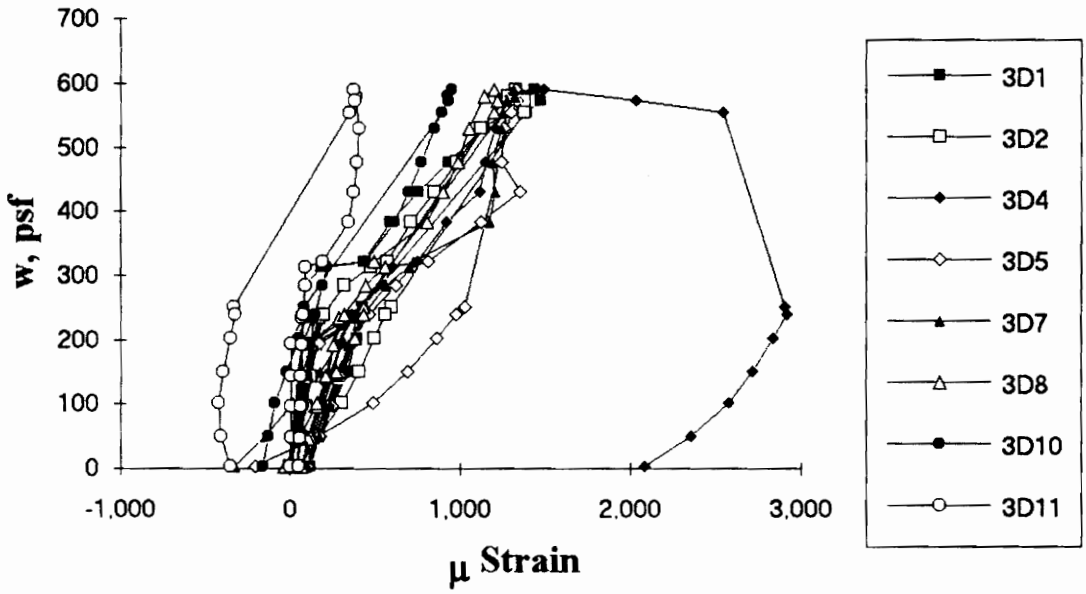

Figure A.103 SDI-2/20-P3-9 Load vs. Strain in Deck Bottom Flange along the Span

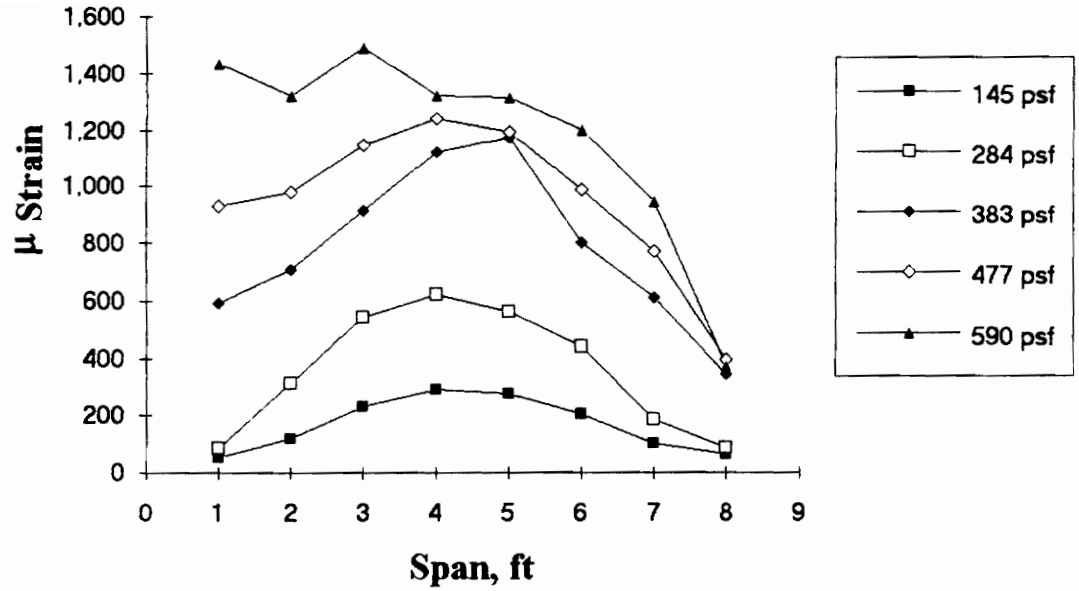

Figure A.104 SDI-2/20-P3-9 Strain Variation in Deck Bottom Flange along the Span (from centerline of exterior support)

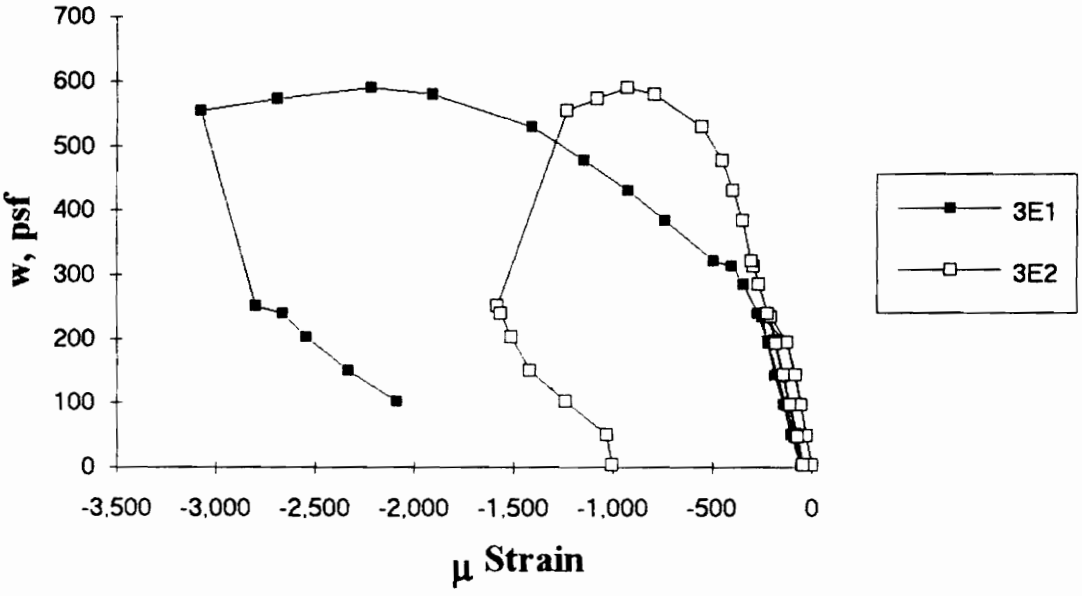

Figure A.105 SDI-2/20-P3-9 Load vs. Strain in Concrete at Maximum Moment

Test Designation: SDI-2/20-PX1-9
Test Date: December 15, 1993

MATERIALS AND DIMENSIONS

General:

width:	6 ft. (2 panels)
span length:	9 ft. end span
end details:	1 ft. cantilever, interior support deck joint
deck anchorage type:	arc spot weld, 3/4 in. dia.
average anchorage spacing:	1.0 ft.

Deck:

thickness:	0.0345 in. (20 gage)
depth:	2 in.
area:	0.519 $in.^2/ft.$
yield stress:	45.4 ksi
ultimate strength:	52.6 ksi
web embossment type:	N/A

embossment dimensions:

N_b :	1.76 in.	W_b :	0.81 in.	s :	3.07 in.
N_t :	1.19 in.	W_t :	0.58 in.	p_h :	0.15 in.

Concrete:

type:	normal weight
test strength:	3,770 psi
total depth:	4.5 in.
cover depth:	2.5 in.

RESULTS

midspan strain due to fresh concrete:	320 x 10^{-6} in./in.
maximum load:	369 psf
deflection at maximum load:	1.59 in.
deflection at termination of test:	3.13 in.
end slip at maximum load:	0.10 in.
end slip at termination of test:	0.43 in.

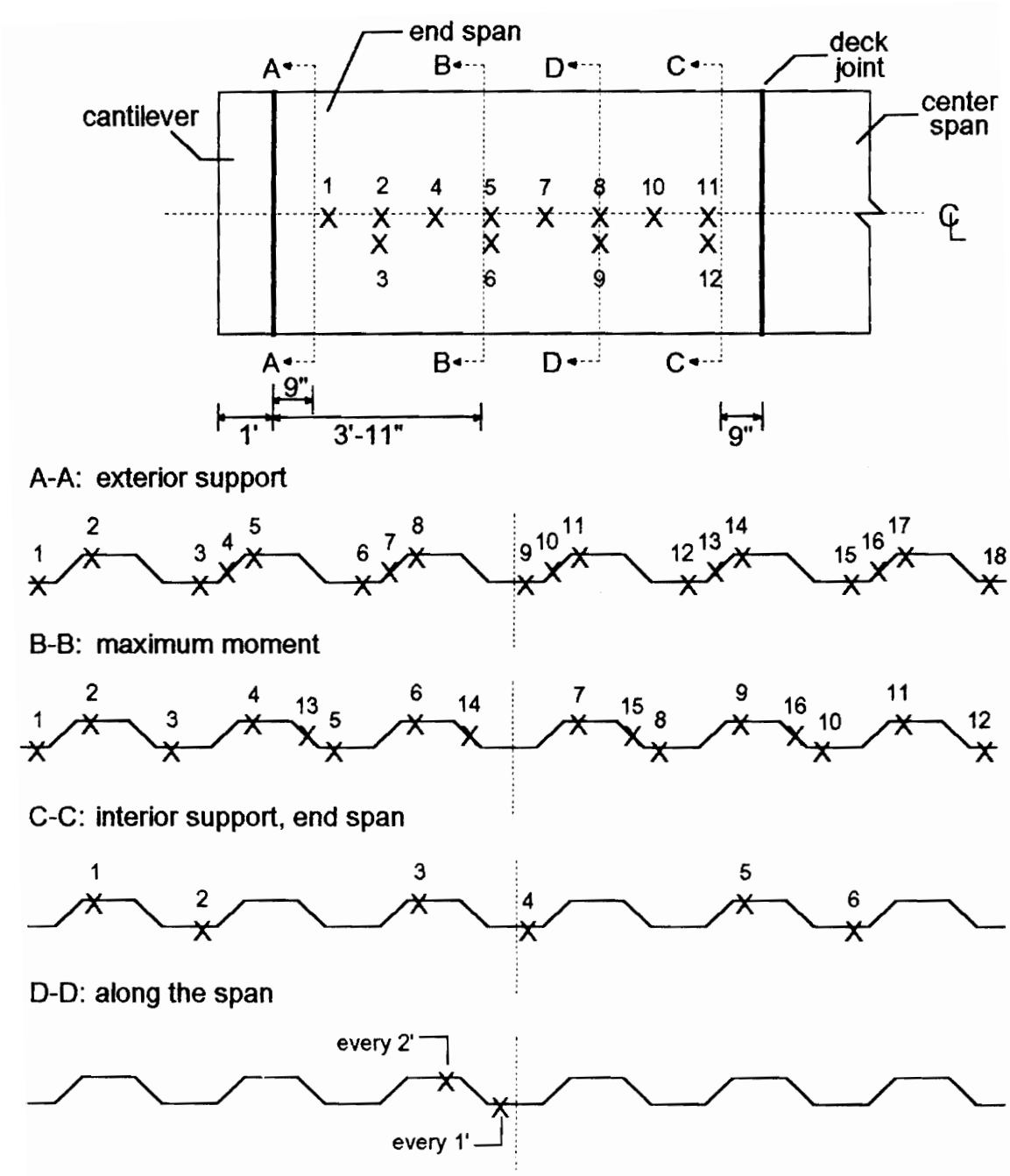

Figure A.106 SDI-2/20-PX1-9 Steel Deck Strain Gage Locations

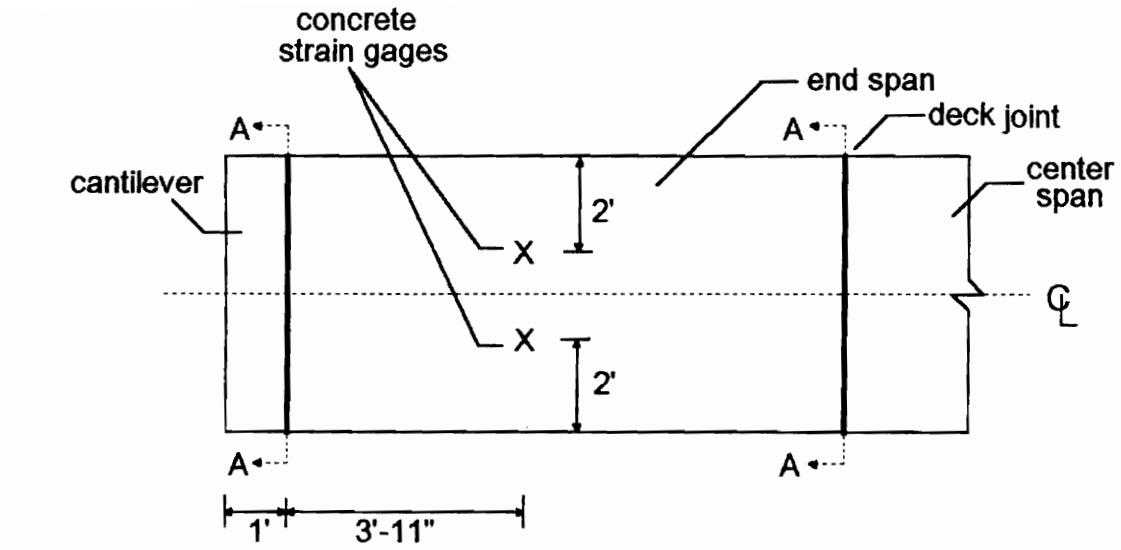

A-A: arc spot welds over supports

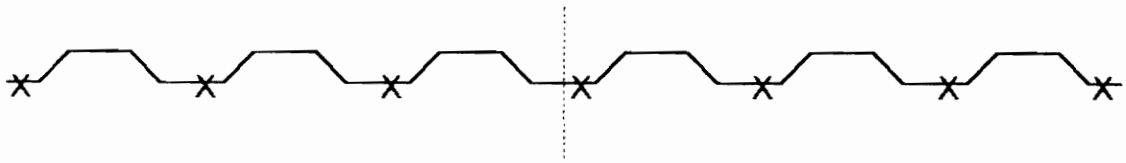

Figure A.107 SDI-2/20-PX1-9 Concrete Strain Gage and Arc Spot Weld Locations

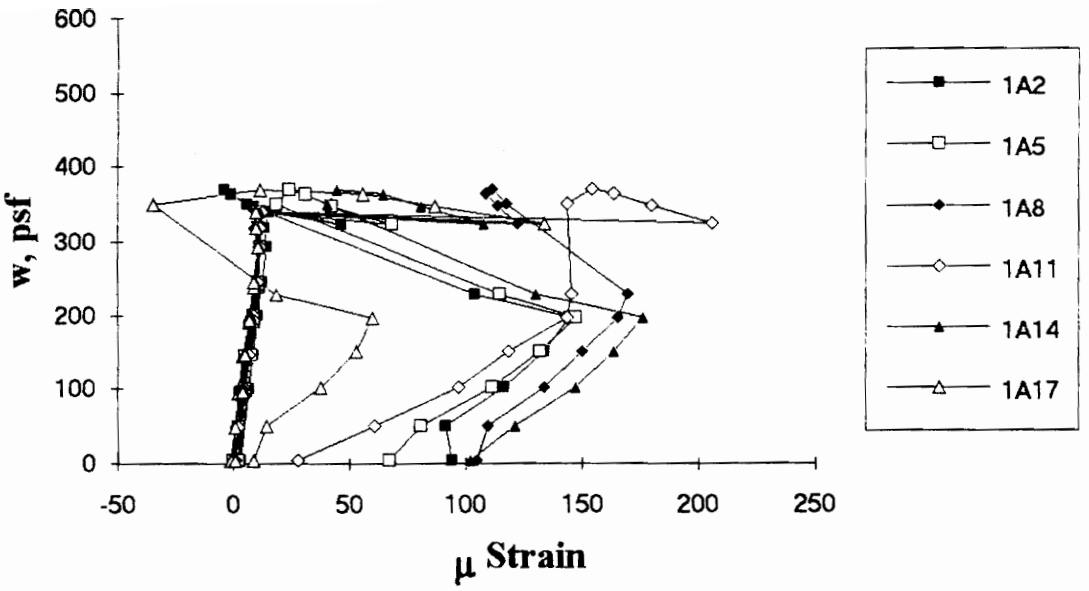

Figure A.108 SDI-2/20-PX1-9 Load vs. Strain in Deck Top Flange at Exterior Support

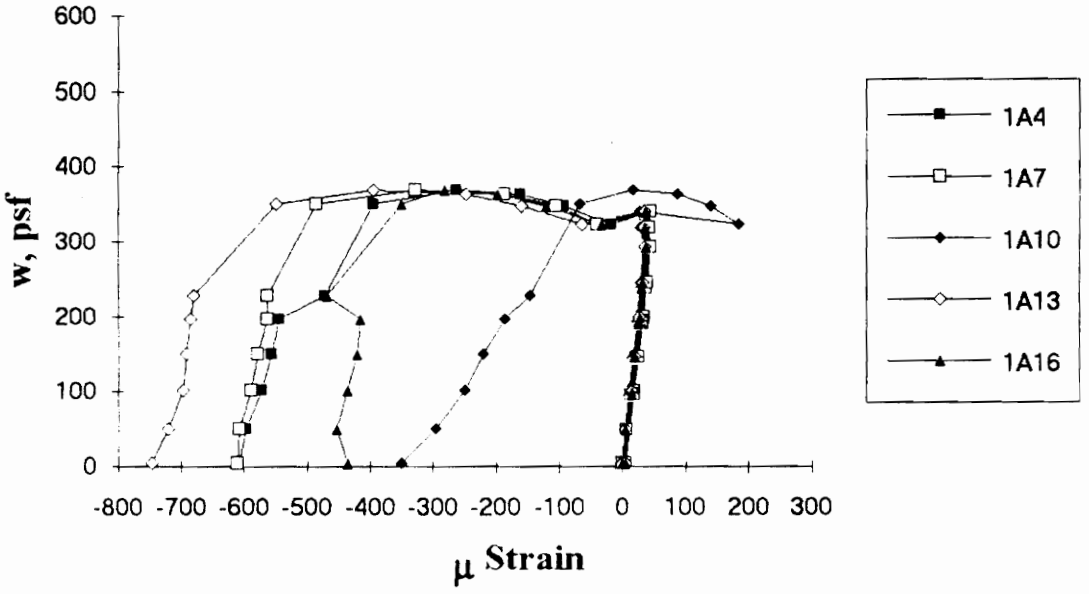

Figure A.109 SDI-2/20-PX1-9 Load vs. Strain in Deck Web at Exterior Support

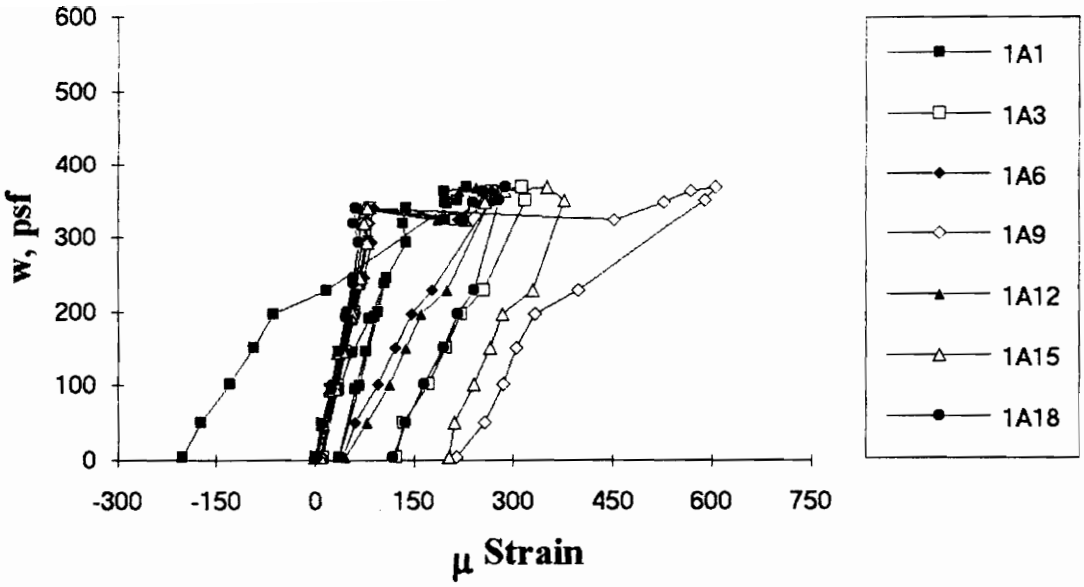

Figure A.110 SDI-2/20-PX1-9 Load vs. Strain in Deck Bottom Flange at Exterior Support

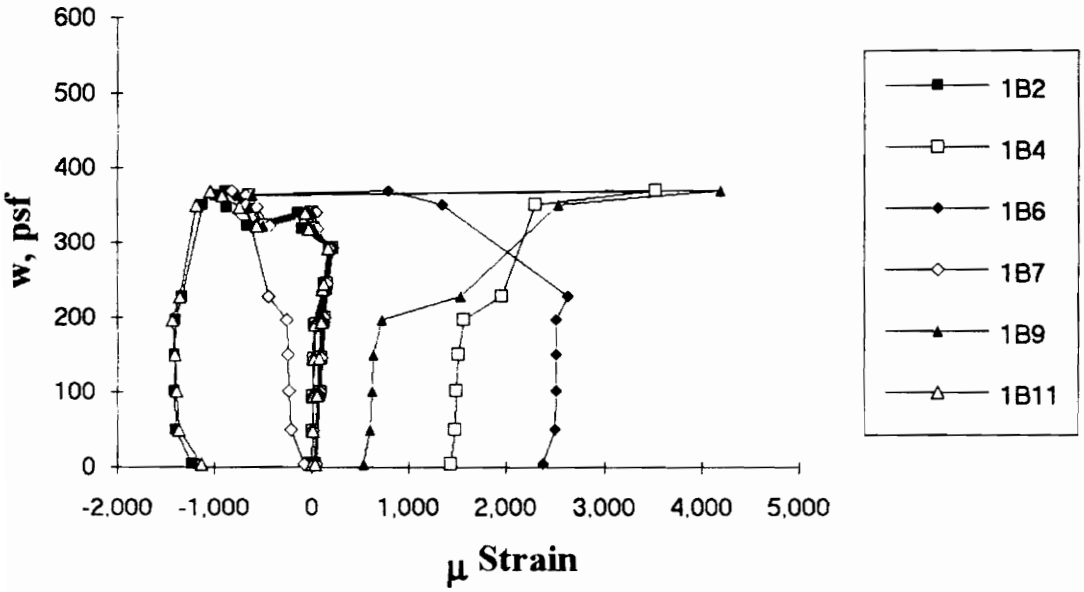

Figure A.111 SDI-2/20-PX1-9 Load vs. Strain in Deck Top Flange at Maximum Moment

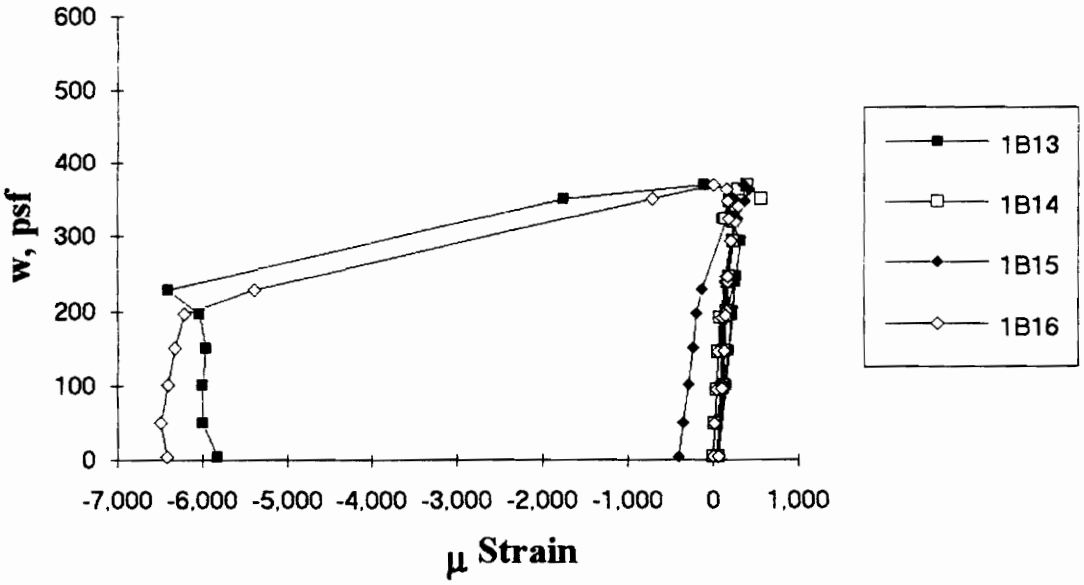

Figure A.112 SDI-2/20-PX1-9 Load vs. Strain in Deck Web at Maximum Moment

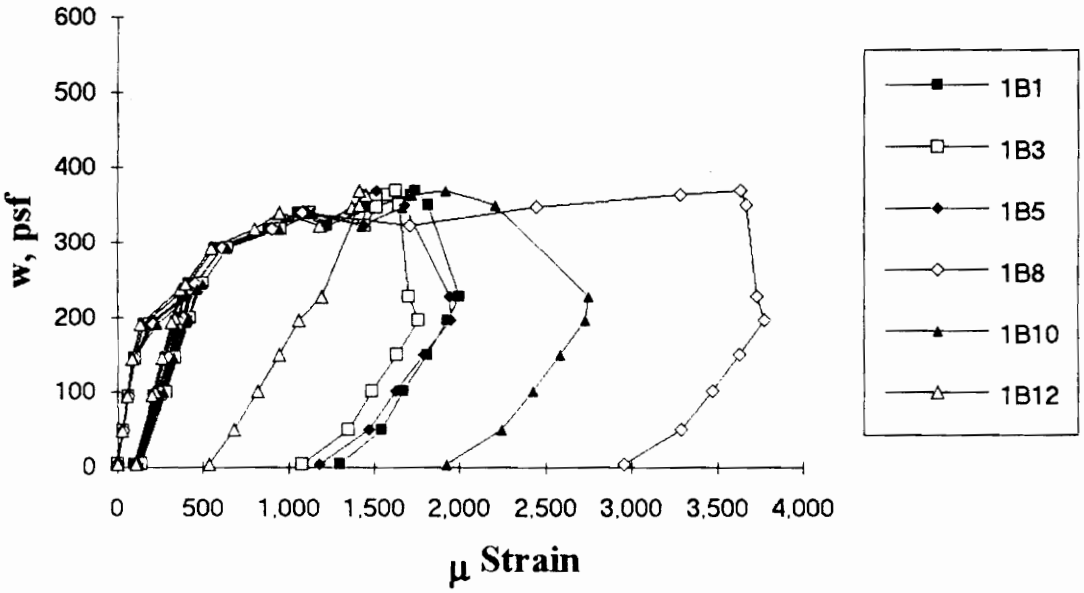

Figure A.113 SDI-2/20-PX1-9 Load vs. Strain in Deck Bottom Flange at Maximum Moment

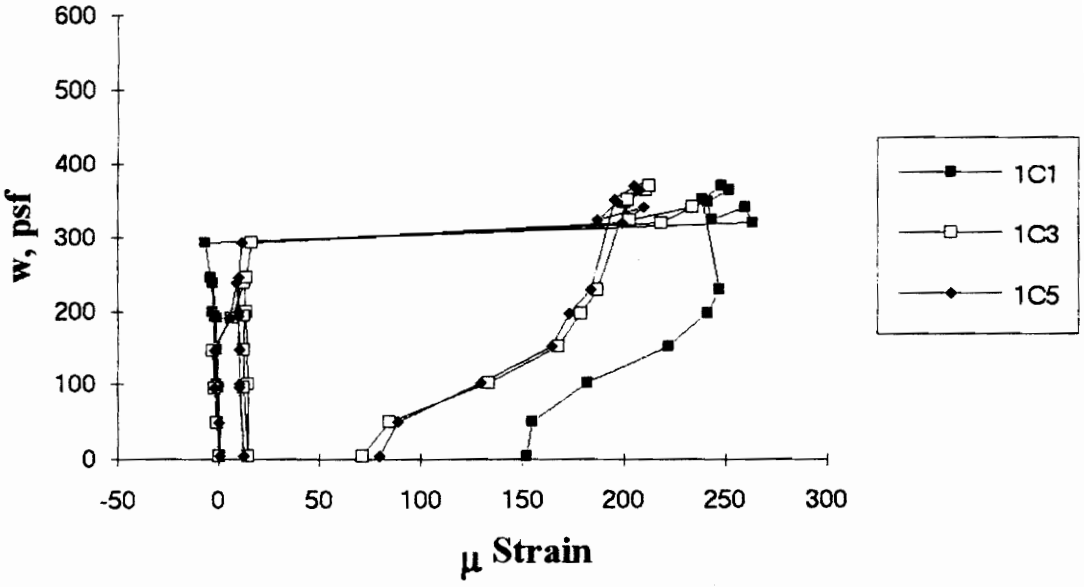

Figure A.114 SDI-2/20-PX1-9 Load vs. Strain in Deck Top Flange at Interior Support

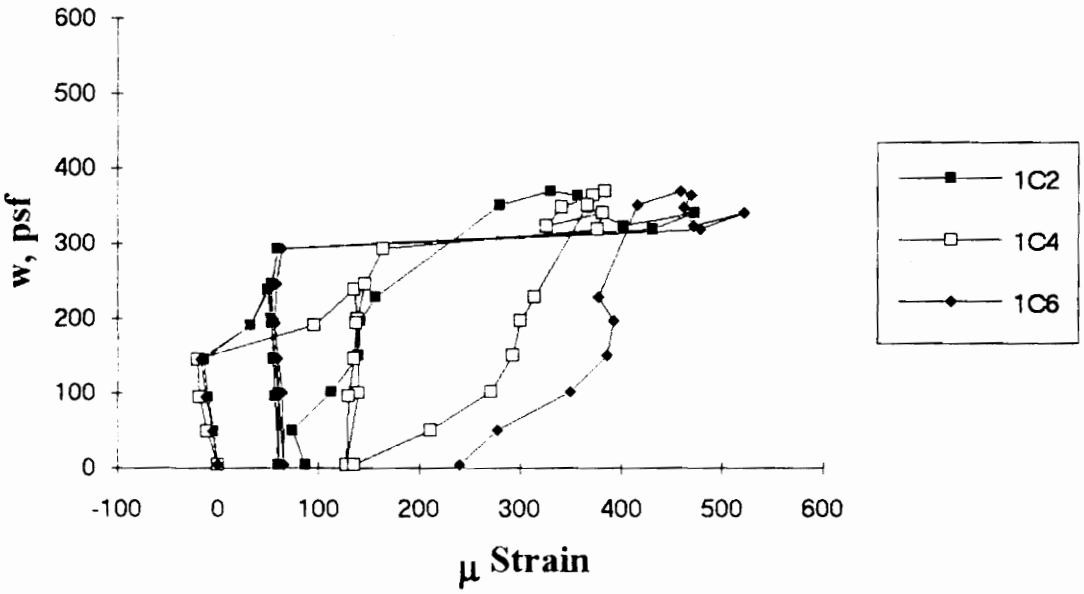

Figure A.115 SDI-2/20-PX1-9 Load vs. Strain in Deck Bottom Flange at Interior Support

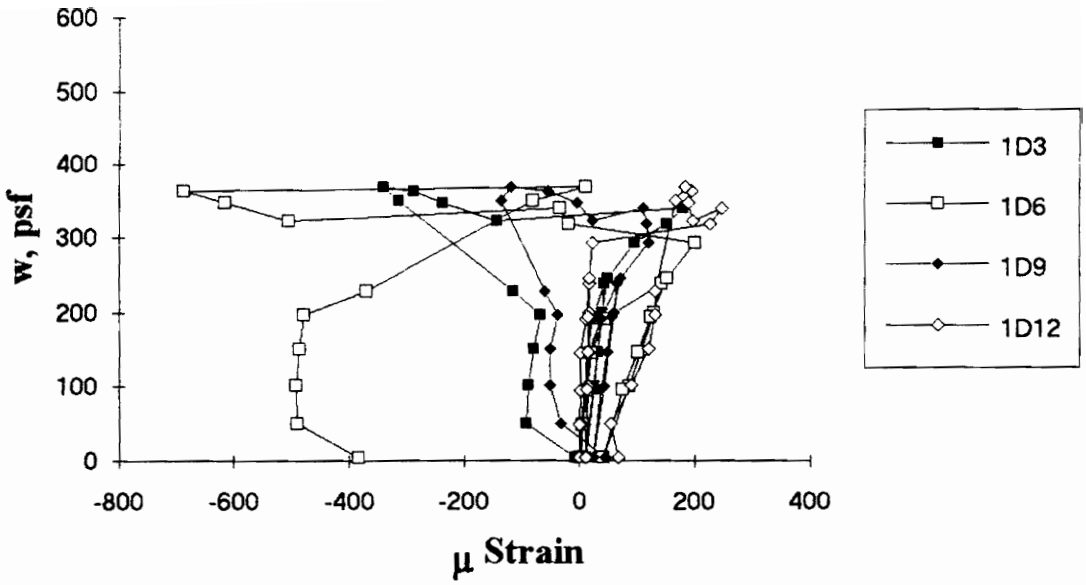

Figure A.116 SDI-2/20-PX1-9 Load vs. Strain in Deck Top Flange along the Span

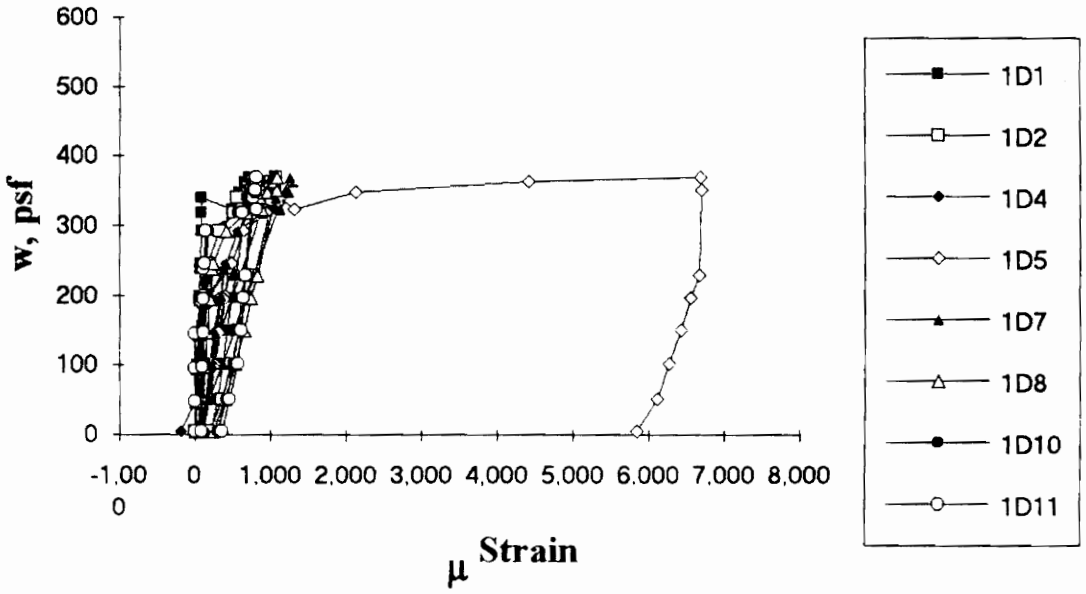

Figure A.117 SDI-2/20-PX1-9 Load vs. Strain in Deck Bottom Flange along the Span

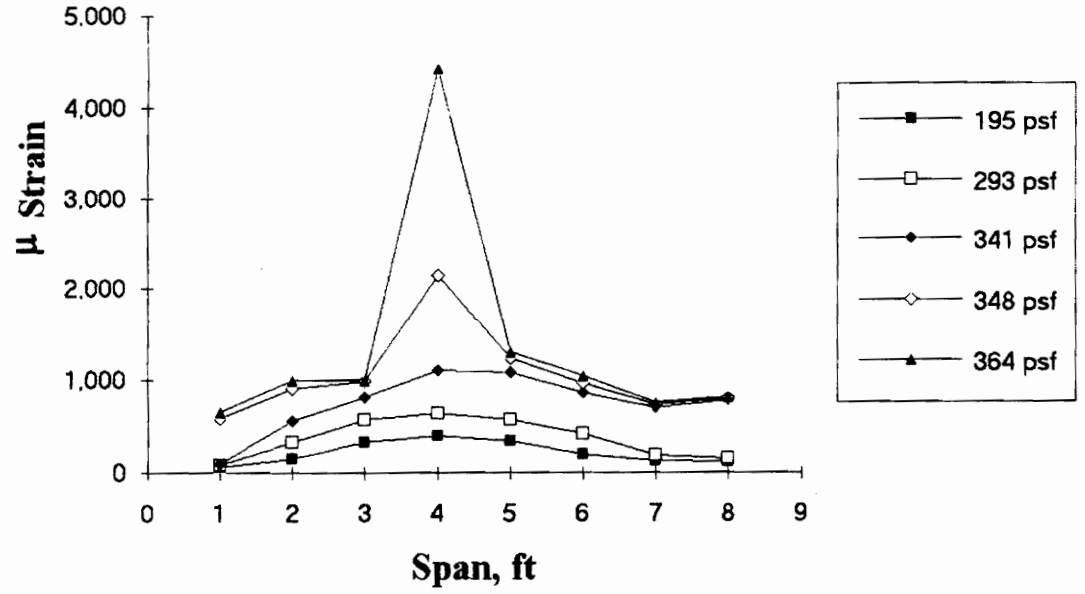

Figure A.118 SDI-2/20-PX1-9 Strain Variation in Deck Bottom Flange along the Span (from centerline of exterior support)

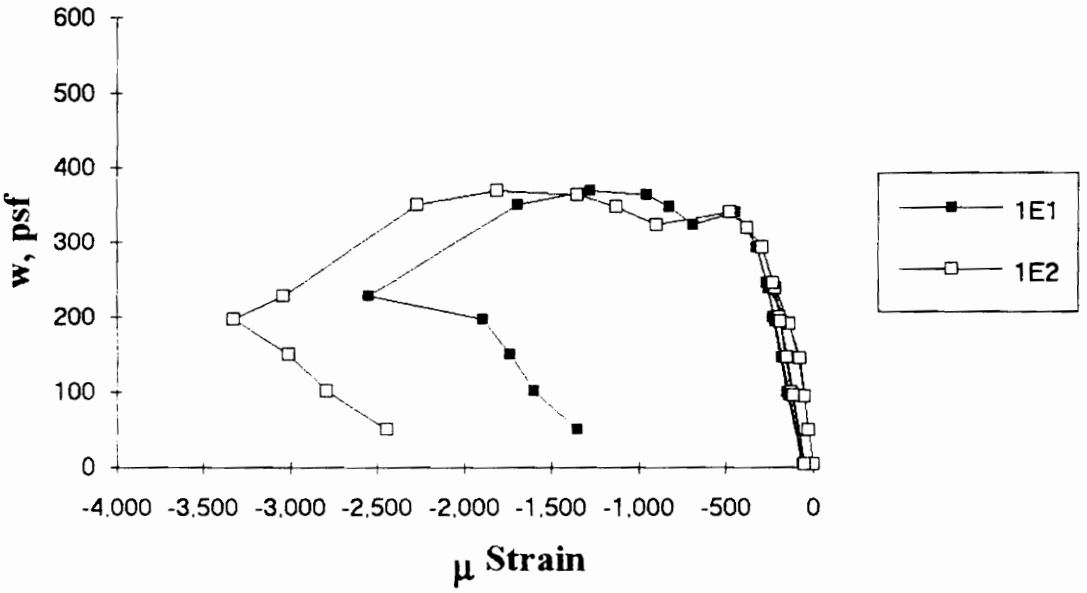

Figure A.119 SDI-2/20-PX1-9 Load vs. Strain in Concrete at Maximum Moment

Test Designation: SDI-2/20-PX2-9
Test Date: December 17, 1993

MATERIALS AND DIMENSIONS

General:

width:	6 ft. (2 panels)
span length:	9 ft. center span
end details:	deck joints
deck anchorage type:	arc spot weld, 3/4 in. dia.
average anchorage spacing:	1.0 ft.

Deck:

thickness:	0.0345 in. (20 gage)
depth:	2 in.
area:	0.519 $in.^2/ft.$
yield stress:	45.4 ksi
ultimate strength:	52.6 ksi
web embossment type:	N/A

embossment dimensions:

N_b :	1.76 in.	W_b :	0.81 in.	s :	3.07 in.
N_t :	1.19 in.	W_t :	0.58 in.	p_h :	0.15 in.

Concrete:

type:	normal weight
test strength:	3,770 psi
total depth:	4.5 in.
cover depth:	2.5 in.

RESULTS

midspan strain due to fresh concrete:	320 x 10^{-6} in./in.
maximum load:	344 psf
deflection at maximum load:	1.82 in.
deflection at termination of test:	2.31 in.
end slip at maximum load:	N/A
end slip at termination of test:	N/A

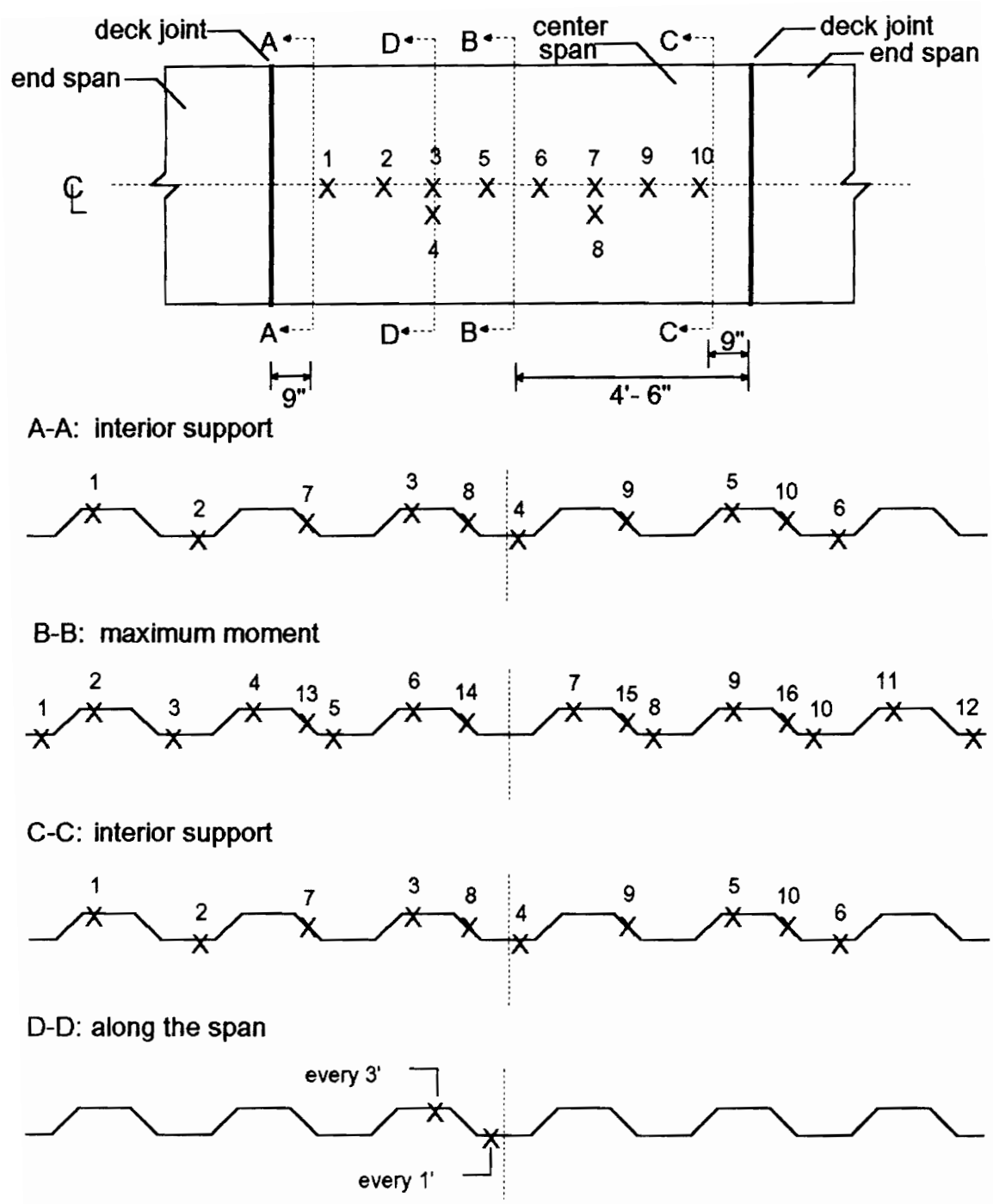

Figure A.120 SDI-2/20-PX2-9 Steel Deck Strain Gage Locations

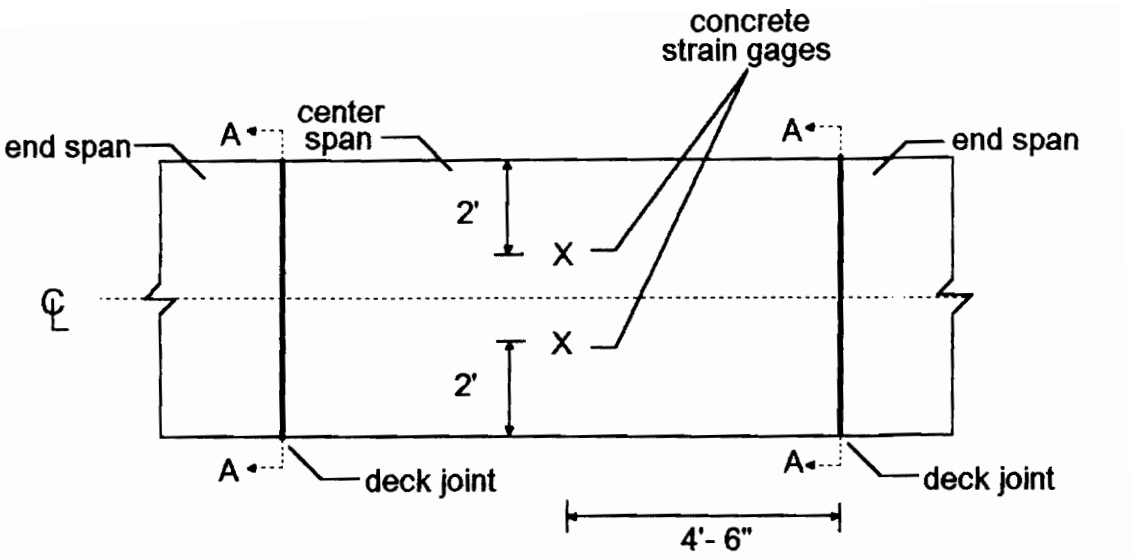

A-A: arc spot welds over supports

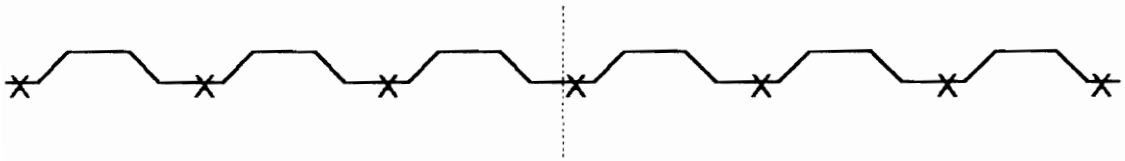

Figure A.121 SDI-2/20-PX2-9 Concrete Strain Gage and Arc Spot Weld Locations

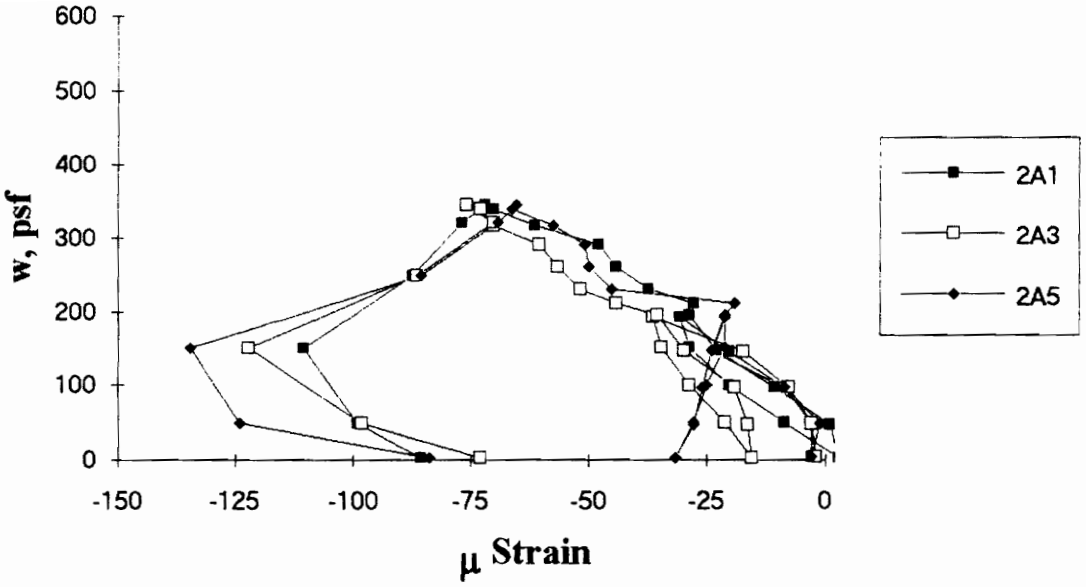

Figure A.122 SDI-2/20-PX2-9 Load vs. Strain in Deck Top Flange at Interior Support

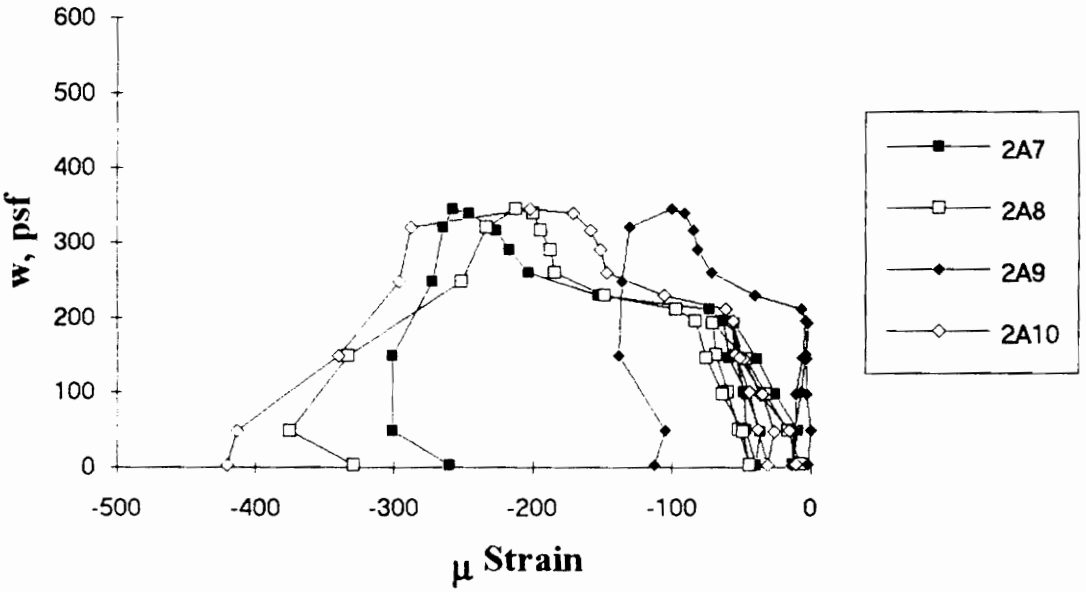

Figure A.123 SDI-2/20-PX2-9 Load vs. Strain in Deck Web at Interior Support

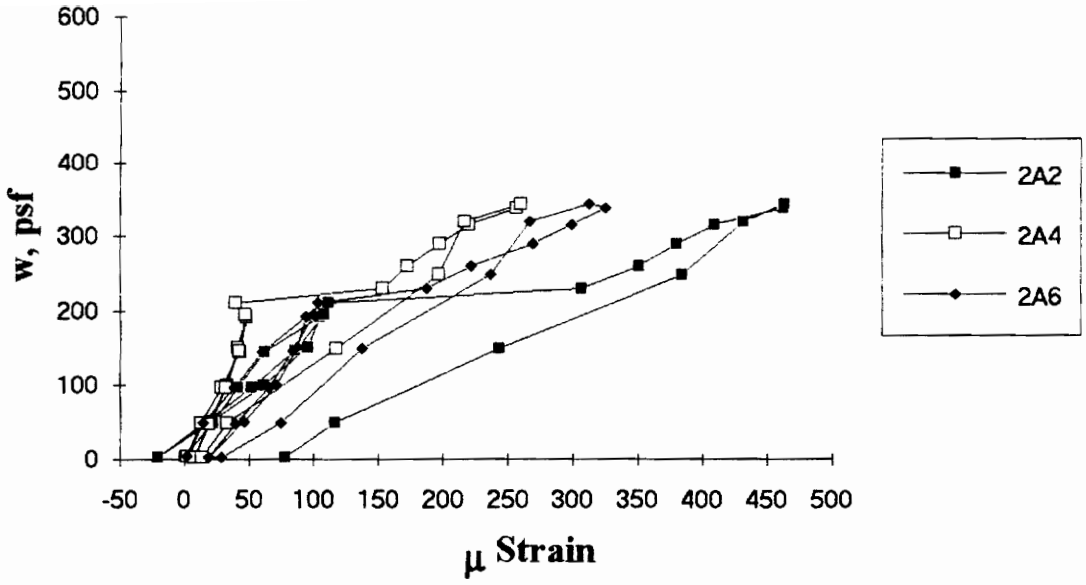

Figure A.124 SDI-2/20-PX2-9 Load vs. Strain in Deck Bottom Flange at Interior Support

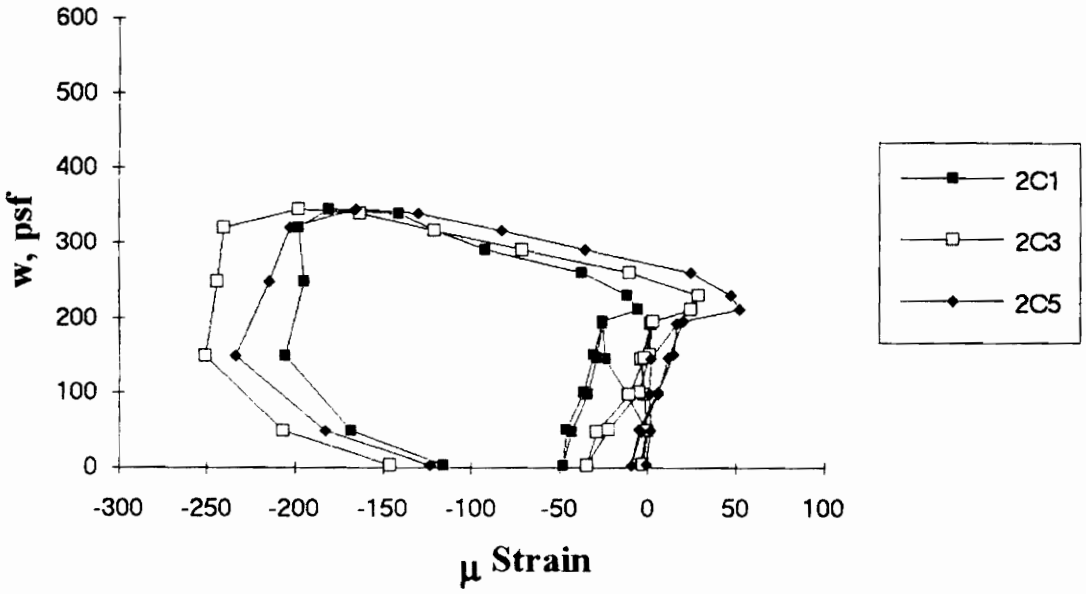

Figure A.125 SDI-2/20-PX2-9 Load vs. Strain in Deck Top Flange at Interior Support

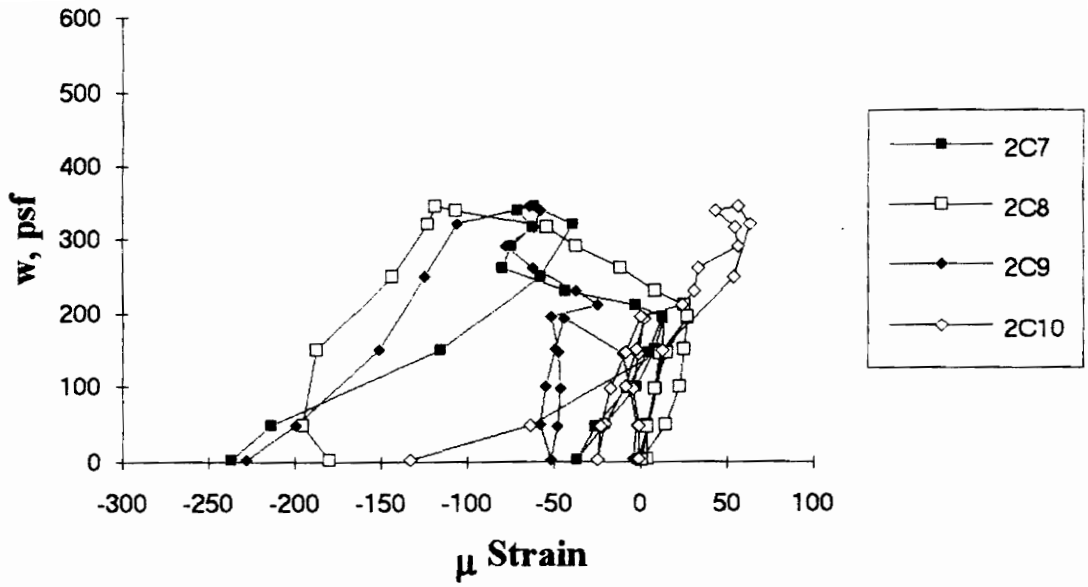

Figure A.126 SDI-2/20-PX2-9 Load vs. Strain in Deck Web at Interior Support

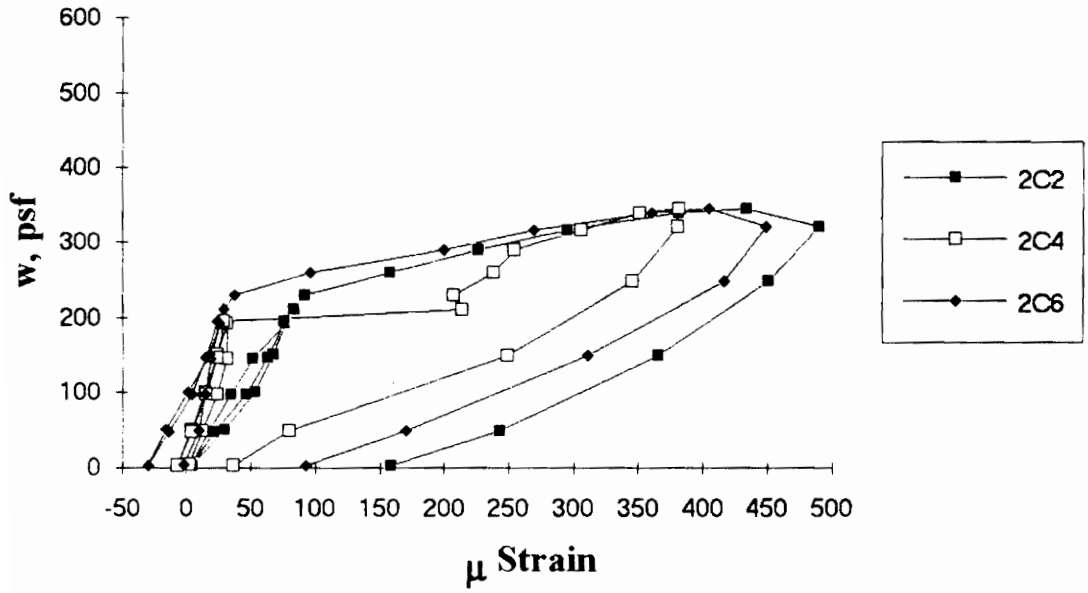

Figure A.127 SDI-2/20-PX2-9 Load vs. Strain in Deck Bottom Flange at Interior Support

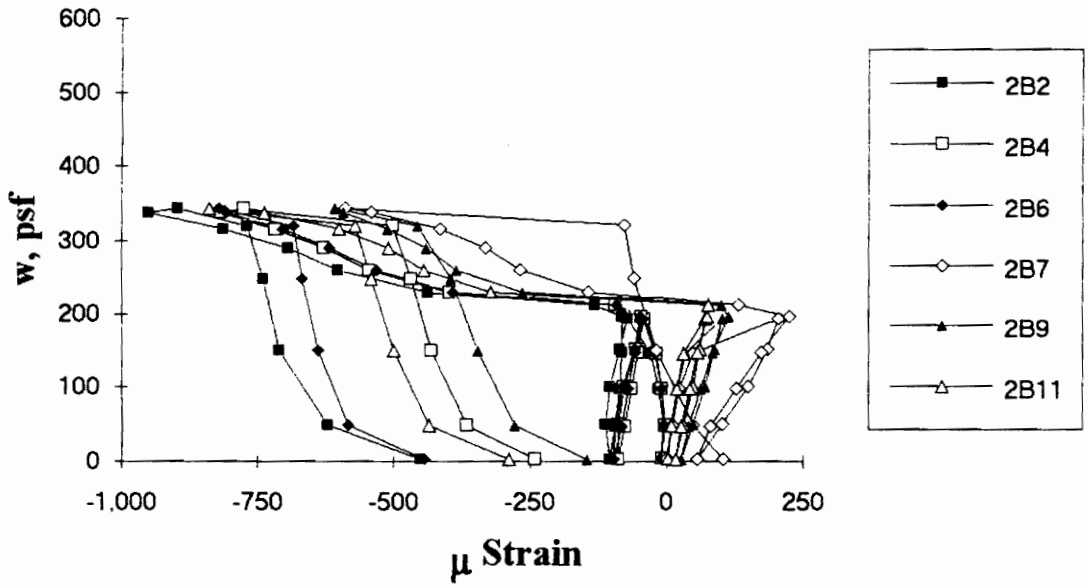

Figure A.128 SDI-2/20-PX2-9 Load vs. Strain in Deck Top Flange at Maximum Moment

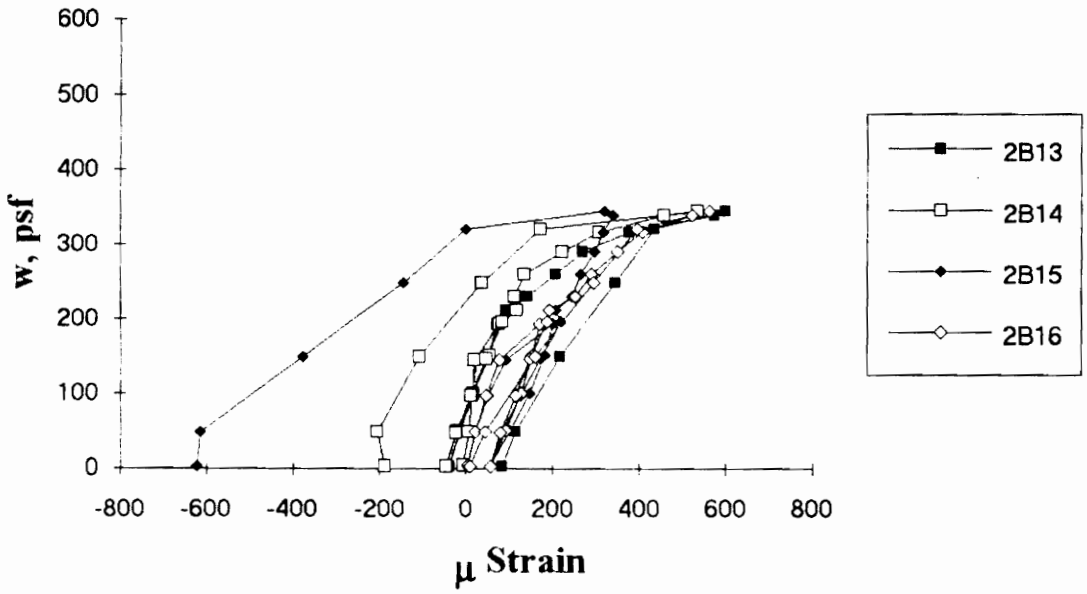

Figure A.129 SDI-2/20-PX2-9 Load vs. Strain in Deck Web at Maximum Moment

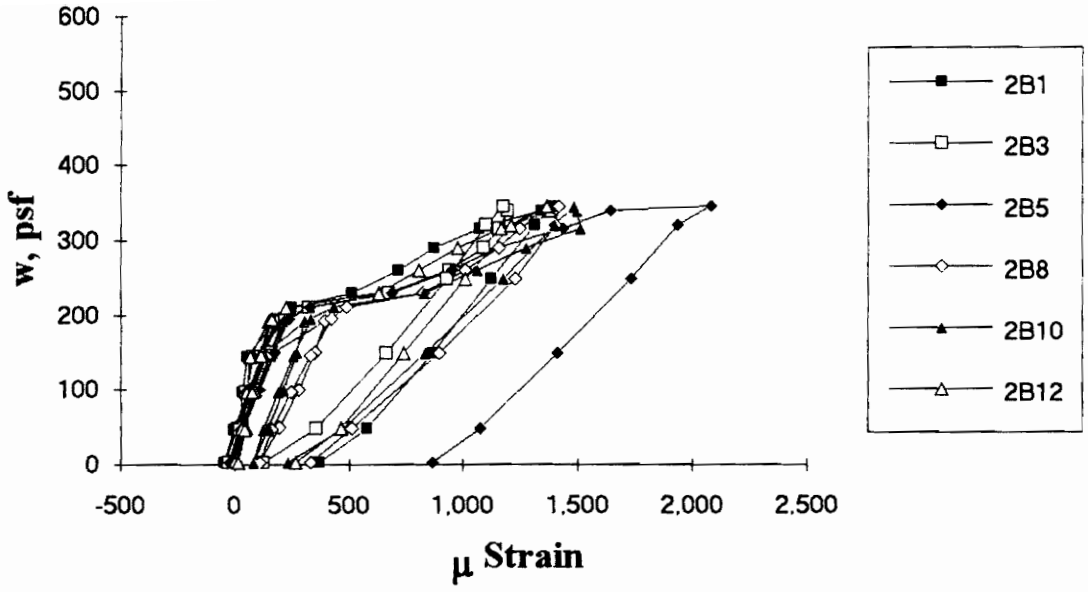

Figure A.130 SDI-2/20-PX2-9 Load vs. Strain in Deck Bottom Flange at Maximum Moment

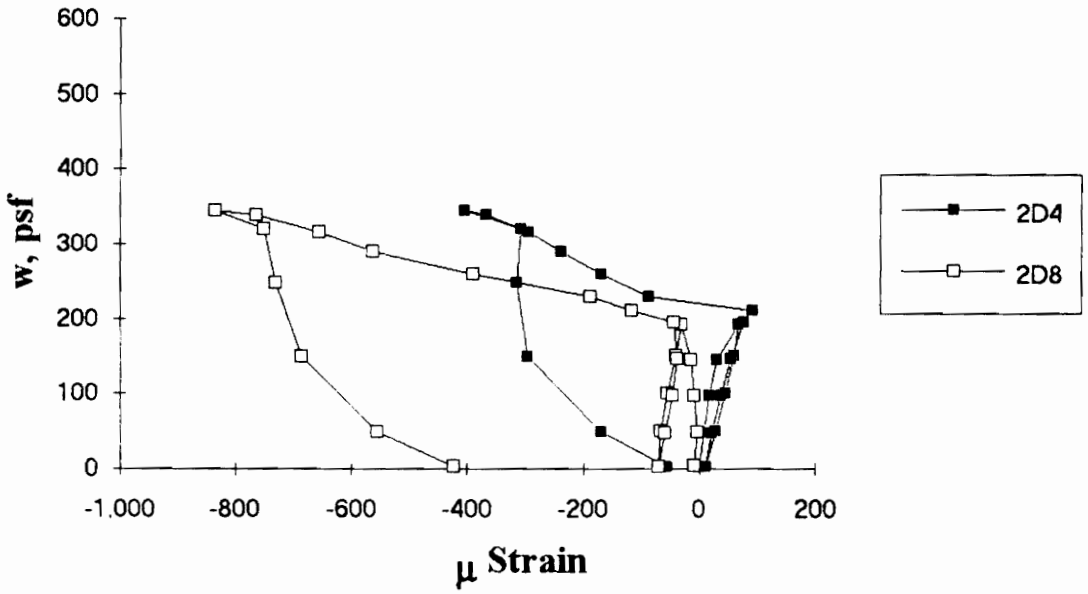

Figure A.131 SDI-2/20-PX2-9 Load vs. Strain in Deck Top Flange along the Span

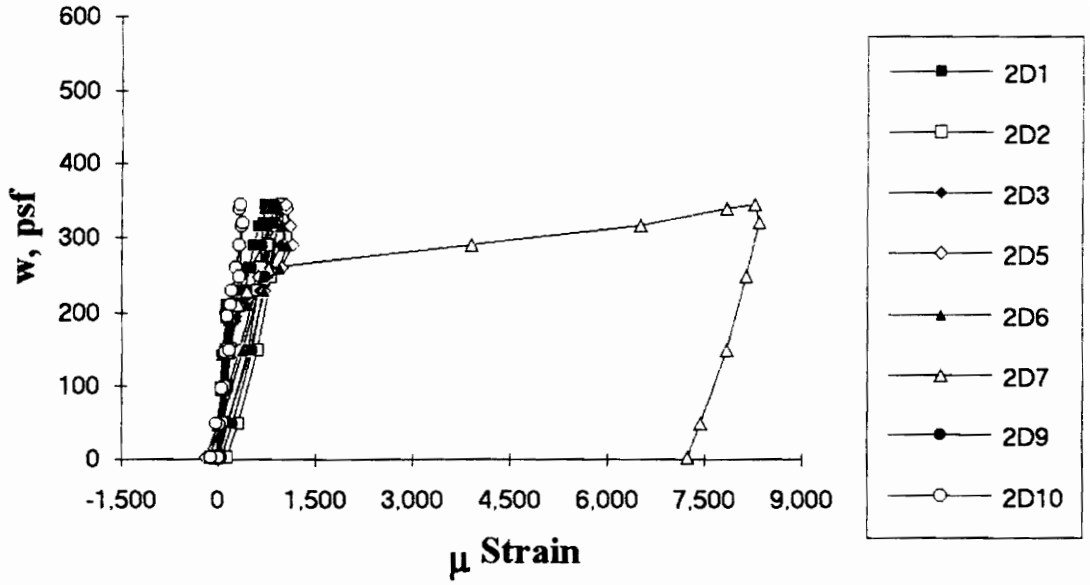

Figure A.132 SDI-2/20-PX2-9 Load vs. Strain in Deck Bottom Flange along the Span

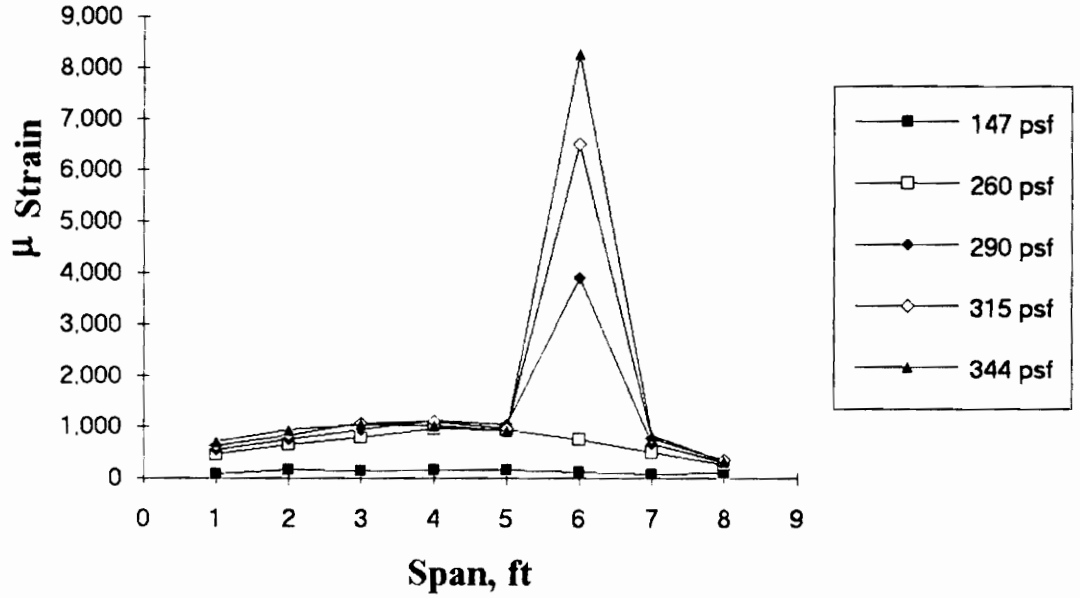

Figure A.133 SDI-2/20-PX2-9 Strain Variation in Deck Bottom Flange along the Span (from centerline of support)

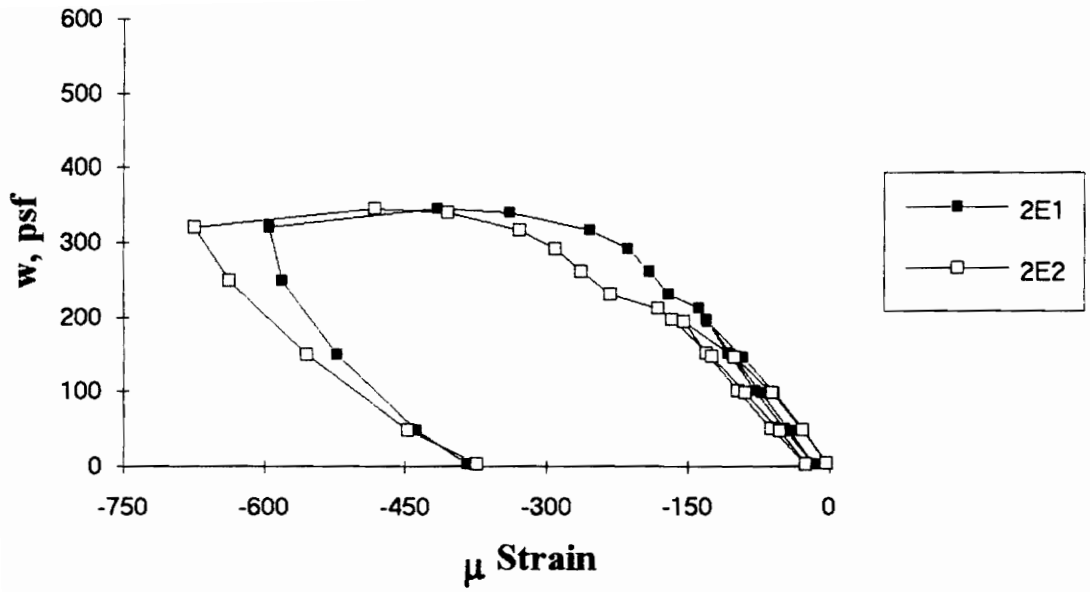

Figure A.134 SDI-2/20-PX2-9 Load vs. Strain in Concrete at Maximum Moment

Test Designation: SDI-2/20-PX3-9
Test Date: December 16, 1993

MATERIALS AND DIMENSIONS

General:

width:	6 ft. (2 panels)
span length:	9 ft. end span
end details:	angle with return lip, int. support deck joint
deck anchorage type:	arc spot weld, 3/4 in. dia.
average anchorage spacing:	1.0 ft.

Deck:

thickness:	0.0345 in. (20 gage)
depth:	2 in.
area:	0.519 $in.^2/ft.$
yield stress:	45.4 ksi
ultimate strength:	52.6 ksi
web embossment type:	N/A

embossment dimensions:

N_b :	1.76 in.	W_b :	0.81 in.	s :	3.07 in.
N_t :	1.19 in.	W_t :	0.58 in.	p_h :	0.15 in.

Concrete:

type:	normal weight
test strength:	3,770 psi
total depth:	4.5 in.
cover depth:	2.5 in.

RESULTS

midspan strain due to fresh concrete:	320 x 10^{-6} in./in.
maximum load:	488 psf
deflection at maximum load:	1.77 in.
deflection at termination of test:	3.91 in.
end slip at maximum load:	0.00 in.
end slip at termination of test:	0.00 in.

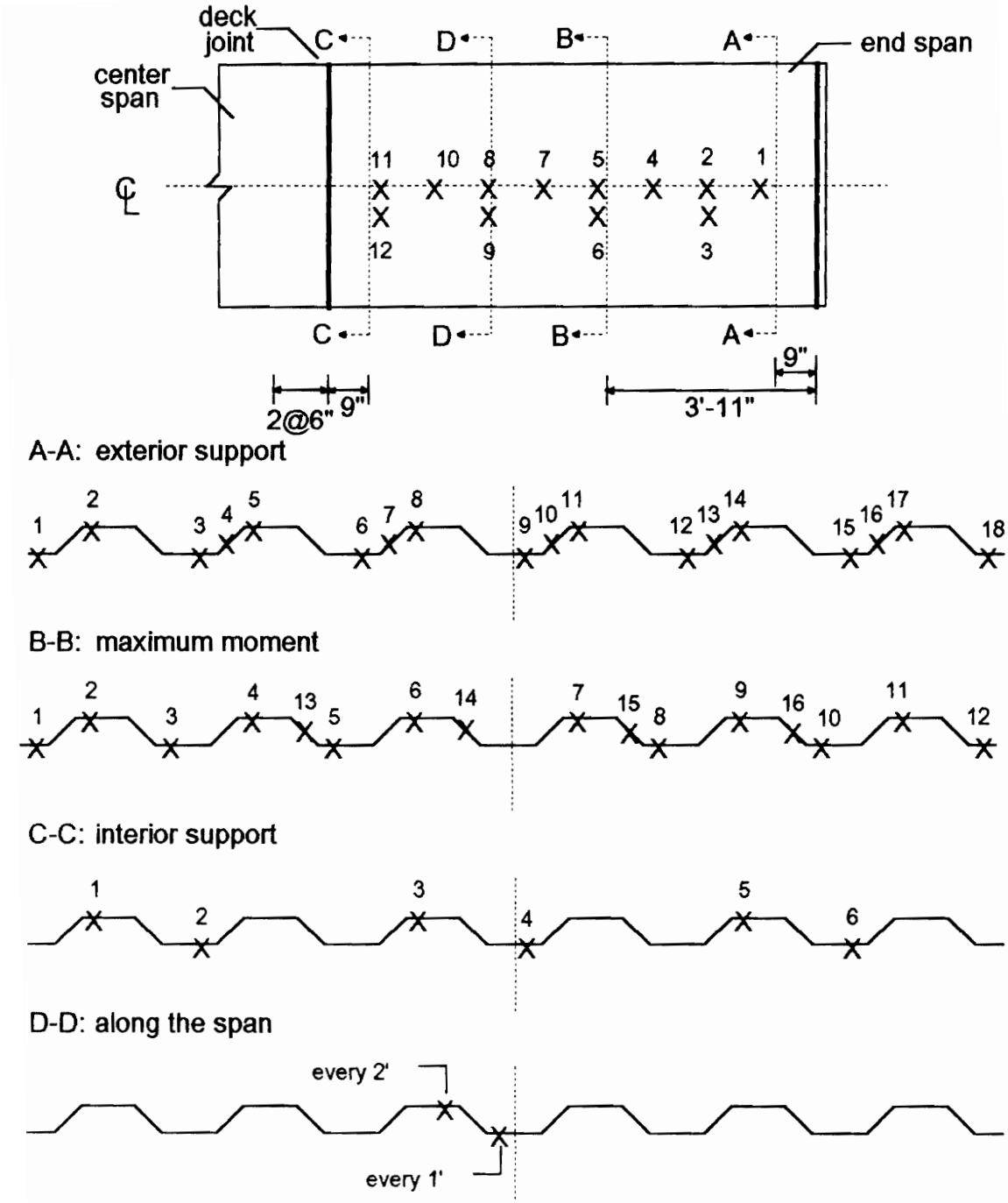

Figure A.135 SDI-2/20-PX3-9 Steel Deck Strain Gage Locations

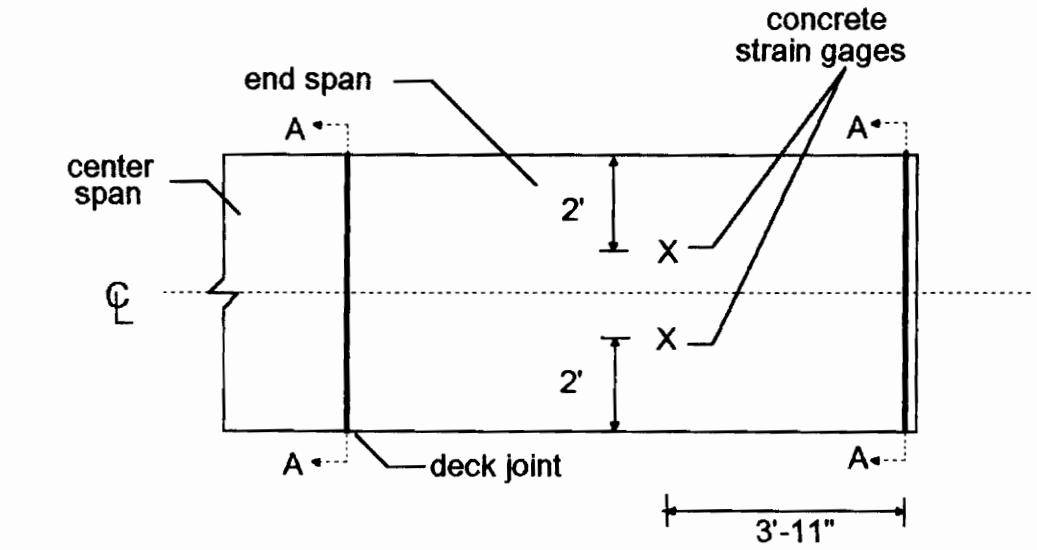

A-A: arc spot welds over supports

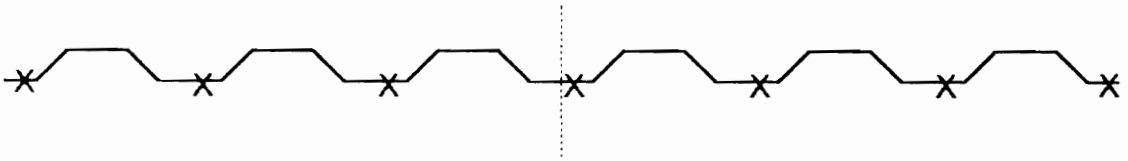

Figure A.136 SDI-2/20-PX3-9 Concrete Strain Gage and Arc Spot Weld Locations

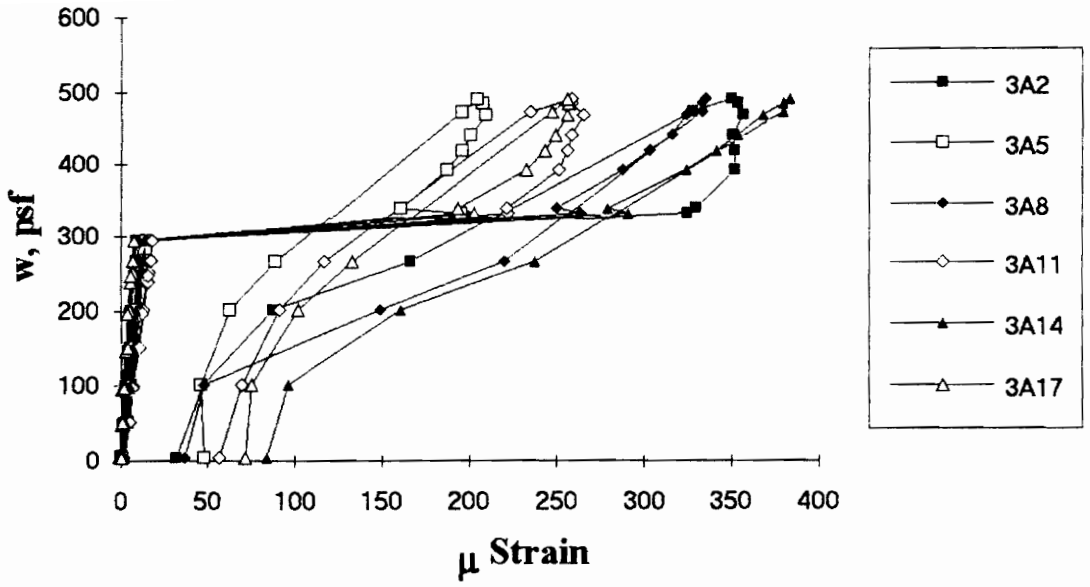

Figure A.137 SDI-2/20-PX3-9 Load vs. Strain in Deck Top Flange at Exterior Support

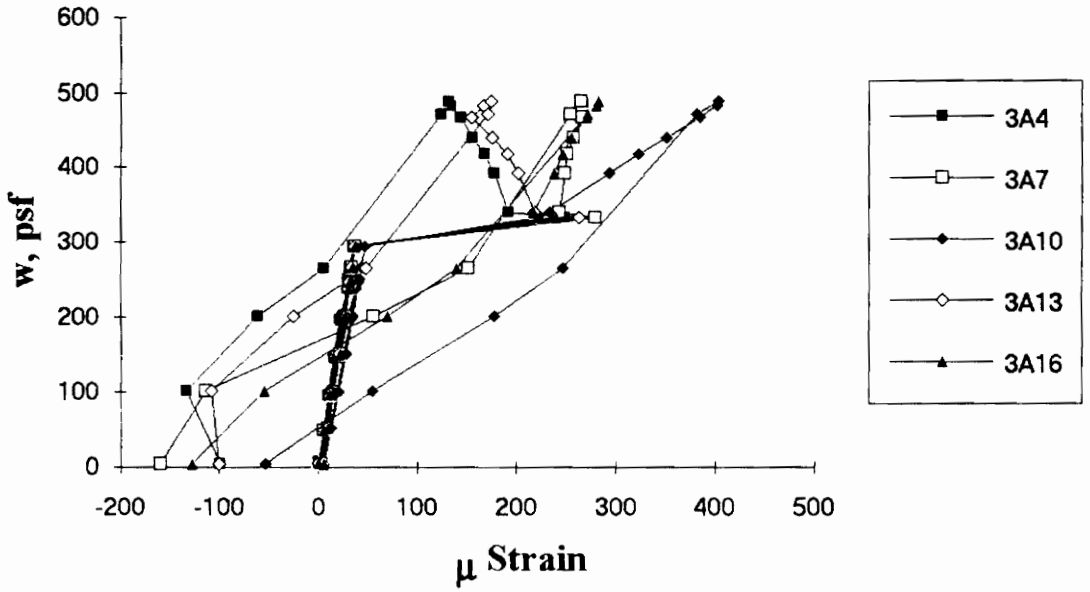

Figure A.138 SDI-2/20-PX3-9 Load vs. Strain in Deck Web at Exterior Support

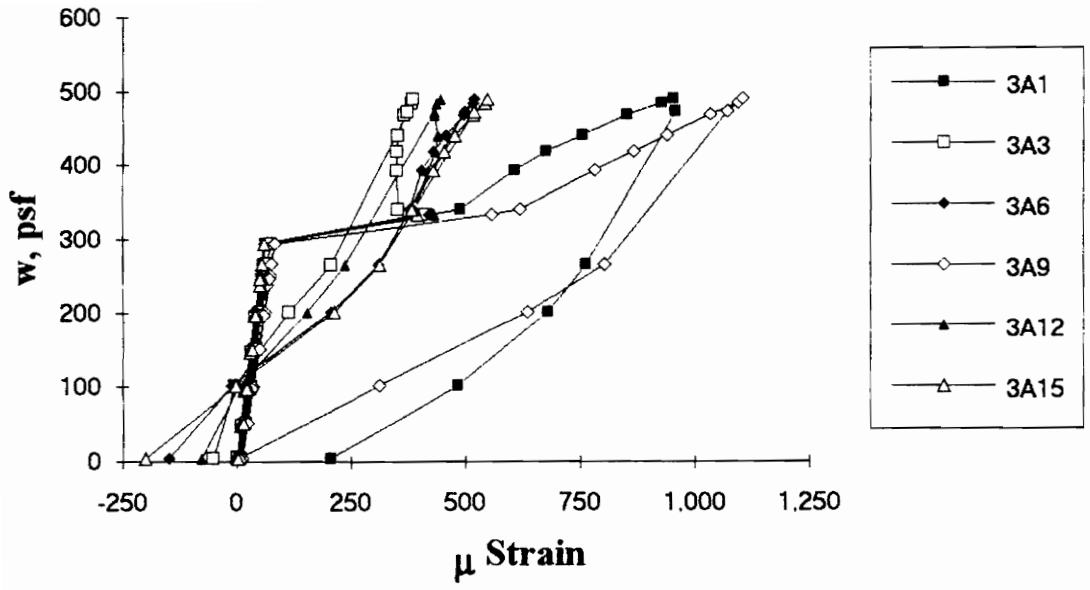

Figure A.139 SDI-2/20-PX3-9 Load vs. Strain in Deck Bottom Flange at Exterior Support

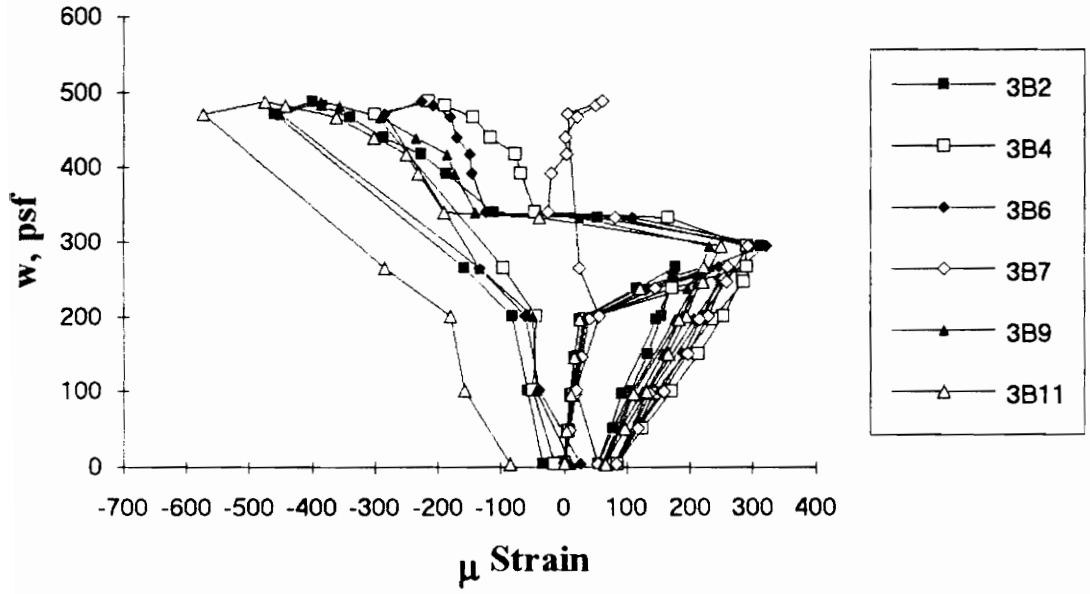

Figure A.140 SDI-2/20-PX3-9 Load vs. Strain in Deck Top Flange at Maximum Moment

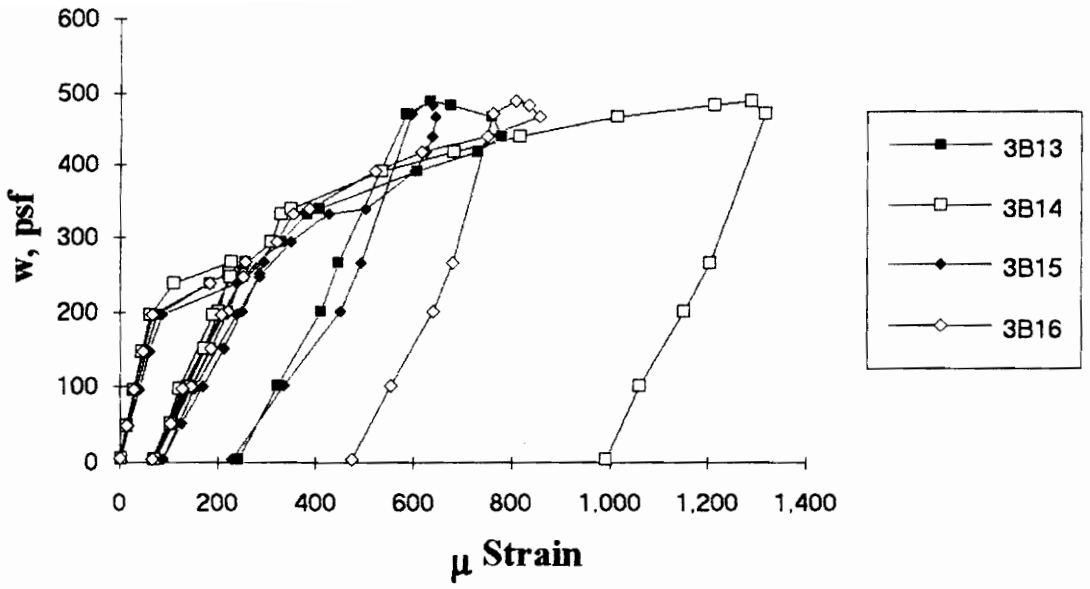

Figure A.141 SDI-2/20-PX3-9 Load vs. Strain in Deck Web at Maximum Moment

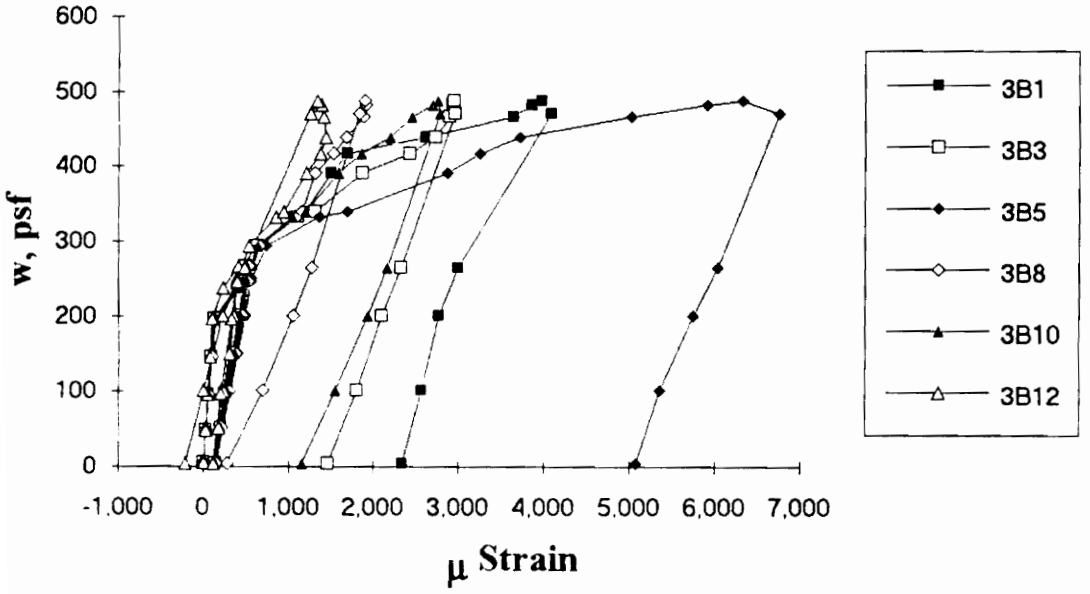

Figure A.142 SDI-2/20-PX3-9 Load vs. Strain in Deck Bottom Flange at Maximum Moment

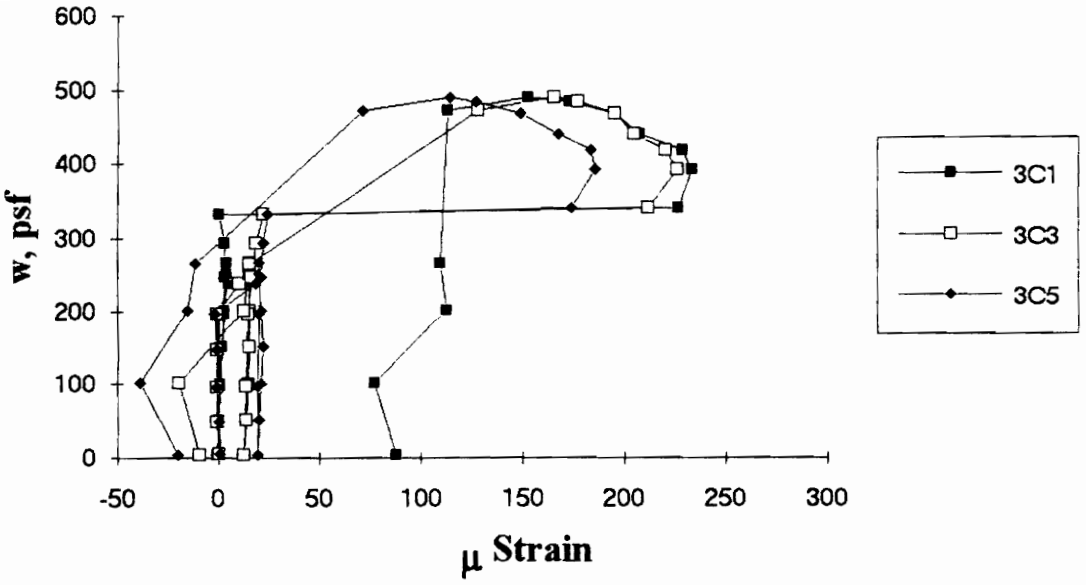

Figure A.143 SDI-2/20-PX3-9 Load vs. Strain in Deck Top Flange at Interior Support

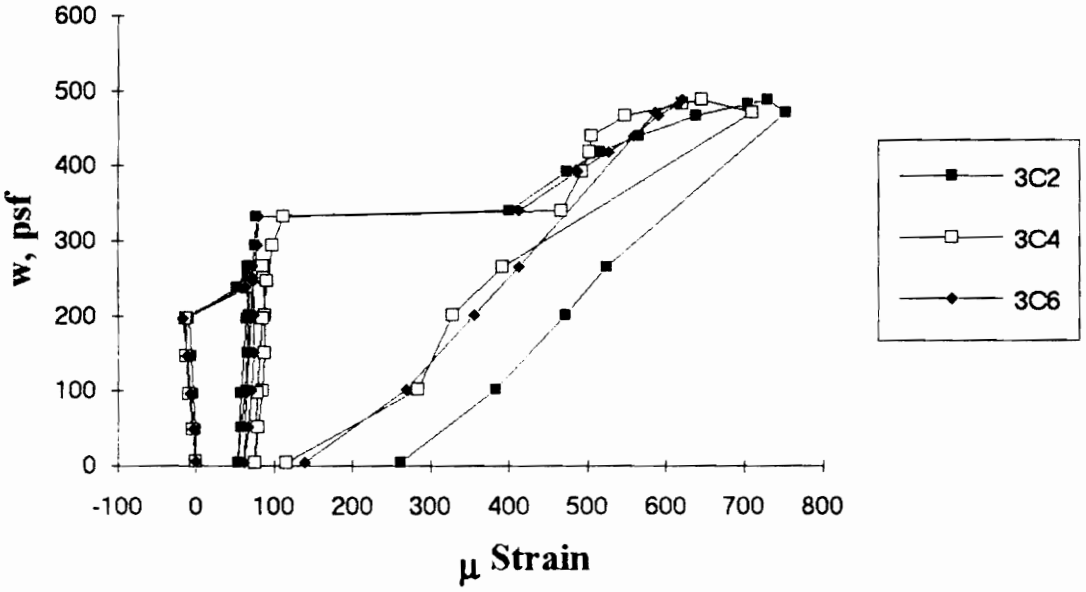

Figure A.144 SDI-2/20-PX3-9 Load vs. Strain in Deck Bottom Flange at Interior Support

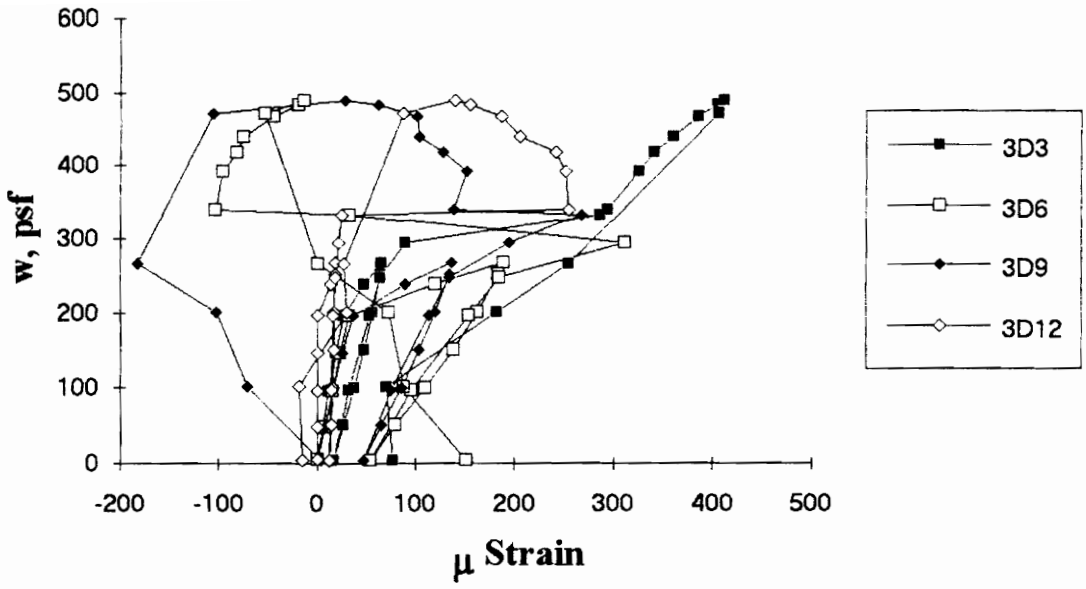

Figure A.145 SDI-2/20-PX3-9 Load vs. Strain in Deck Top Flange along the Span

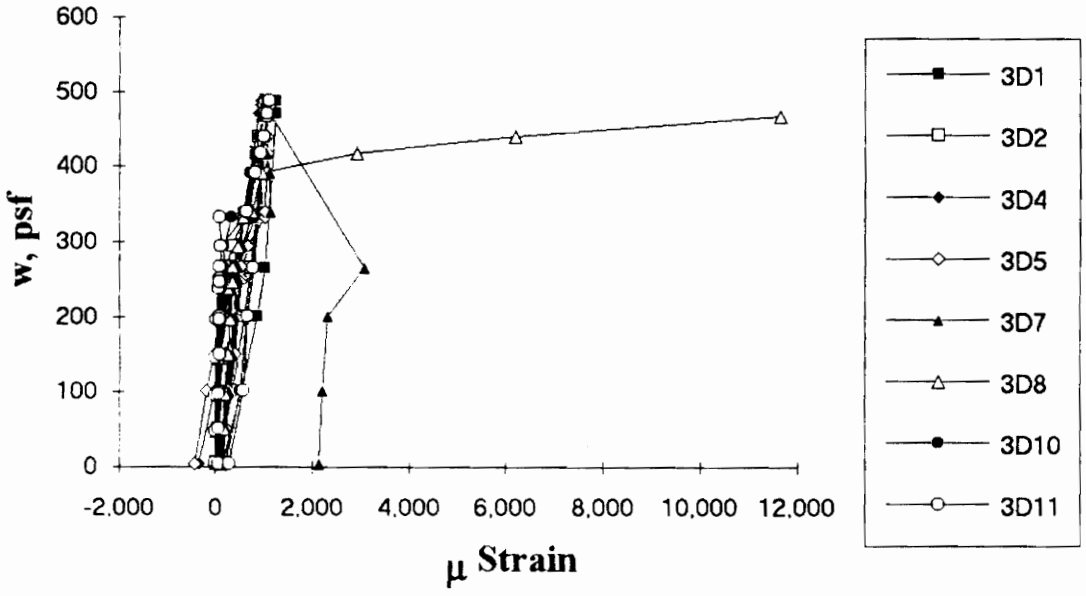

Figure A.146 SDI-2/20-PX3-9 Load vs. Strain in Deck Bottom Flange along the Span

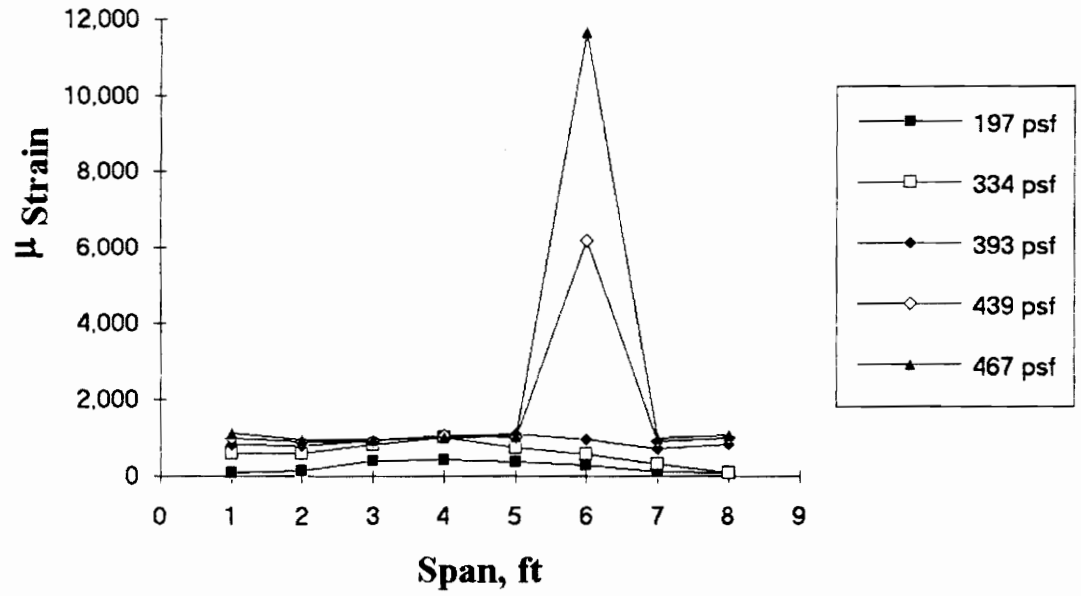

Figure A.147 SDI-2/20-PX3-9 Strain Variation in Deck Bottom Flange along the Span (from centerline of exterior support)

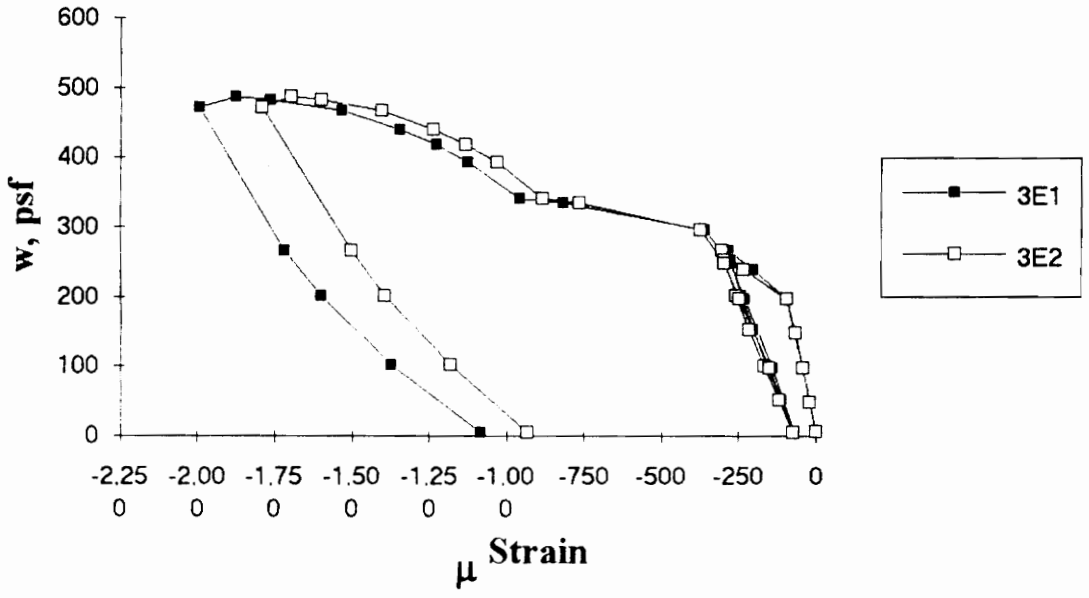

Figure A.148 SDI-2/20-PX3-9 Load vs. Strain in Concrete at Maximum Moment

Test Designation: SDI-2/18-3-9
Test Date: January 13, 1994

MATERIALS AND DIMENSIONS

General:

width:	6 ft. (2 panels)
span length:	9 ft. end span
end details:	1 ft. cantilever
deck anchorage type:	shear stud, 3-7/8 in. long, 3/4 in. dia.
average anchorage spacing:	2.1 ft.

Deck:

thickness:	0.0470 in. (18 gage)
depth:	2 in.
area:	0.696 $in.^2/ft.$
yield stress:	46.5 ksi
ultimate strength:	59.6 ksi
web embossment type:	I

embossment dimensions:

N_b : 2.28 in.	W_b : 0.44 in.	s : 1.59 in.
N_t : 1.68 in.	W_t : 0.24 in.	p_h : 0.08 in.

Concrete:

type:	normal weight
test strength:	5,300 psi
total depth:	4.5 in.
cover depth:	2.5 in.

RESULTS

midspan strain due to fresh concrete:	220 x 10^{-6} in./in.
maximum load:	903 psf
deflection at maximum load:	2.50 in.
deflection at termination of test:	4.82 in.
end slip at maximum load:	0.17 in.
end slip at termination of test:	0.68 in.

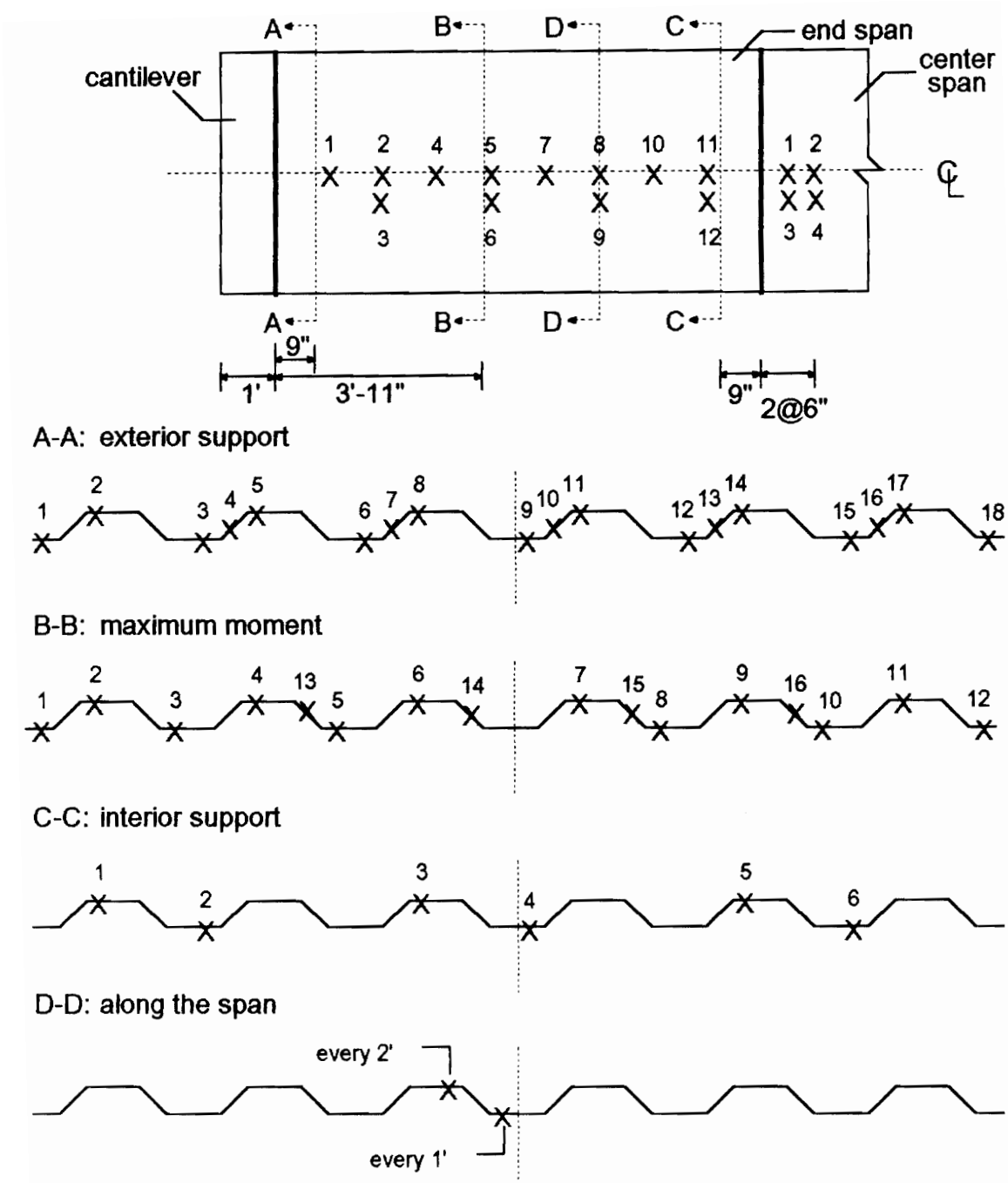

Figure A.149 SDI-2/18-3-9 Steel Deck Strain Gage Locations

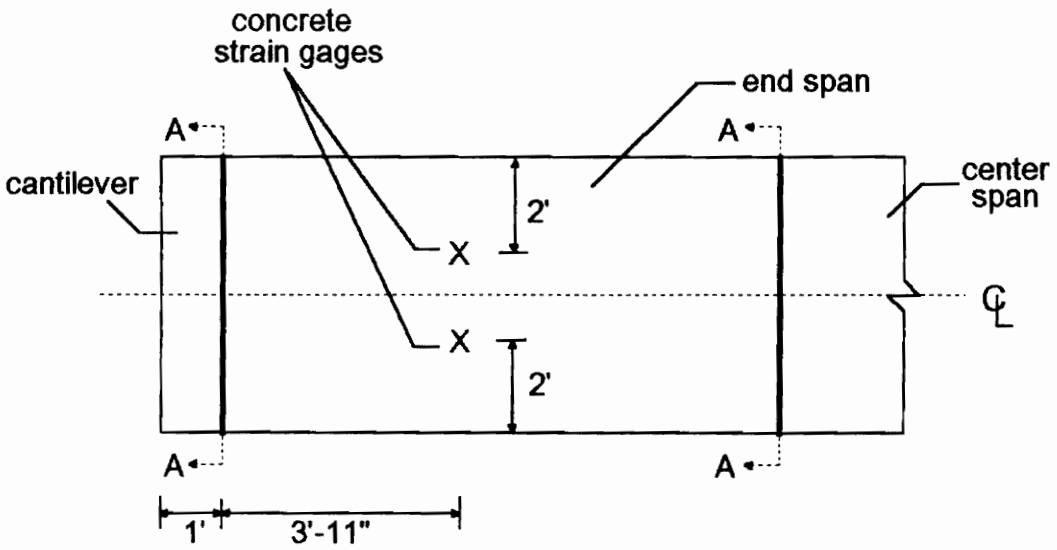

A-A: shear studs over supports

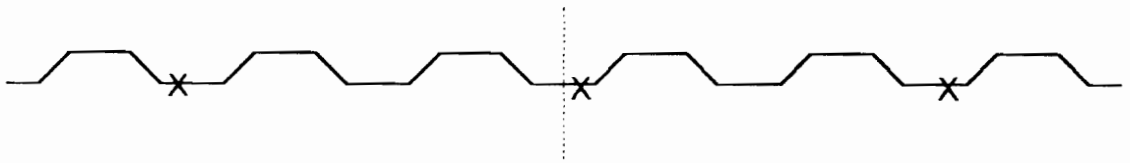

Figure A.150 SDI-2/18-3-9 Concrete Strain Gage and Shear Stud Locations

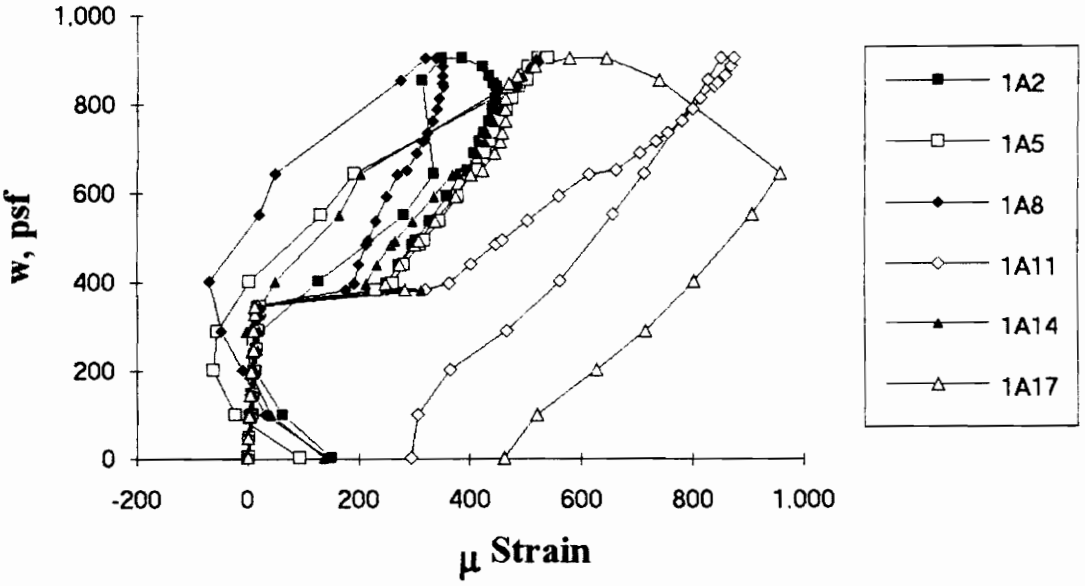

Figure A.151 SDI-2/18-3-9 Load vs. Strain in Deck Top Flange at Exterior Support

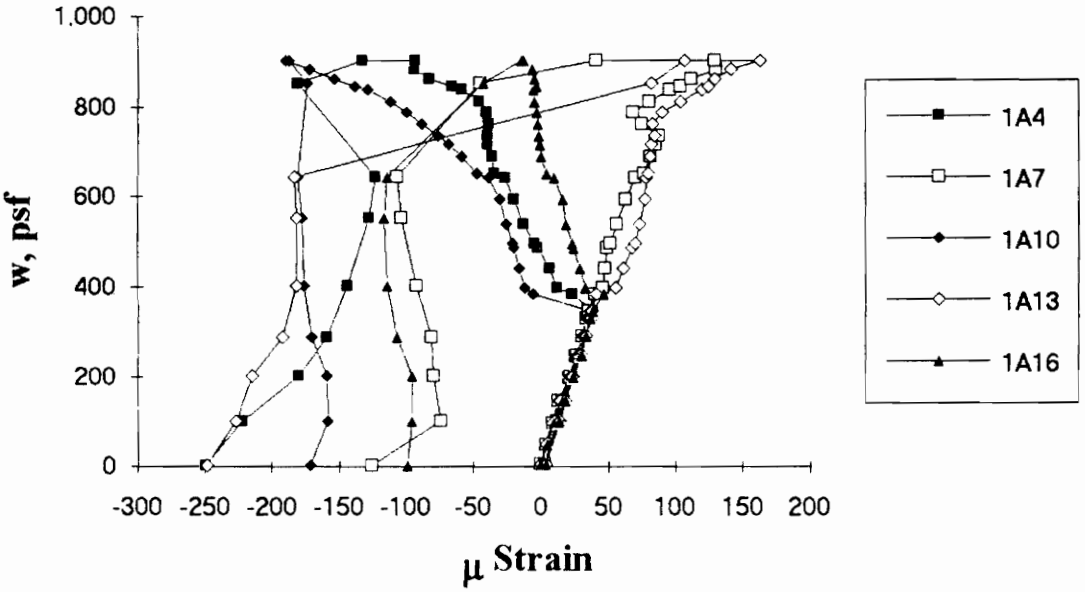

Figure A.152 SDI-2/18-3-9 Load vs. Strain in Deck Web at Exterior Support

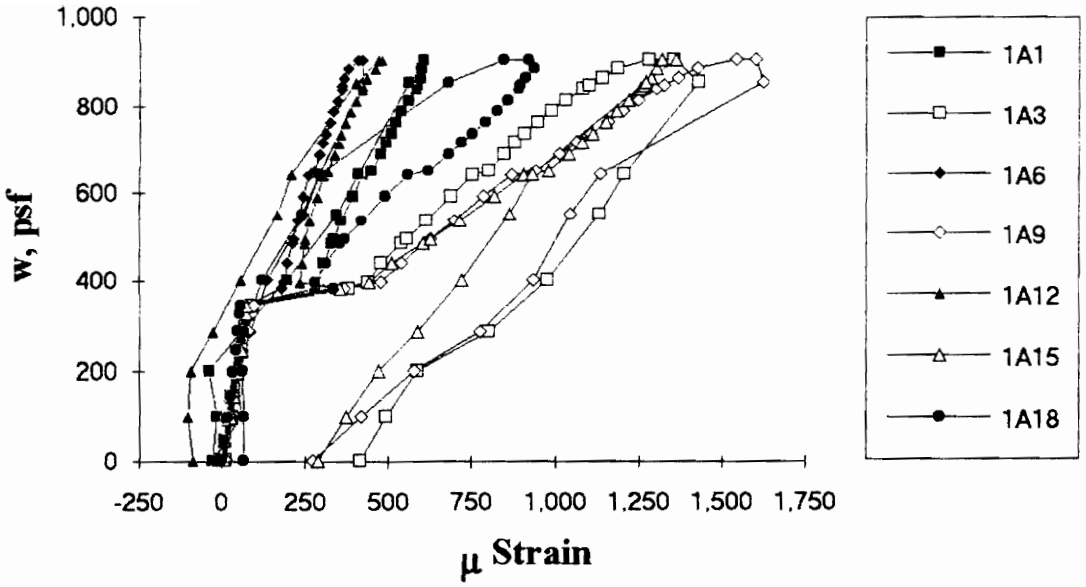

Figure A.153 SDI-2/18-3-9 Load vs. Strain in Deck Bottom Flange at Exterior Support

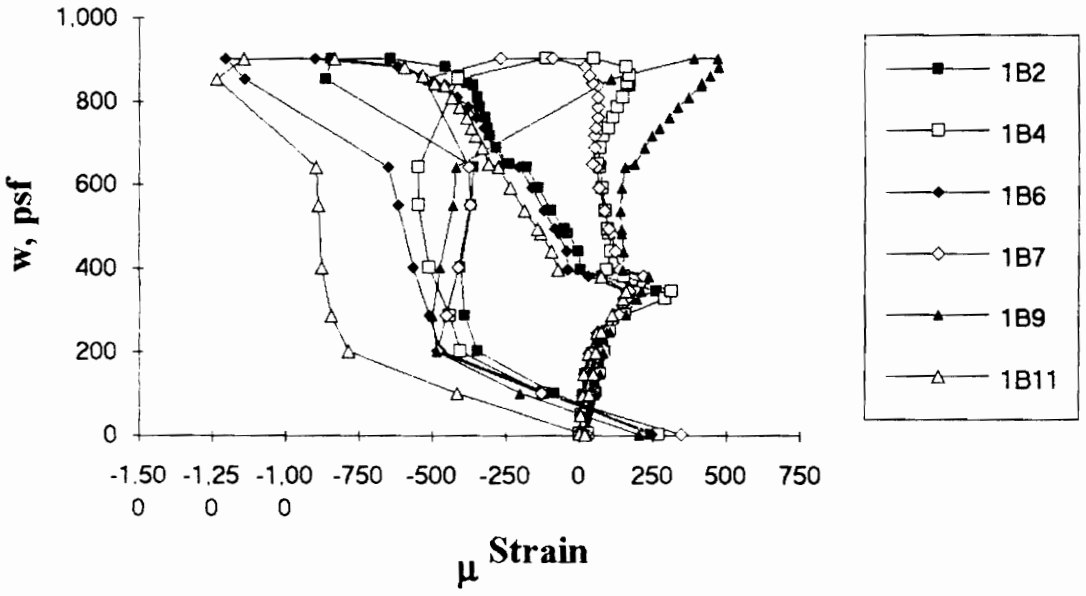

Figure A.154 SDI-2/18-3-9 Load vs. Strain in Deck Top Flange at Maximum Moment

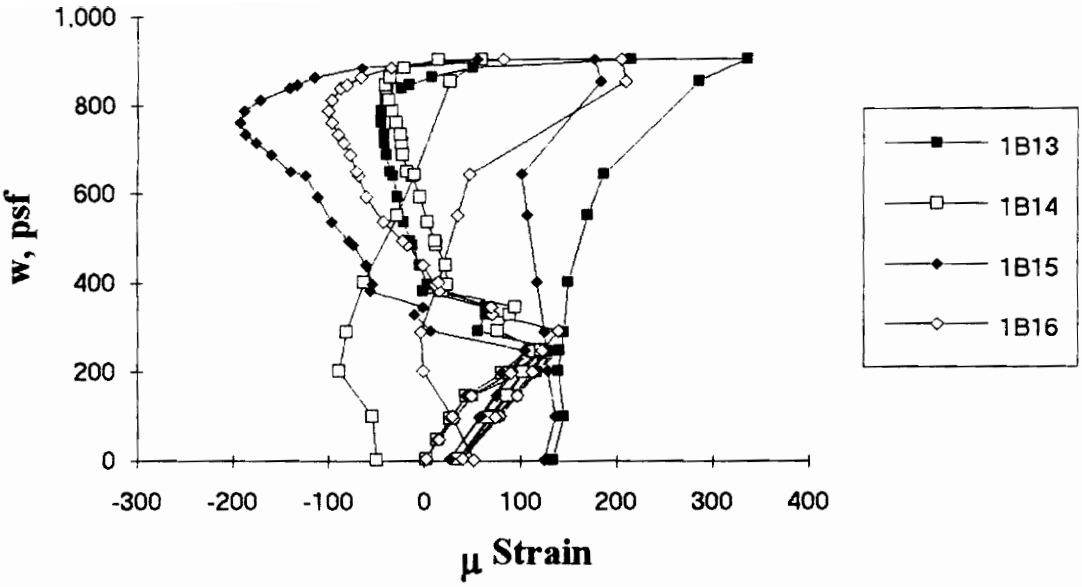

Figure A.155 SDI-2/18-3-9 Load vs. Strain in Deck Web at Maximum Moment

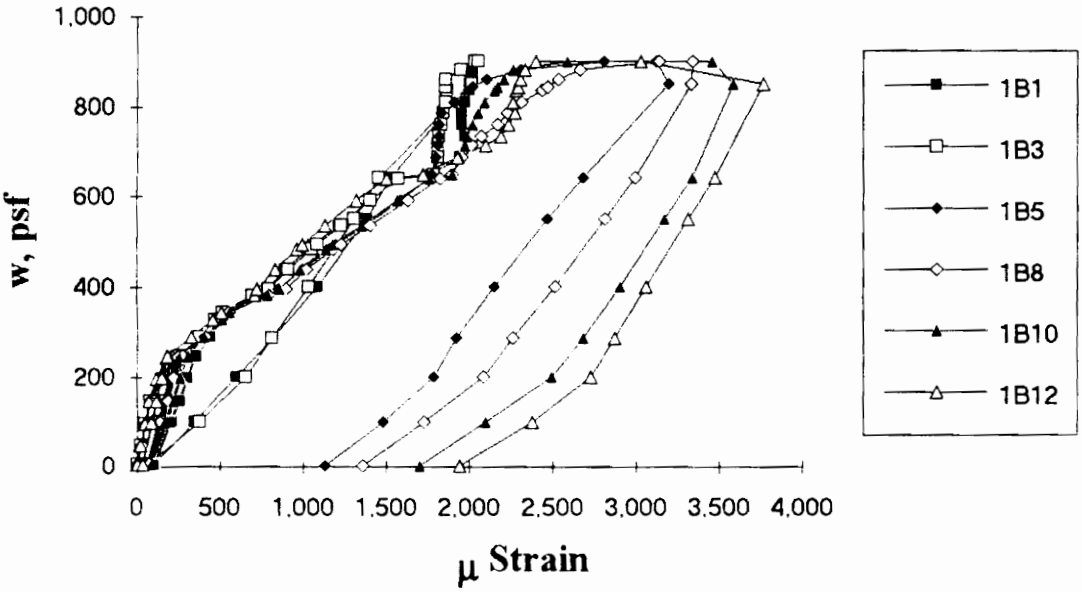

Figure A.156 SDI-2/18-3-9 Load vs. Strain in Deck Bottom Flange at Maximum Moment

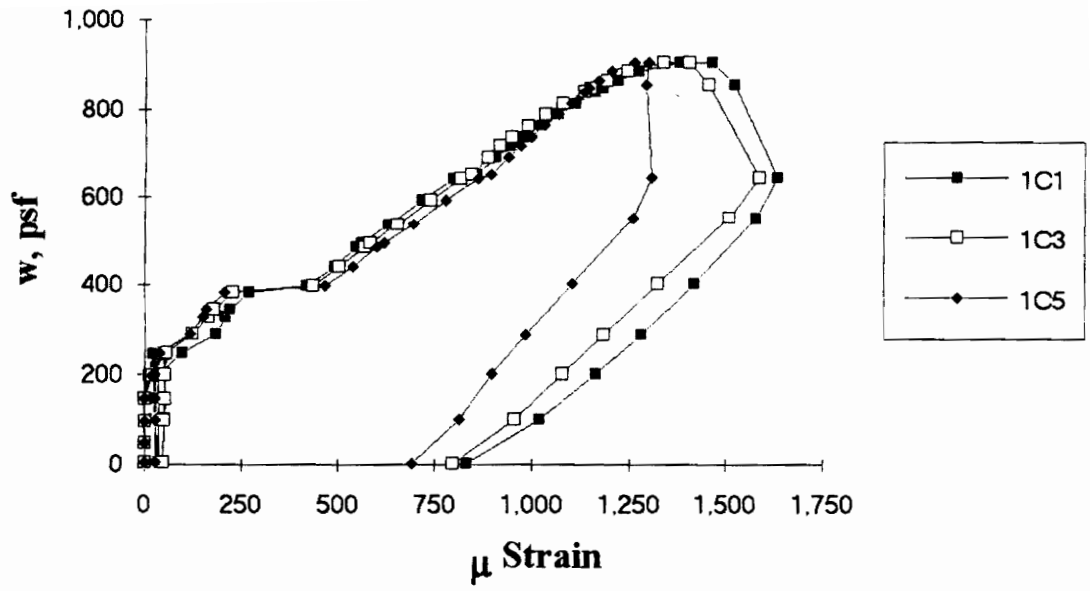

Figure A.157 SDI-2/18-3-9 Load vs. Strain in Deck Top Flange at Interior Support

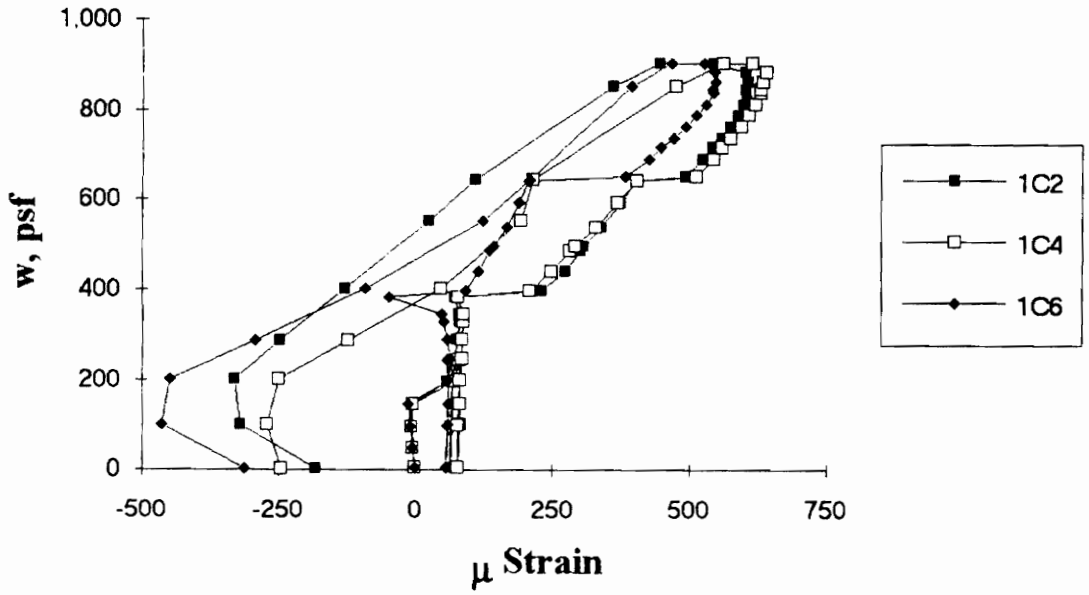

Figure A.158 SDI-2/18-3-9 Load vs. Strain in Deck Bottom Flange at Interior Support

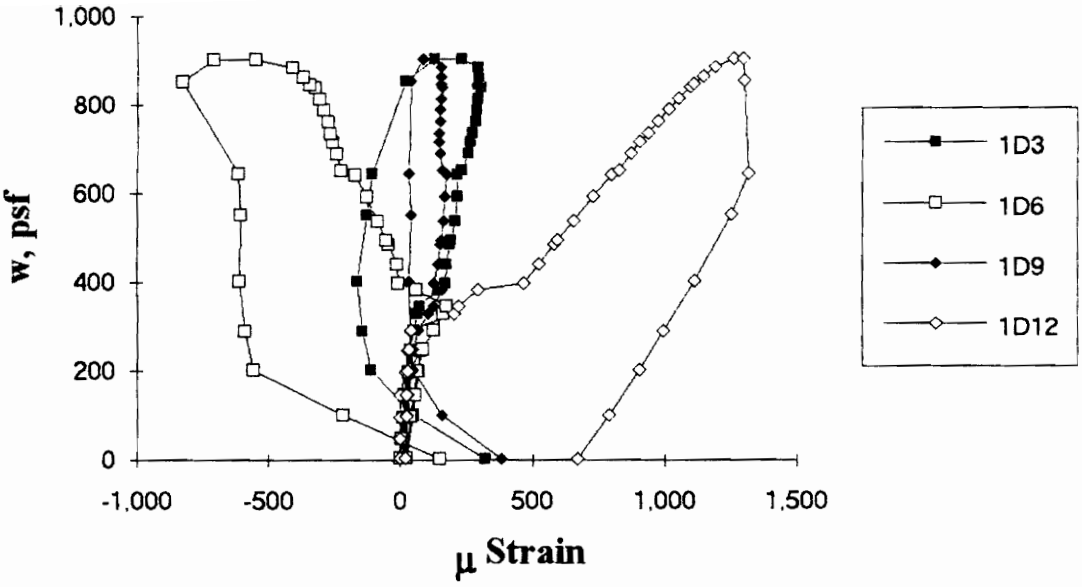

Figure A.159 SDI-2/18-3-9 Load vs. Strain in Deck Top Flange along the Span

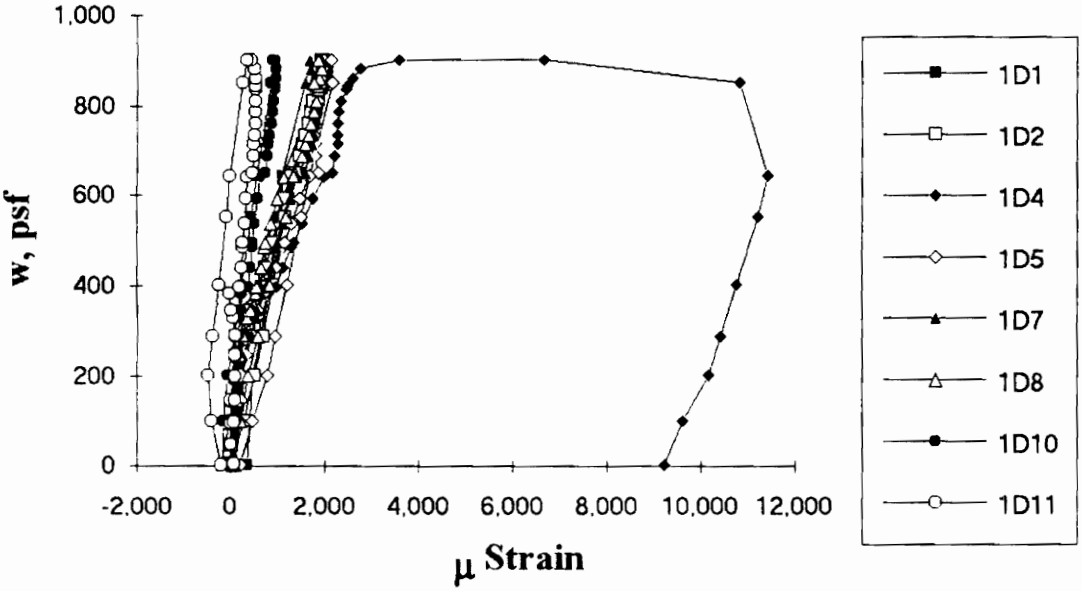

Figure A.160 SDI-2/18-3-9 Load vs. Strain in Deck Bottom Flange along the Span

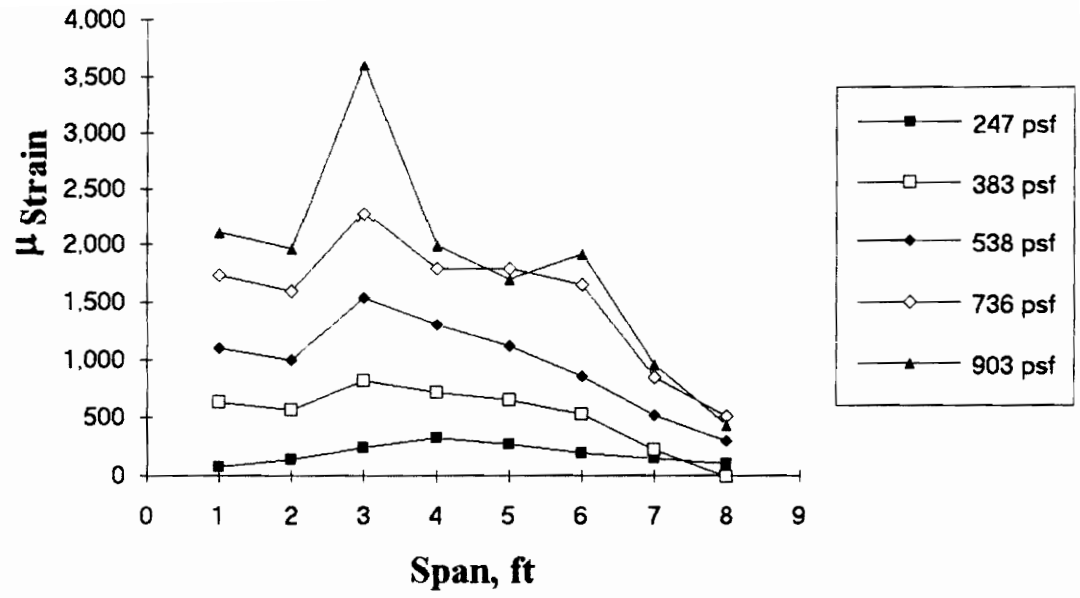

Figure A.161 SDI-2/18-3-9 Strain Variation in Deck Bottom Flange along the Span (from centerline of exterior support)

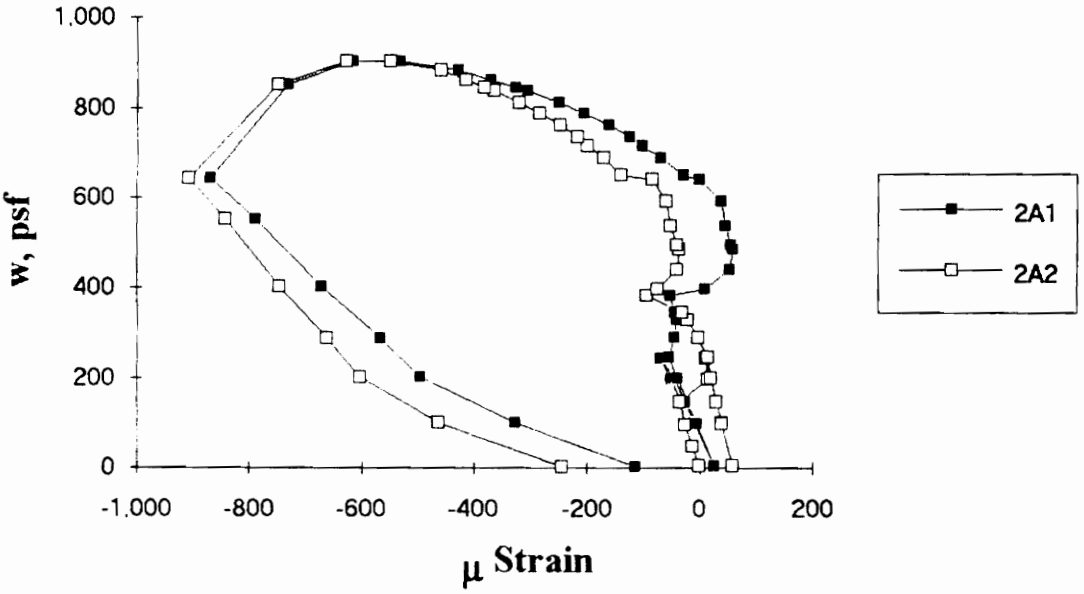

Figure A.162 SDI-2/18-3-9 Load vs. Strain in Deck Bottom Flange in Center Span

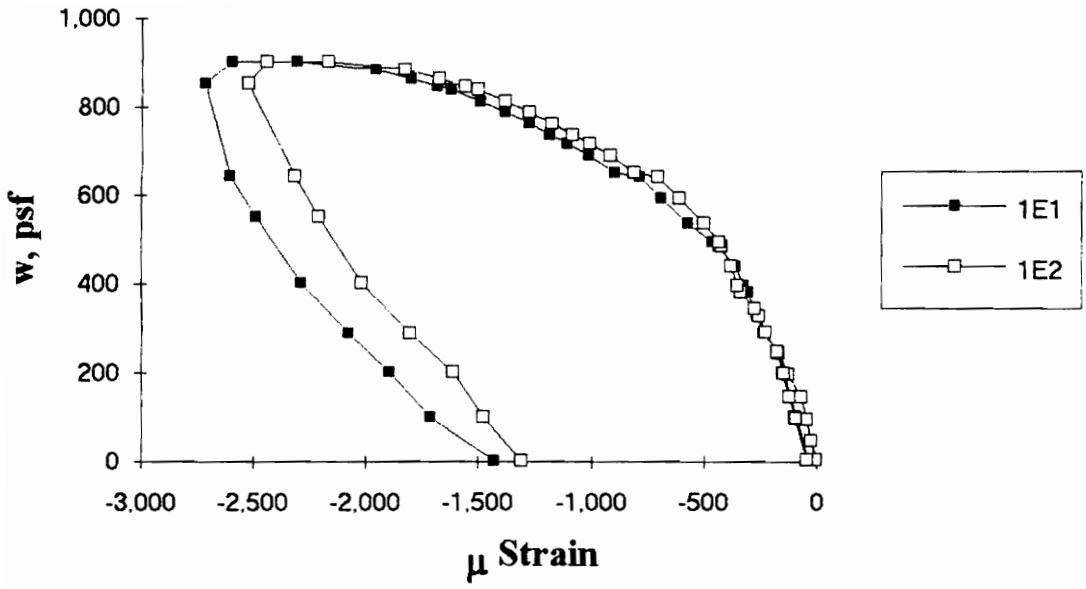

Figure A.163 SDI-2/18-3-9 Load vs. Strain in Concrete at Maximum Moment

Test Designation: SDI-2/18-35-9
Test Date: January 20, 1994

MATERIALS AND DIMENSIONS

General:

width:	6 ft. (2 panels)
span length:	9 ft. center span
end details:	N/A
deck anchorage type:	shear stud, 3-7/8 in. long, 3/4 in. dia.
average anchorage spacing:	2.1 ft. and 1.0 ft.

Deck:

thickness:	0.0470 in. (18 gage)
depth:	2 in.
area:	0.696 $in.^2$/ft.
yield stress:	46.5 ksi
ultimate strength:	59.6 ksi
web embossment type:	I

embossment dimensions:

N_b :	2.28 in.	W_b :	0.44 in.	s :	1.59 in.
N_t :	1.68 in.	W_t :	0.24 in.	p_h :	0.08 in.

Concrete:

type:	normal weight
test strength:	5,300 psi
total depth:	4.5 in.
cover depth:	2.5 in.

RESULTS

midspan strain due to fresh concrete:	220 x 10^{-6} in./in.
maximum load:	891 psf
deflection at maximum load:	3.10 in.
deflection at termination of test:	3.95 in.
end slip at maximum load:	N/A
end slip at termination of test:	N/A

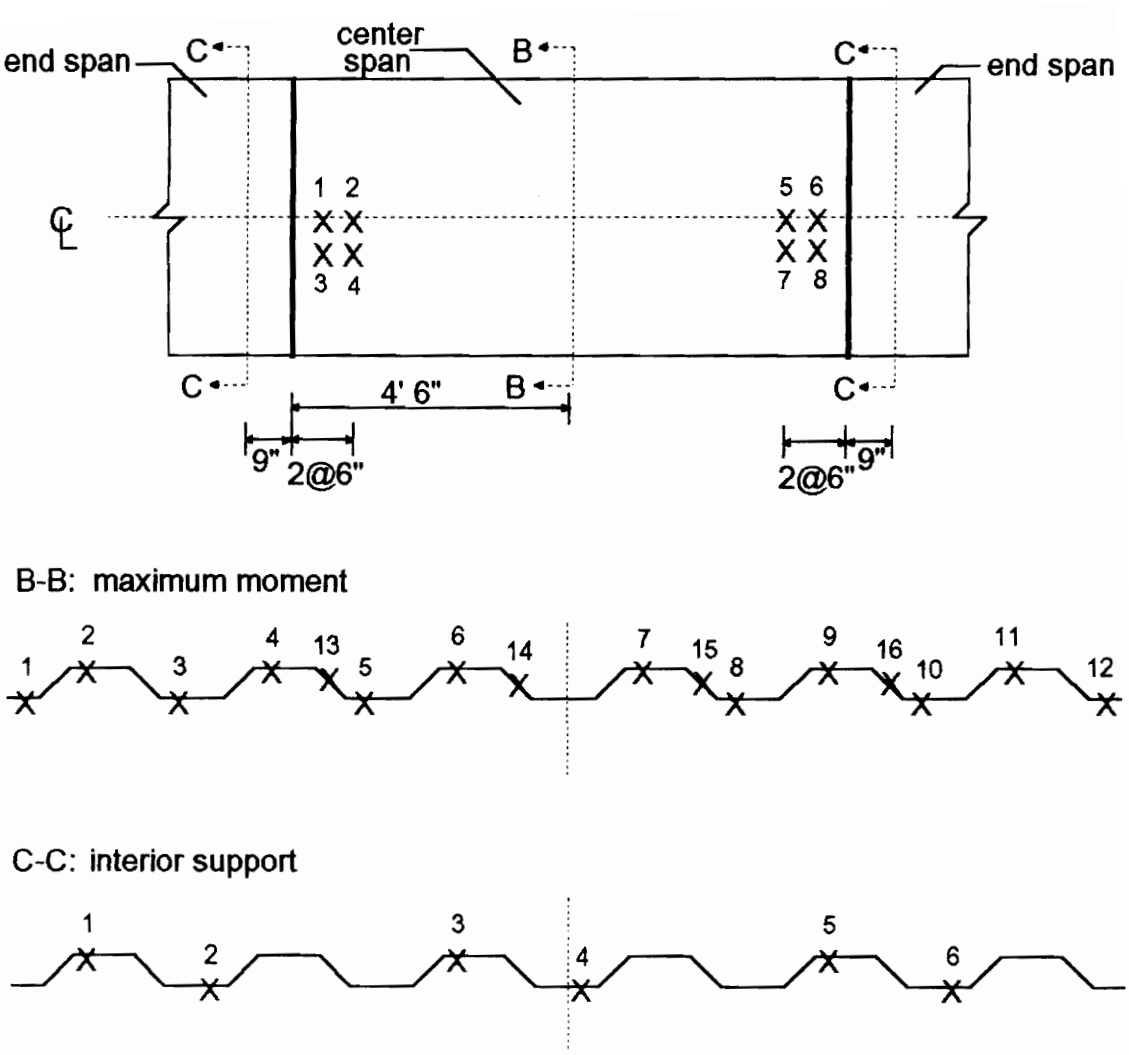

Figure A.164 SDI-2/18-35-9 Steel Deck Strain Gage Locations

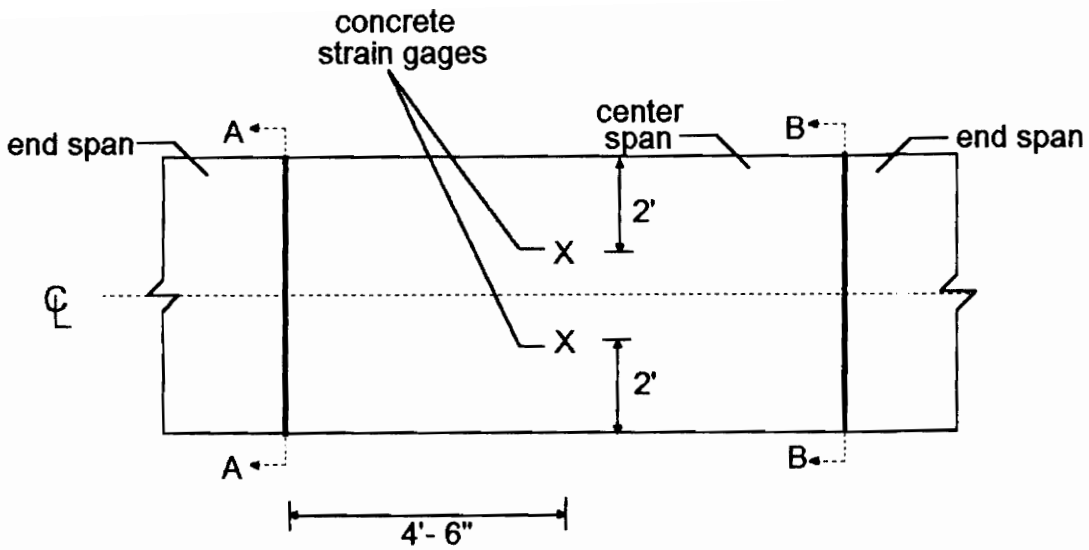

A-A: shear studs over supports

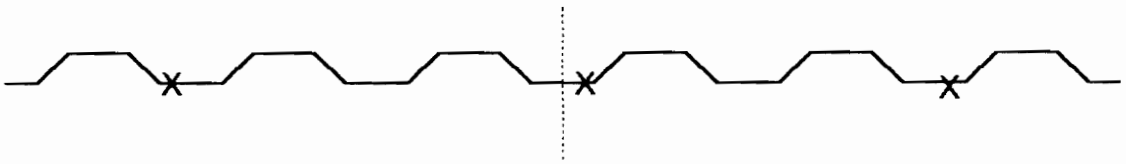

B-B: shear studs over supports

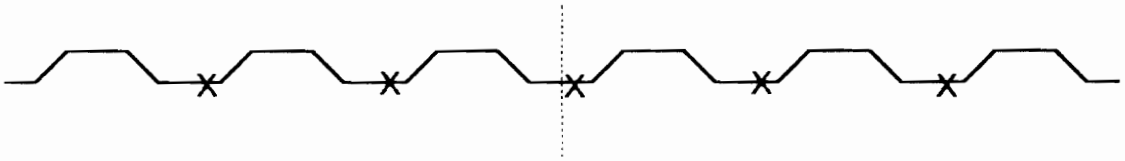

Figure A.165 SDI-2/18-35-9 Concrete Strain Gage and Shear Stud Locations

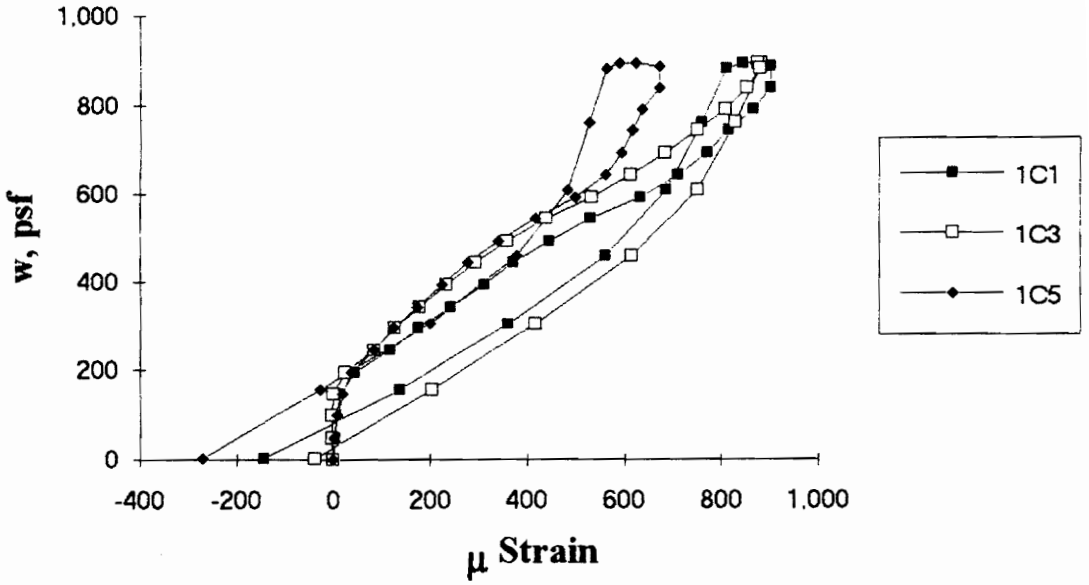

Figure A.166 SDI-2/18-35-9 Load vs. Strain in Deck Top Flange at Interior Support in End Span

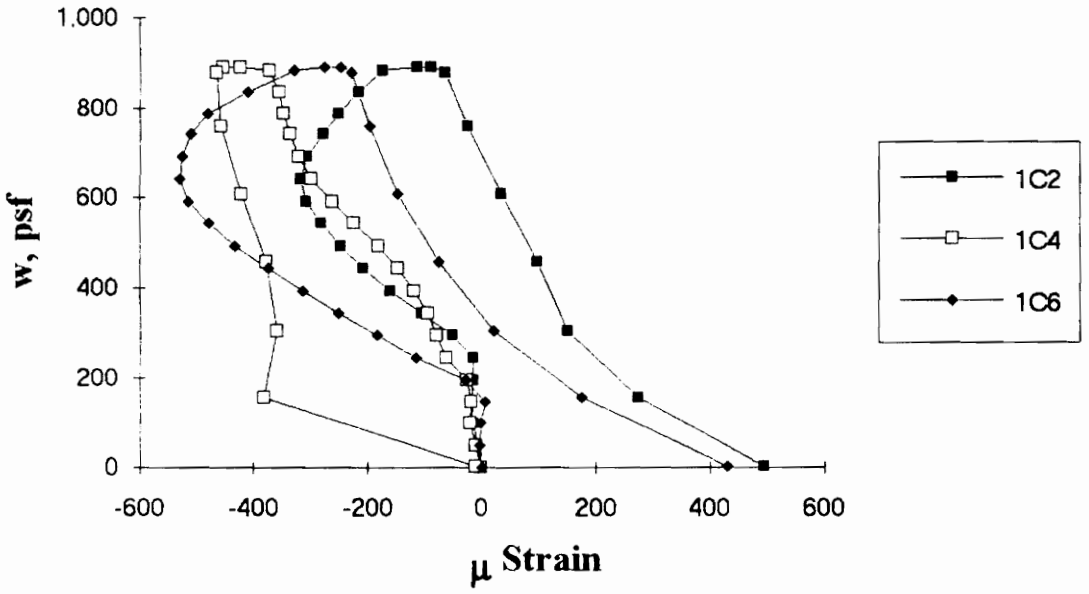

Figure A.167 SDI-2/18-35-9 Load vs. Strain in Deck Bottom Flange at Interior Support in End Span

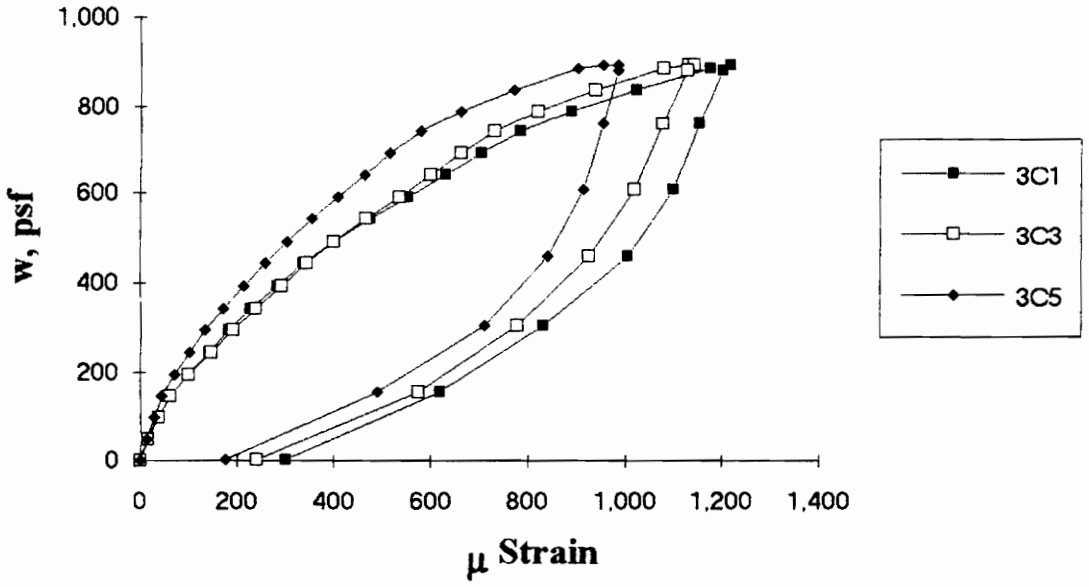

Figure A.168 SDI-2/18-35-9 Load vs. Strain in Deck Top Flange at Interior Support in End Span

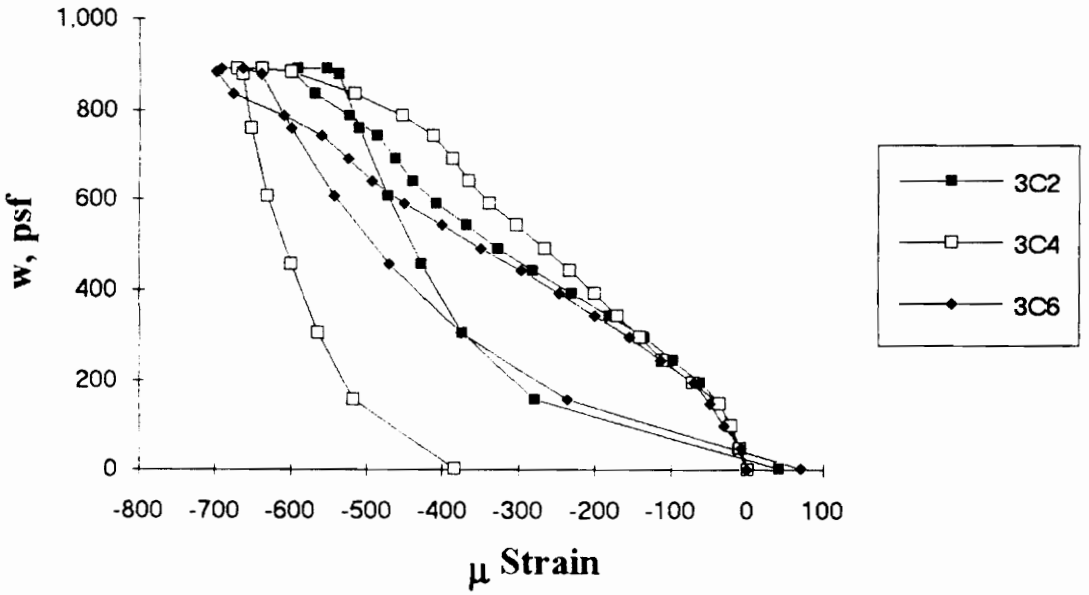

Figure A.169 SDI-2/18-35-9 Load vs. Strain in Deck Bottom Flange at Interior Support in End Span

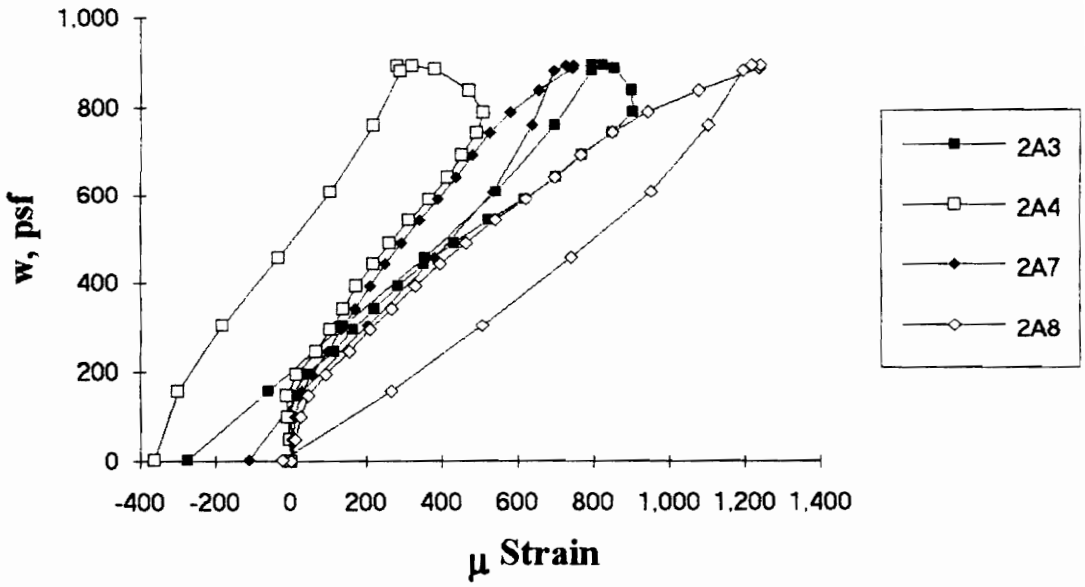

Figure A.170 SDI-2/18-35-9 Load vs. Strain in Deck Top Flange at Interior Support in Center Span

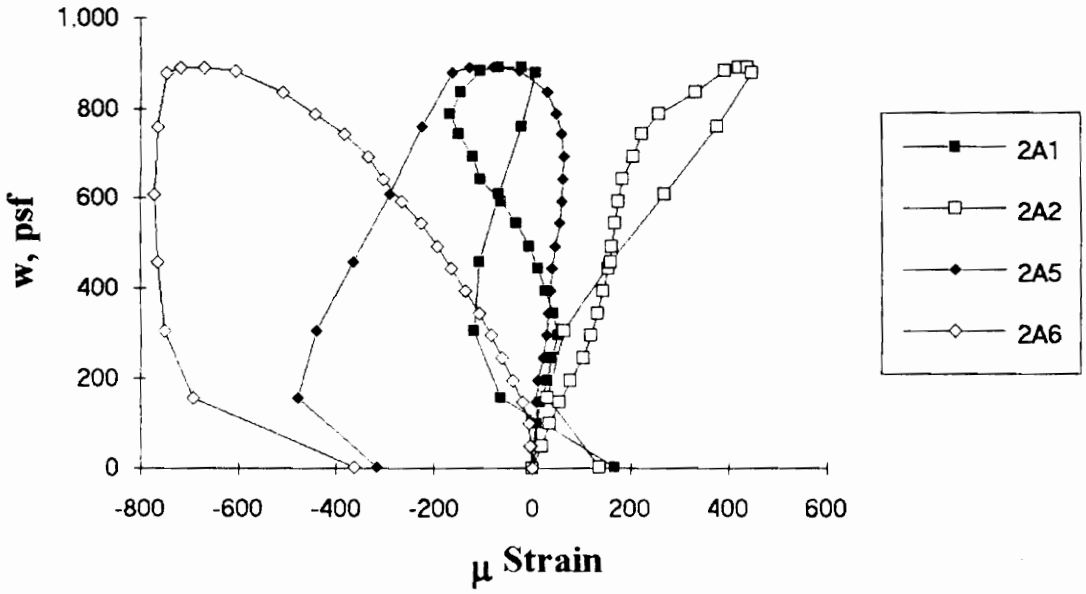

Figure A.171 SDI-2/18-35-9 Load vs. Strain in Deck Bottom Flange at Interior Support in Center Span

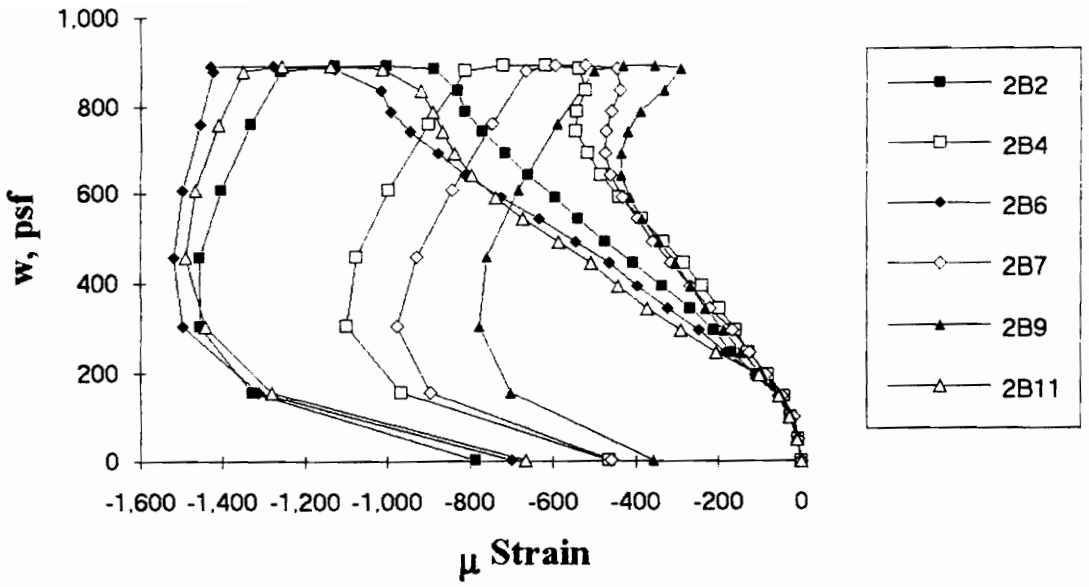

Figure A.172 SDI-2/18-35-9 Load vs. Strain in Deck Top Flange at Maximum Moment

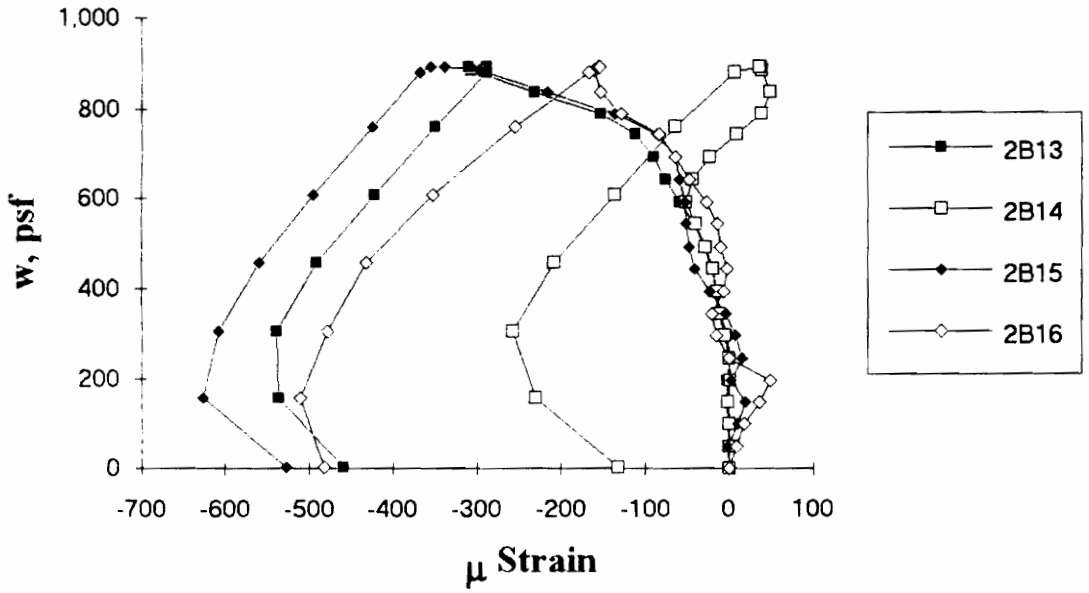

Figure A.173 SDI-2/18-35-9 Load vs. Strain in Deck Web at Maximum Moment

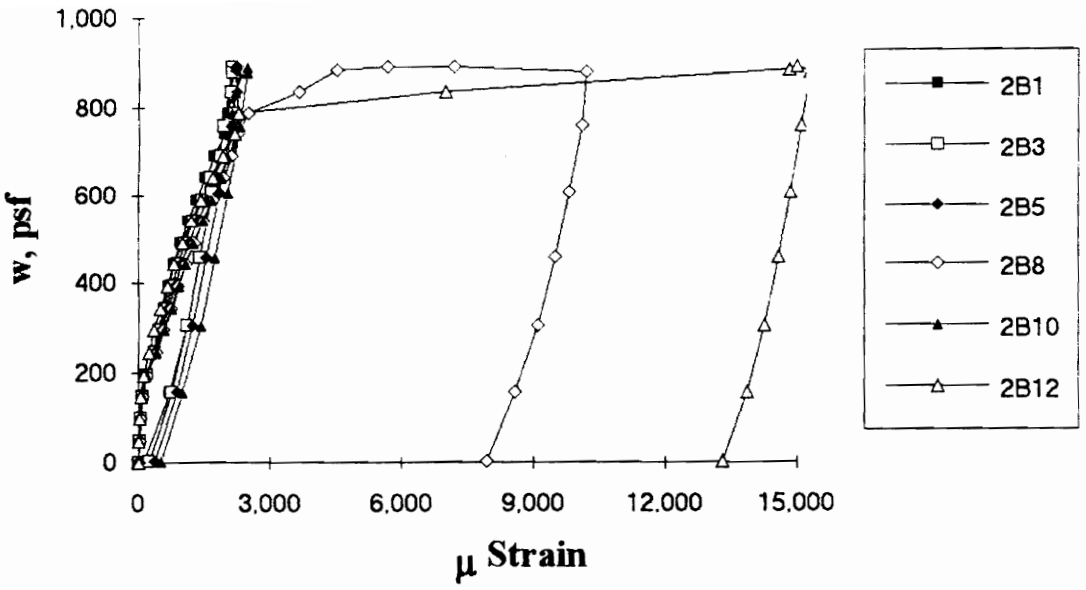

Figure A.174 SDI-2/18-35-9 Load vs. Strain in Deck Bottom Flange at Maximum Moment

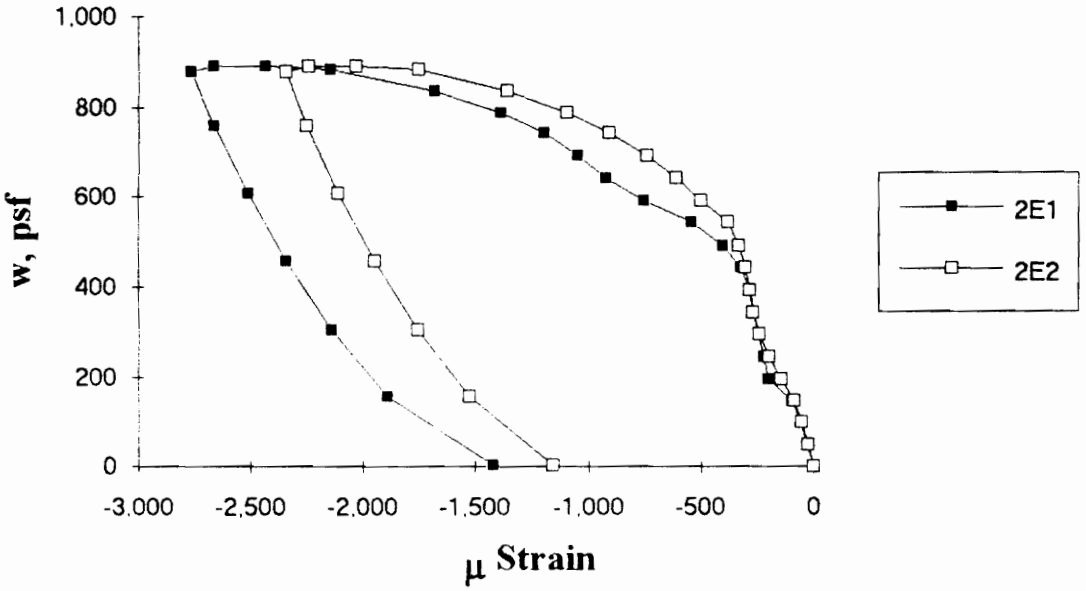

Figure A.175 SDI-2/18-35-9 Load vs. Strain in Concrete at Maximum Moment

Test Designation: SDI-2/18-5-9
Test Date: January 17, 1994

MATERIALS AND DIMENSIONS

General:

width:	6 ft. (2 panels)
span length:	9 ft. end span
end details:	1 ft. cantilever
deck anchorage type:	shear stud, 3-7/8 in. long, 3/4 in. dia.
average anchorage spacing:	1.0 ft.

Deck:

thickness:	0.0470 in. (18 gage)
depth:	2 in.
area:	0.696 $in.^2/ft.$
yield stress:	46.5 ksi
ultimate strength:	59.6 ksi
web embossment type:	I

embossment dimensions:

N_b :	2.28 in.	W_b :	0.44 in.	s :	1.59 in.
N_t :	1.68 in.	W_t :	0.24 in.	p_h :	0.08 in.

Concrete:

type:	normal weight
test strength:	5,300 psi
total depth:	4.5 in.
cover depth:	2.5 in.

RESULTS

midspan strain due to fresh concrete:	220 x 10^{-6} in./in.
maximum load:	912 psf
deflection at maximum load:	2.70 in.
deflection at termination of test:	3.50 in.
end slip at maximum load:	0.21 in.
end slip at termination of test:	0.35 in.

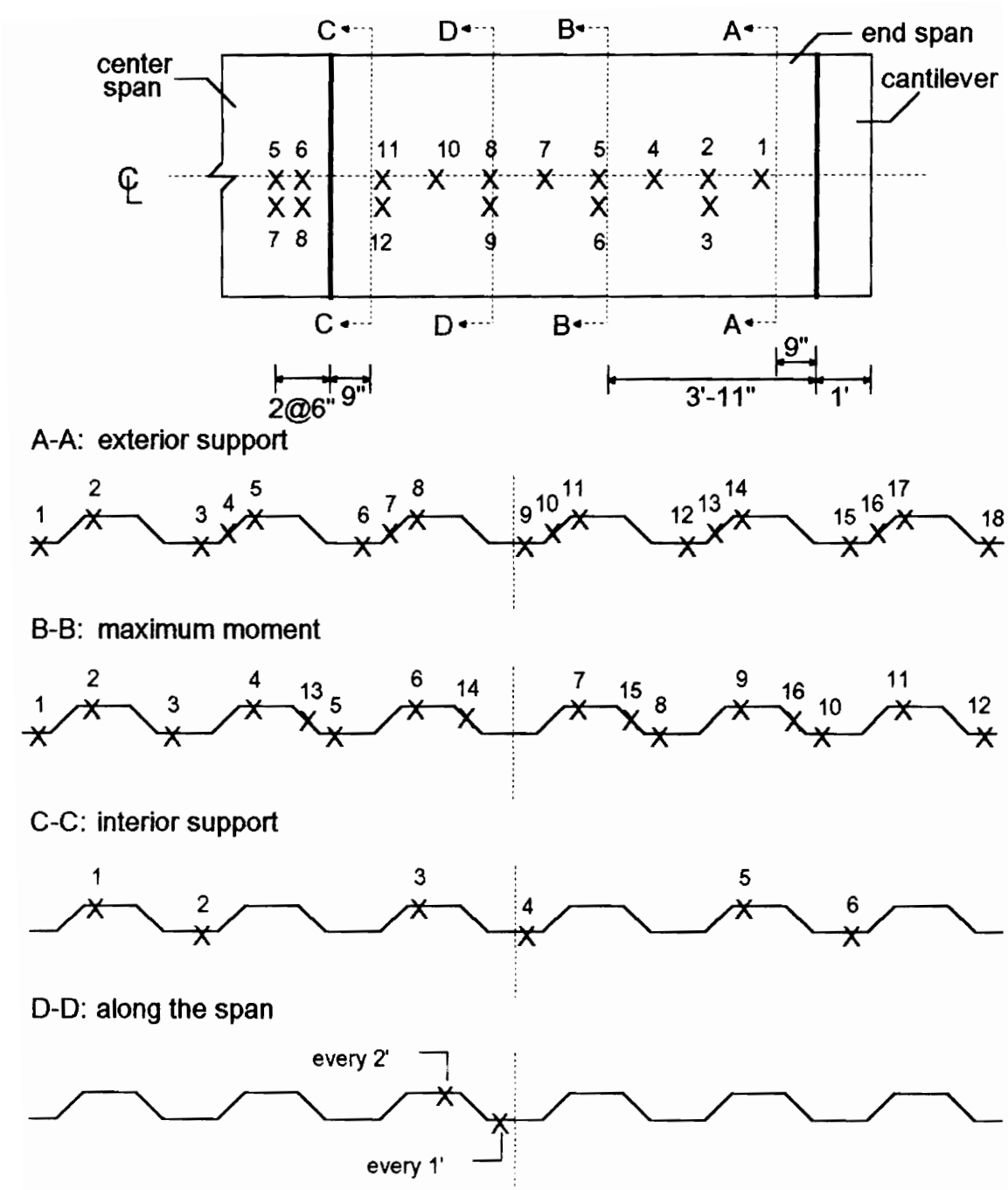

Figure A.176 SDI-2/18-5-9 Steel Deck Strain Gage Locations

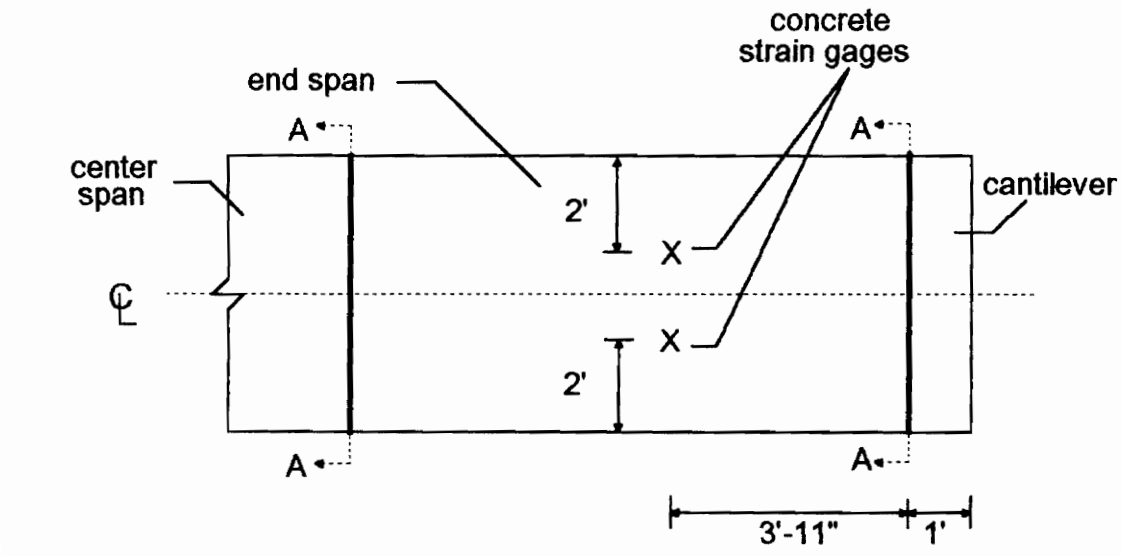

A-A: shear studs over supports

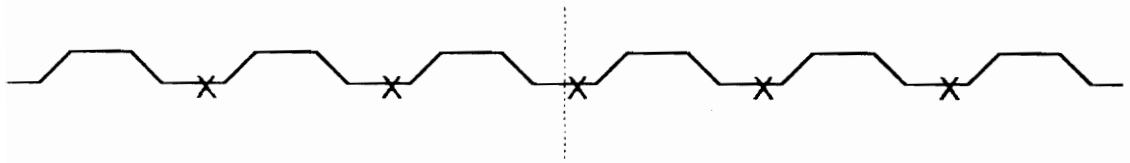

Figure A.177 SDI-2/18-5-9 Concrete Strain Gage and Shear Stud Locations

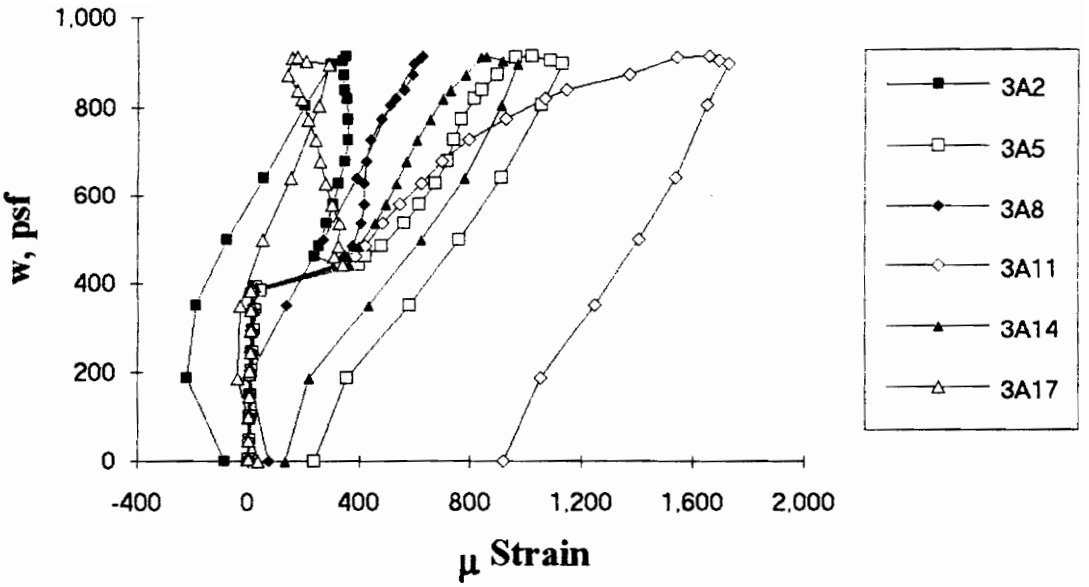

Figure A.178 SDI-2/18-5-9 Load vs. Strain in Deck Top Flange at Exterior Support

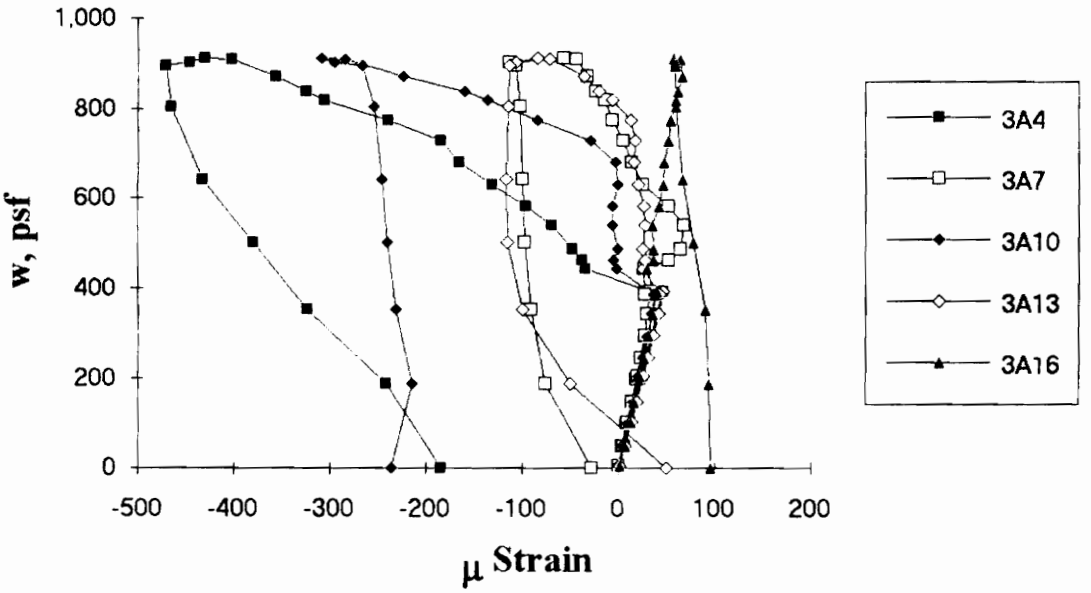

Figure A.179 SDI-2/18-5-9 Load vs. Strain in Deck Web at Exterior Support

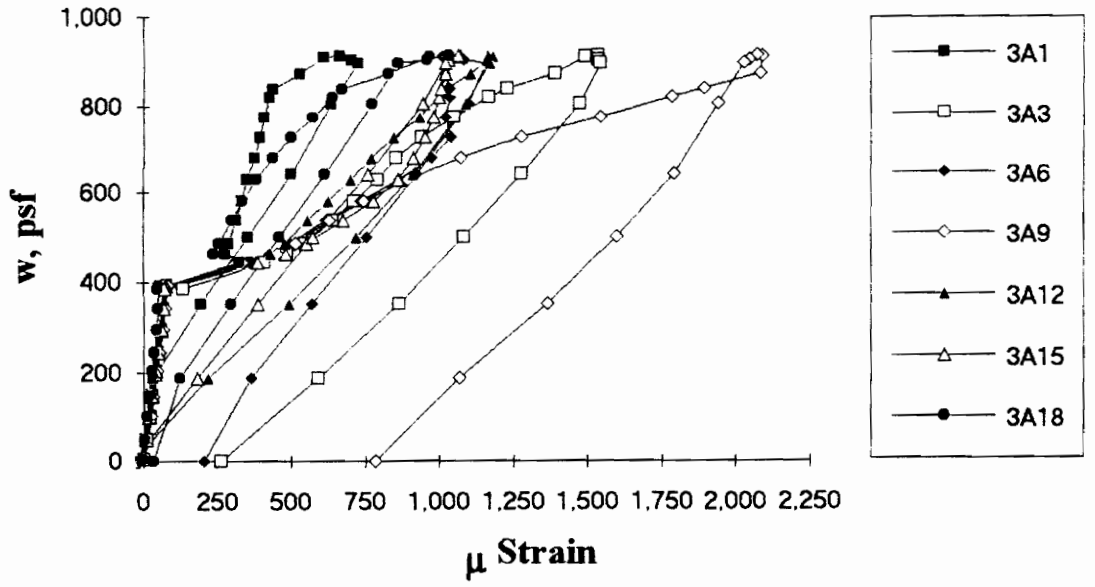

Figure A.180 SDI-2/18-5-9 Load vs. Strain in Deck Bottom Flange at Exterior Support

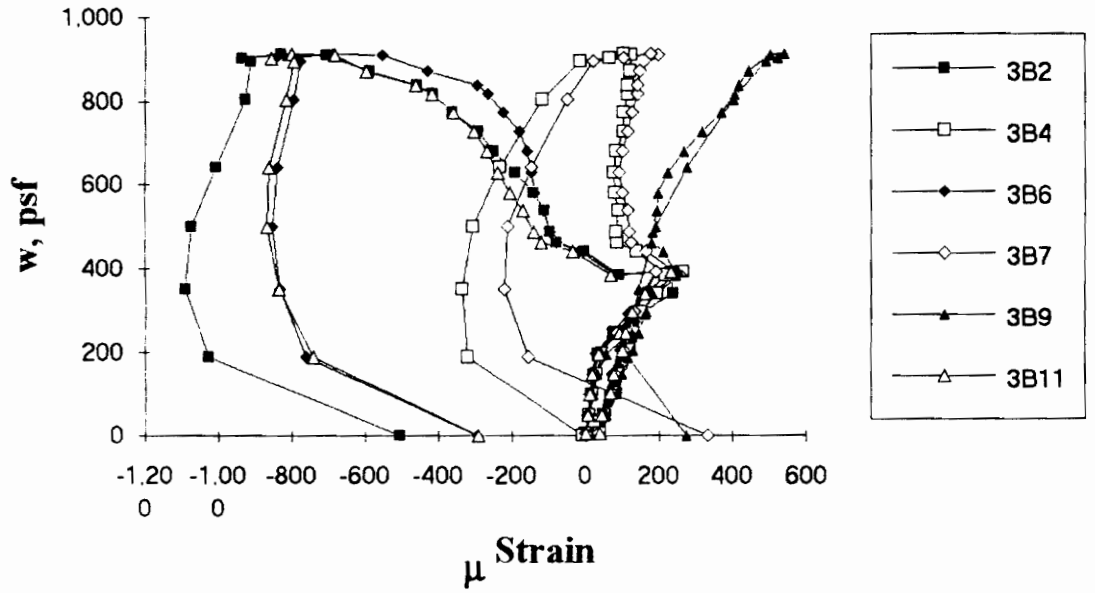

Figure A.181 SDI-2/18-5-9 Load vs. Strain in Deck Top Flange at Maximum Moment

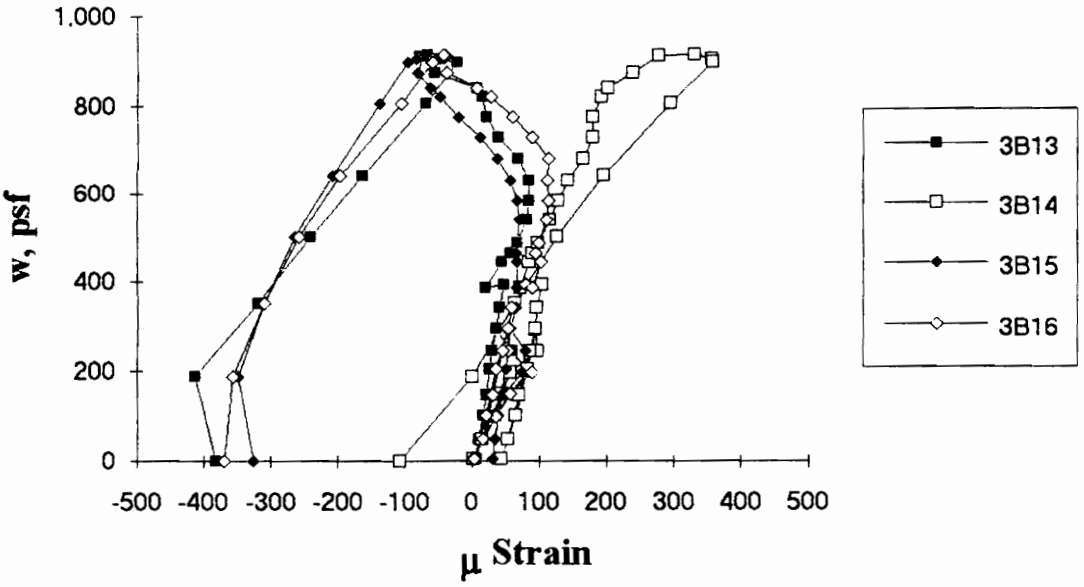

Figure A.182 SDI-2/18-5-9 Load vs. Strain in Deck Web at Maximum Moment

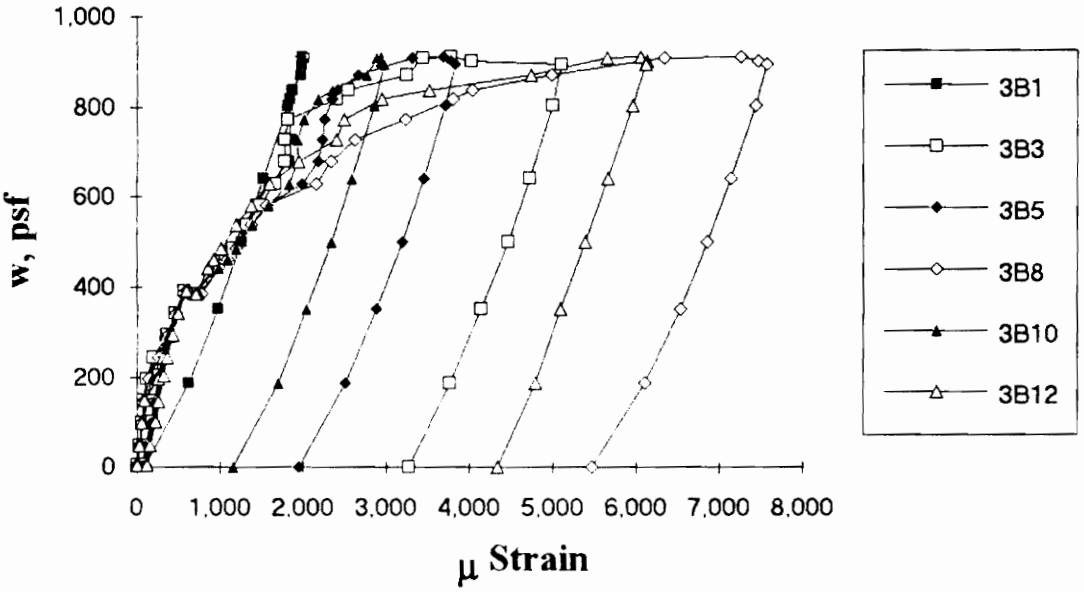

Figure A.183 SDI-2/18-5-9 Load vs. Strain in Deck Bottom Flange at Maximum Moment

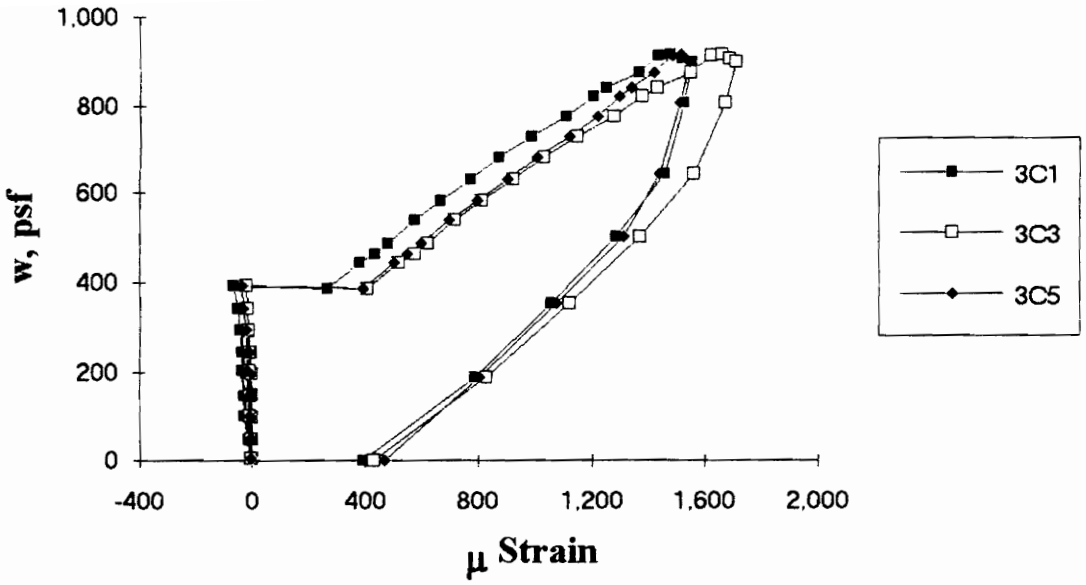

Figure A.184 SDI-2/18-5-9 Load vs. Strain in Deck Top Flange at Interior Support

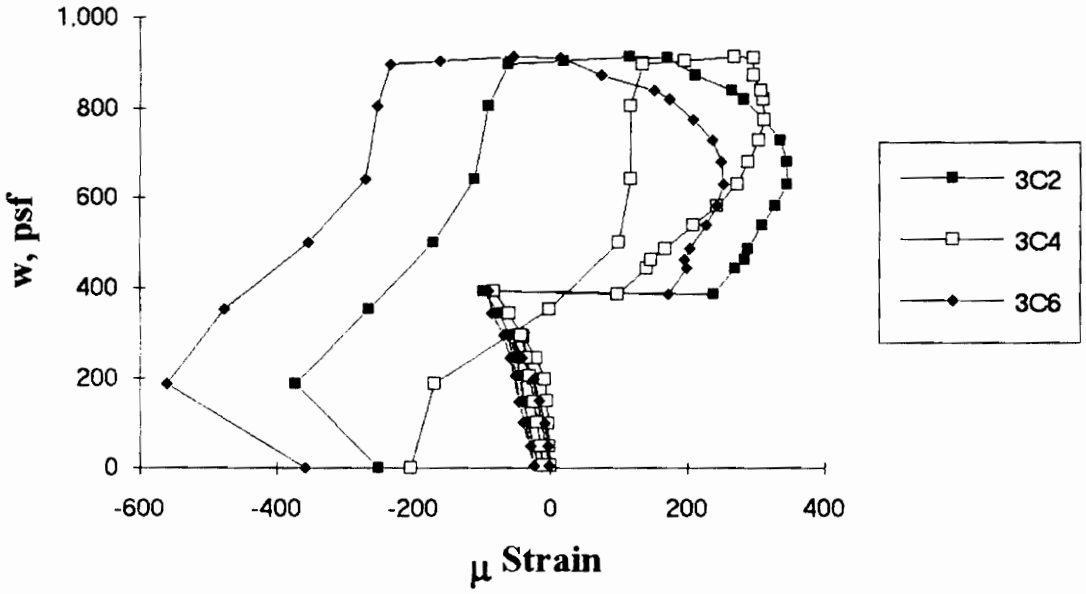

Figure A.185 SDI-2/18-5-9 Load vs. Strain in Deck Bottom Flange at Interior Support

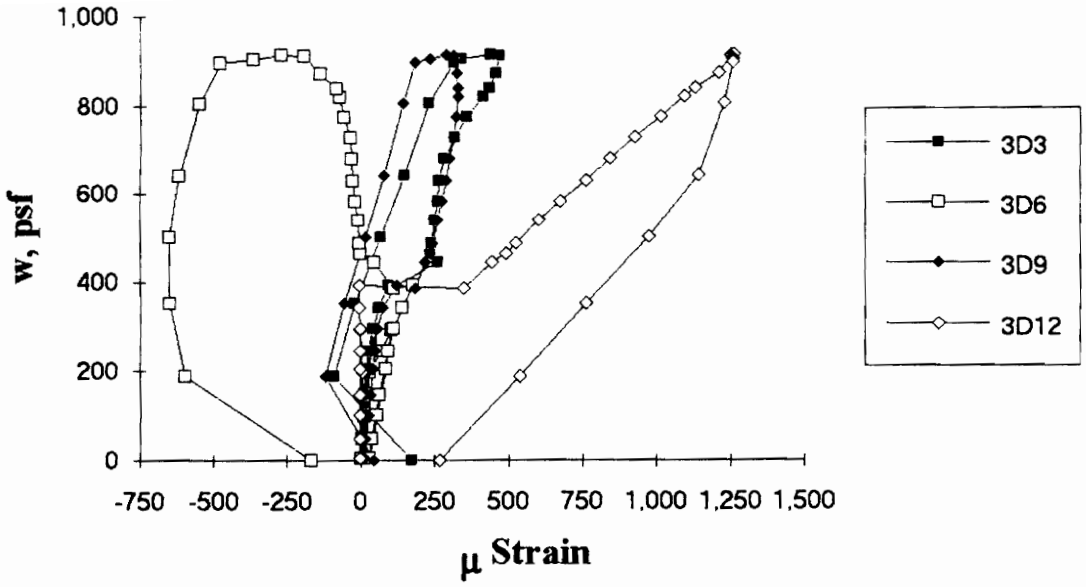

Figure A.186 SDI-2/18-5-9 Load vs. Strain in Deck Top Flange along the Span

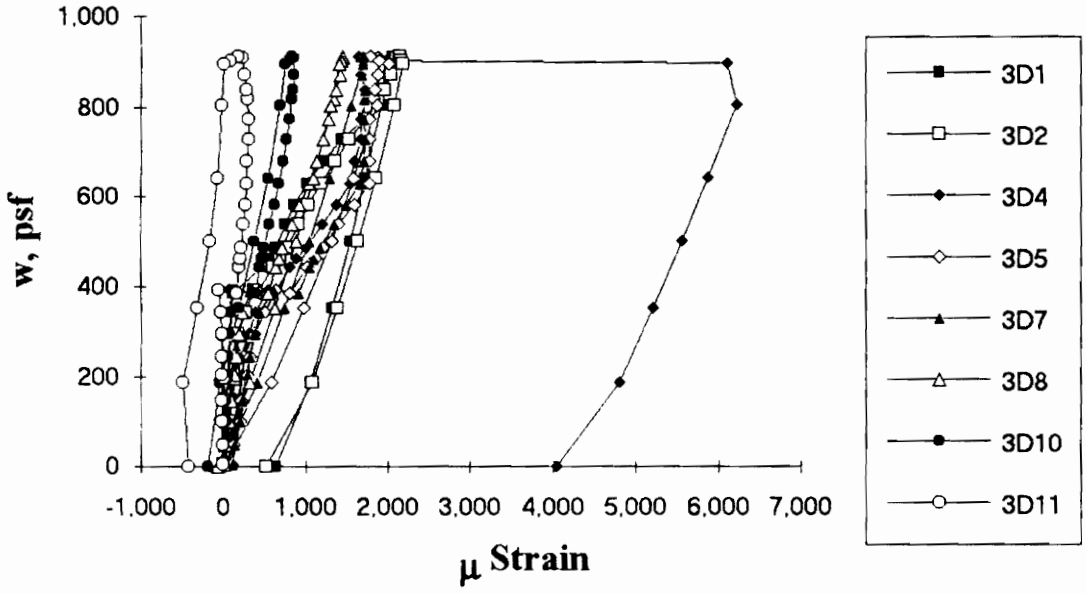

Figure A.187 SDI-2/18-5-9 Load vs. Strain in Deck Bottom Flange along the Span

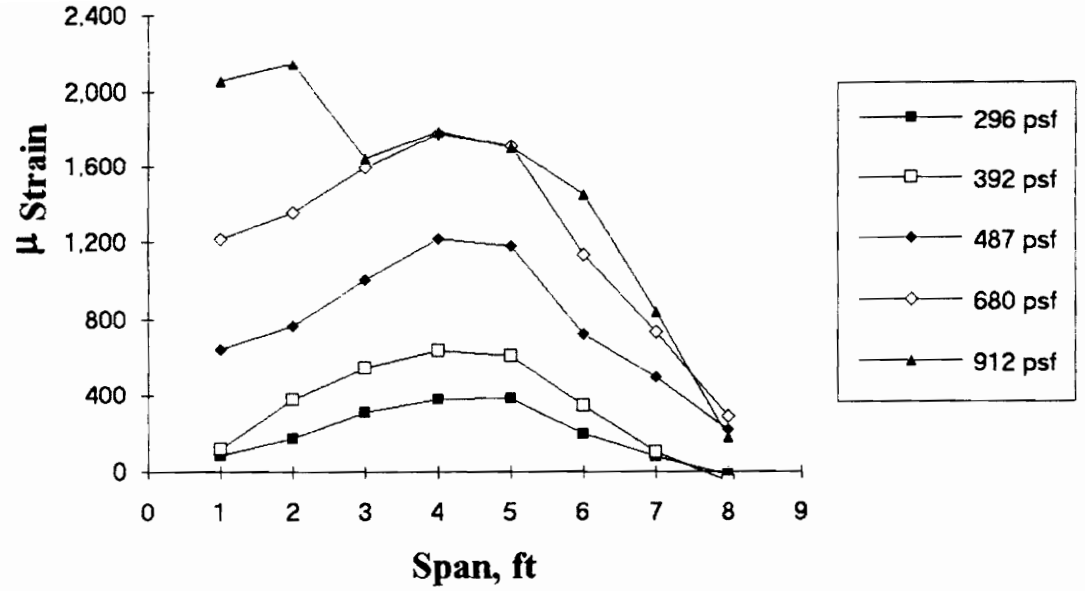

Figure A.188 SDI-2/18-5-9 Strain Variation in Deck Bottom Flange along the Span (from centerline of exterior support)

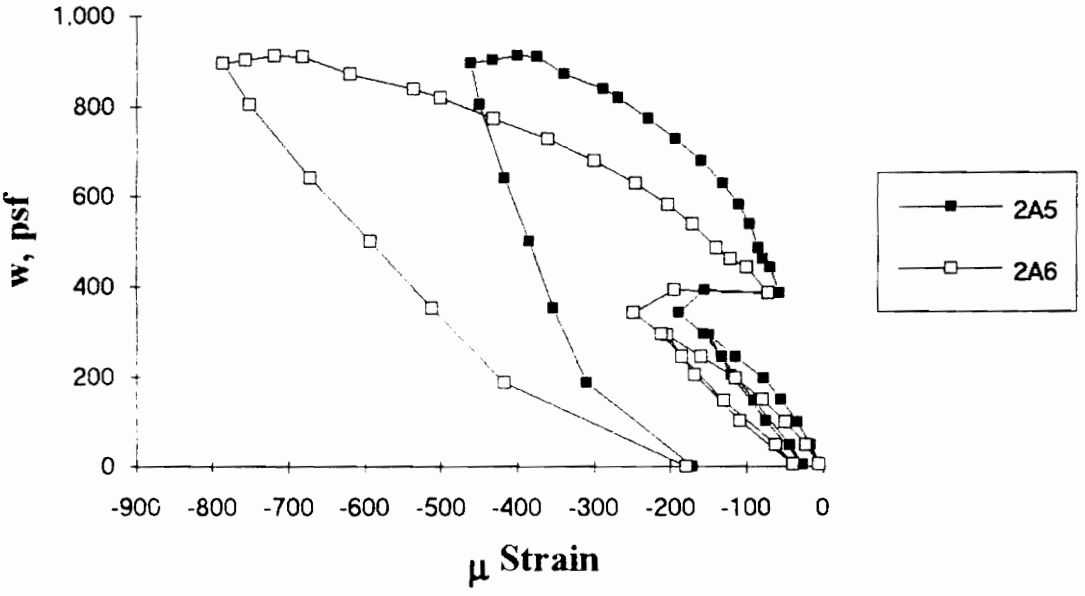

Figure A.189 SDI-2/18-5-9 Load vs. Strain in Deck Bottom Flange in Center Span

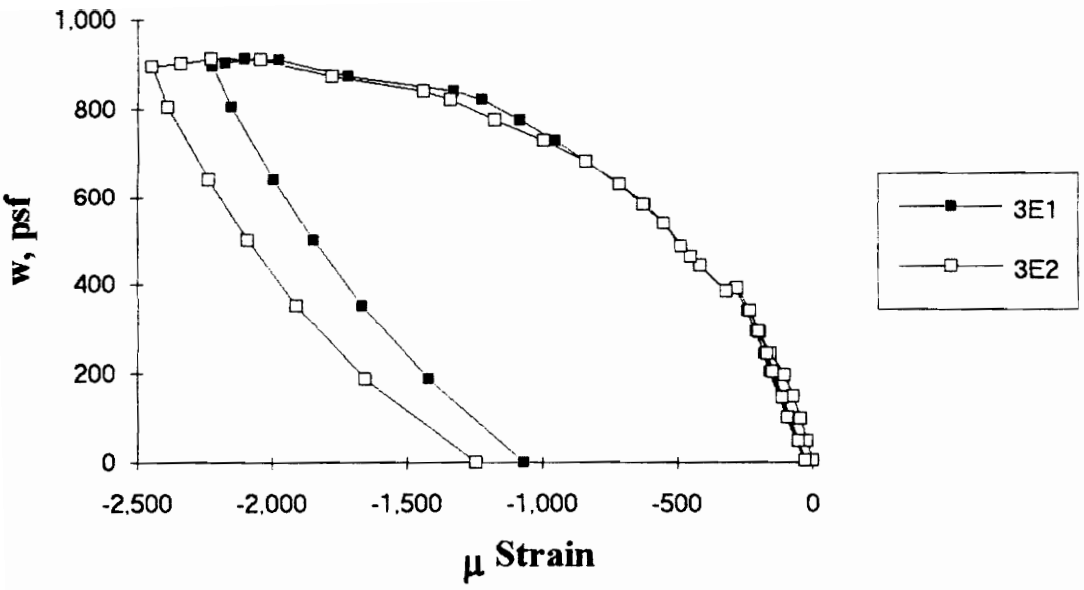

Figure A.190 SDI-2/18-5-9 Load vs. Strain in Concrete at Maximum Moment

Test Designation: SDI-3/20-3-10
Test Date: March 1, 1994

MATERIALS AND DIMENSIONS

General:

width:	6 ft. (2 panels)
span length:	10 ft. end span
end details:	1 ft. cantilever
deck anchorage type:	shear stud, 4-7/8 in. long, 3/4 in. dia.
average anchorage spacing:	2.1 ft.

Deck:

thickness:	0.0355 in. (20 gage)
depth:	3 in.
area:	0.572 in.^{2}/ft.
yield stress:	50.1 ksi
ultimate strength:	61.4 ksi
web embossment type:	III

embossment dimensions:

horizontal		vertical					
N_b :	1.81 in.	N_b :	2.30 in.	W_b :	0.53 in.	s :	3.42 in.
N_t :	1.52 in.	N_t :	2.07 in.	W_t :	0.30 in.	p_h :	0.10 in.

Concrete:

type:	normal weight
test strength:	3,750 psi
total depth:	5.5 in.
cover depth:	2.5 in.

RESULTS

midspan strain due to fresh concrete:	230 x 10^{-6} in./in.
maximum load:	743 psf
deflection at maximum load:	2.58 in.
deflection at termination of test:	3.57 in.
end slip at maximum load:	0.12 in.
end slip at termination of test:	0.24 in.

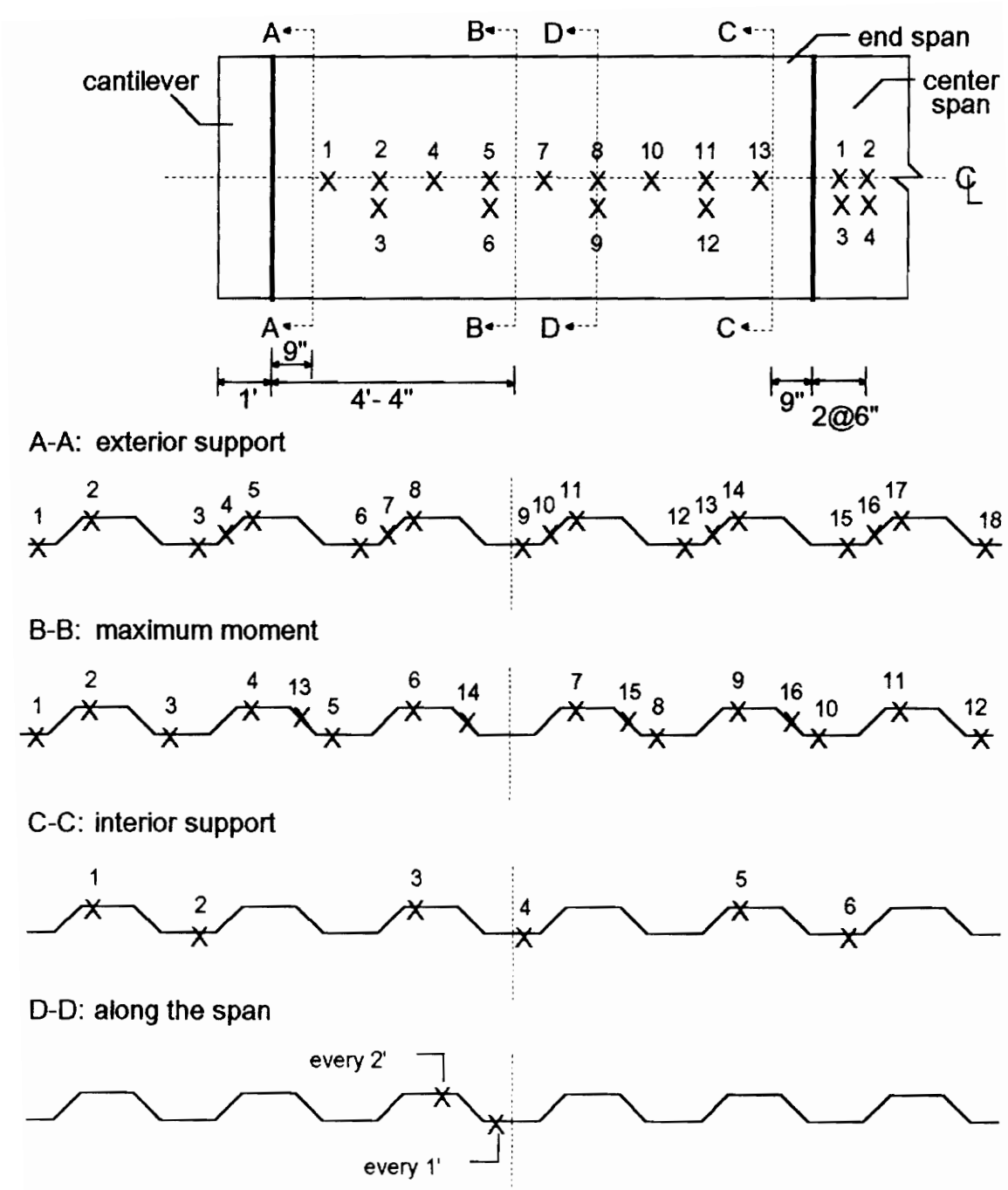

Figure A.191 SDI-3/20-3-10 Steel Deck Strain Gage Locations

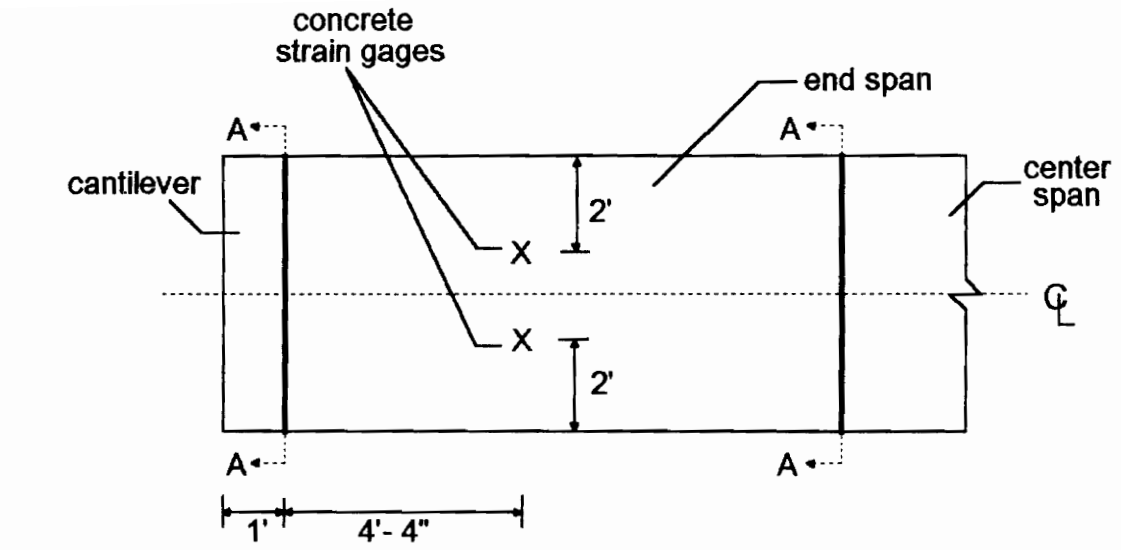

A-A: shear studs over supports

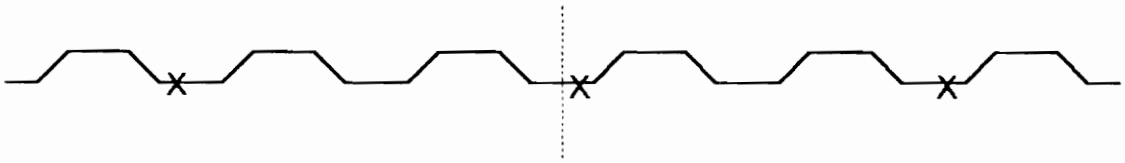

Figure A.192 SDI-3/20-3-10 Concrete Strain Gage and Shear Stud Locations

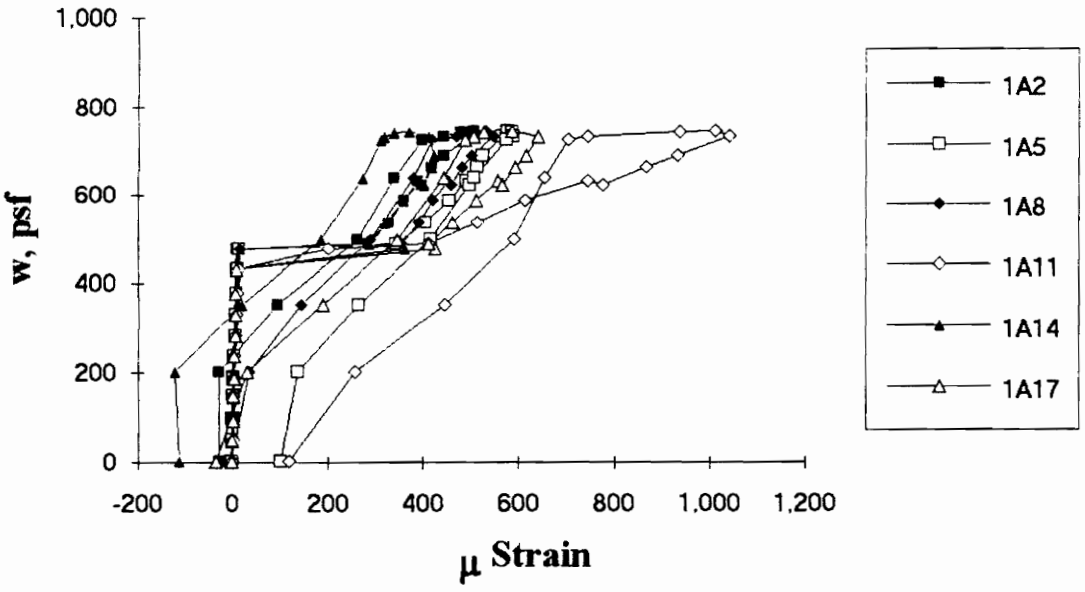

Figure A.193 SDI-3/20-3-10 Load vs. Strain in Deck Top Flange at Exterior Support

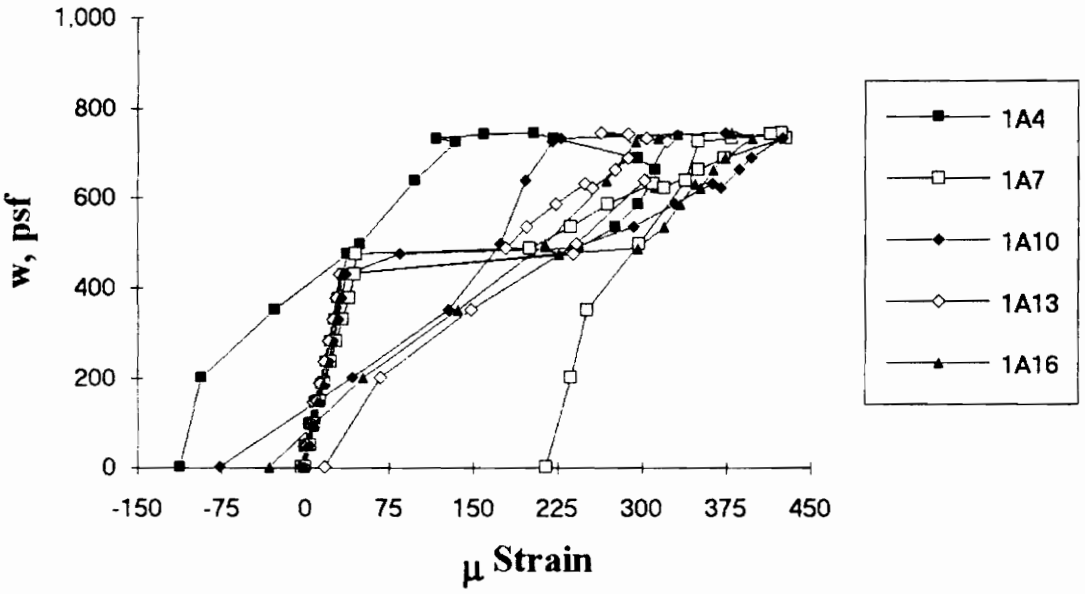

Figure A.194 SDI-3/20-3-10 Load vs. Strain in Deck Web at Exterior Support

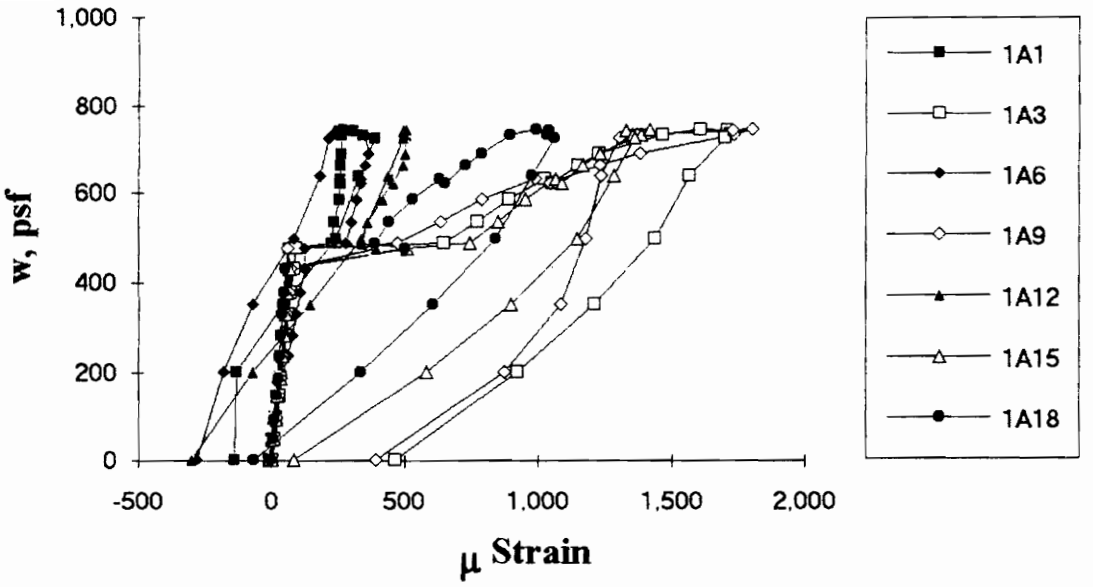

Figure A.195 SDI-3/20-3-10 Load vs. Strain in Deck Bottom Flange at Exterior Support

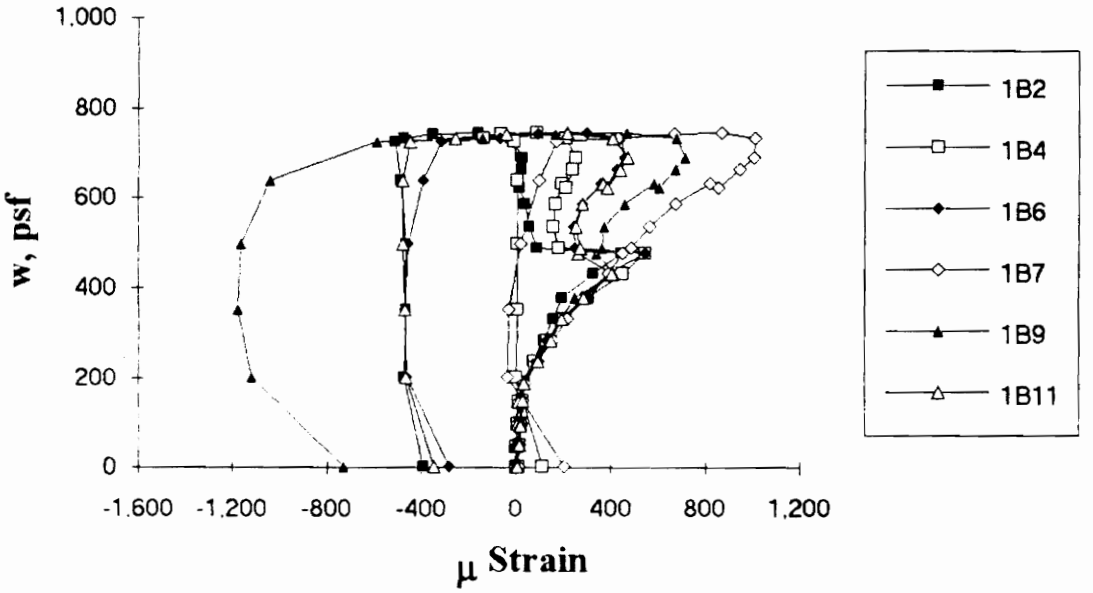

Figure A.196 SDI-3/20-3-10 Load vs. Strain in Deck Top Flange at Maximum Moment

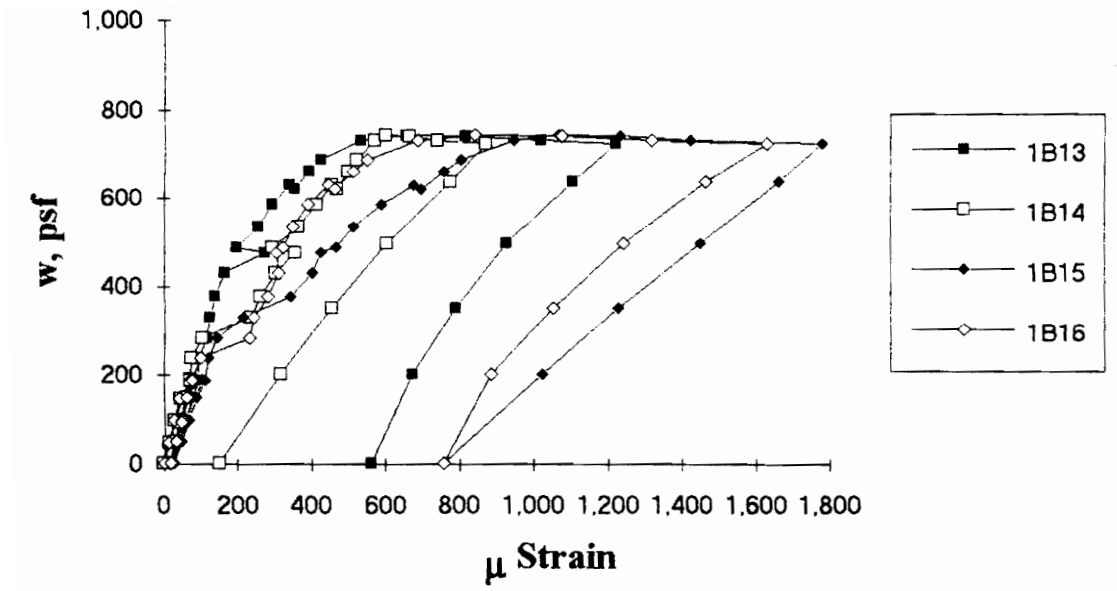

Figure A.197 SDI-3/20-3-10 Load vs. Strain in Deck Web at Maximum Moment

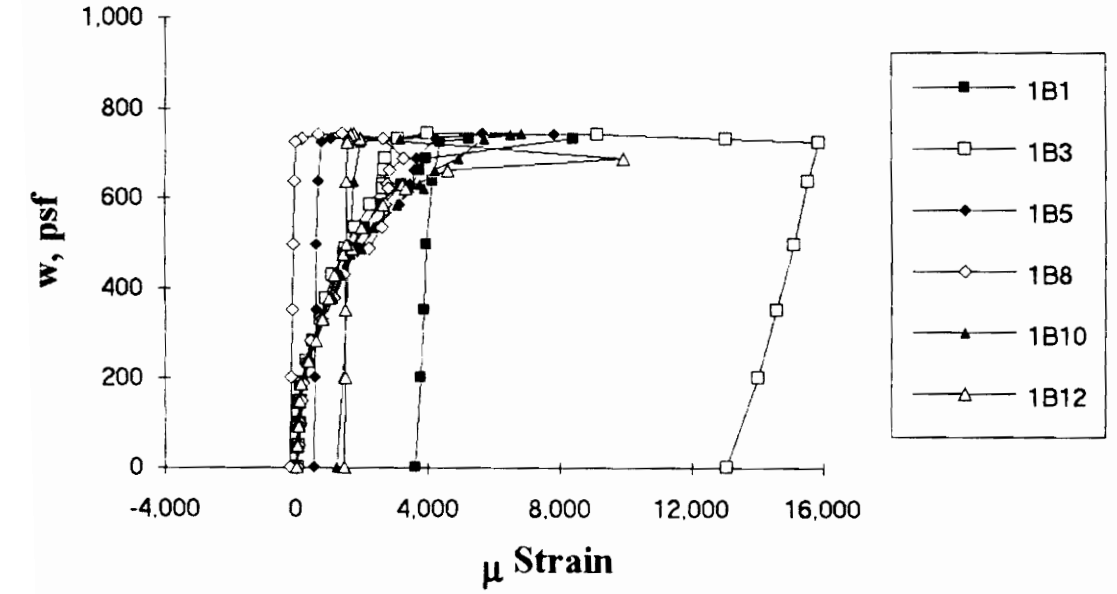

Figure A.198 SDI-3/20-3-10 Load vs. Strain in Deck Bottom Flange at Maximum Moment

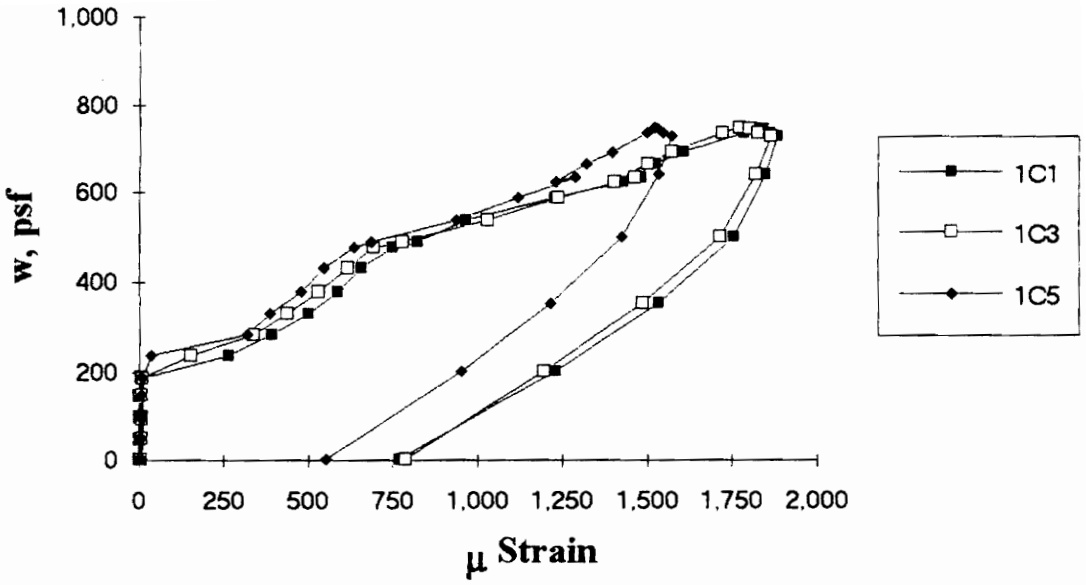

Figure A.199 SDI-3/20-3-10 Load vs. Strain in Deck Top Flange at Interior Support

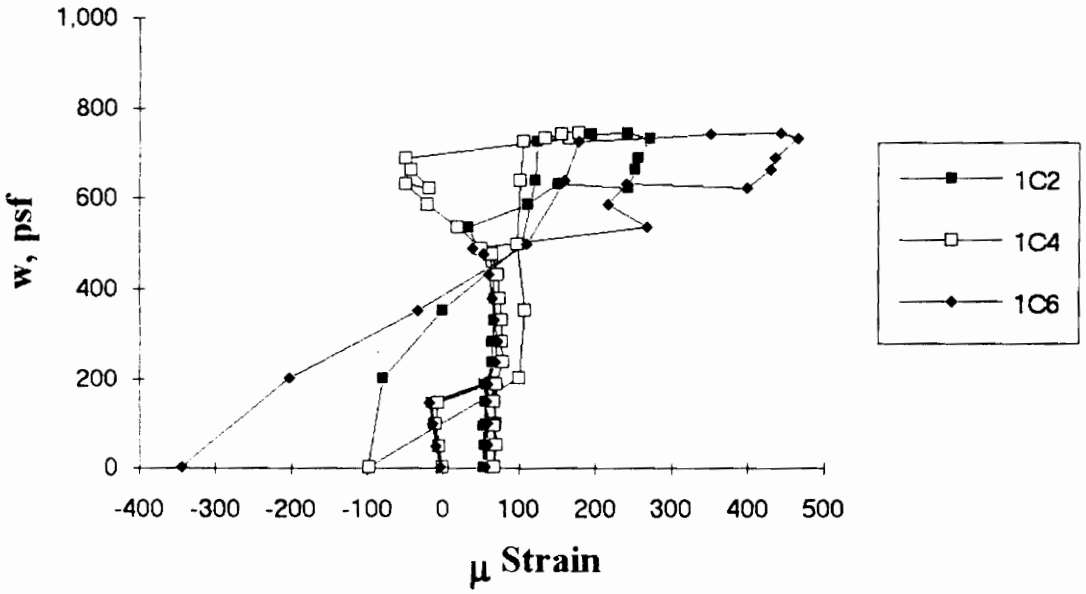

Figure A.200 SDI-3/20-3-10 Load vs. Strain in Deck Bottom Flange at Interior Support

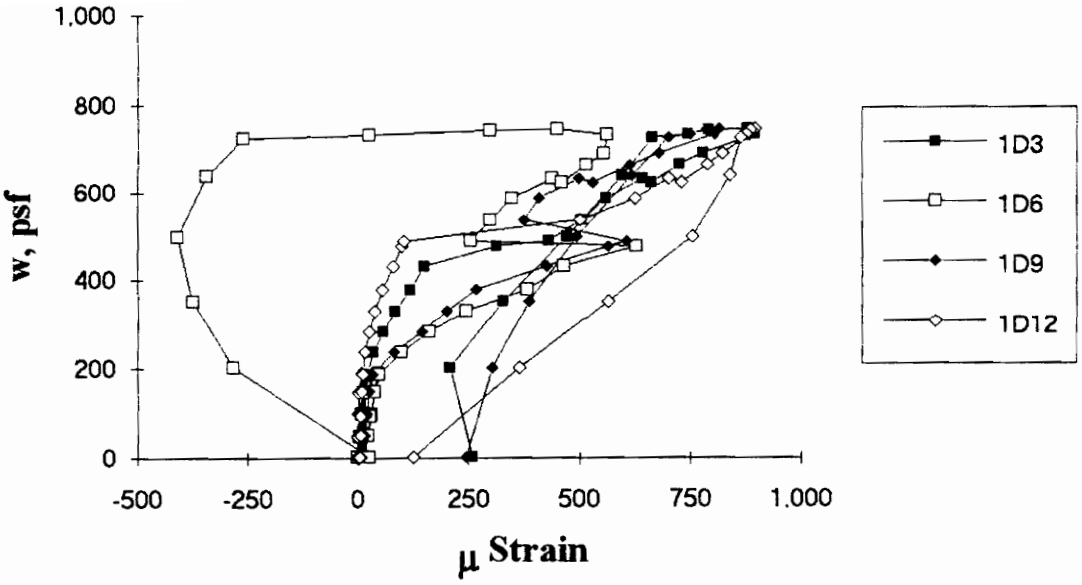

Figure A.201 SDI-3/20-3-10 Load vs. Strain in Deck Top Flange along the Span

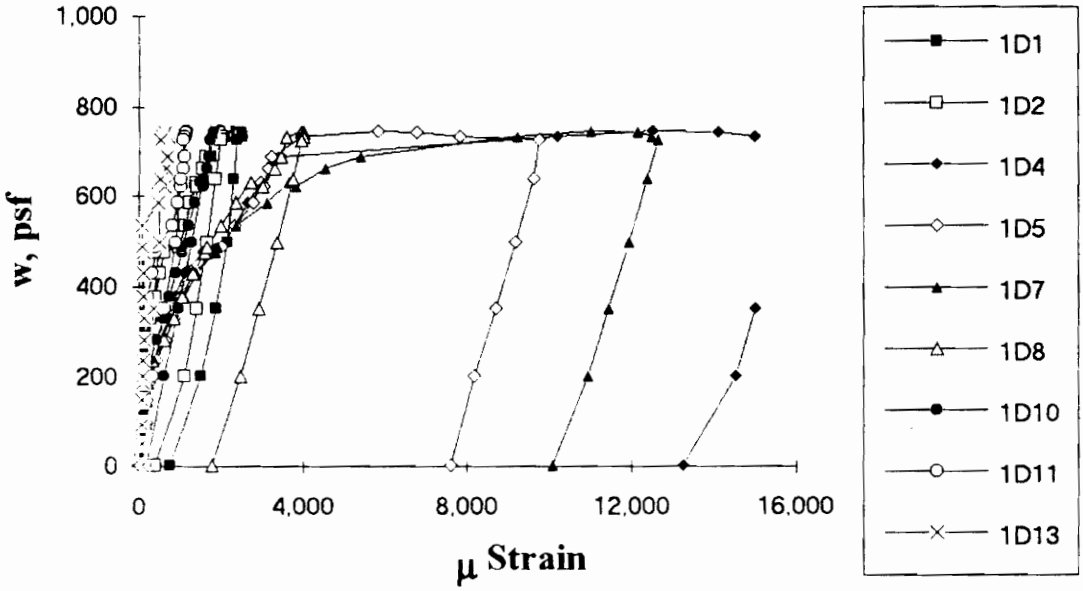

Figure A.202 SDI-3/20-3-10 Load vs. Strain in Deck Bottom Flange along the Span

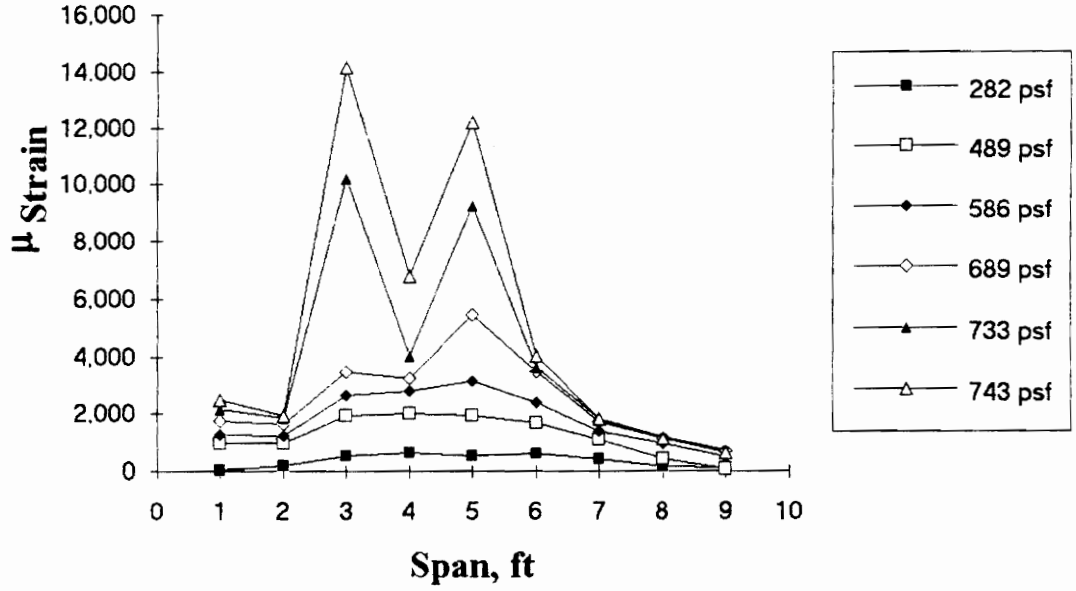

Figure A.203 SDI-3/20-3-10 Strain Variation in Deck Bottom Flange along the Span (from centerline of exterior support)

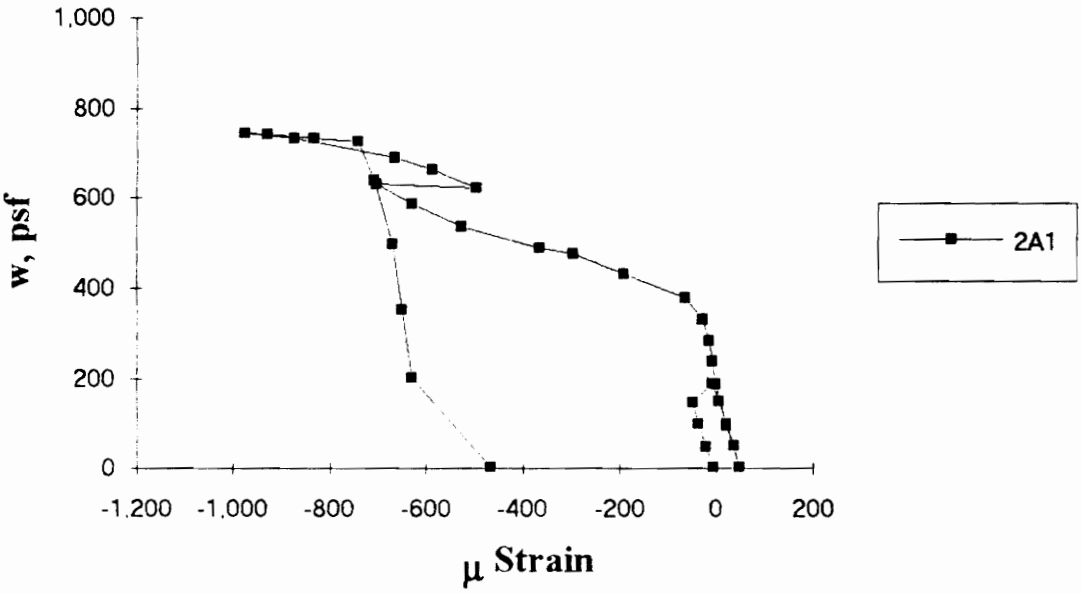

Figure A.204 SDI-3/20-3-10 Load vs. Strain in Deck Bottom Flange in Center Span

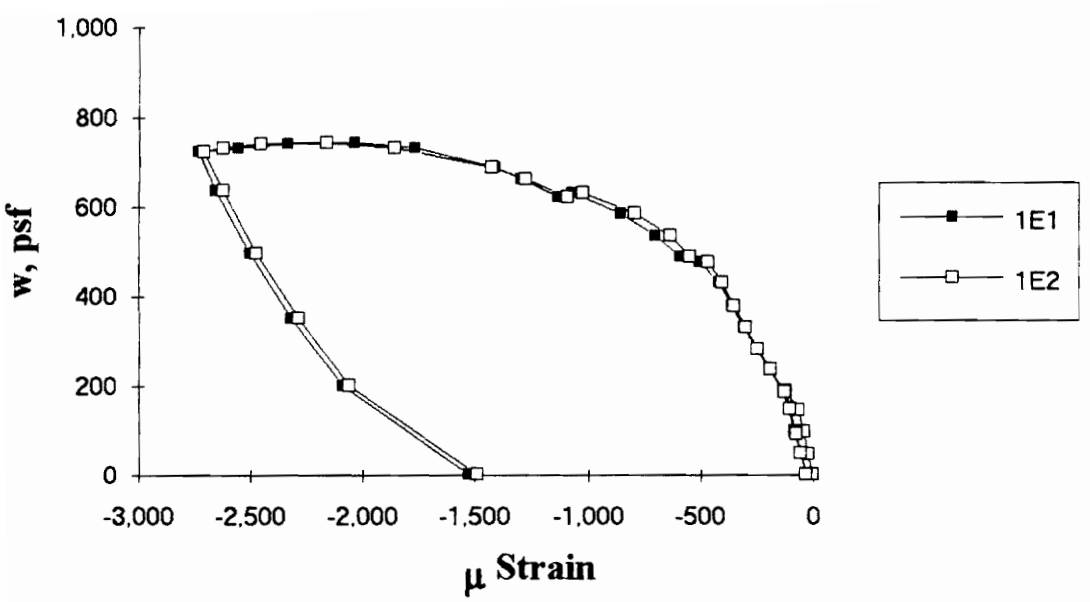

Figure A.205 SDI-3/20-3-10 Load vs. Strain in Concrete at Maximum Moment

Test Designation: SDI-3/20-35-10
Test Date: March 4, 1994

MATERIALS AND DIMENSIONS

General:

width:	6 ft. (2 panels)
span length:	9 ft. center span
end details:	N/A
deck anchorage type:	shear stud, 4-7/8 in. long, 3/4 in. dia.
average anchorage spacing:	2.1 ft. and 1.0 ft.

Deck:

thickness:	0.0355 in. (20 gage)
depth:	3 in.
area:	0.572 $in.^2/ft.$
yield stress:	50.1 ksi
ultimate strength:	61.4 ksi
web embossment type:	III

embossment dimensions:

horizontal:		vertical:					
N_b :	1.81 in.	N_b :	2.30 in.	W_b :	0.53 in.	s :	3.42 in.
N_t :	1.52 in.	N_t :	2.07 in.	W_t :	0.30 in.	p_h :	0.10 in.

Concrete:

type:	normal weight
test strength:	3,750 psi
total depth:	5.5 in.
cover depth:	2.5 in.

RESULTS

midspan strain due to fresh concrete:	230 x 10^{-6} in./in.
maximum load:	787 psf
deflection at maximum load:	3.83 in.
deflection at termination of test:	4.17 in.
end slip at maximum load:	N/A
end slip at termination of test:	N/A

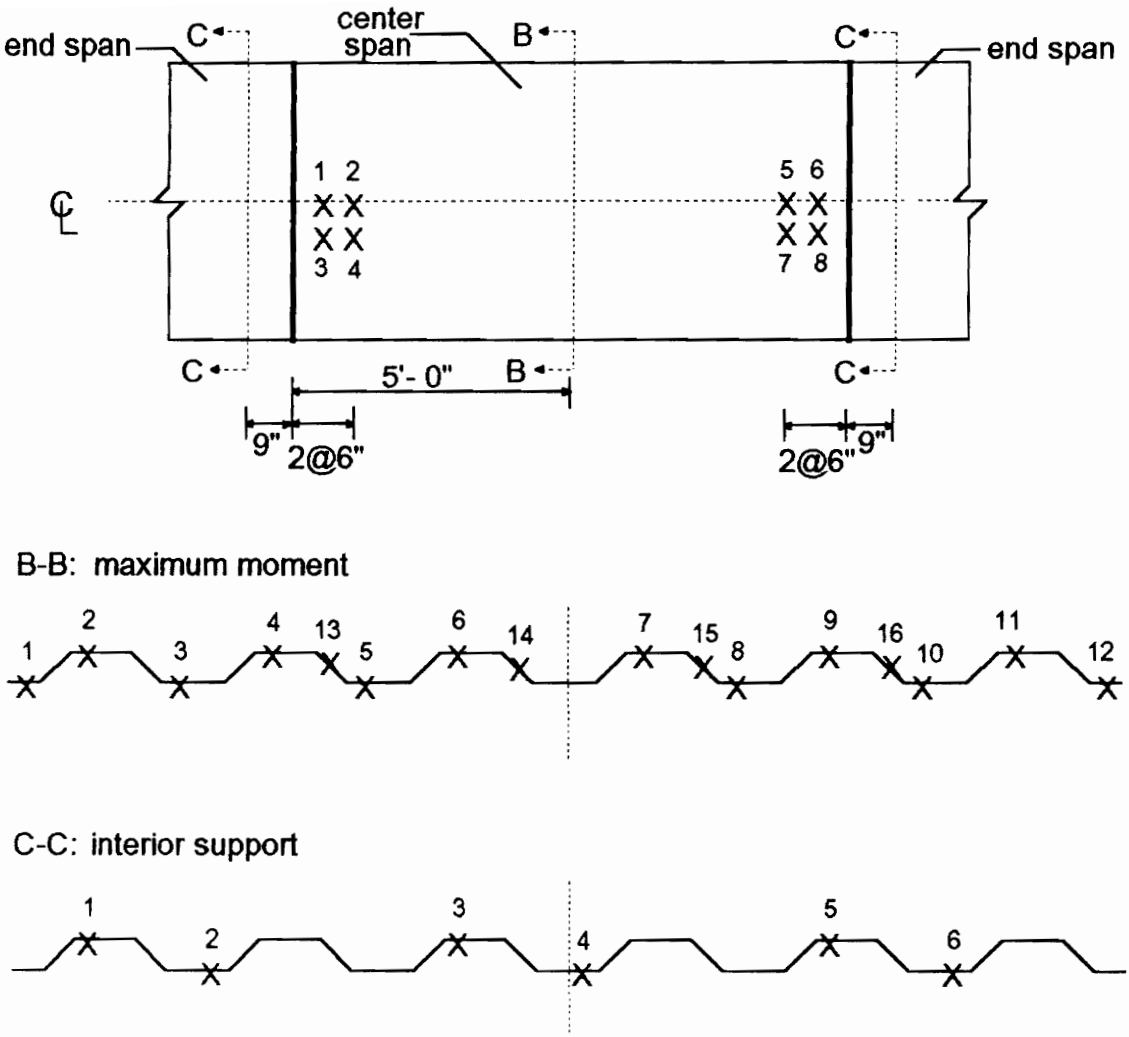

Figure A.206 SDI-3/20-35-10 Steel Deck Strain Gage Locations

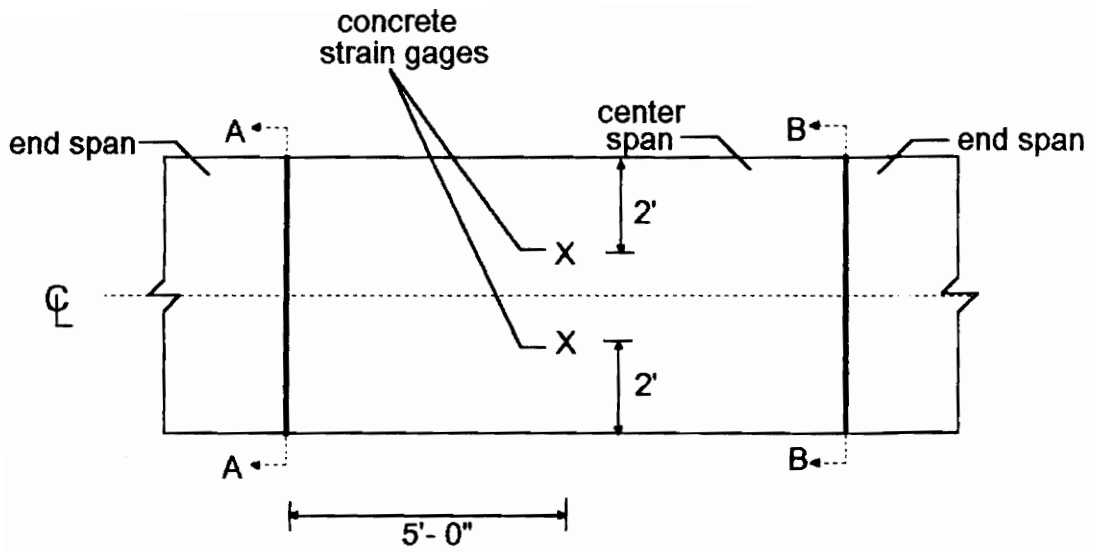

A-A: shear studs over supports

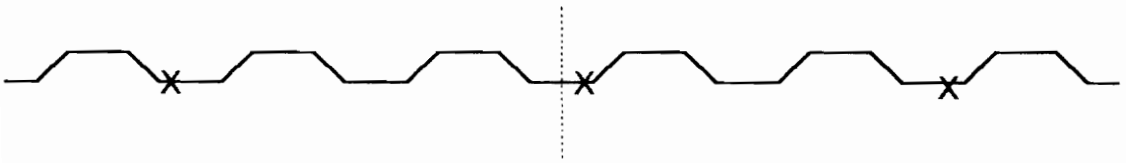

B-B: shear studs over supports

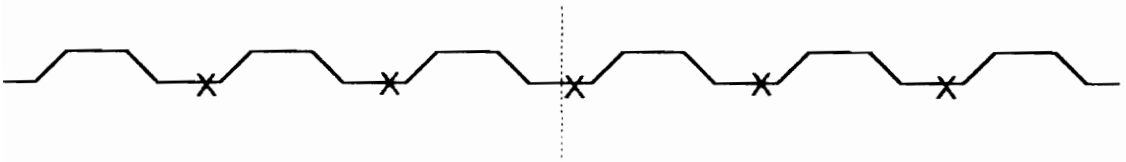

Figure A.207 SDI-3/20-35-10 Concrete Strain Gage and Shear Stud Locations

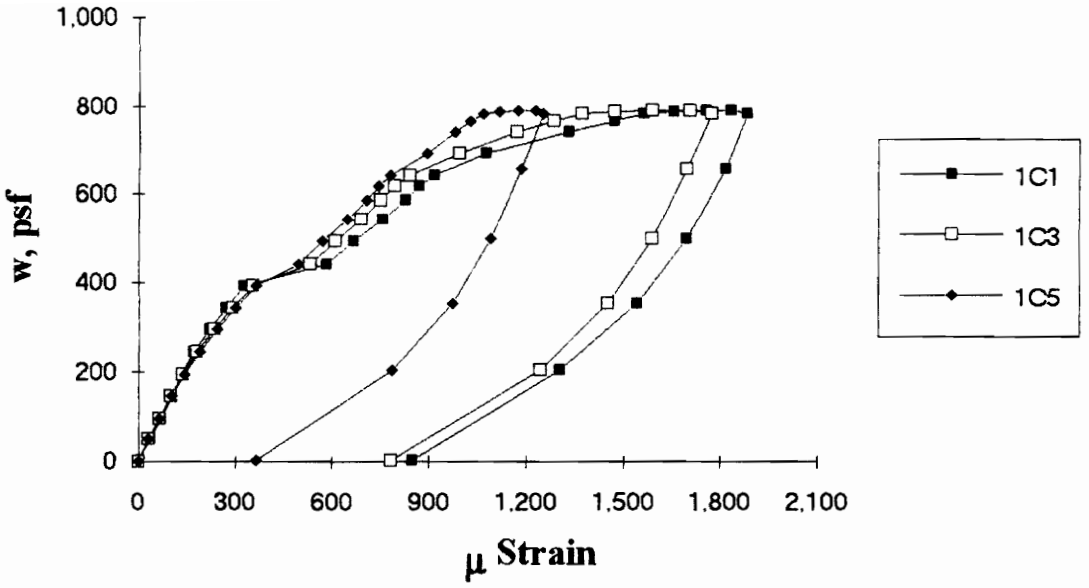

Figure A.208 SDI-3/20-35-10 Load vs. Strain in Deck Top Flange at Interior Support in End Span

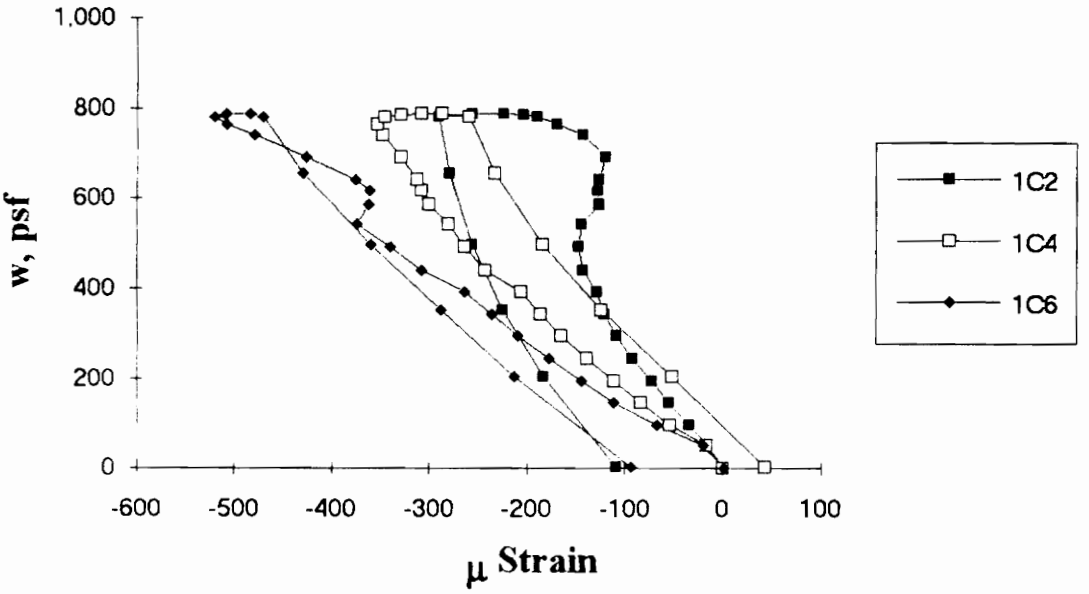

Figure A.209 SDI-3/20-35-10 Load vs. Strain in Deck Bottom Flange at Interior Support in End Span

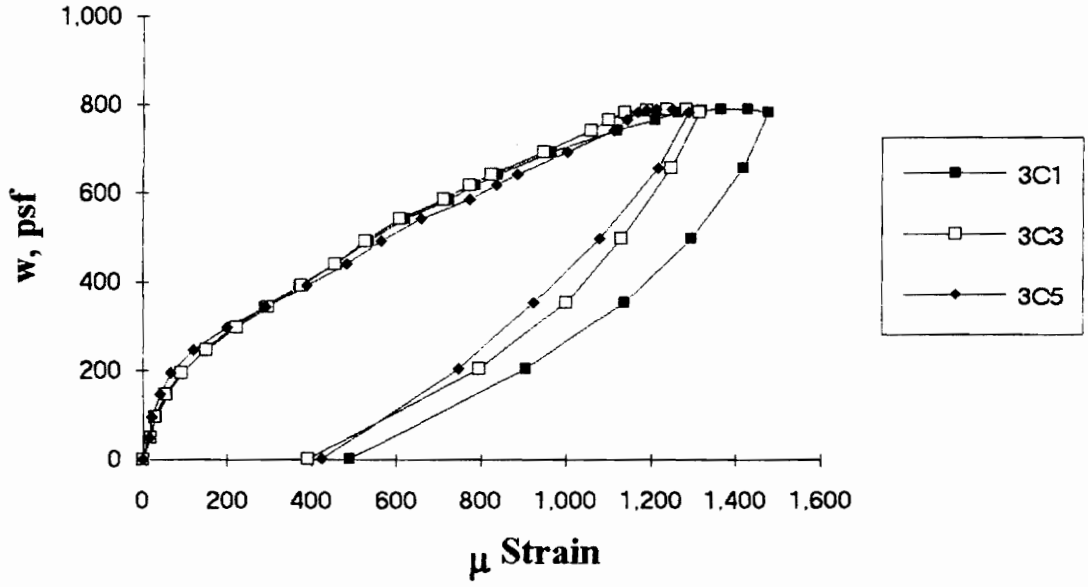

Figure A.210 SDI-3/20-35-10 Load vs. Strain in Deck Top Flange at Interior Support in End Span

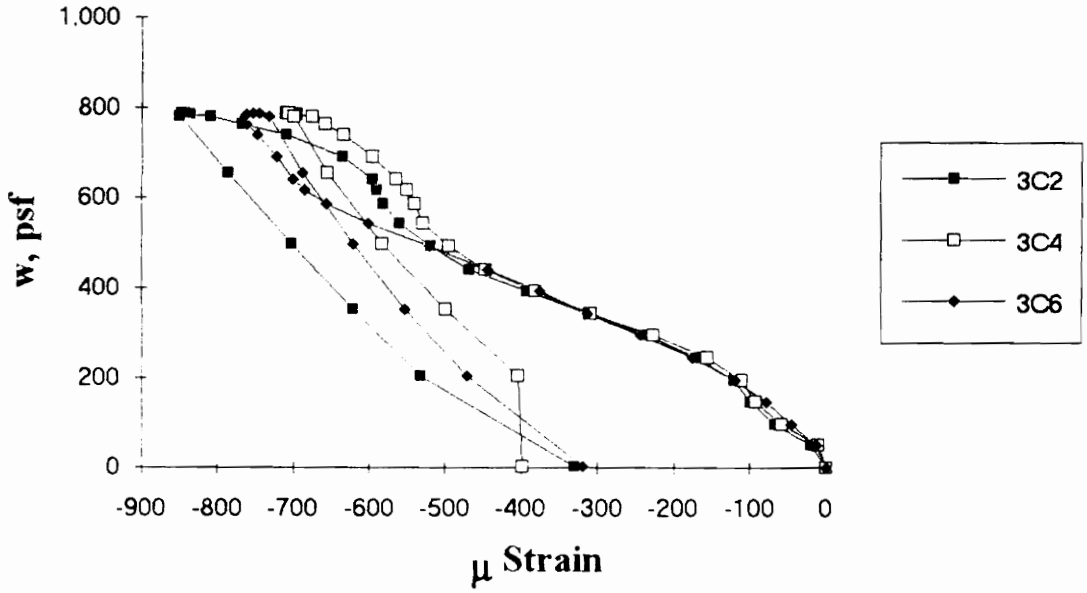

Figure A.211 SDI-3/20-35-10 Load vs. Strain in Deck Bottom Flange at Interior Support in End Span

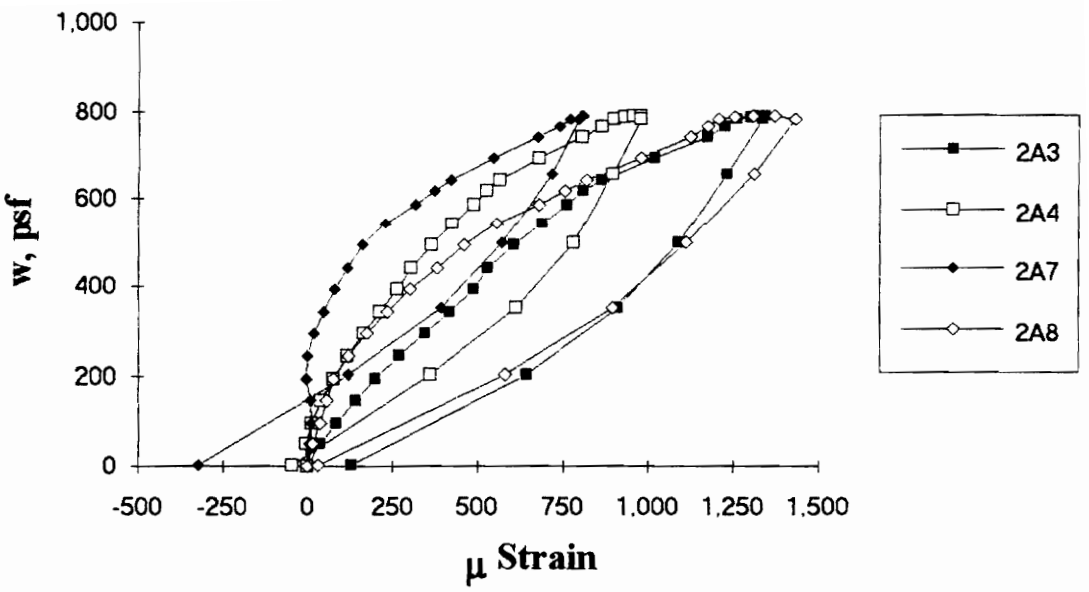

Figure A.212 SDI-3/20-35-10 Load vs. Strain in Deck Top Flange at Interior Support in Center Span

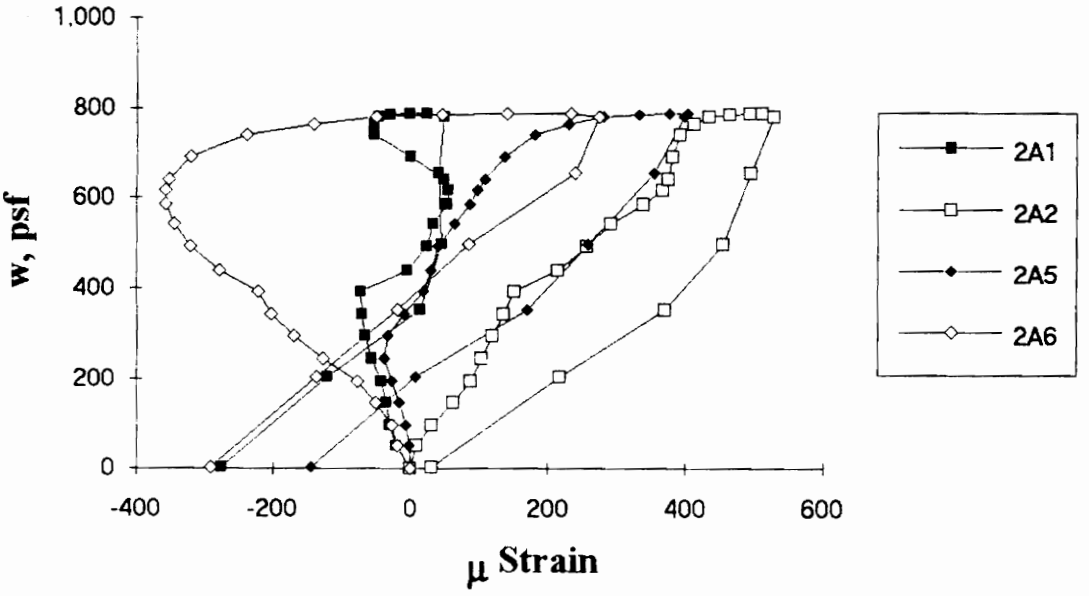

Figure A.213 SDI-3/20-35-10 Load vs. Strain in Deck Bottom Flange at Interior Support in Center Span

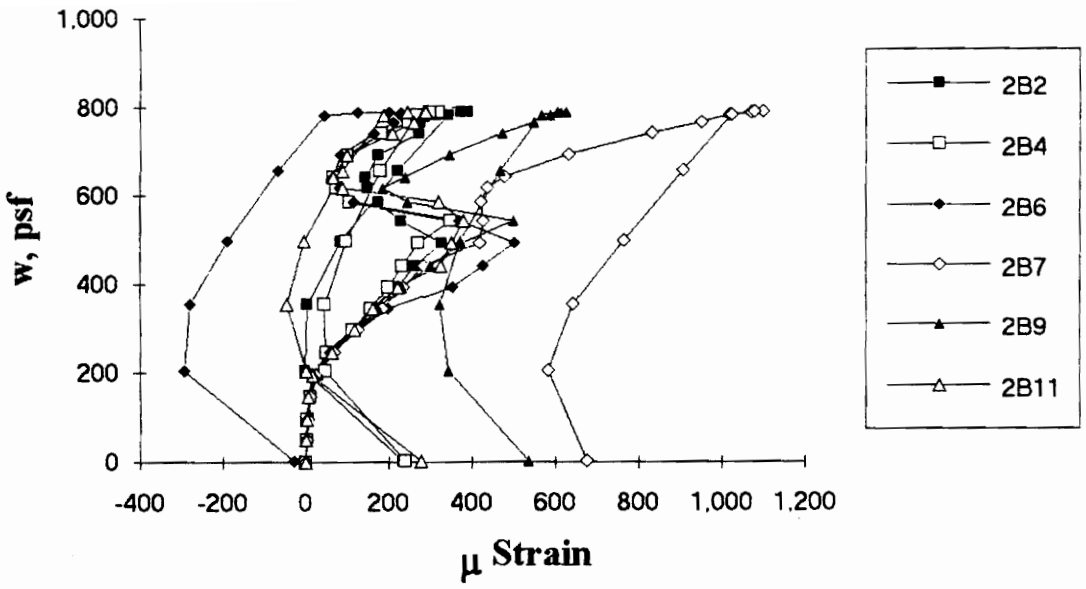

Figure A.214 SDI-3/20-35-10 Load vs. Strain in Deck Top Flange at Maximum Moment

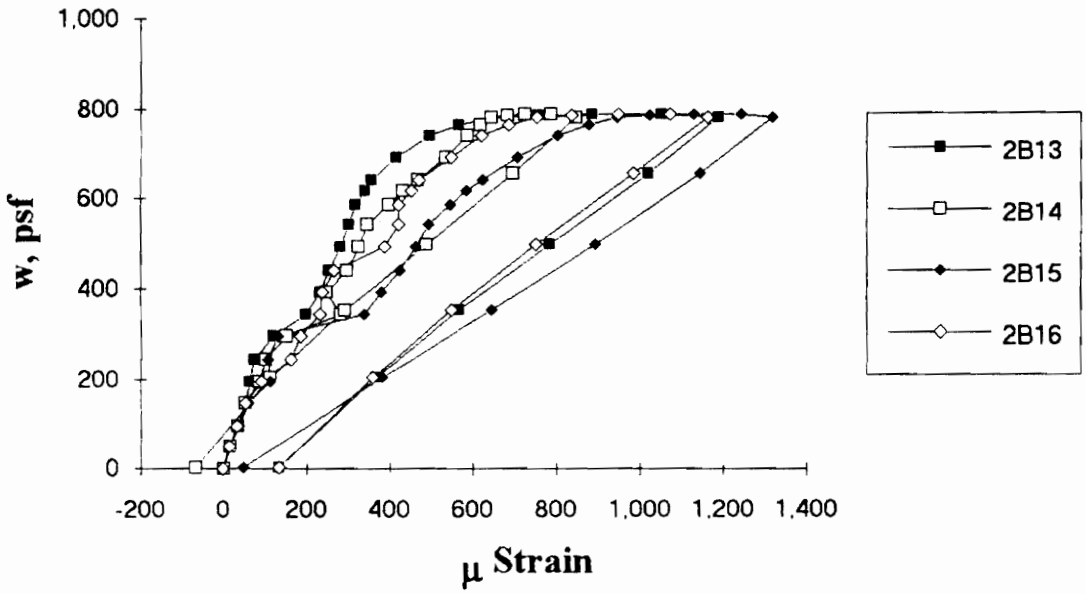

Figure A.215 SDI-3/20-35-10 Load vs. Strain in Deck Web at Maximum Moment

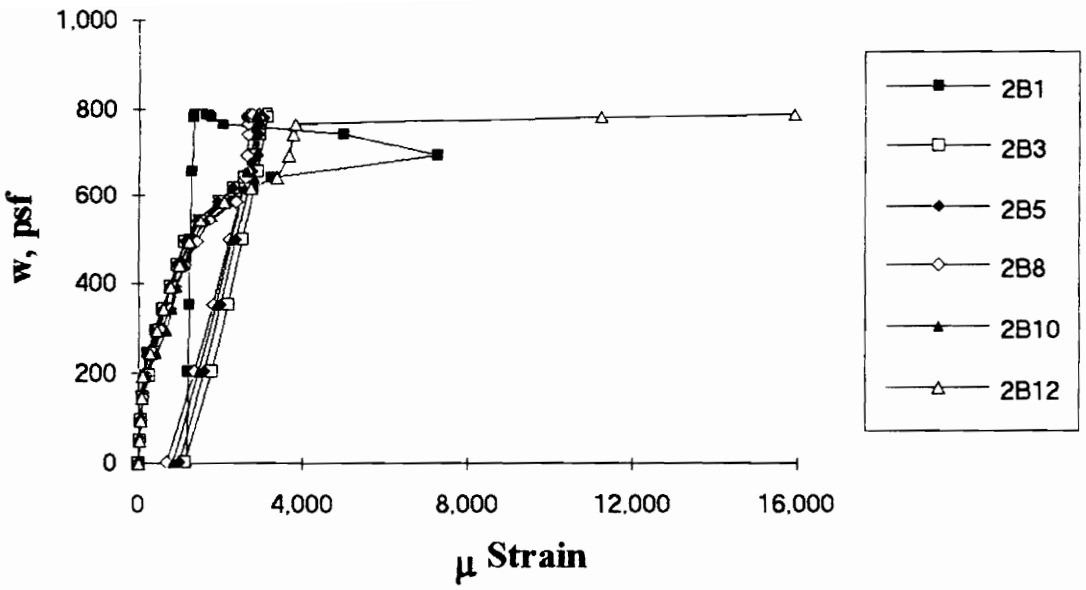

Figure A.216 SDI-3/20-35-10 Load vs. Strain in Deck Bottom Flange at Maximum Moment

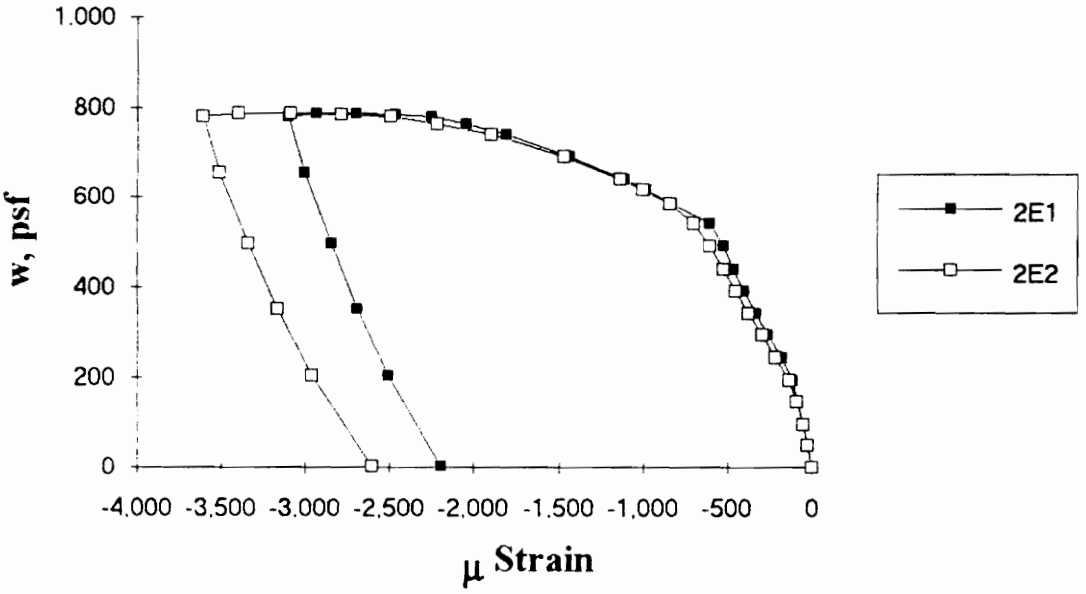

Figure A.217 SDI-3/20-35-10 Load vs. Strain in Concrete at Maximum Moment

Test Designation: SDI-3/20-5-10
Test Date: March 2, 1994

MATERIALS AND DIMENSIONS

General:

width:	6 ft. (2 panels)
span length:	10 ft. end span
end details:	1 ft. cantilever
deck anchorage type:	shear stud, 4-7/8 in. long, 3/4 in. dia.
average anchorage spacing:	1.0 ft.

Deck:

thickness:	0.0355 in. (20 gage)
depth:	3 in.
area:	0.572 $in.^2/ft.$
yield stress:	50.1 ksi
ultimate strength:	61.4 ksi
web embossment type:	III

embossment dimensions:

horizontal:		vertical:					
N_b :	1.81 in.	N_b :	2.30 in.	W_b :	0.53 in.	s :	3.42 in.
N_t :	1.52 in.	N_t :	2.07 in.	W_t :	0.30 in.	p_h :	0.10 in.

Concrete:

type:	normal weight
test strength:	3,750 psi
total depth:	5.5 in.
cover depth:	2.5 in.

RESULTS

midspan strain due to fresh concrete:	230 x 10^{-6} in./in.
maximum load:	891 psf
deflection at maximum load:	3.49 in.
deflection at termination of test:	4.24 in.
end slip at maximum load:	0.12 in.
end slip at termination of test:	0.21 in.

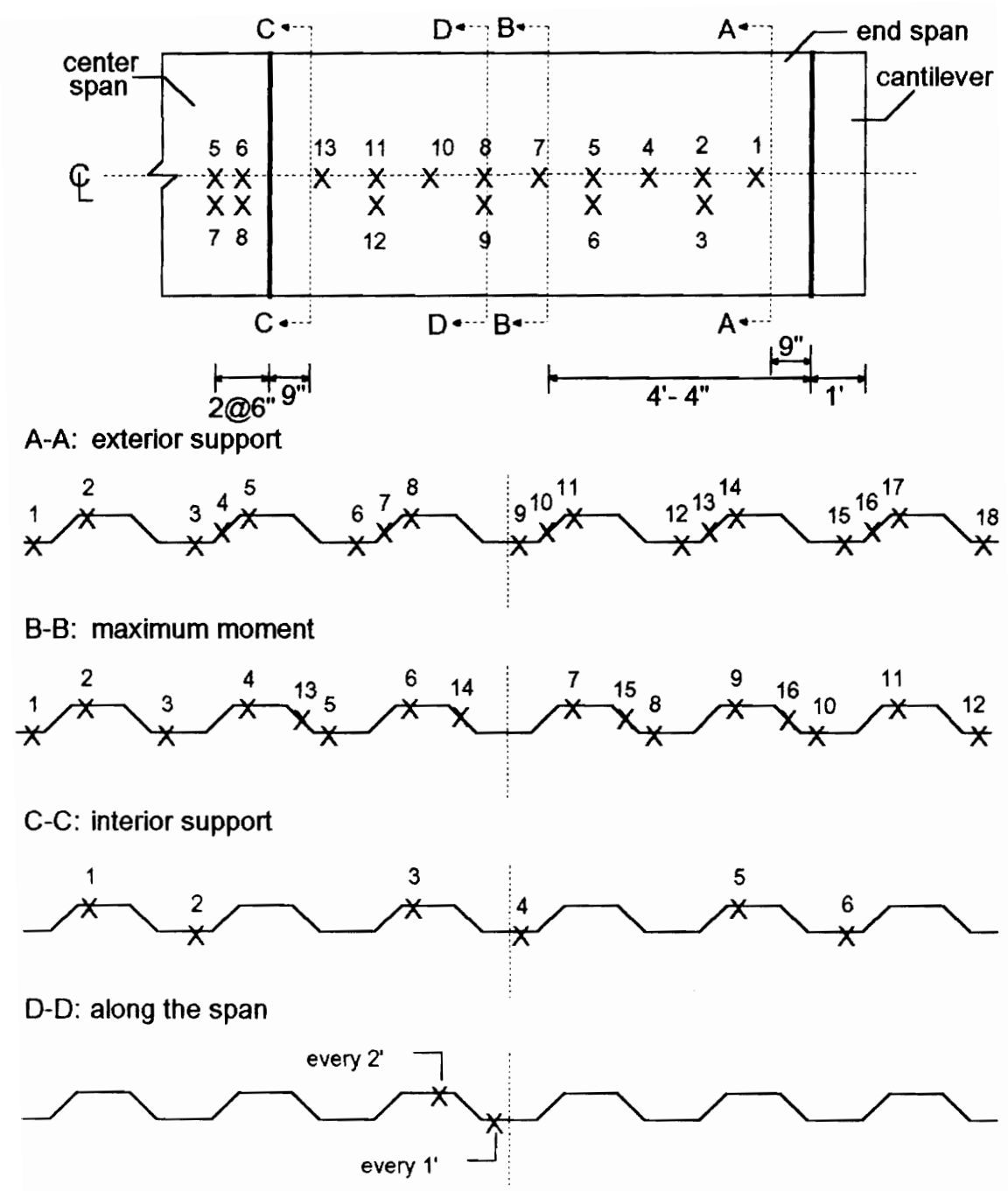

Figure A.218 SDI-3/20-5-10 Steel Deck Strain Gage Locations

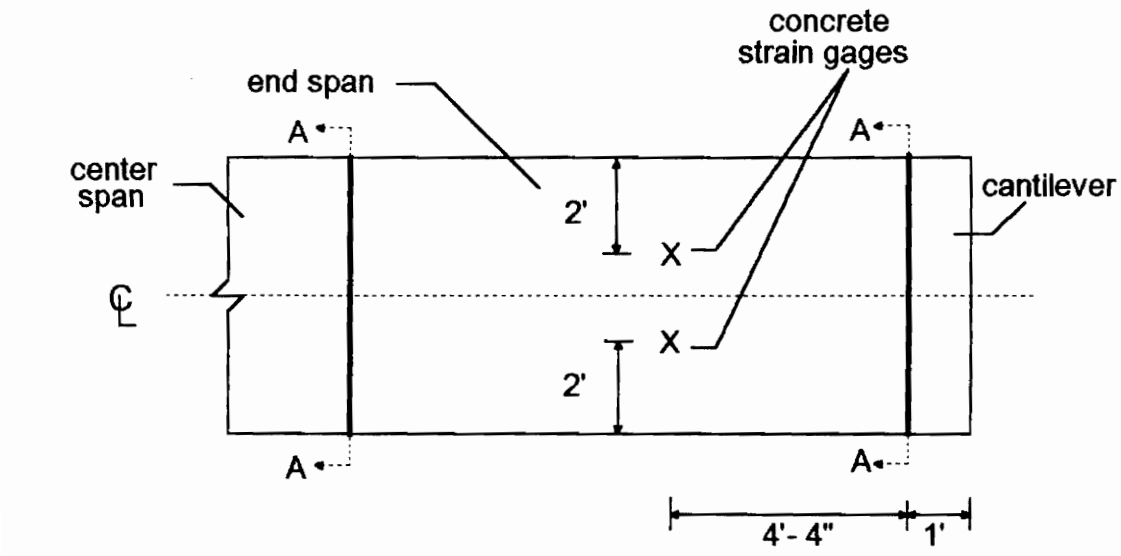

A-A: shear studs over supports

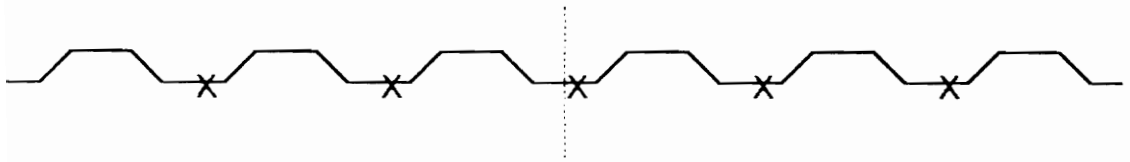

Figure A.219 SDI-3/20-5-10 Concrete Strain Gage and Shear Stud Locations

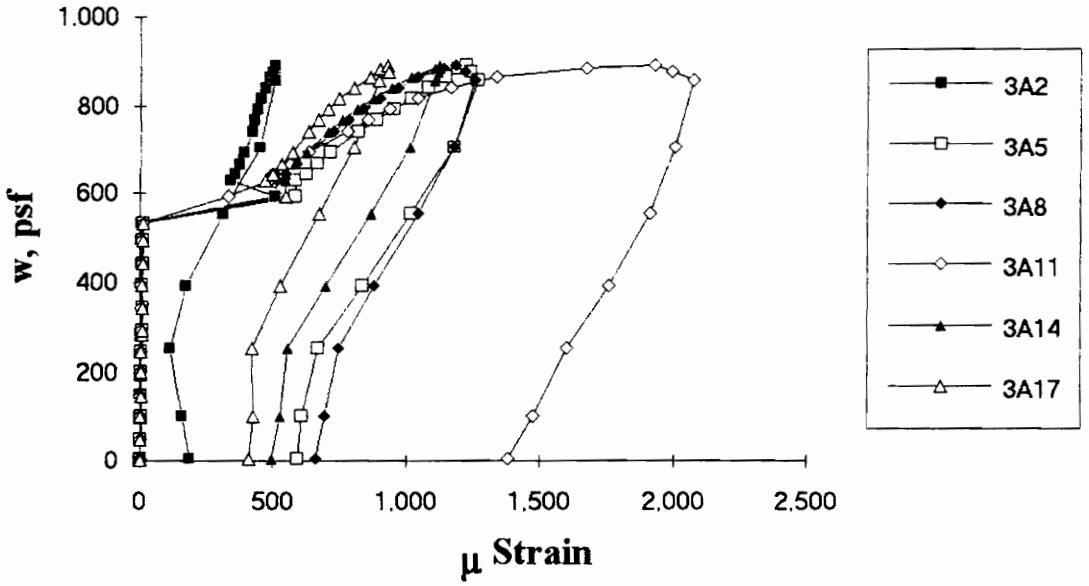

Figure A.220 SDI-3/20-5-10 Load vs. Strain in Deck Top Flange at Exterior Support

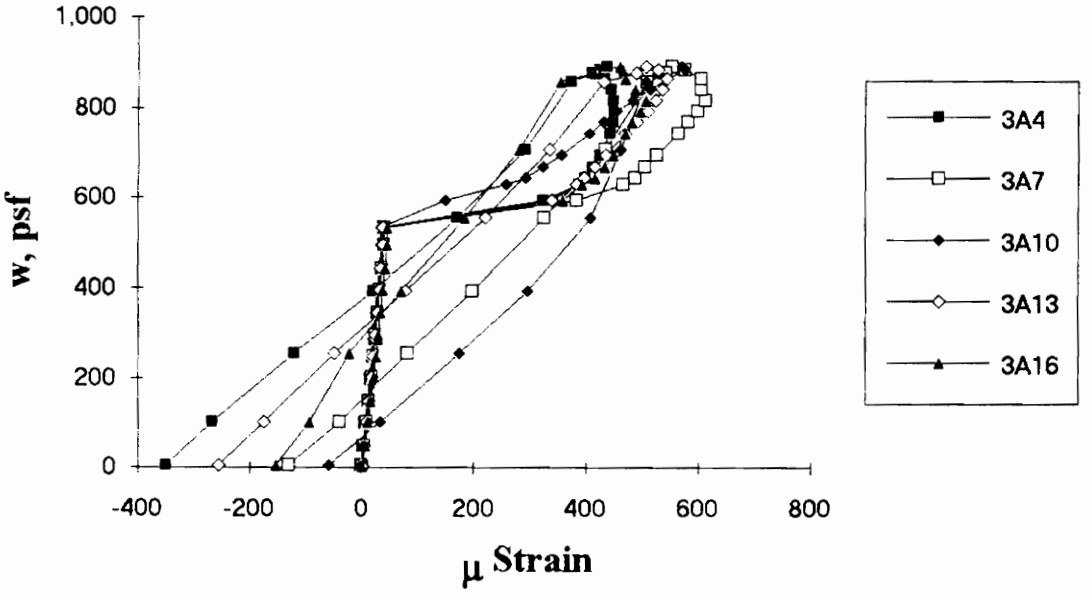

Figure A.221 SDI-3/20-5-10 Load vs. Strain in Deck Web at Exterior Support

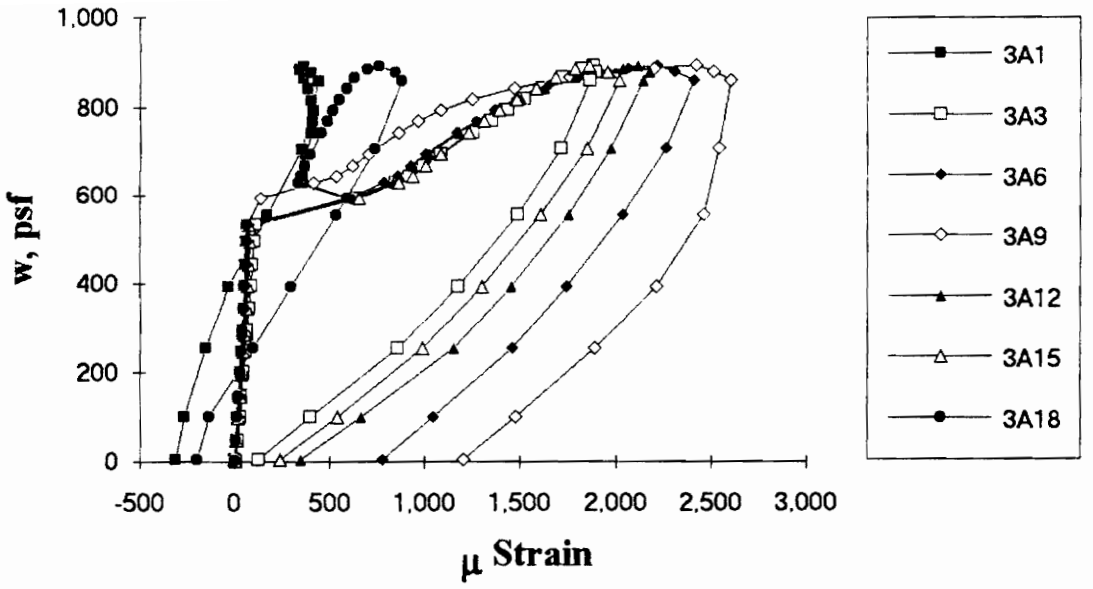

Figure A.222 SDI-3/20-5-10 Load vs. Strain in Deck Bottom Flange at Exterior Support

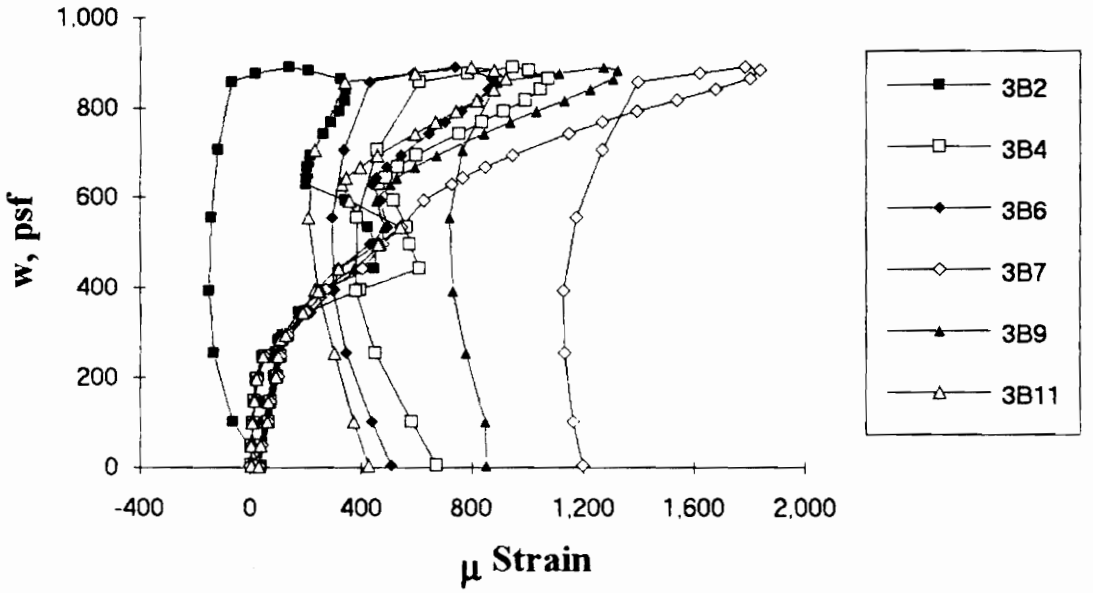

Figure A.223 SDI-3/20-5-10 Load vs. Strain in Deck Top Flange at Maximum Moment

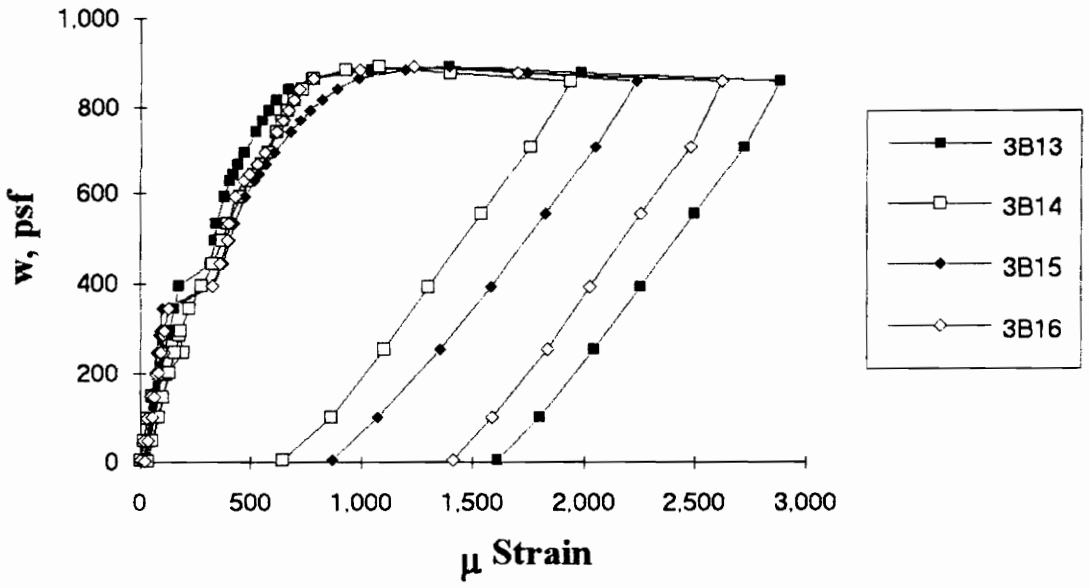

Figure A.224 SDI-3/20-5-10 Load vs. Strain in Deck Web at Maximum Moment

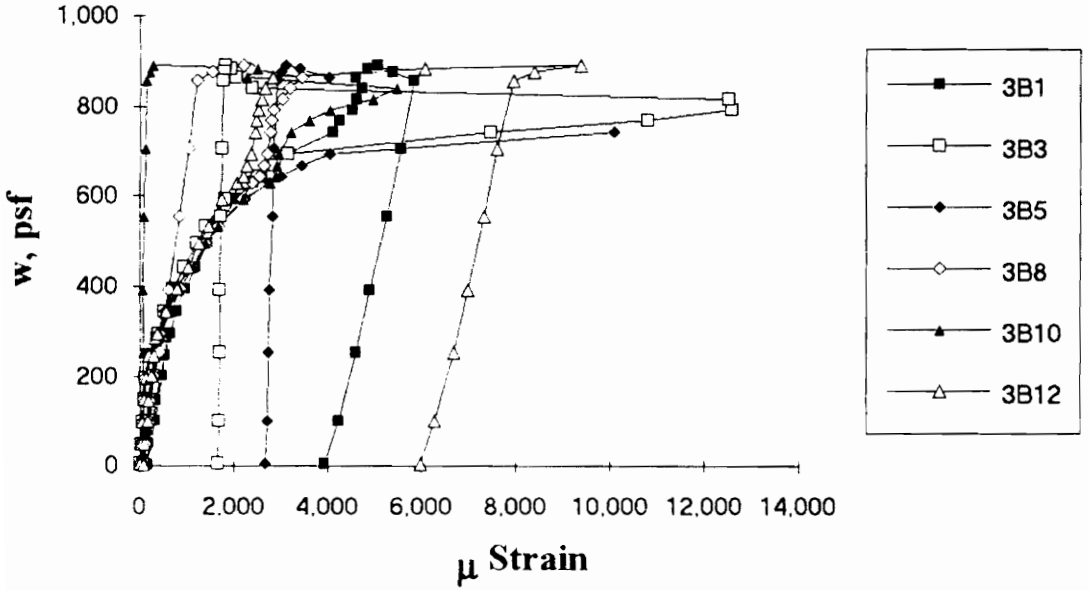

Figure A.225 SDI-3/20-5-10 Load vs. Strain in Deck Bottom Flange at Maximum Moment

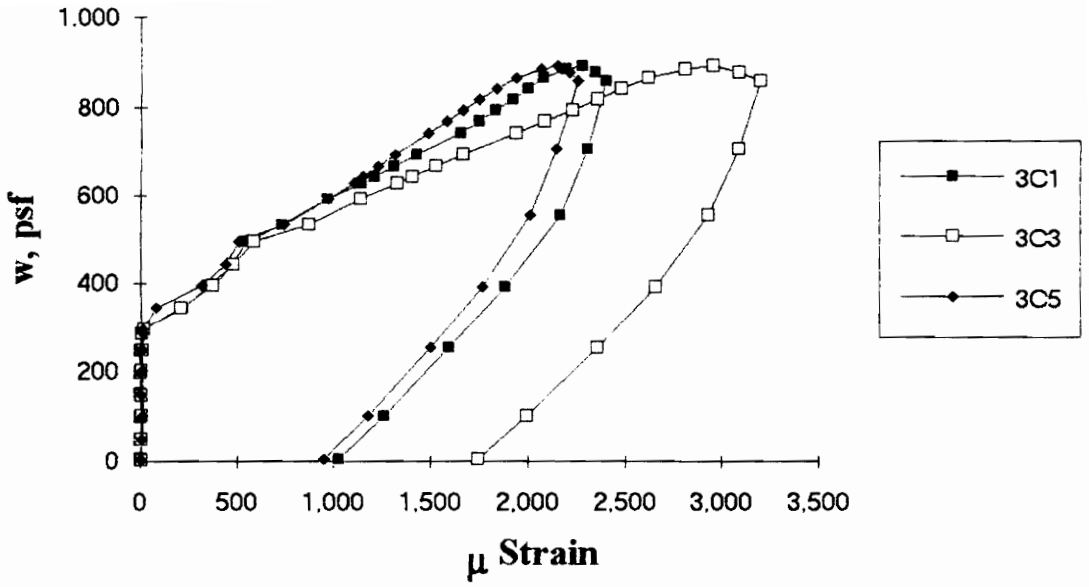

Figure A.226 SDI-3/20-5-10 Load vs. Strain in Deck Top Flange at Interior Support

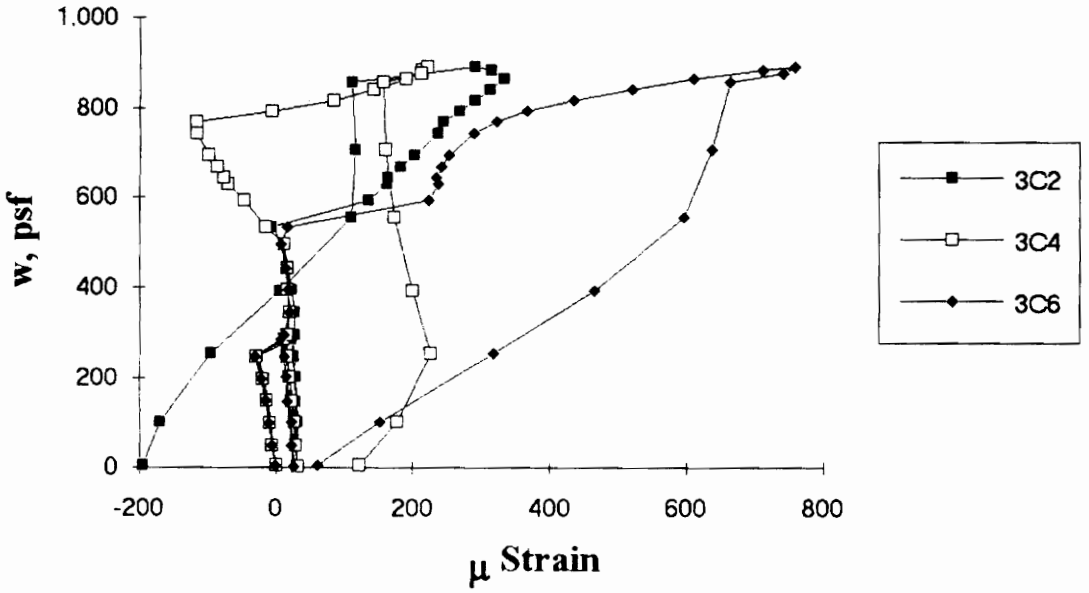

Figure A.227 SDI-3/20-5-10 Load vs. Strain in Deck Bottom Flange at Interior Support

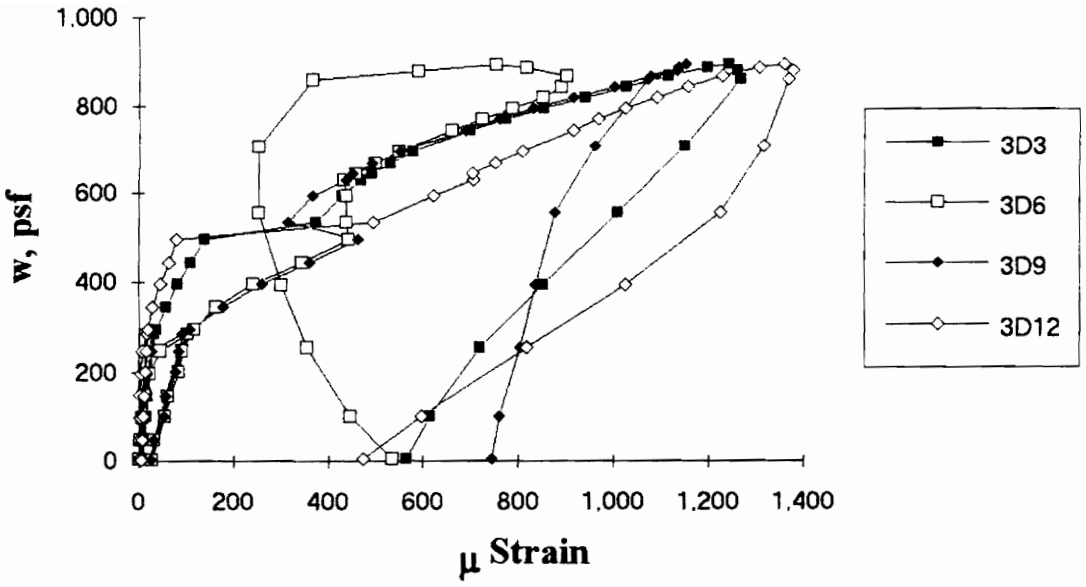

Figure A.228 SDI-3/20-5-10 Load vs. Strain in Deck Top Flange along the Span

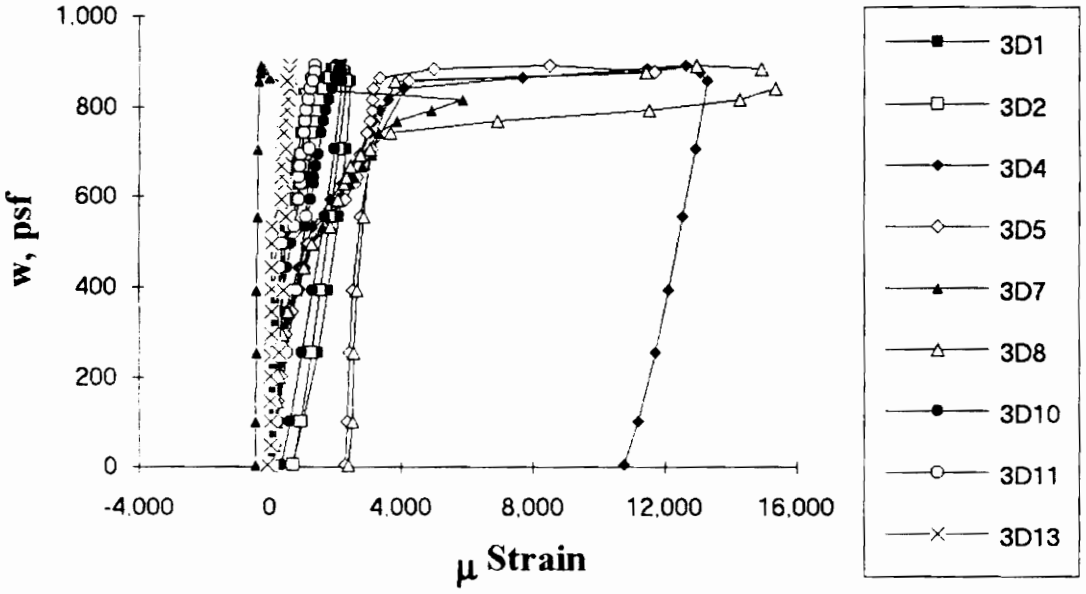

Figure A.229 SDI-3/20-5-10 Load vs. Strain in Deck Bottom Flange along the Span

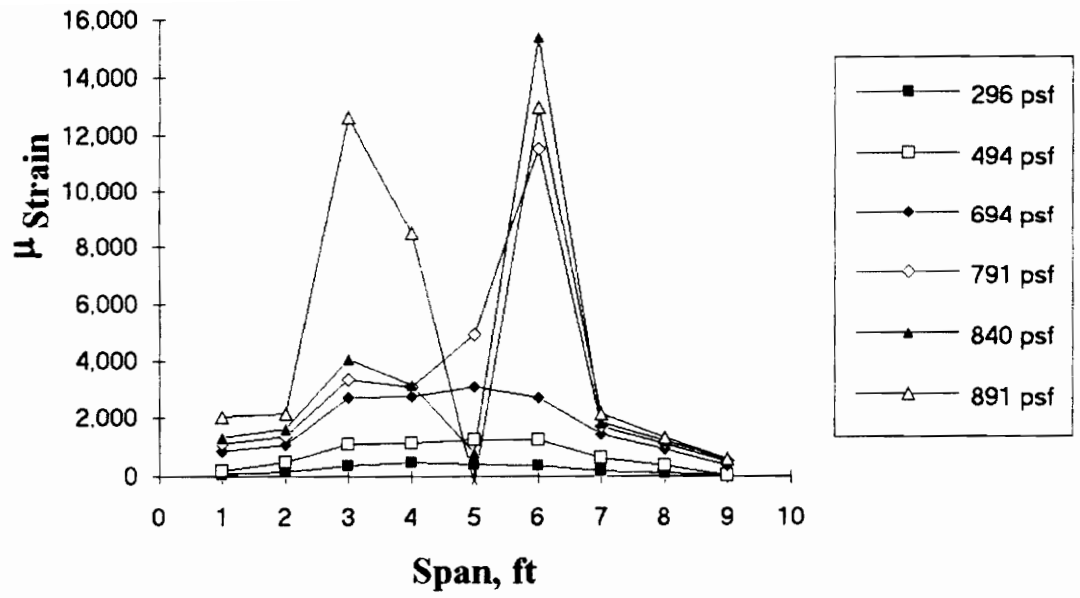

Figure A.230 SDI-3/20-5-10 Strain Variation in Deck Bottom Flange along the Span (from centerline of exterior support)

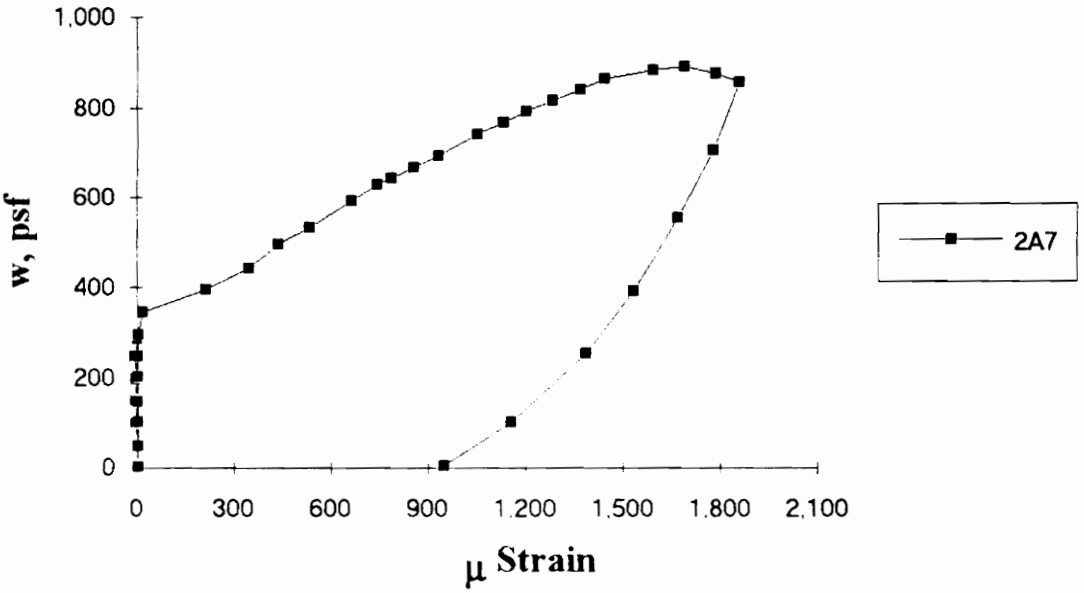

Figure A.231 SDI-3/20-5-10 Load vs. Strain in Deck Bottom Flange in Center Span

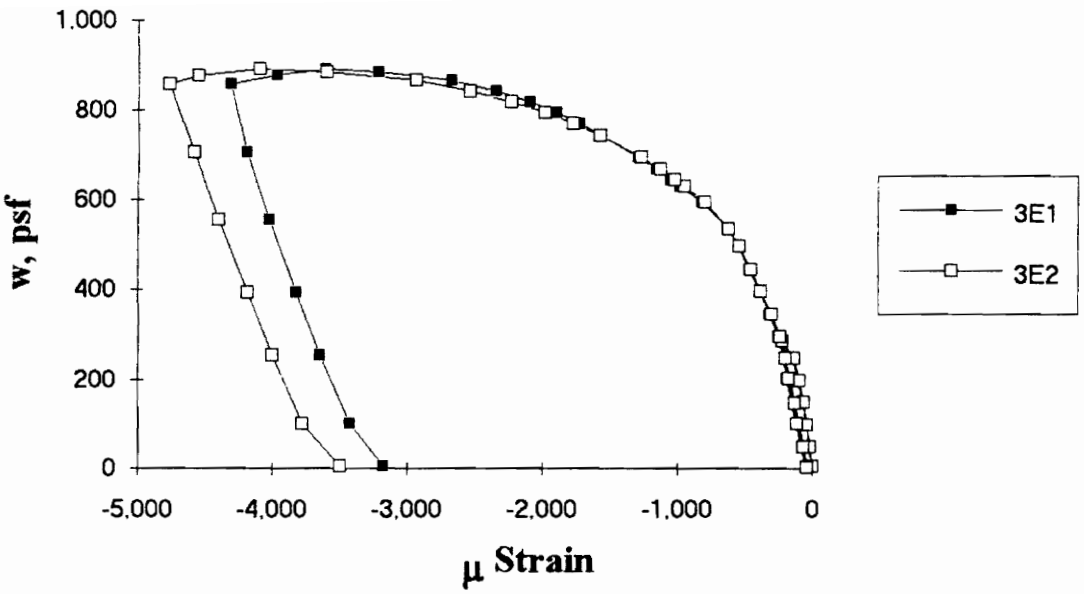

Figure A.232 SDI-3/20-5-10 Load vs. Strain in Concrete at Maximum Moment

Test Designation: SDI-3/20-PX1-10
Test Date: April 1, 1994

MATERIALS AND DIMENSIONS

General:

width:	6 ft. (2 panels)
span length:	10 ft. end span
end details:	1 ft. cantilever, interior support deck joint
deck anchorage type:	arc spot weld, 3/4 in. dia.
average anchorage spacing:	1.0 ft.

Deck:

thickness:	0.0355 in. (20 gage)
depth:	3 in.
area:	0.572 $in.^2/ft.$
yield stress:	50.1 ksi
ultimate strength:	61.4 ksi
web embossment type:	III

embossment dimensions:

horizontal:		vertical:					
N_b :	1.81 in.	N_b :	2.30 in.	W_b :	0.53 in.	s :	3.42 in.
N_t :	1.52 in.	N_t :	2.07 in.	W_t :	0.30 in.	p_h :	0.10 in.

Concrete:

type:	normal weight
test strength:	3,370 psi
total depth:	5.5 in.
cover depth:	2.5 in.

RESULTS

midspan strain due to fresh concrete:	400 x 10^{-6} in./in.
maximum load:	478 psf
deflection at maximum load:	0.60 in.
deflection at termination of test:	2.95 in.
end slip at maximum load:	0.00 in.
end slip at termination of test:	0.56 in.

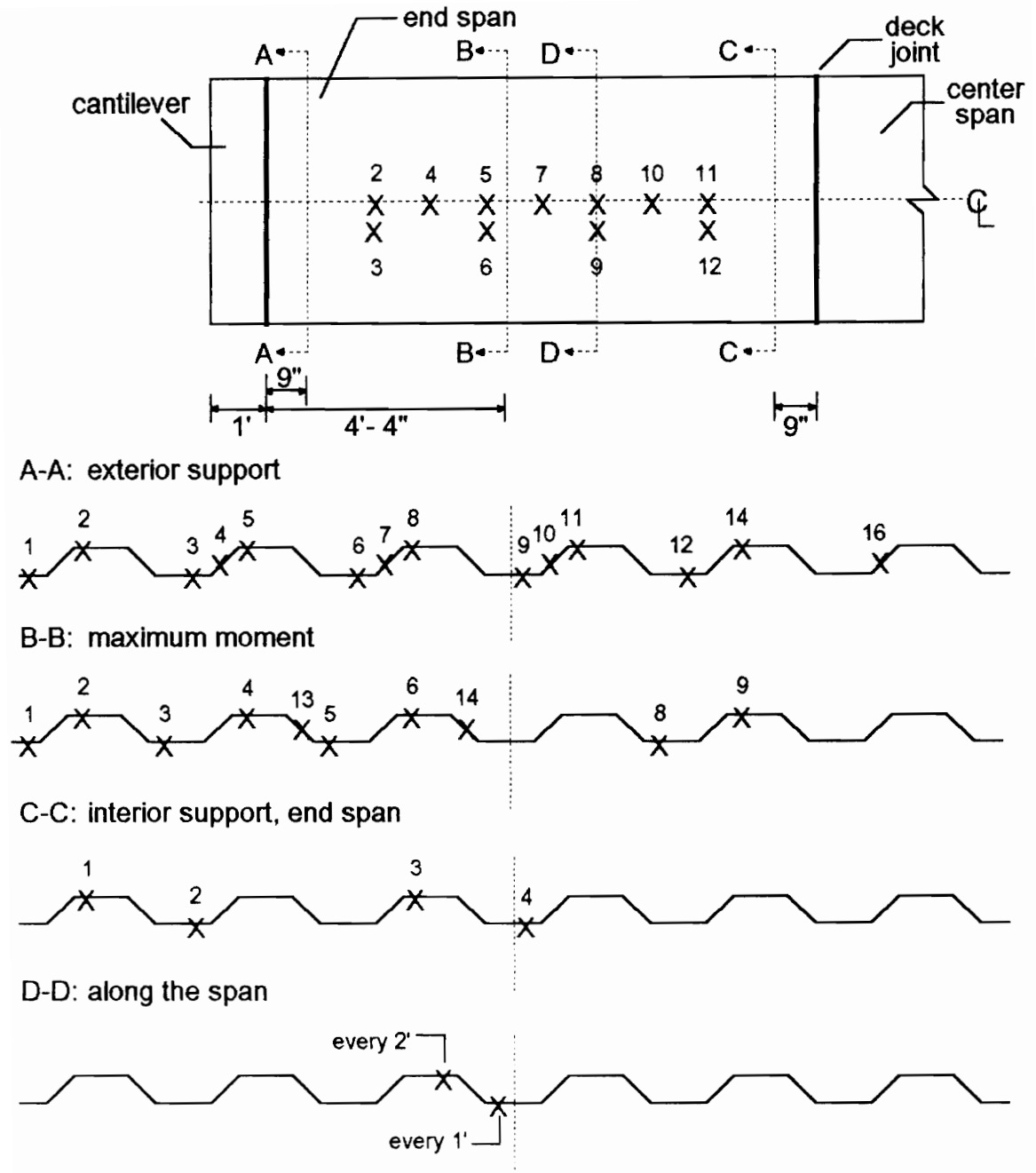

Figure A.233 SDI-3/20-PX1-10 Steel Deck Strain Gage Locations

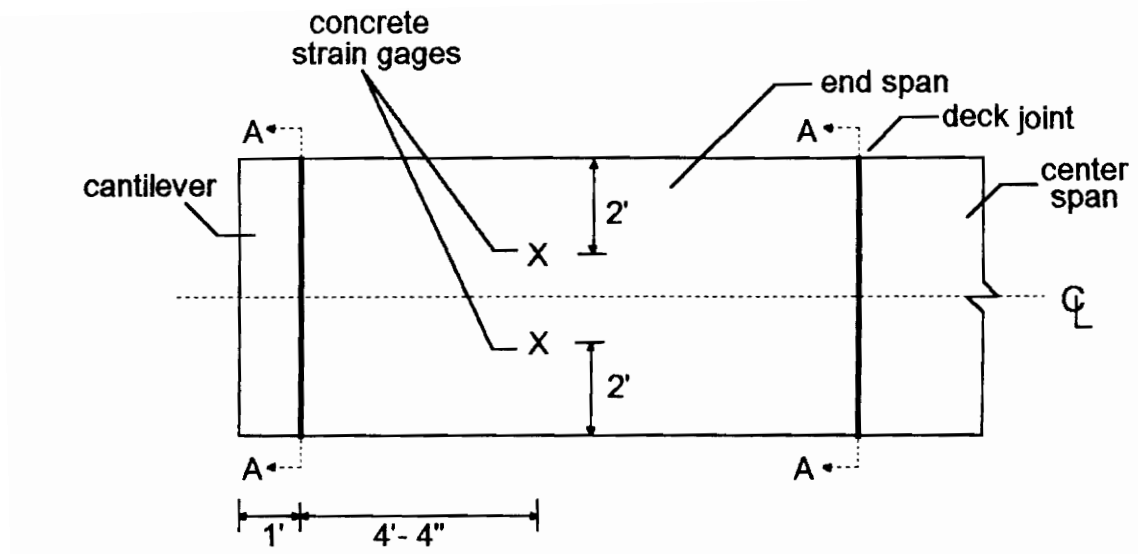

A-A: arc spot welds over supports

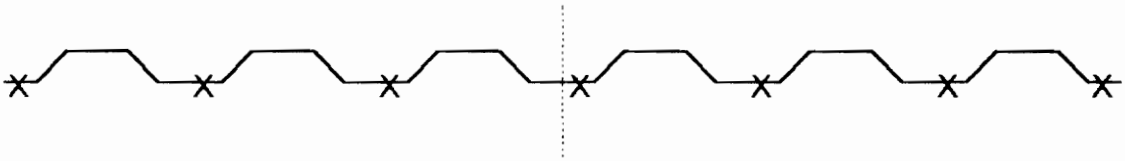

Figure A.234 SDI-3/20-PX1-10 Concrete Strain Gage and Arc Spot Weld Locations

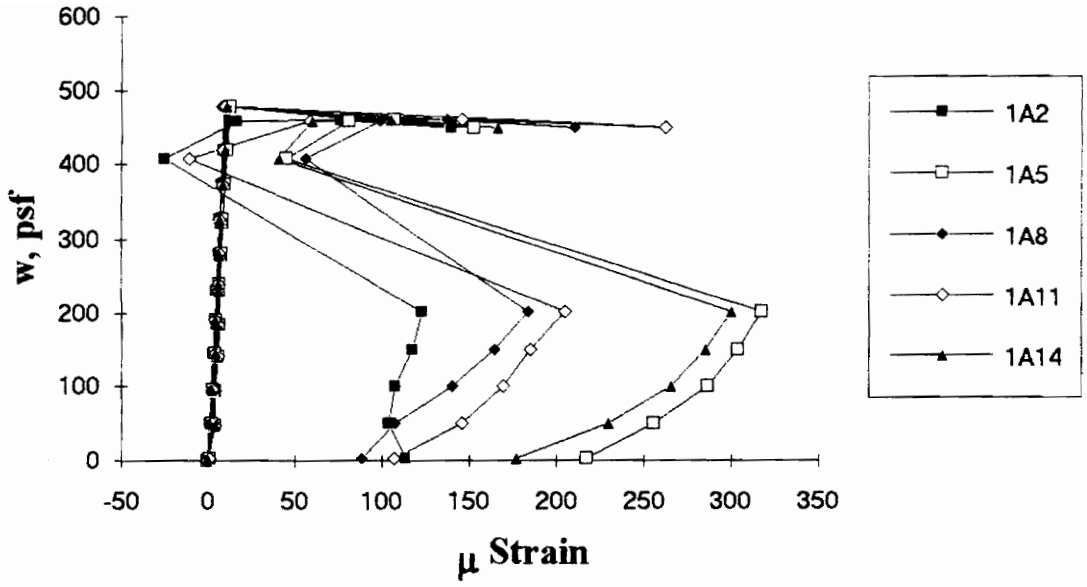

Figure A.235 SDI-3/20-PX1-10 Load vs. Strain in Deck Top Flange at Exterior Support

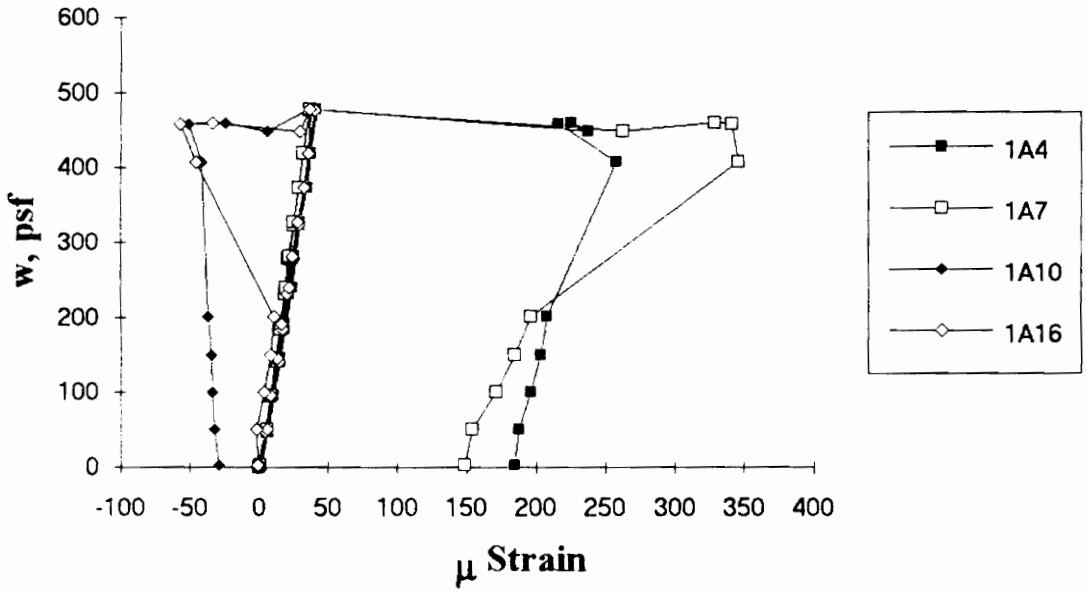

Figure A.236 SDI-3/20-PX1-10 Load vs. Strain in Deck Web at Exterior Support

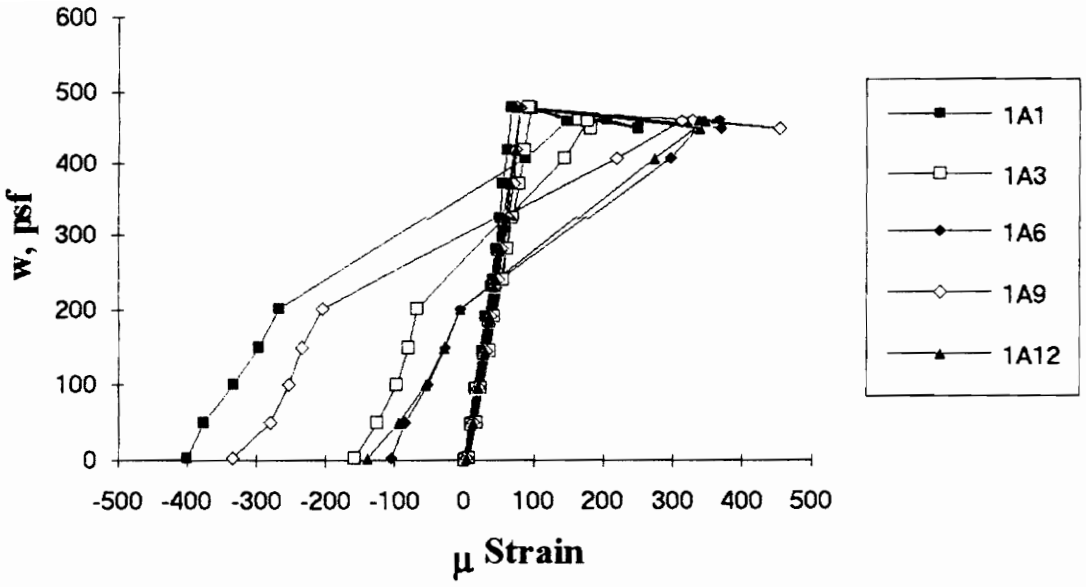

Figure A.237 SDI-3/20-PX1-10 Load vs. Strain in Deck Bottom Flange at Exterior Support

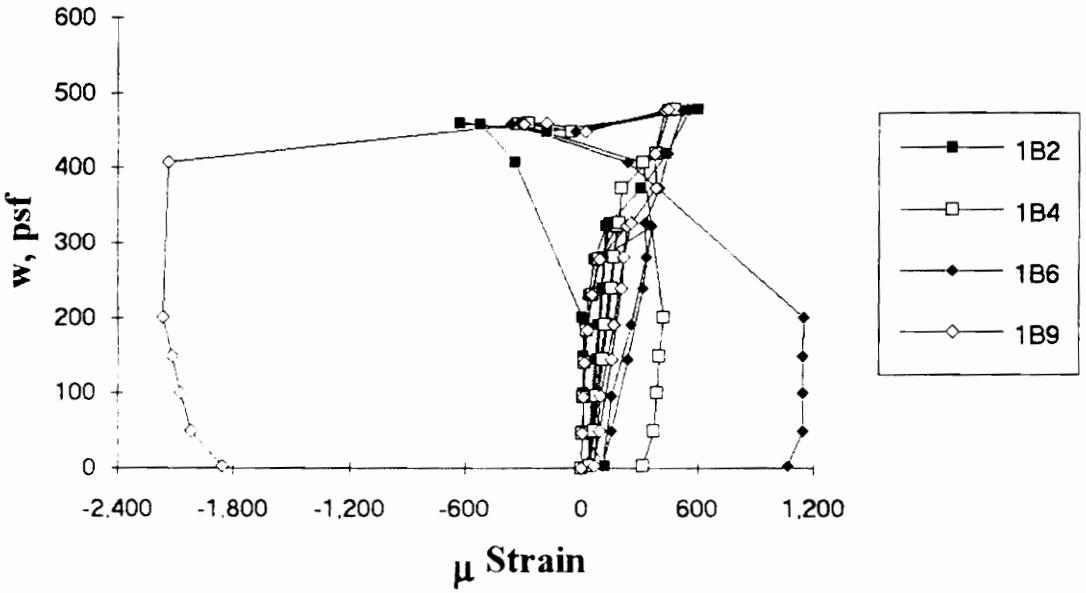

Figure A.238 SDI-3/20-PX1-10 Load vs. Strain in Deck Top Flange at Maximum Moment

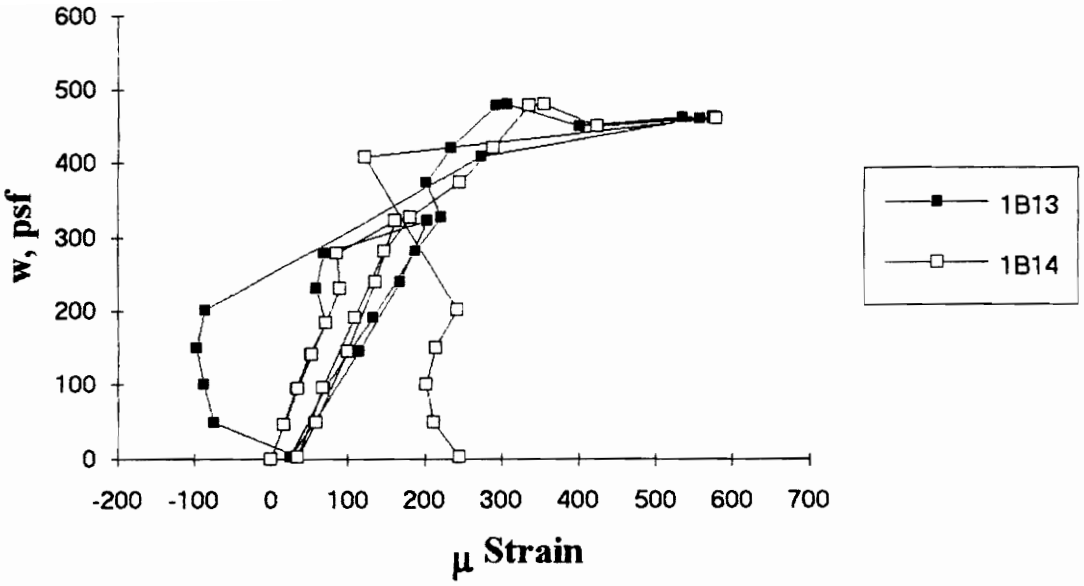

Figure A.239 SDI-3/20-PX1-10 Load vs. Strain in Deck Web at Maximum Moment

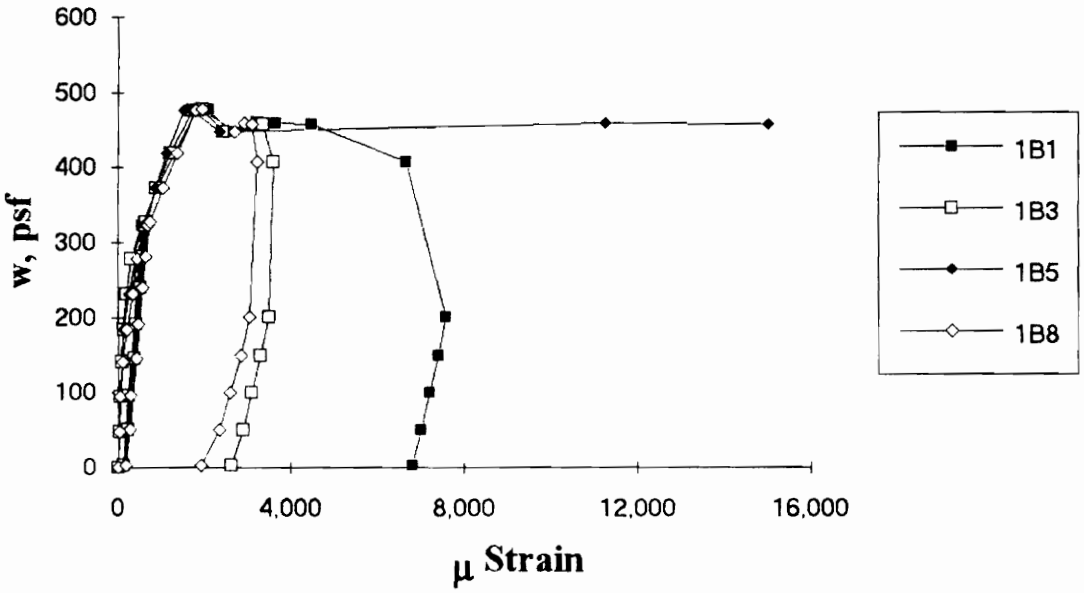

Figure A.240 SDI-3/20-PX1-10 Load vs. Strain in Deck Bottom Flange at Maximum Moment

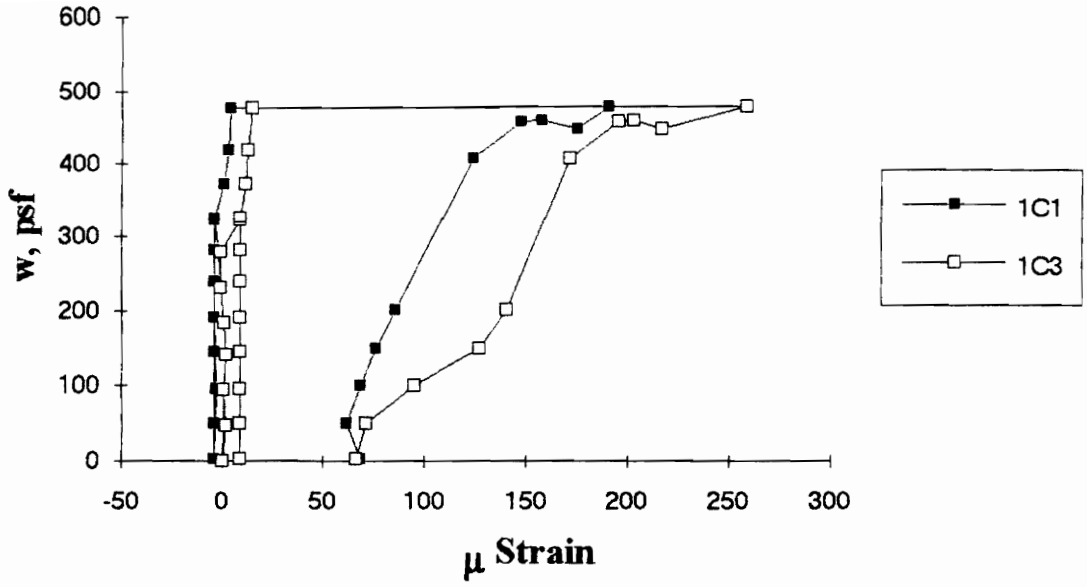

Figure A.241 SDI-3/20-PX1-10 Load vs. Strain in Deck Top Flange at Interior Support

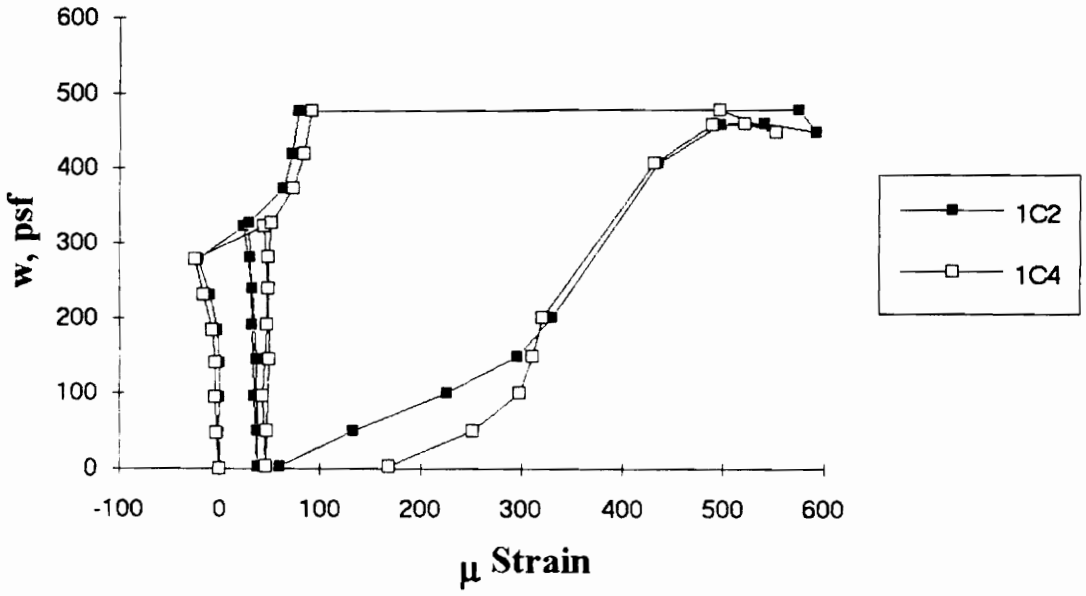

Figure A.242 SDI-3/20-PX1-10 Load vs. Strain in Deck Bottom Flange at Interior Support

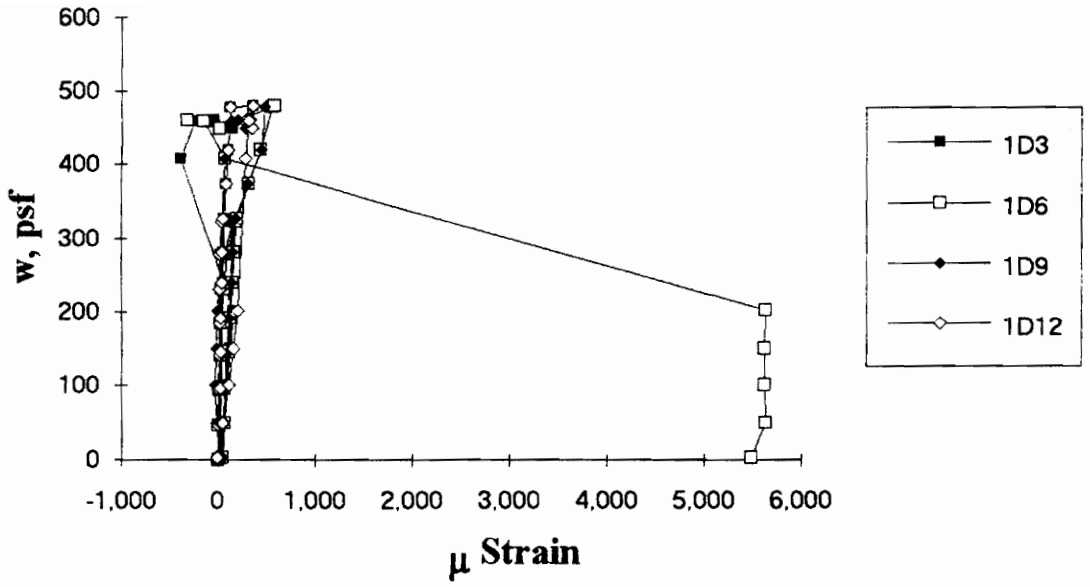

Figure A.243 SDI-3/20-PX1-10 Load vs. Strain in Deck Top Flange along the Span

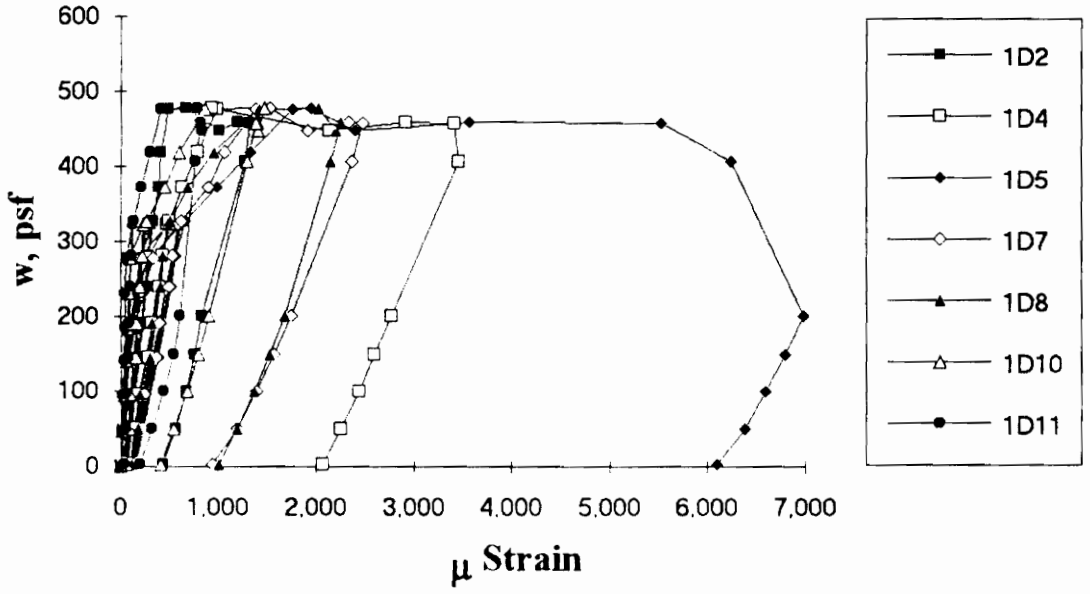

Figure A.244 SDI-3/20-PX1-10 Load vs. Strain in Deck Bottom Flange along the Span

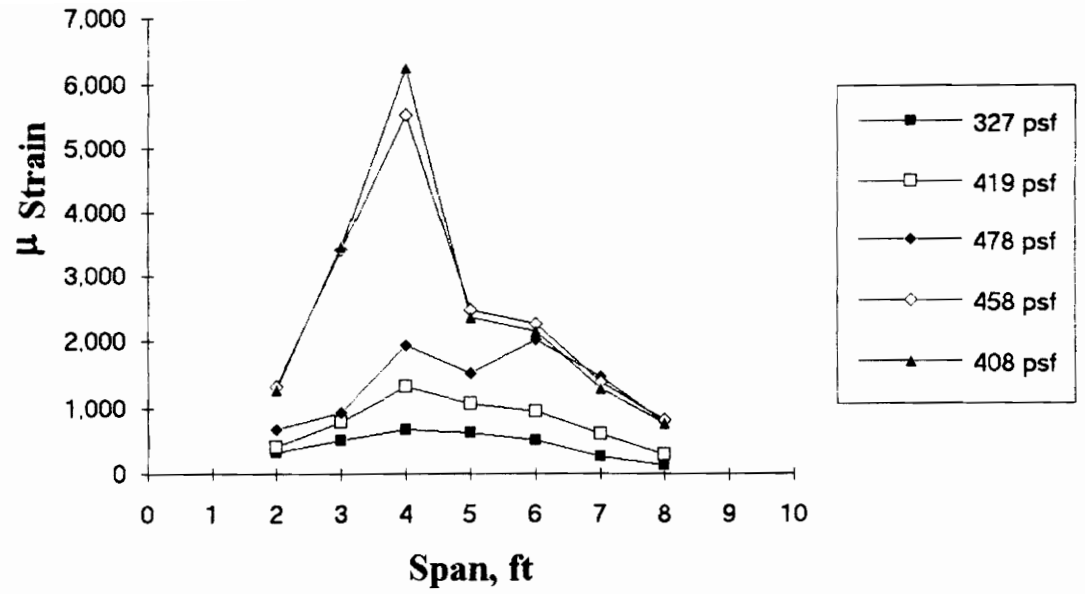

Figure A.245 SDI-3/20-PX1-10 Strain Variation in Deck Bottom Flange along the Span (from centerline of exterior support)

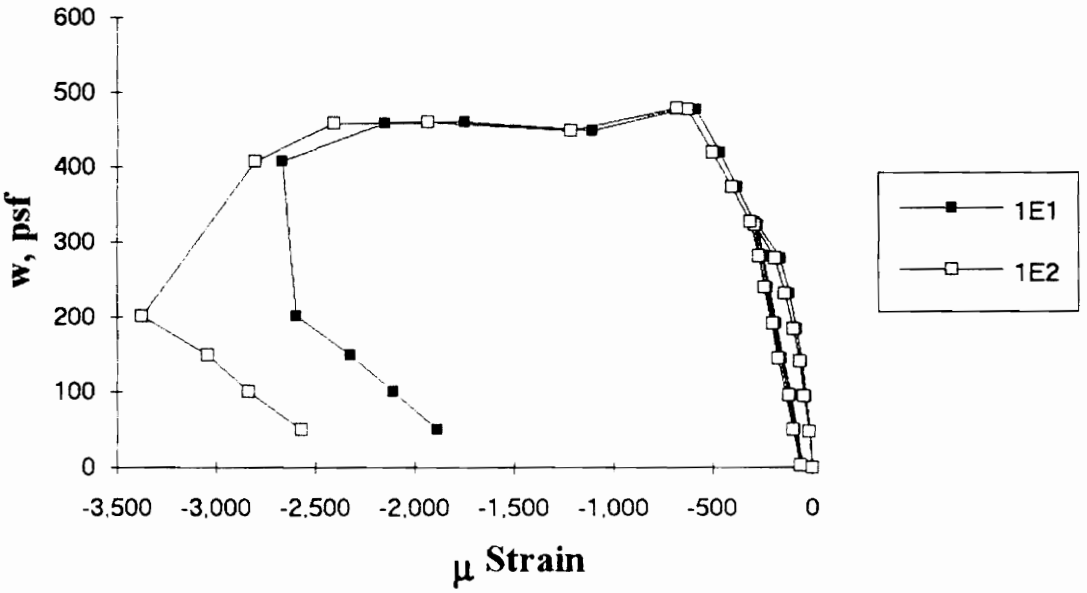

Figure A.246 SDI-3/20-PX1-10 Load vs. Strain in Concrete at Maximum Moment

Test Designation: SDI-2/18-PX3-9
Test Date: April 4, 1994

MATERIALS AND DIMENSIONS

General:

width:	6 ft. (2 panels)
span length:	9 ft. end span
end details:	1 ft. cantilever, int. support deck joint
deck anchorage type:	arc spot weld, 3/4 in. dia.
average anchorage spacing:	1.0 ft.

Deck:

thickness:	0.0470 in. (18 gage)
depth:	2 in.
area:	0.696 $in.^2/ft.$
yield stress:	46.5 ksi
ultimate strength:	59.6 ksi
web embossment type:	I

embossment dimensions:

N_b :	2.28 in.	W_b :	0.44 in.	s :	1.59 in.
N_t :	1.68 in.	W_t :	0.24 in.	p_h :	0.08 in.

Concrete:

type:	normal weight
test strength:	3,400 psi
total depth:	4.5 in.
cover depth:	2.5 in.

RESULTS

midspan strain due to fresh concrete:	310 x 10^{-6} in./in.
maximum load:	499 psf
deflection at maximum load:	1.57 in.
deflection at termination of test:	3.11 in.
end slip at maximum load:	0.16 in.
end slip at termination of test:	0.72 in.

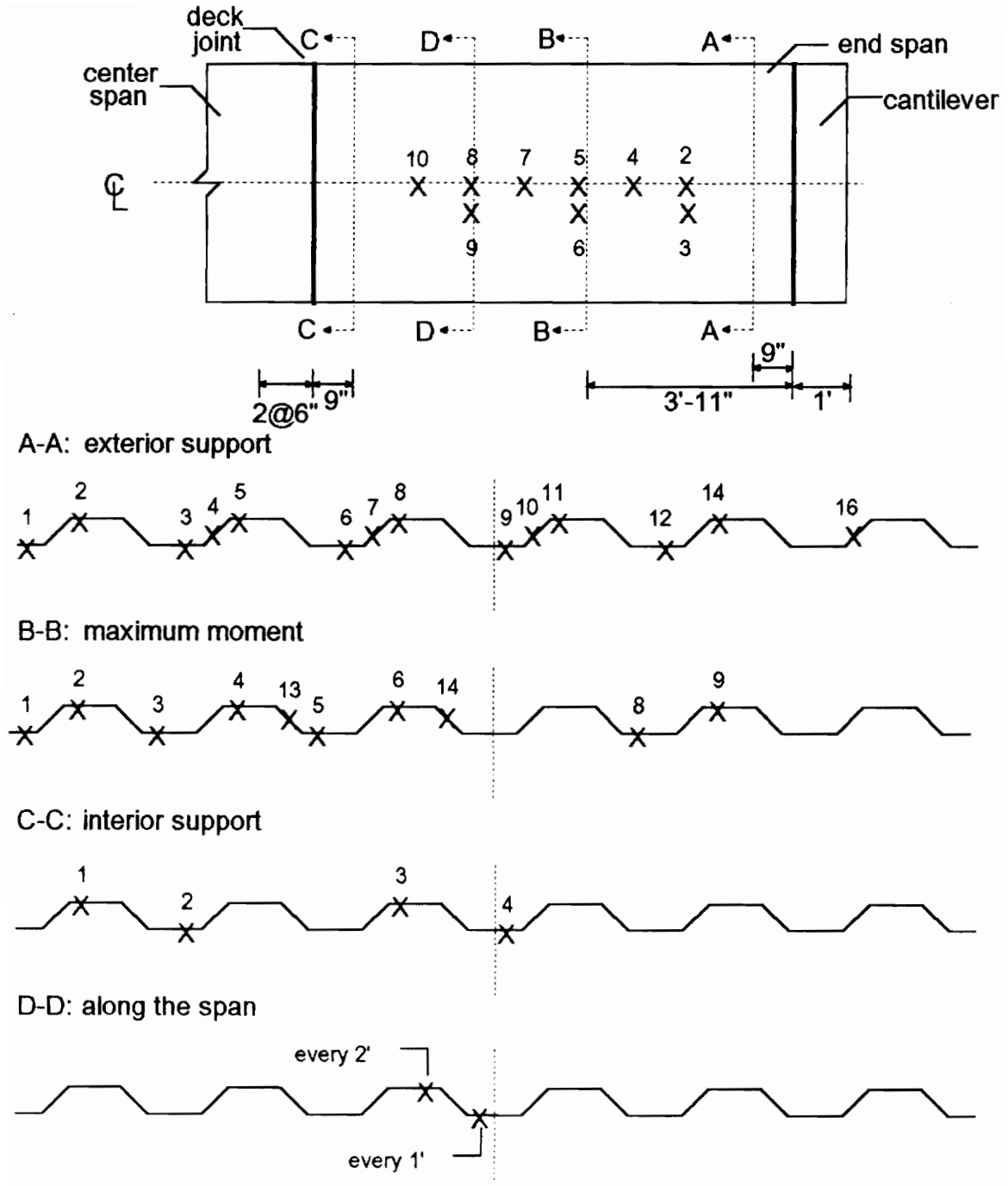

Figure A.247 SDI-2/18-PX3-9 Steel Deck Strain Gage Locations

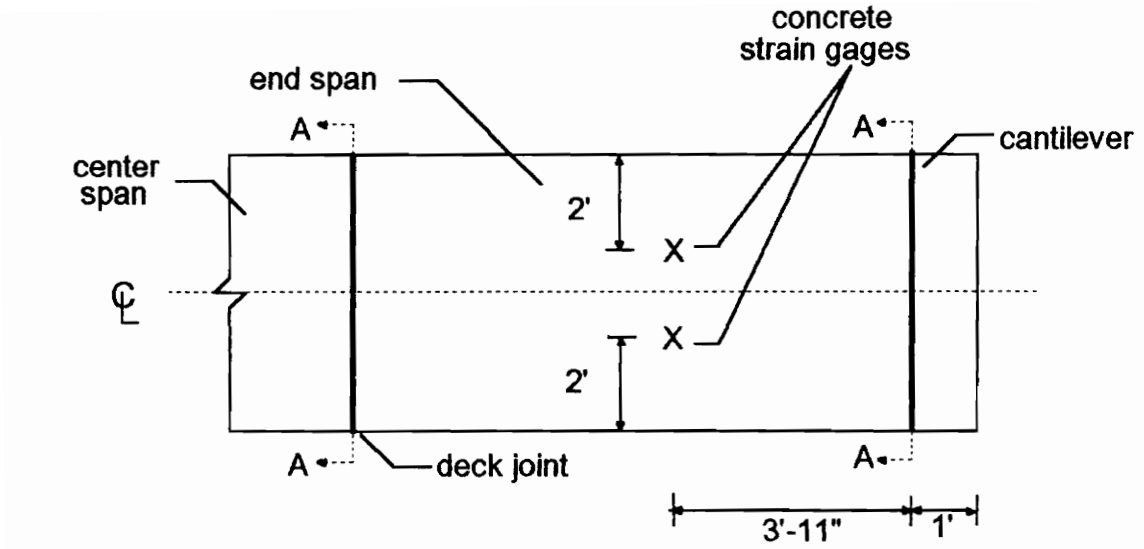

A-A: arc spot welds over supports

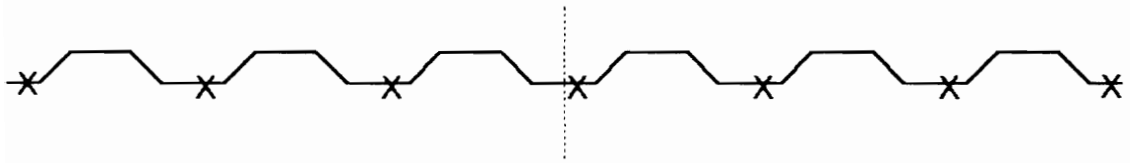

Figure A.248 SDI-2/18-PX3-9 Concrete Strain Gage and Arc Spot Weld Locations

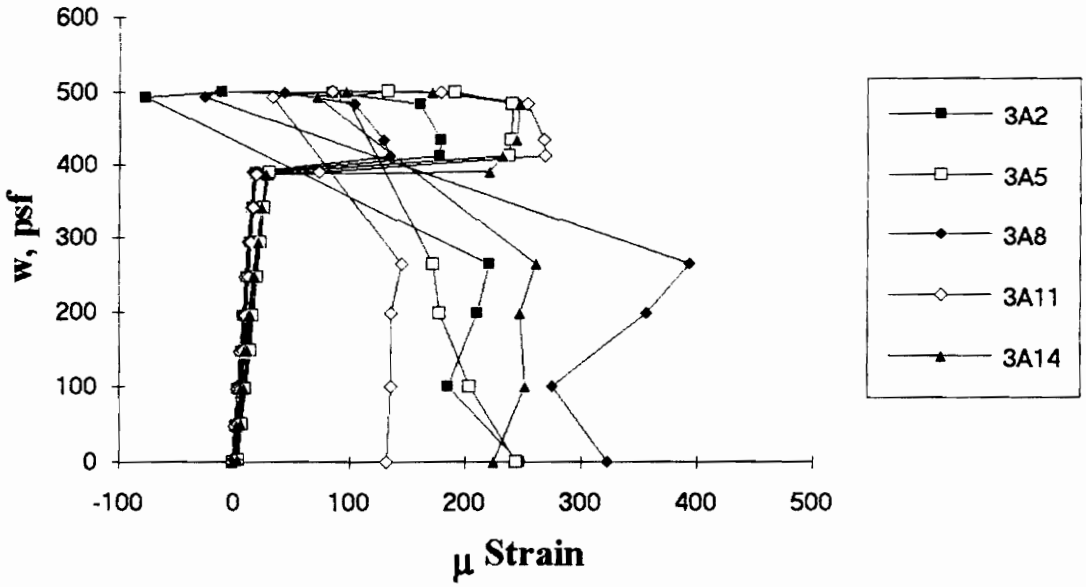

Figure A.249 SDI-2/18-PX3-9 Load vs. Strain in Deck Top Flange at Exterior Support

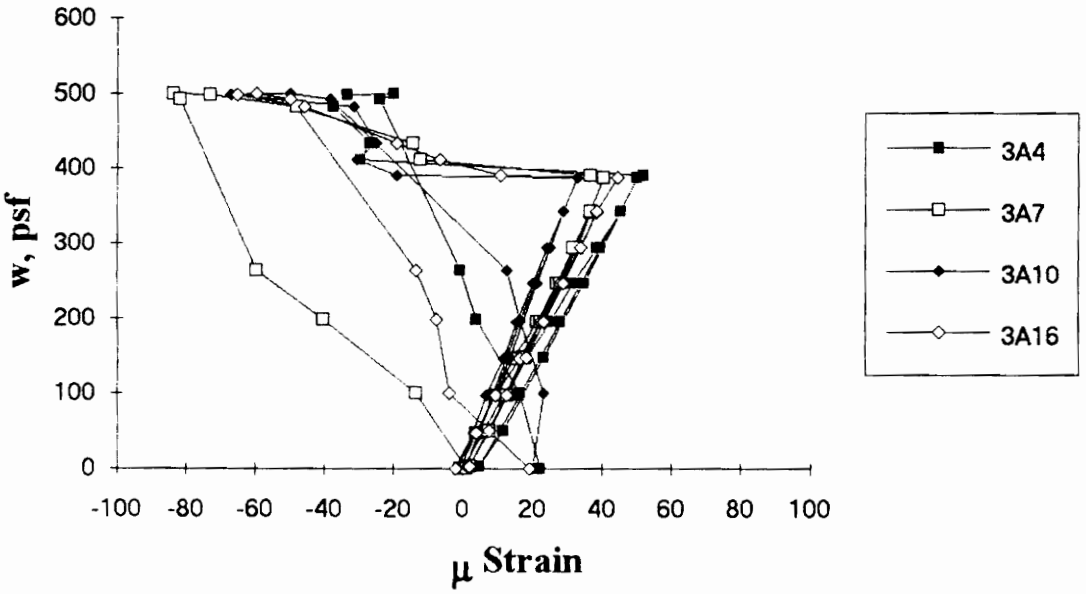

Figure A.250 SDI-2/18-PX3-9 Load vs. Strain in Deck Web at Exterior Support

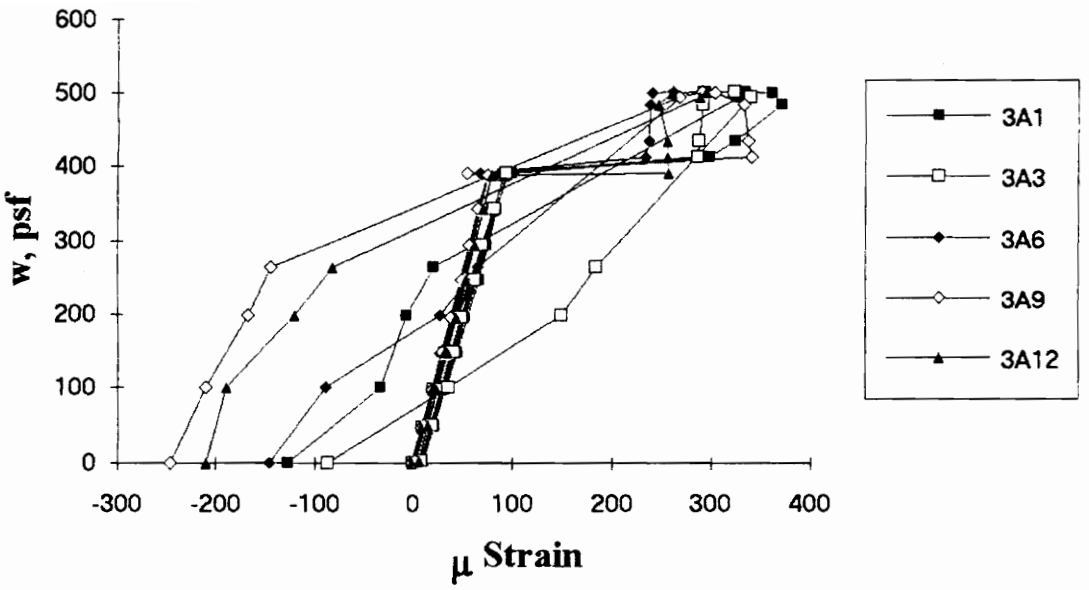

Figure A.251 SDI-2/18-PX3-9 Load vs. Strain in Deck Bottom Flange at Exterior Support

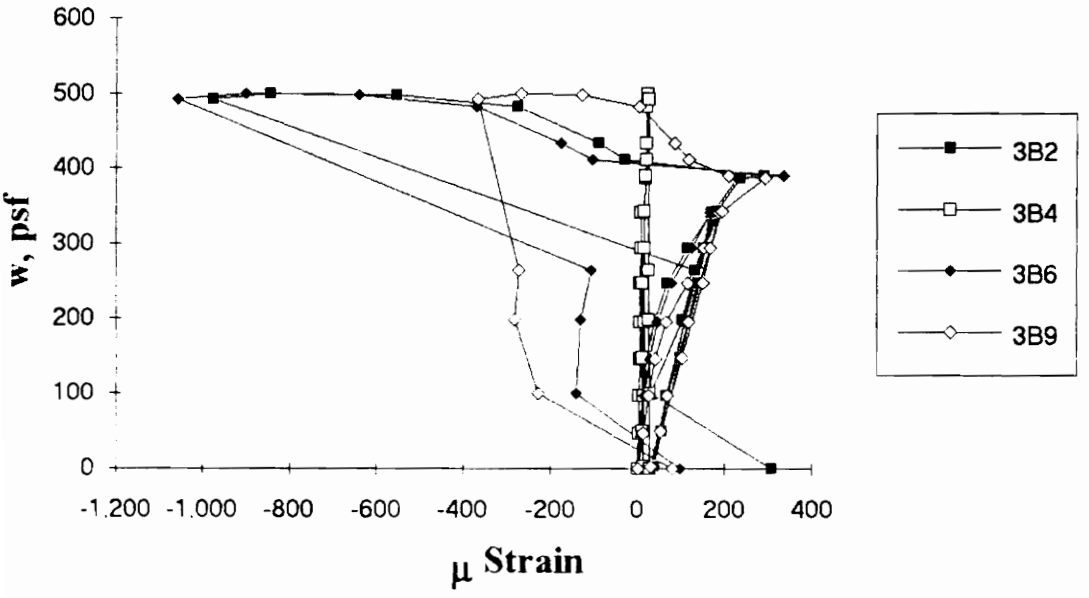

Figure A.252 SDI-2/18-PX3-9 Load vs. Strain in Deck Top Flange at Maximum Moment

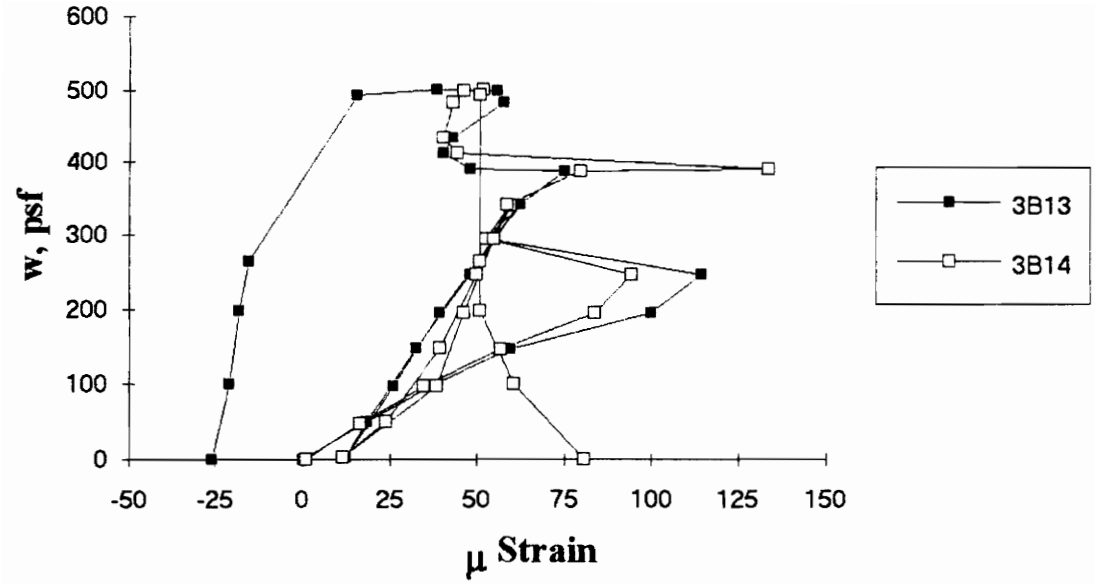

Figure A.253 SDI-2/18-PX3-9 Load vs. Strain in Deck Web at Maximum Moment

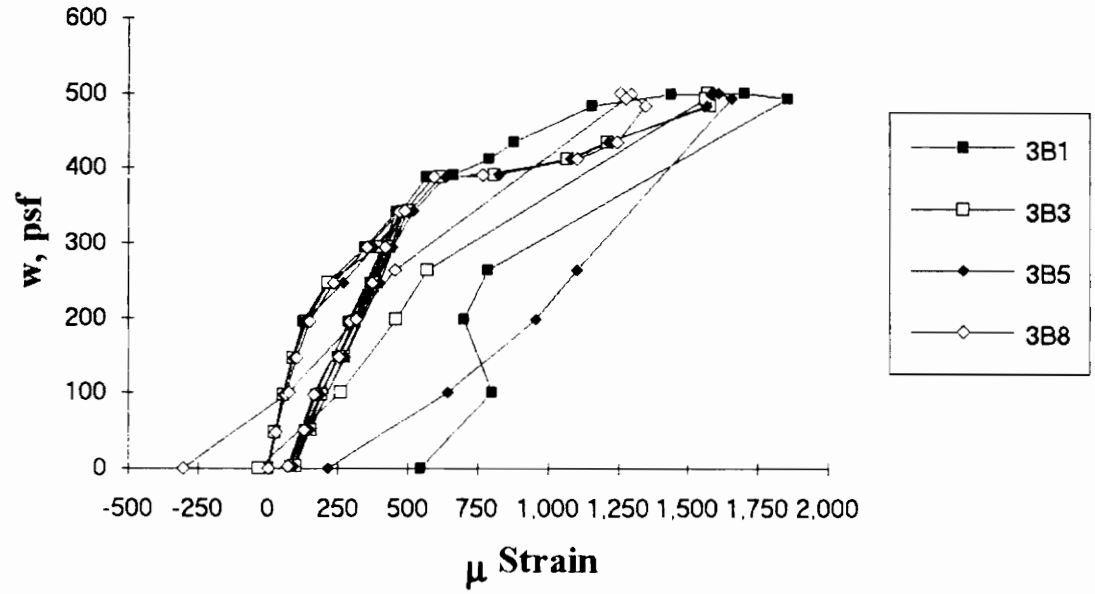

Figure A.254 SDI-2/18-PX3-9 Load vs. Strain in Deck Bottom Flange at Maximum Moment

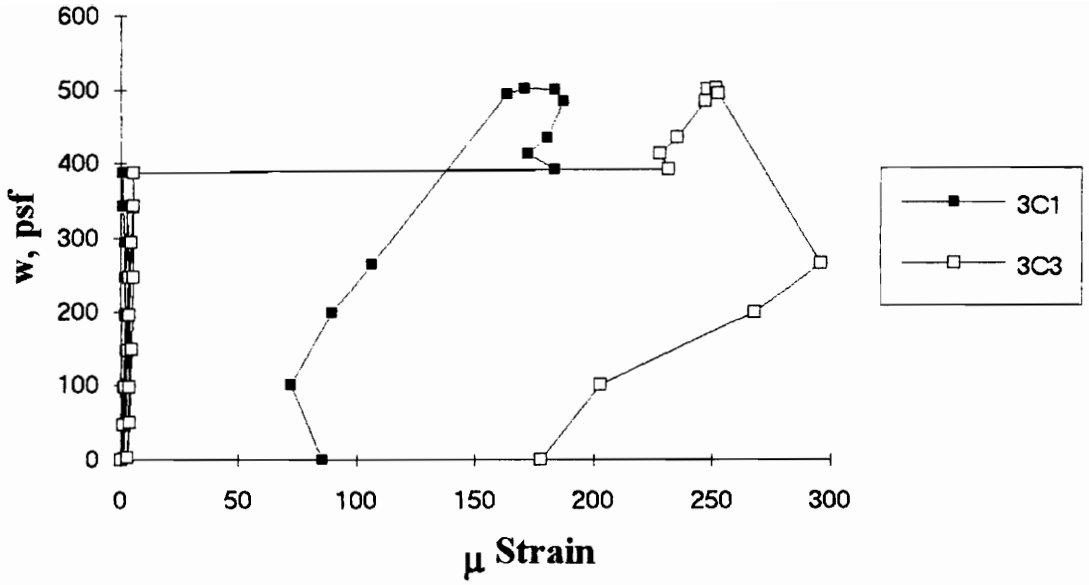

Figure A.255 SDI-2/18-PX3-9 Load vs. Strain in Deck Top Flange at Interior Support

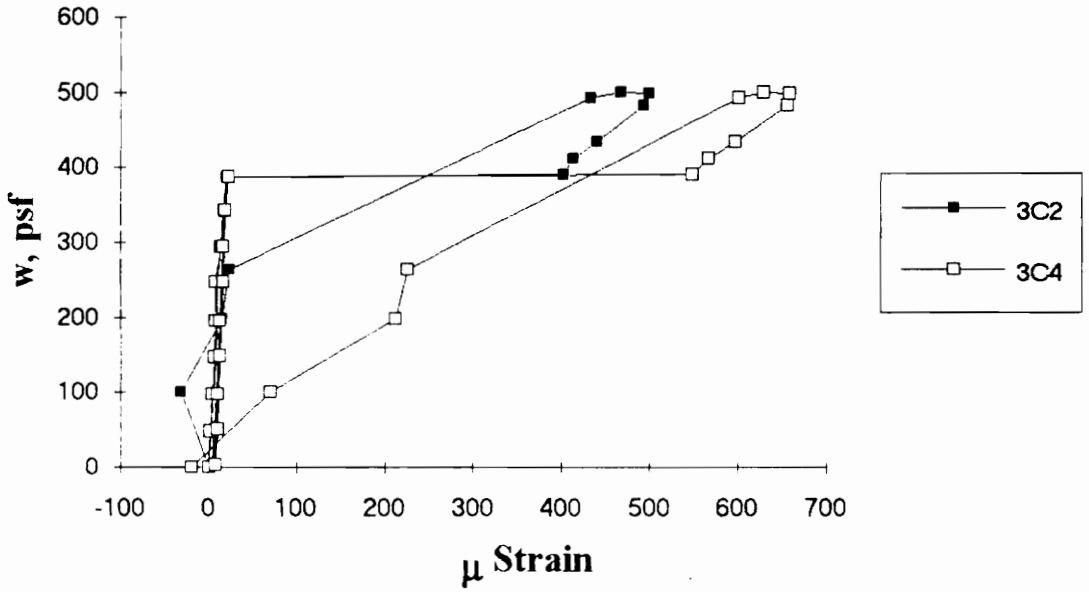

Figure A.256 SDI-2/18-PX3-9 Load vs. Strain in Deck Bottom Flange at Interior Support

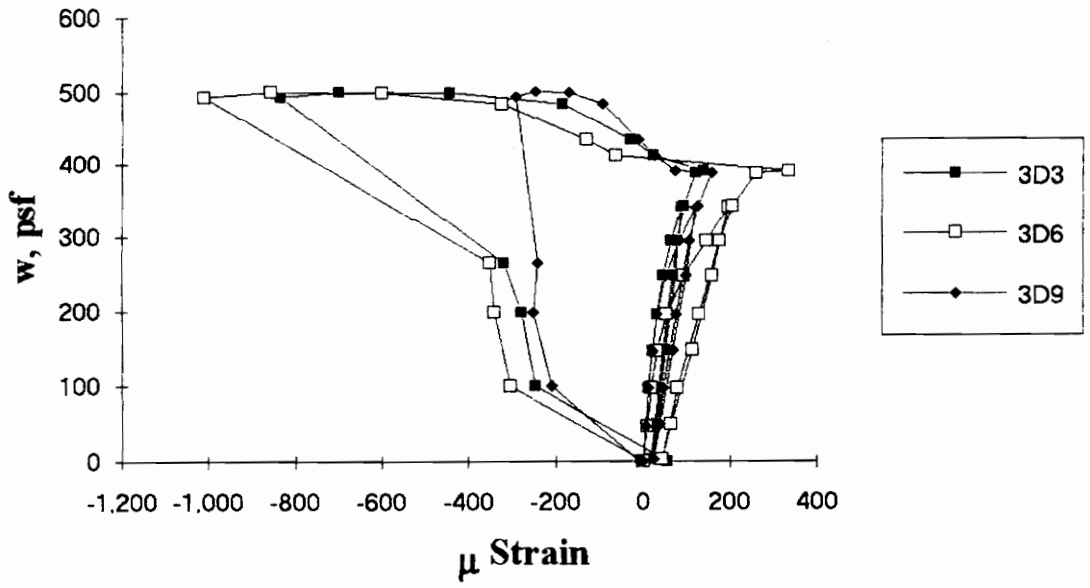

Figure A.257 SDI-2/18-PX3-9 Load vs. Strain in Deck Top Flange along the Span

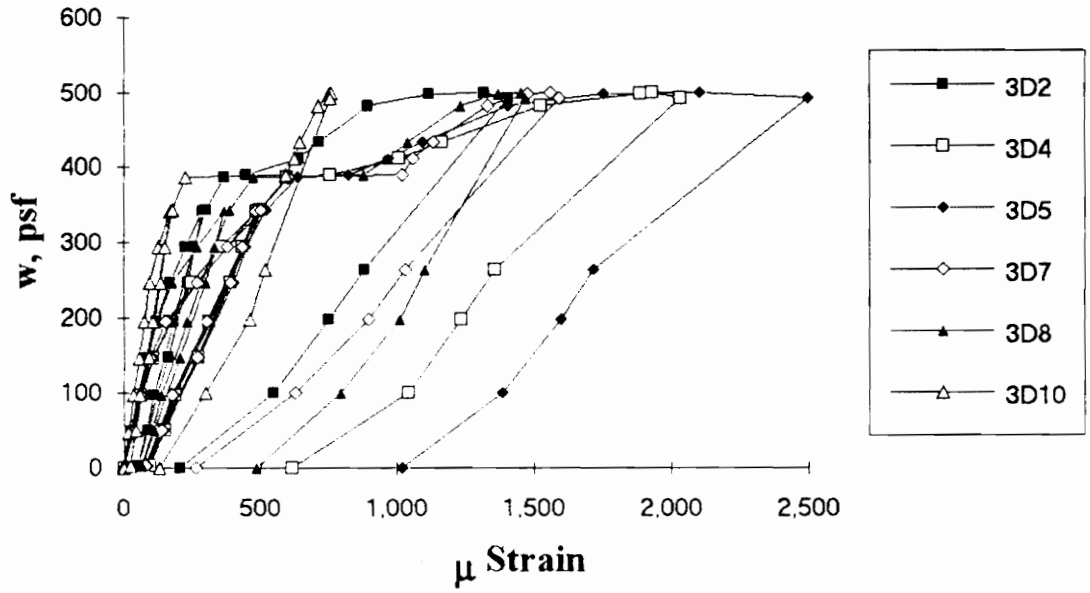

Figure A.258 SDI-2/18-PX3-9 Load vs. Strain in Deck Bottom Flange along the Span

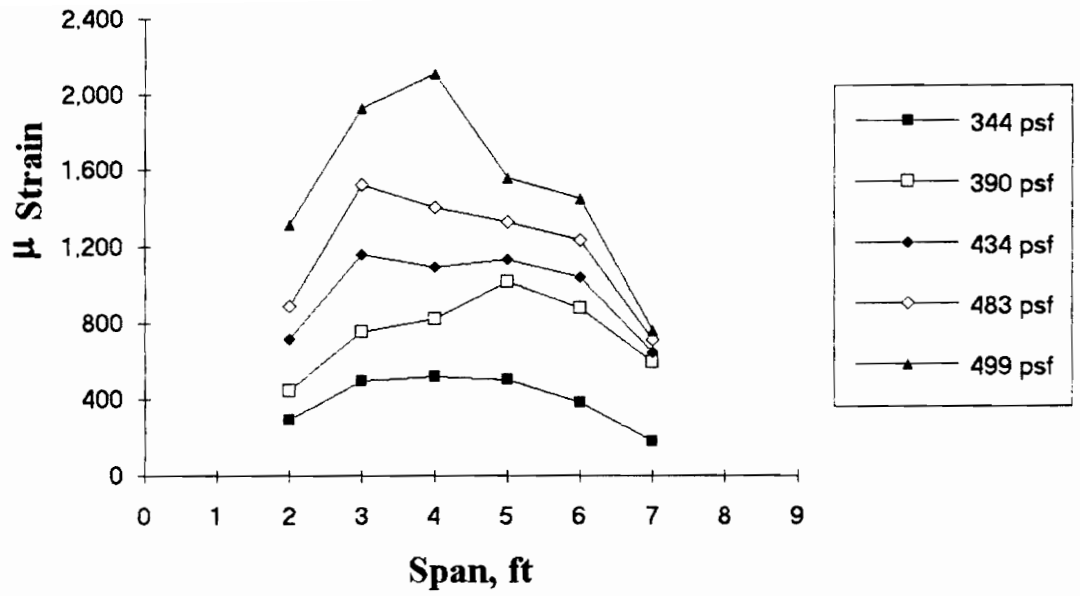

Figure A.259 SDI-2/18-PX3-9 Strain Variation in Deck Bottom Flange along the Span (from centerline of exterior support)

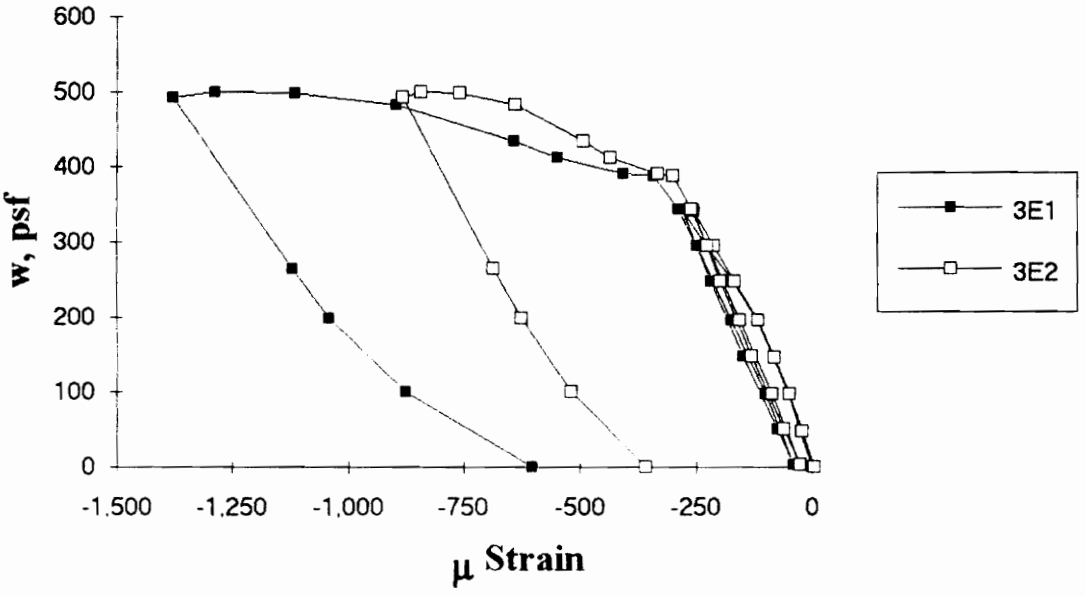

Figure A.260 SDI-2/18-PX3-9 Load vs. Strain in Concrete at Maximum Moment

Test Designation: SDI-3/20-33-10
Test Date: May 7, 1994

MATERIALS AND DIMENSIONS

General:

width:	6 ft. (2 panels)
span length:	10 ft. center span
end details:	N/A
deck anchorage type:	shear stud,4-7/8 in. long 3/4 in. dia.
average anchorage spacing:	2.1 ft.

Deck:

thickness:	0.0355 in. (20 gage)
depth:	3 in.
area:	0.572 $in.^2/ft.$
yield stress:	50.1 ksi
ultimate strength:	61.4 ksi
web embossment type:	III

embossment dimensions:

horizontal:		vertical:					
N_b :	1.81 in.	N_b :	2.30 in.	W_b :	0.53 in.	s :	3.42 in.
N_t :	1.52 in.	N_t :	2.07 in.	W_t :	0.30 in.	p_h :	0.10 in.

Concrete:

type:	normal weight
test strength:	3,220 psi
total depth:	5.5 in.
cover depth:	2.5 in.

RESULTS

midspan strain due to fresh concrete:	120 x 10^{-6} in./in.
maximum load:	911 psf
deflection at maximum load:	3.33 in.
deflection at termination of test:	4.29 in.
end slip at maximum load:	N/A
end slip at termination of test:	N/A

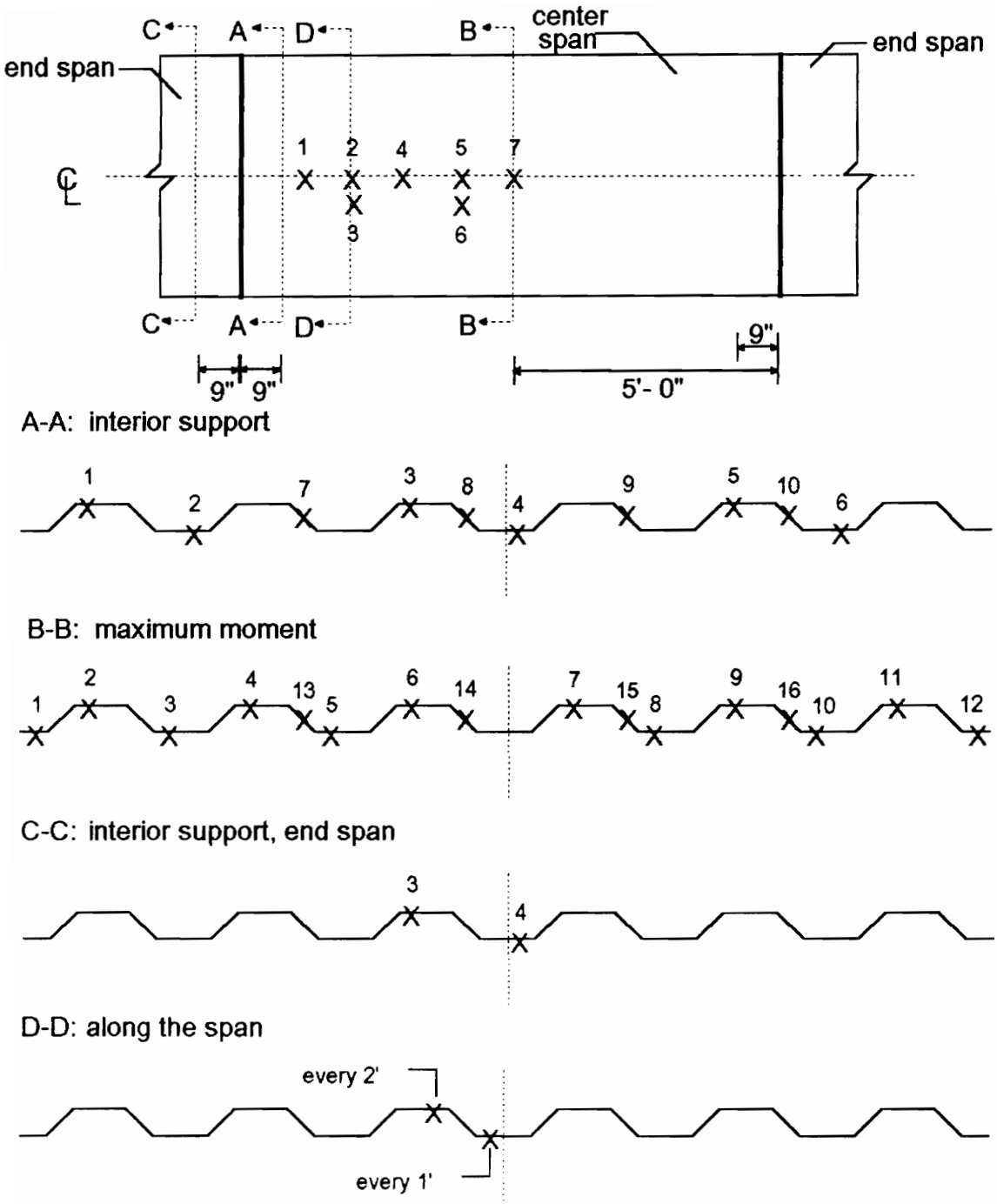

Figure A.261 SDI-3/20-33-10 Steel Deck Strain Gage Locations

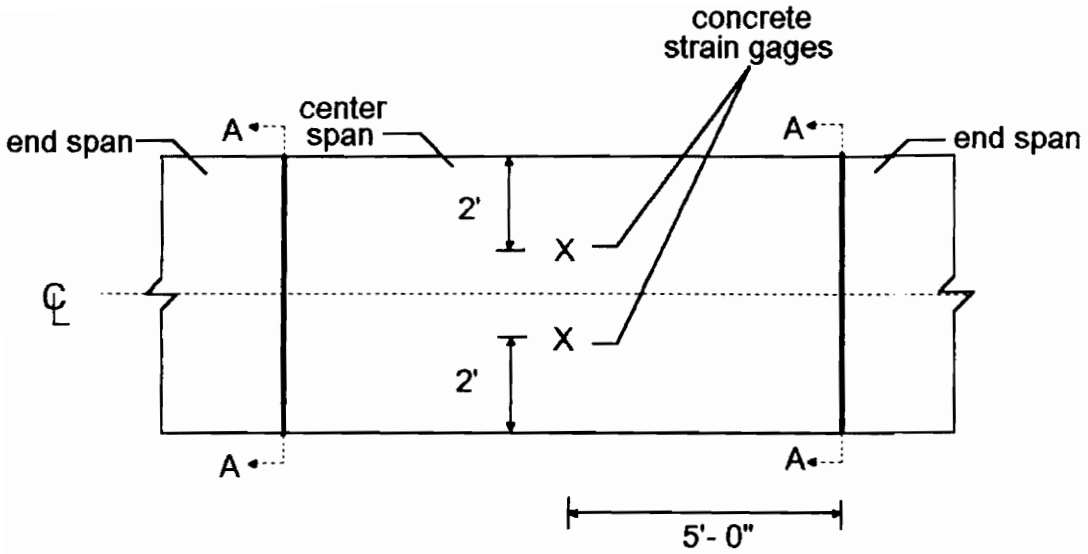

A-A: shear studs over supports

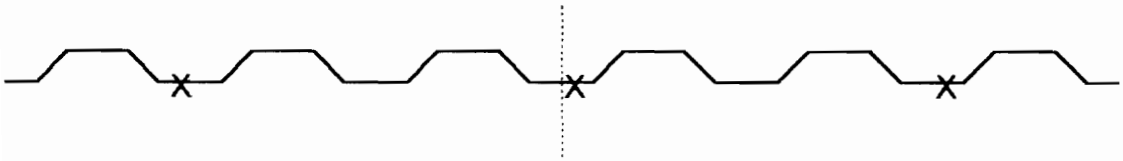

Figure A.262 SDI-3/20-33-10 Concrete Strain Gage and Shear Stud Locations

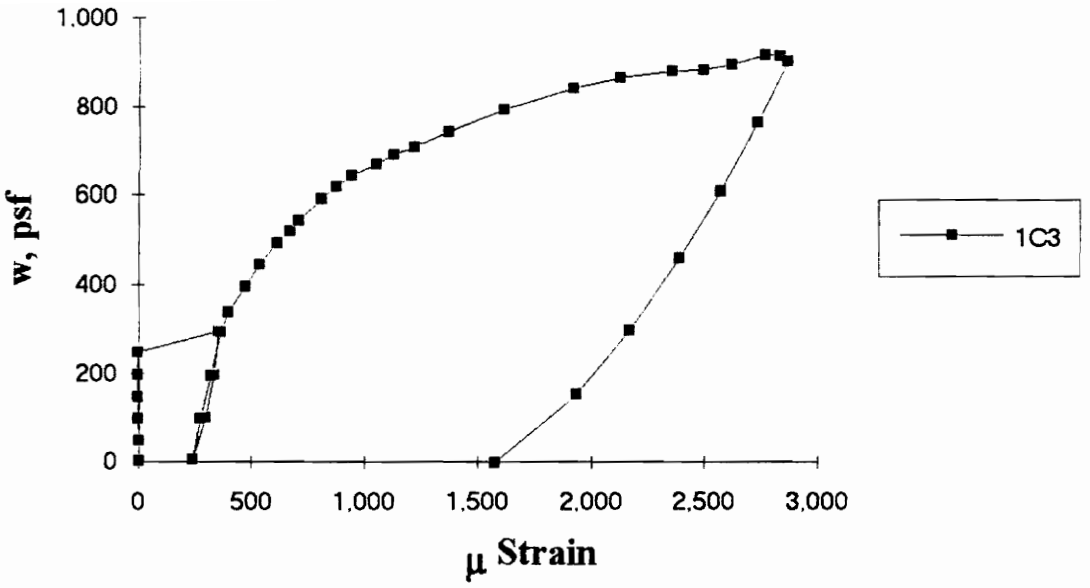

Figure A.263 SDI-3/20-33-10 Load vs. Strain in Deck Top Flange at Interior Support in End Span

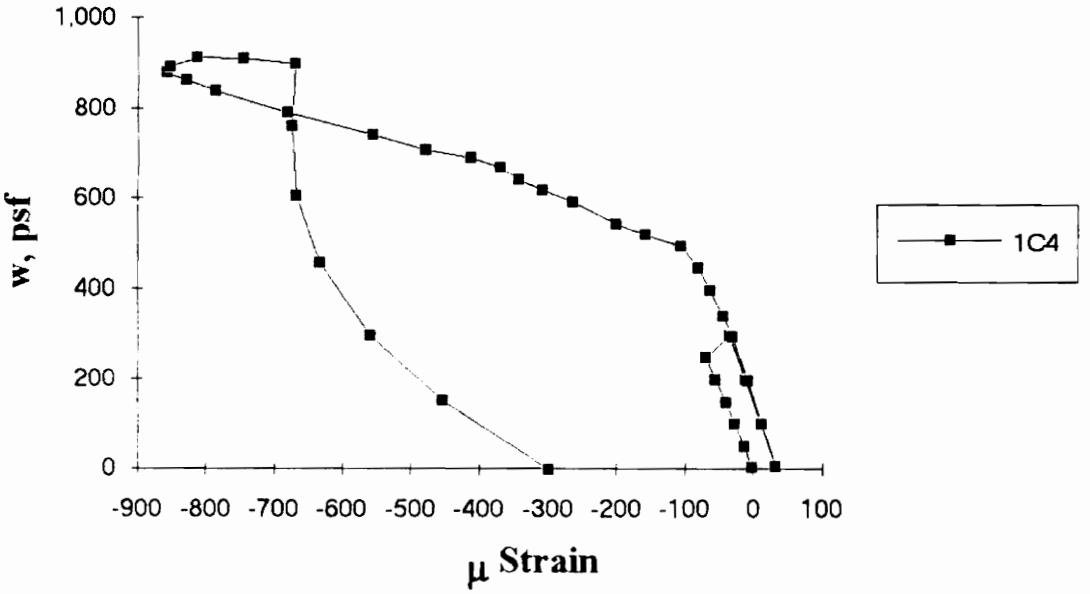

Figure A.264 SDI-3/20-33-10 Load vs. Strain in Deck Bottom Flange at Interior Support in End Span

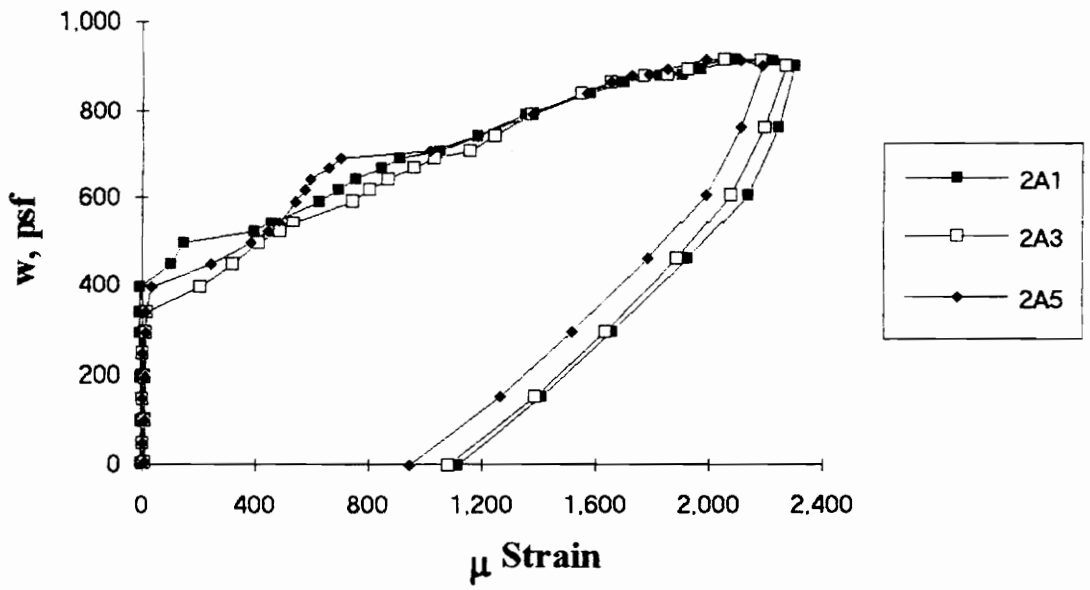

Figure A.265 SDI-3/20-33-10 Load vs. Strain in Deck Top Flange at Interior Support in Center Span

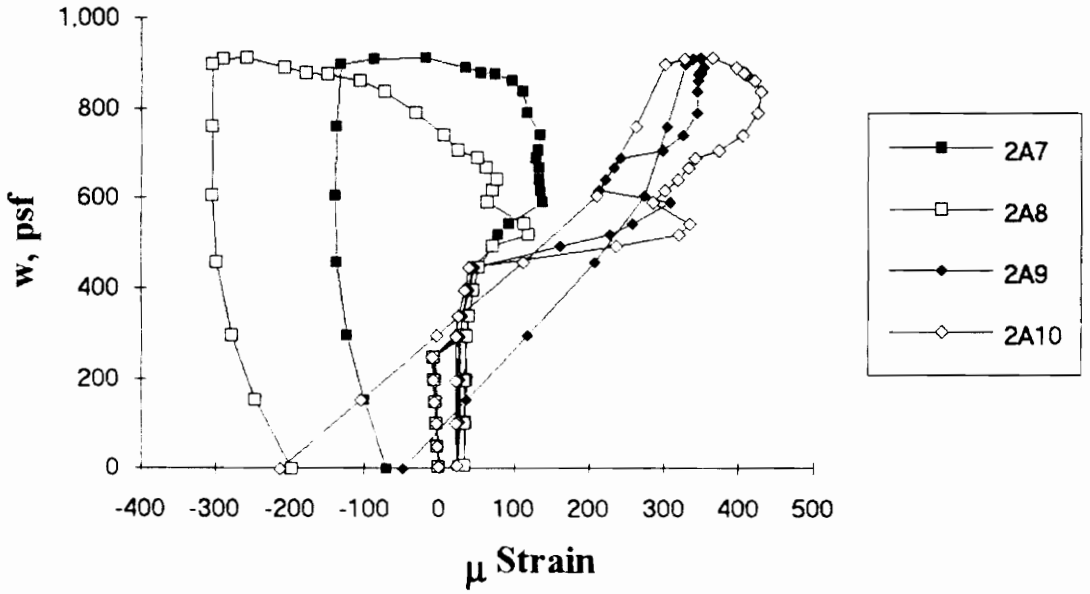

Figure A.266 SDI-3/20-33-10 Load vs. Strain in Deck Web at Interior Support in Center Span

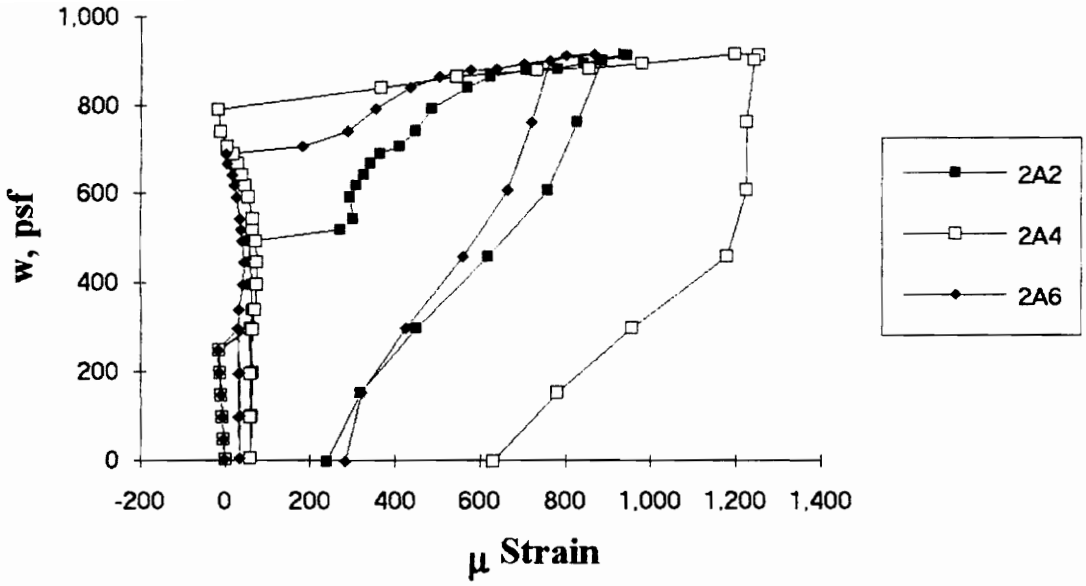

Figure A.267 SDI-3/20-33-10 Load vs. Strain in Deck Bottom Flange at Interior Support in Center Span

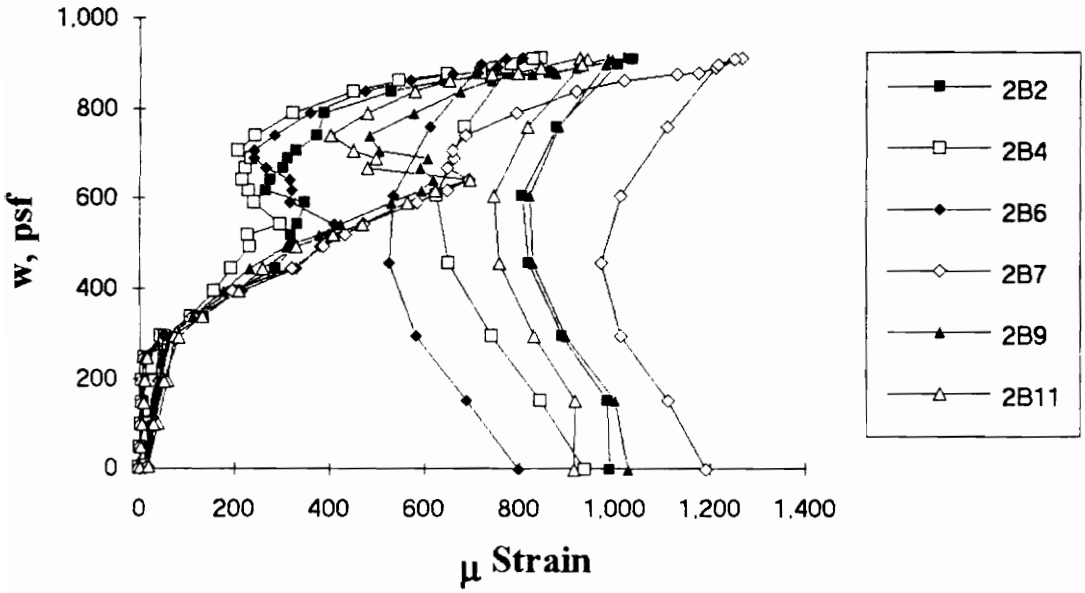

Figure A.268 SDI-3/20-33-10 Load vs. Strain in Deck Top Flange at Maximum Moment

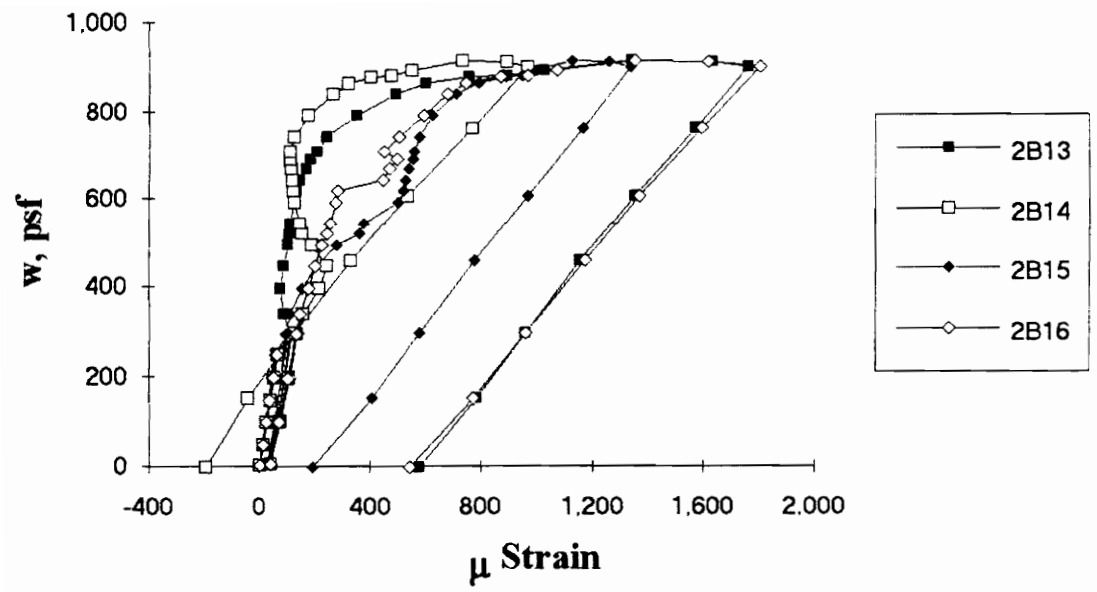

Figure A.269 SDI-3/20-33-10 Load vs. Strain in Deck Web at Maximum Moment

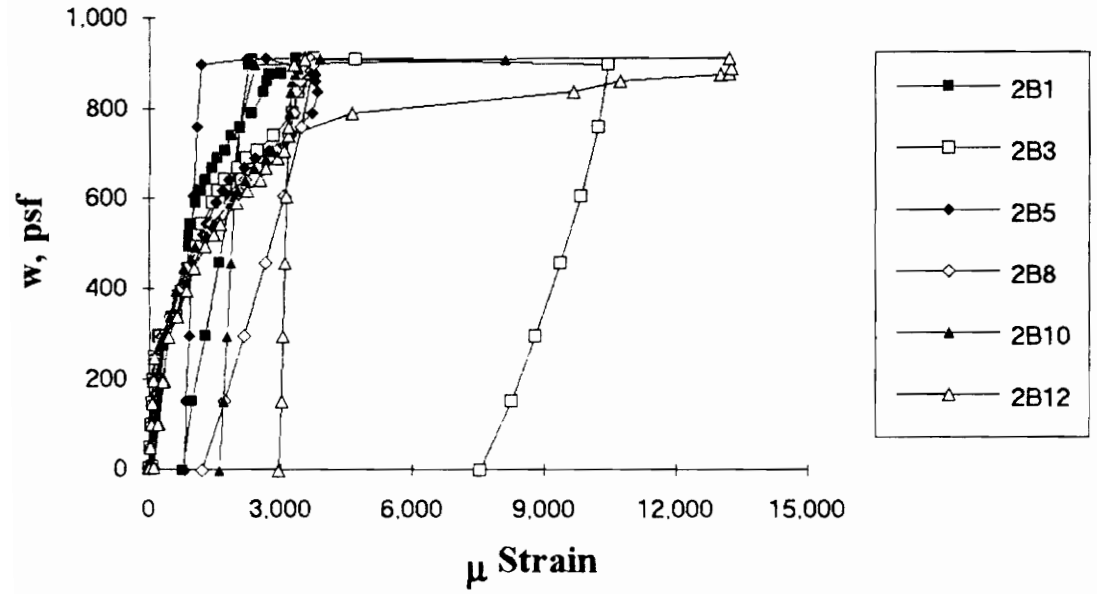

Figure A.270 SDI-3/20-33-10 Load vs. Strain in Deck Bottom Flange at Maximum Moment

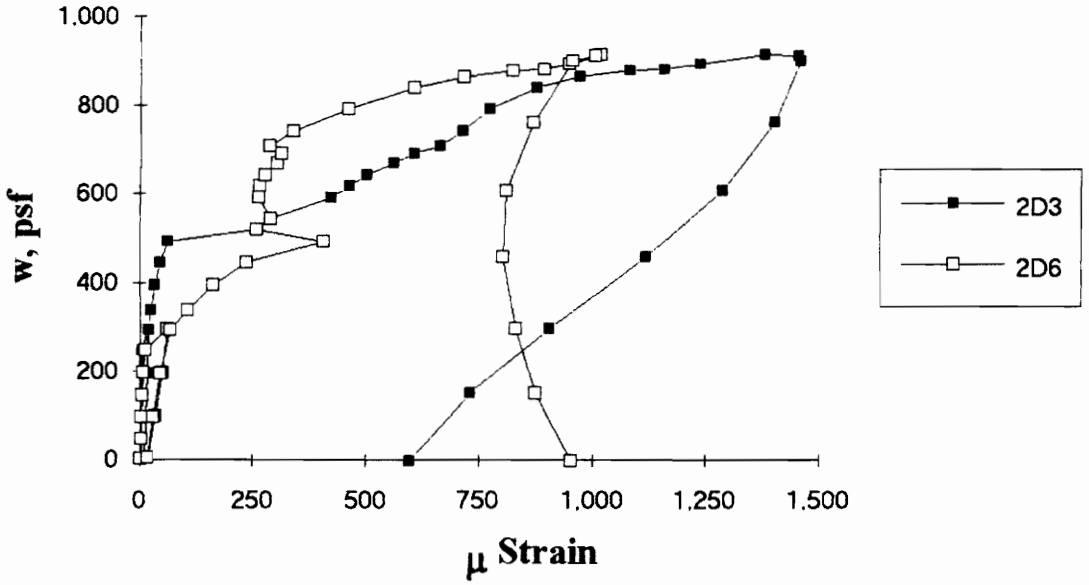

Figure A.271 SDI-3/20-33-10 Load vs. Strain in Deck Top Flange along the Span

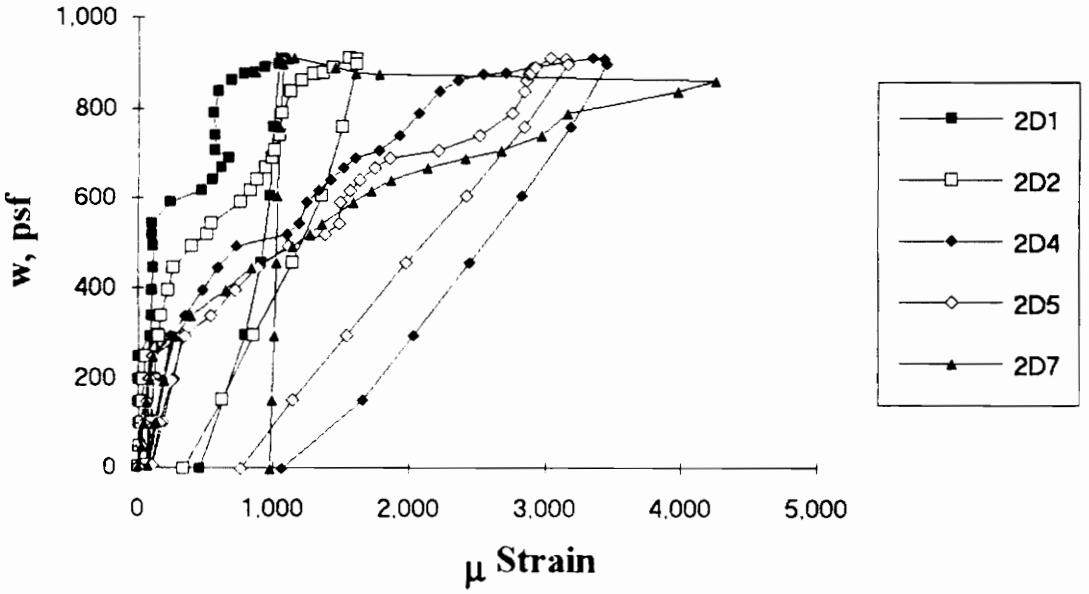

Figure A.272 SDI-3/20-33-10 Load vs. Strain in Deck Bottom Flange along the Span

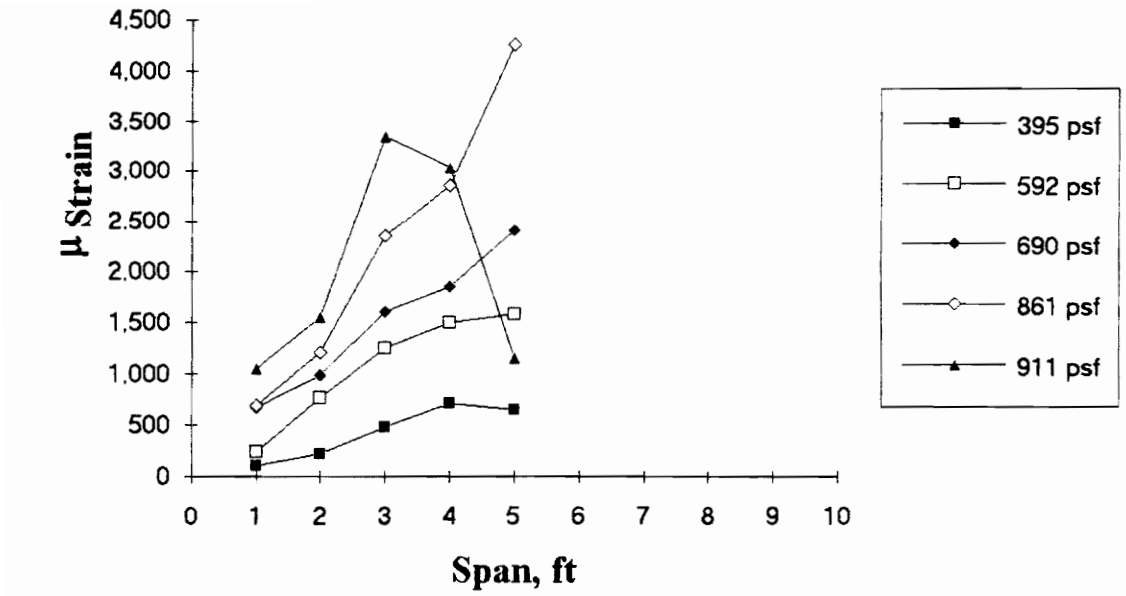

Figure A.273 SDI-3/20-33-10 Strain Variation in Deck Bottom Flange along the Span (from centerline of support)

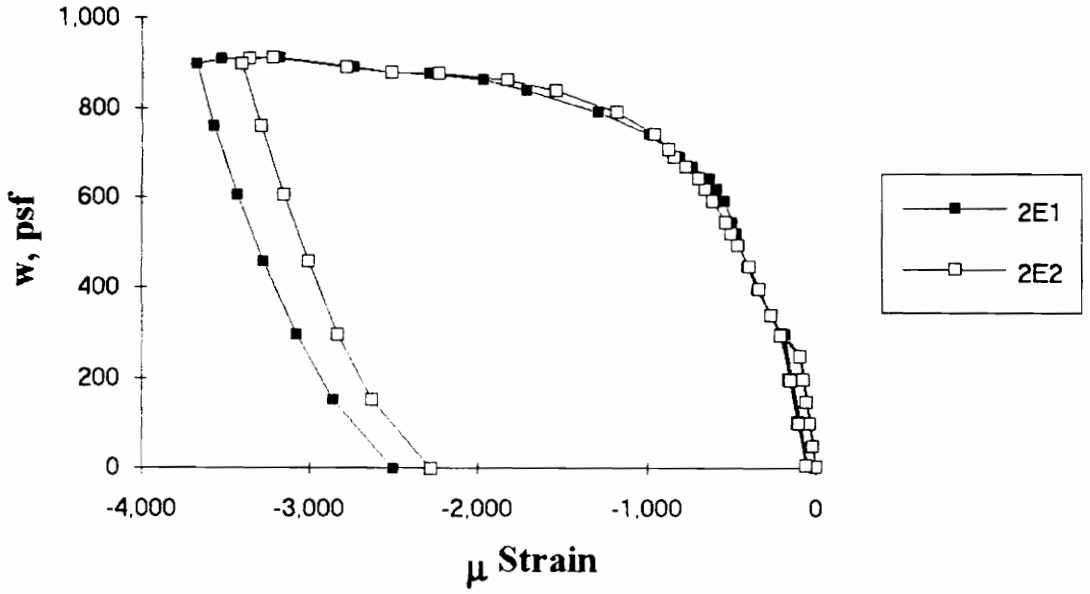

Figure A.274 SDI-3/20-33-10 Load vs. Strain in Concrete at Maximum Moment

Appendix B

VERTICAL SHEAR STRENGTH

Very little research has been conducted on the vertical shear strength of composite slabs. A procedure for checking the vertical shear strength has yet to be developed based on the actual behavior of composite slabs. Current checks are either based on the reinforced concrete design provisions for vertical shear derived by Zsutty (1968) or consider only the vertical shear strength of the concrete and not the steel deck. These checks produce very conservative vertical shear strengths and lead to thick slabs.

The SDI has recognized the need for a model to determine the vertical shear strength of composite slabs. As a first step in the development process a literature search was conducted to determine what research had been done on the subject. The results of this search are presented.

Daniels and Crisinel (1987) conducted tests to investigate flexural failure, horizontal shear debonding failure and vertical shear failure. The specimens tested to investigate vertical shear failure were actually portions of specimens previously tested for flexural

capacity. Some of the vertical shear specimens had existing flexural cracks from the flexural tests, others were uncracked.

Two loading conditions were used, a line load and a point load. The specimens that were loaded with a line load across the width of the specimen experienced a single transverse crack at the edge of the applied load. Pre-existing flexural cracks did not influence the shear capacity of the specimens. For point-loaded specimens the load was placed above the thick portion of the slab in the center of a rib. If there were no pre-existing flexural cracks, one or two formed near the load. Longitudinal and transverse cracks formed on all four sides of the load. Two slab thicknesses were tested, 115 mm (4.5 in.) and 165 mm (6.5 in.). The vertical shear strengths of the thicker specimens were adversely affected by pre-existing flexural cracks whereas the thinner slabs were not.

The test results were compared to the vertical shear design limits of Eurocode 4. The failure loads of the specimens, deemed to have failed by vertical shear, were much higher than the design limits of Eurocode 4. An alternative approach to predicting vertical shear strength was not presented.

A second study on the design of composite slabs for vertical shear was directed by Patrick and Bridge (1992). They describe the tests in their study as the "first tests known to produce vertical shear failures in simply-supported composite slabs" (Patrick and Bridge 1992). Patrick and Bridge make reference to the work by Daniels and Crisinel, but suggest that the failures they observed were incorrectly classified. "They reported that the ultimate mode of failure was for the concrete, after having formed a dominant crack near the

loading point, to break into two pieces and slip at each end over the supports (which is a normal feature of a longitudinal slip failure). However, they classified the failures as vertical shear failures (seemingly on account of increased brittleness of the load-deflection and load-slip behaviour, and a tendency for the flexural cracks to be more inclined, compared with longer slabs)..."

The experimental program conducted by Patrick and Bridge focused exclusively on vertical shear. Four composite slabs were constructed using Bondek II deck which has a reentrant or dovetail shaped rib. Significant planning was put into the design of the slabs so that a vertical shear failure would occur when loaded to failure with concentrated line loads.

Three factors needed to be considered in the design of the specimens: (1) the length of the shear span, (2) the length of the cantilever, and (3) the possibility of strut action. A range of shear spans for which vertical shear failures would result was determined using the empirical equations derived by Zsutty for the ultimate strength of reinforced concrete beams failing in vertical shear given by:

$$V_s = 2.3\left(\frac{f_{cm}\,A_s}{L_s}\right)^{1/3} d \qquad \text{for} \frac{L_s}{d} \geq 2.5 \qquad \text{(B-1)}$$

$$V_s = 2.3\left(\frac{f_{cm}\,A_s}{L_s}\right)^{1/3} d\left(2.5\frac{d}{L_s}\right) \qquad \text{for } \frac{L_s}{d} \leq 2.5 \qquad \text{(B-2)}$$

where,

V_s = shear force for vertical shear failure

f_{cm} = mean compressive strength

A_s = area of steel per unit width

L_s = shear span

d = effective depth of reinforcement

In the Australian Concrete Structures Standard AS 3600 Eqs. B-1 and B-2 have been modified "to account for the apparent increase in average shear stress at failure in shallow members" and are given by:

$$V_s = \left(1.4 - \frac{d}{2000}\right)\left(\frac{L_s}{d}\right)^{1/3}\left(\frac{f_{cm}\,A_s}{L_s}\right)^{1/3} d \qquad \text{for} \frac{L_s}{d} \geq 2.0 \qquad \text{(B-3)}$$

$$V_s = \left(1.4 - \frac{d}{2000}\right)\left(\frac{L_s}{d}\right)^{1/3}\left(\frac{f_{cm}\,A_s}{L_s}\right)^{1/3} d\left(2.0\frac{d}{L_s}\right) \qquad \text{for } \frac{L_s}{d} \leq 2.0 \qquad \text{(B-4)}$$

For under-reinforced slabs the shear force corresponding to flexural failure is given by:

$$V_m = 0.9\,A_p\,f_{sy.sh}\,\frac{d}{L_s} \qquad \text{(B-5)}$$

where,

V_m = shear force for flexural failure

A_p = area of steel deck per unit width

$f_{sy.sh}$ = yield stress of steel deck

Two slab depths, 140 mm (5.5 in.) and 175 mm (6.9 in.), and two deck thicknesses, 0.75 mm (0.0295 in.) and 1.00 mm (0.0394 in.), were chosen. A concrete strength of 35 MPa (5070 psi) and a steel yield stress of 650 MPa (94 ksi) were assumed for analysis. Using these dimensions and material properties the ratio of V_s to V_m was plotted vs. the shear span-to-effective depth ratio, L_s/d, for both the Zsutty and the AS 3600 equations. The AS 3600 plot is shown in Figure B.1. The selection of a shear span that would cause vertical shear failure, i.e., $V_s/V_m < 1$, was made from these plots. The researchers chose a range of L_s/d between 1.5 and 3.0.

Partial shear connection strength theory was also used to design the test specimens. The partial shear connection strength model can calculate the ultimate strength of slabs controlled by flexural or longitudinal slip failure but not vertical shear. The model was used to rule out longitudinal slip as a possible failure mode in the test specimens by determining the necessary length of the cantilever portion of the slab to provide adequate anchorage against slip. The model assumes negligible adhesion bond and perfectly ductile shear connection performance. However in order to use the model, the capacity of the deck profile to resist longitudinal slip had to be investigated. A slip block test, discussed in Chapter 2 and illustrated in Figure 2.6, was used to gather this information.

The length of the specimens was predetermined by the testing rig to be 4250 mm (13.9 ft.) Using the partial shear connection strength model slabs were analyzed with the length of cantilever portions, L_c, ranging from zero to 1000 mm (3.3 ft.) The shear bond curves for L_c = 1000 mm (3.3 ft.), shown in Figure B.2, predicted flexural failures for the

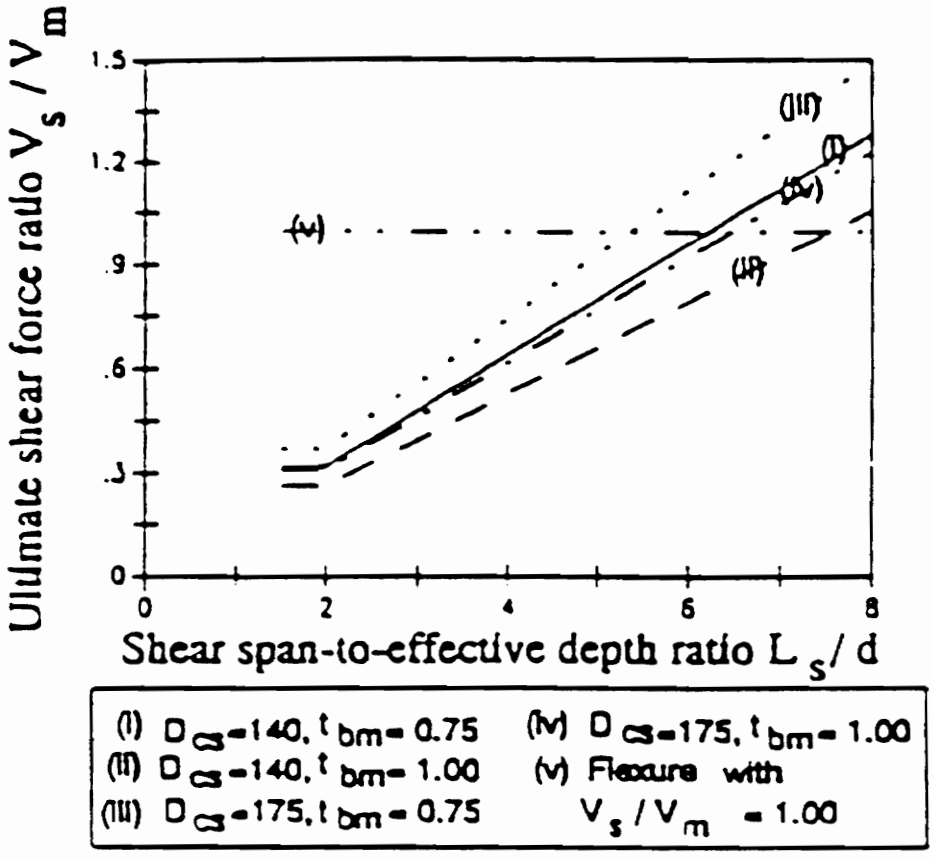

Figure B.1 Predicting Vertical Shear Failures of Proposed Test Specimens Using Zsutty's Equations Modified According to AS 3600 (Patrick and Bridge 1992)

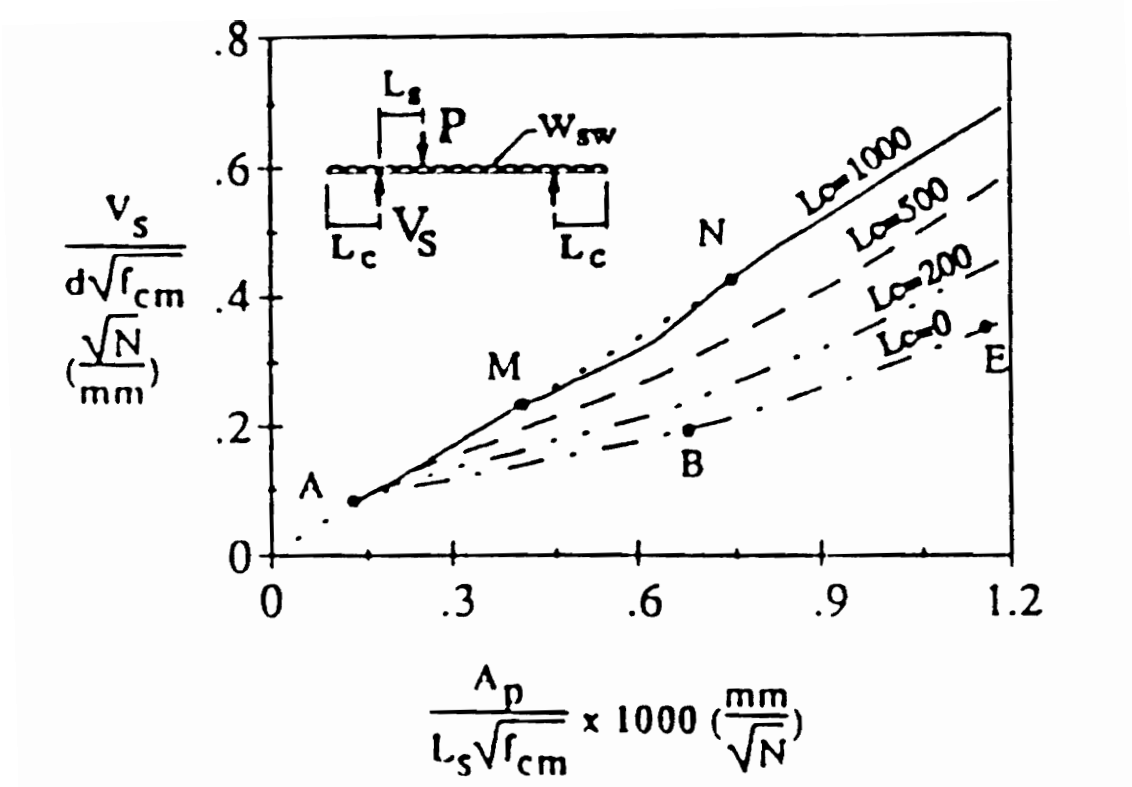

Figure B.2 Shear-Bond Graph Showing Effect of L_c on Failure Mode of Shear Span (Patrick and Bridge 1992)

entire range of shear spans and was chosen as the length of the cantilever. The slabs had an overall length of 6250 mm (20.5 ft.).

The last factor to be considered to prevent longitudinal slip failure was strut action. Strut action between the loading point and the support allows the slab to transmit shear force, and can facilitate a longitudinal slip failure. From simple statics, the diagonal strut that forms between the support and the load point is in compression. Horizontal compressive forces at the top and bottom of the strut must be resisted by the concrete. Although the horizontal resistance of the concrete was found through analysis to be greater than the horizontal compressive force on the strut, pinned pan connectors were attached to the deck within the cantilever portion as an extra precaution against longitudinal slip failure.

With all the possibilities for longitudinal slip failure accounted for, four specimens were constructed with the following dimensions:

span length	=	4250 mm (13.9 ft.)
cantilever length	=	1000 mm (3.3 ft.)
width	=	1180 mm (3.9 ft.) (2 panels)
total depth	=	140 mm (5.5 in.) and 175 mm (6.9 in.)
deck thickness	=	0.75 mm (0.0295 in.) and 1.00 mm (0.0394 in.)

Two hydraulic jacks applied load to the specimens. The jacks applied equal forces to a beam positioned parallel to the slab. This beam then transferred to the load to two cross beams, one at each end of the slab, that ran parallel to the supports. The test setup is pictured in Figure B.3. The specimens were unrestrained horizontally.

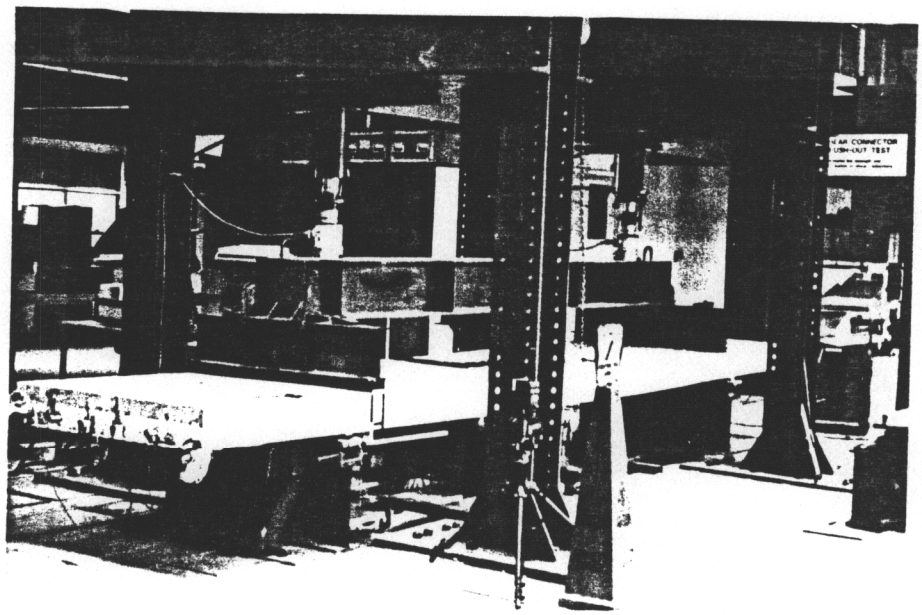

Figure B.3 Overview of Test Setup (Patrick and Bridge 1992)

Each specimen was first tested for flexural capacity. The specimens were unloaded just prior to ultimate load before the specimen sustained any damage. A shear test was then performed at each end of the specimen. During the test on the first end the jack on the second end was positioned directly over the support so that a single load was applied within the span. If vertical shear failure occurred at the first end the second end was tested at the same shear span. If not the shear span was adjusted. Out of seven tests four failed by vertical shear and three by flexure.

Patrick and Bridge reported the following mode of failure:

(1) A single flexural crack formed adjacent to the loading point early in the test which grew in height as the load increased.

(2) Within one percent of the maximum load the first sign of failure appeared. A fine diagonal crack formed at mid-height of the slab in the middle of the shear span. The slab was still able to support the load.

(3) Additional load caused the top of the crack to propagate towards the loading point and the bottom towards the support. The slab suddenly split into two parts that pivoted about the loading point, and collapsed.

The test results were compared with the results of Zsutty's equations. Ratios of test shear to predicted shear ranged from 1.52 to 2.06. The equations were very conservative, and inadequate design tools for vertical shear strength of composite slabs. Patrick and Bridge point to the absence of cracks within the shear span as a reason for the poor

correlation. Cracks form within the shear span in reinforced concrete slab tests but not in composite slab tests.

In light of the poor comparison between test results and current design provisions Patrick and Bridge proposed a simple equilibrium model, illustrated in Figure B.4, to predict vertical shear failure. "Just prior to cracking, it is assumed that along the potential crack path (i.e. the straight line joining the loading point and the contact point at the center of the end support) the concrete is in direct compression. Consequently, the elements of concrete orientated in the direction of the strut are assumed to be under zero shear, such that direct tension develops in the concrete at right angles to the potential crack path. Furthermore, it is assumed that the tensile stress is uniform over the full length of the potential crack path." The concrete tensile stress is given by:

$$\sigma_t = \frac{V}{L_s} \qquad \text{(B-6)}$$

where,

V = shear force in slab adjacent to the load P

L_s = shear span

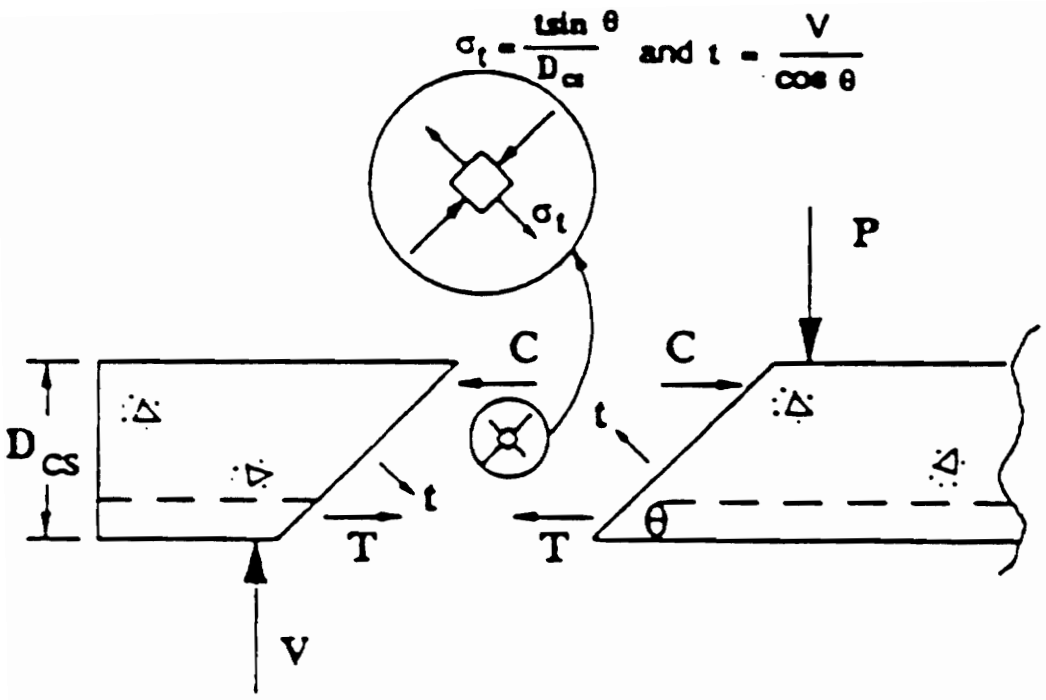

Figure B.4 Assumed State of Equilibrium Just Prior to Diagonal Cracking (Patrick and Bridge 1992)

According to the AS 3600 the tensile stress that is sufficient to cause the concrete to crack is given by:

$$\sigma_t = 0.33 \sqrt{f_{cm}} \tag{B-7}$$

where f_{cm} is the compressive strength of the concrete. Patrick and Bridge assumed that a vertical shear failure occurs when the tensile stress in the concrete reaches this value along the potential crack path. The force necessary to cause a vertical shear failure is therefore given by:

$$V_{dsf} = 0.33 \sqrt{f_{cm}}\ L_s \tag{B-8}$$

The model was plotted on a shear-bond graph along with the line corresponding to flexural failure, shown in Figure B.5. "The curve calculated using the proposed model crosses the flexural line close to the test points [for specimens failing in vertical shear] indicating reasonably good agreement between the tests and the theory."

Patrick and Bridge conclude their study with the following recommendation: "Design provisions should therefore be included in composite slab Design Standards just as they are for reinforced-concrete Standards. The tests reported herein form a basis on which further testing can be performed to develop appropriate rules for the design of the positive moment regions of composite slabs in vertical shear."

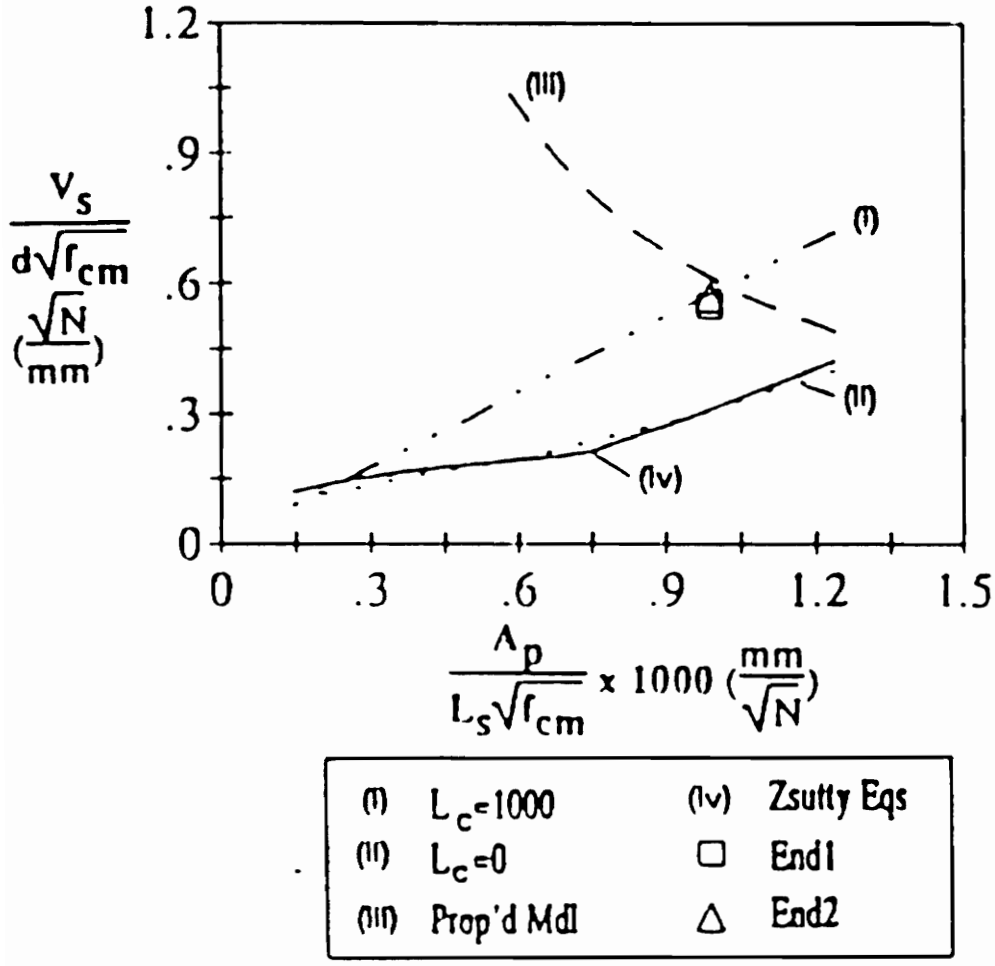

Figure B.5 Shear-Bond Graph of Test Results--Slab D04 (Patrick and Bridge 1992)

VITA

Angela Sellars Terry was born in Roanoke, Virginia on December 5, 1970. She graduated from Staunton River High School in Moneta, Virginia in 1988. She received a Bachelor of Science in Civil Engineering at the University of Virginia (UVA) in Charlottesville, Virginia in 1992. While attending UVA, she worked for the Virginia Transportation Research Council as a Research Assistant. She entered the Virginia Polytechnic Institute and State University Charles Edward Via Department of Civil Engineering, Structures Division, in 1992.